KERNFORSCHUNGSANLAGE JÜLICH GmbH
Institut für Festkörperforschung

SPIN GLASSES

by

Hansjörg Maletta
Werner Zinn

Jül – 2084
September 1986
ISSN 0366 – 0885

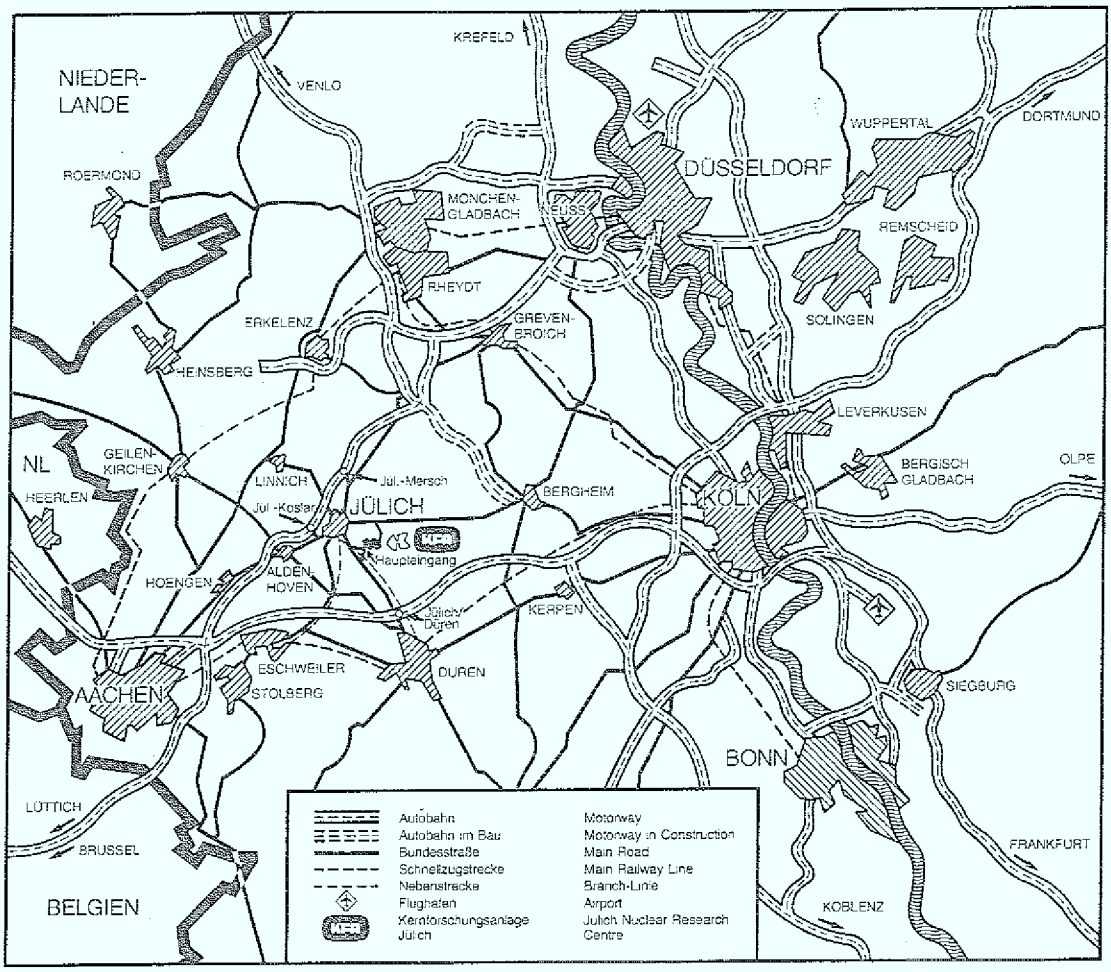

Als Manuskript gedruckt

Berichte der Kernforschungsanlage Jülich – Nr. 2084

Institut für Festkörperforschung Jül – 2084

Zu beziehen durch: ZENTRALBIBLIOTHEK der Kernforschungsanlage Jülich GmbH
Postfach 1913 · D-5170 Jülich (Bundesrepublik Deutschland)
Telefon: 02461/610 · Telex: 833556-0 kf d

SPIN GLASSES

H. Maletta and W. Zinn

Institut für Festkörperforschung
der Kernforschungsanlage Jülich,
D-5170 Jülich, Postfach 1913, W.-Germany

To be published in:

Handbook on the Physics and Chemistry of RARE EARTHS,
ed. K. A. Gschneidner, Jr., and L. Eyring, North-Holland Publ.
Comp., Vol. 12 (1986).

1. Introduction

In recent years there has been an upsurge of interest in the research on the spin-glass phenomenon. The term "spin glass" was introduced in 1968; now about one paper per day is published which uses this word in its title or abstract (For recent reviews see: Fischer, 1983a and 1985; Binder and Young, 1986; Huang, 1985).

There is now general agreement on the "definition" of a spin glass: Spin glass refers to a magnetic state of a system in which interactions between the magnetic moments are "in conflict" with each other due to disorder so that the spins order in a non-periodic fashion - they "freeze" into random directions. Additionally, the state is characterized by very slow equilibration after perturbation and significant history-dependence. Taking these features together means that we are going to apply the term "spin glass" here in the restricted sense, as mostly done, and not to all random non-collinear ordered magnets, e.g. not to systems with random anisotropy axes (see section 9) or to systems with random fields. The new type of magnetic order is represented schematically in Fig. 1 where its magnetization measured in a small applied field is compared (in its magnitude and temperature dependences) with that of two wellknown types of collinear magnetic order, too.

The increasing interest in spin glasses may have the following reasons:

(i) Spin-glass properties are fairly universal. They have been observed in a wide variety of different systems with competing interactions between the spins e.g. in crystalline metals Fe_xAu_{1-x} (Cannella and Mydosh, 1972), in crystalline insulators $Eu_xSr_{1-x}S$ (Maletta and Crecelius, 1976) as well as in amorphous alloys Gd_xAl_{1-x} (Mizoguchi et al., 1977).

(ii) Spin glass behavior is novel; it is an intrinsic effect of disorder and competition of the magnetic interactions. Attempts to understand the origin and behavior of the spin-glass state have led to the appreciation of several new concepts and to the recognition that the fundamental ingredients for these concepts are much more widespread in occurrence than spin glasses. The study has had important impact in statistical mechanics, and recently also applications on complex optimation

problems (Kirkpatrick et al., 1983) and biological problems (memory (Hopfield, 1982), prebiological evoluation (Anderson, 1983)) have been discussed.

(iii) In spite of more than 2000 publications with many important results and in spite of a close interaction between experiment, computer simulation and analytical model calculation the essential questions for instance about the nature of the spin-glass transition and the spin-glass state are still controversially discussed. Spin glasses are still a challenge to solid state physics.

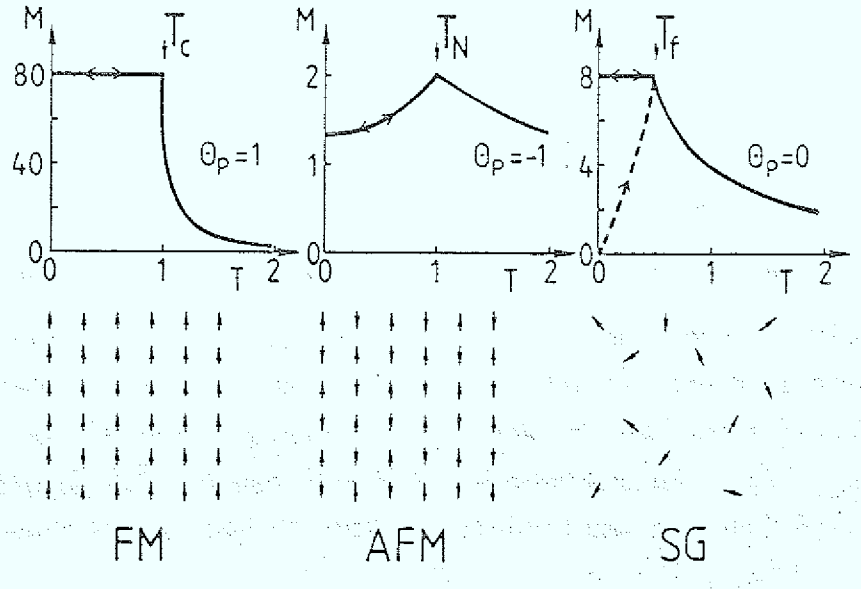

Fig. 1: Comparison of the magnetization measured in a small applied field for (a) a ferromagnet (FM), (b) an antiferromagnet (AFM), and (c) a spin glass (SG). The dashed line indicates the zero-field-cooled behavior of the spin glass. The curves are schematic and the units arbitrary, but the same average magnitude of the exchange interaction is choosen for all three. Values of the paramagnetic Curie-Weiss temperature Θ_p are indicated. At the bottom the corresponding ordering of the magnetic moments is sketched schematically (From Moorjani and Coey, 1984).

The present review attempts to give a survey of the field, including discussions of the most exciting questions which have come up. Obviously, it is nearly impossible to cite all the papers on spin glasses, hence the authors apologize at the outset to those whose work is not explicitely referenced. Additional references are found in other reviews (Fischer, 1983a and 1985; Binder and Young, 1986; Huang, 1985).

The organization of this chapter is as follows: First, two questions are discussed in sec. 2: How to classify any material as a spin glass? What are the ingredients a system needs to be a potential spin glass? Sec. 3 is concerned with some basic requirements for any type of magnetic order such as interactions and anisotropies, and an introduction of some typical systems out of the large variety of rare-earth spin-glasses. We then summarize in sec. 4 the present understanding of the mean-field model of spin glasses, and present very briefly numerical results on short-range models, because no analytical results are available for realistic models. Sec. 5 is devoted to the unusual properties of spin glasses at low temperatures, including irreversibilities, anisotropy and excitations. The upsurge of interest in spin glasses in recent years is related to the "spin-freezing" process near the spin-glass temperature T_f, which is discussed in sec. 6 and 7. Experimental work on the dynamics of spin-glass freezing is reviewed in sec. 6, while attempts devoted to analyzing the data in terms of a phase transition at T_f are discussed in sec. 7. We then give in sec. 8 recent results of studies concerned with the magnetic behavior in the crossover regime from spin-glass to long-range ferro- or antiferromagnetic order. A brief discussion on systems with random anisotropy axis is included in sec. 9. Finally, sec. 10 contains some concluding remarks.

2. Characteristics of a spin glass

Before beginning a survey of experimental results on rare earth spin glasses and their interpretation by model calculations, we would first suggest a brief discussion on two questions: How to classify any material as a spin glass? What are the ingredients a system needs to be a potential spin glass?

2.1 Classification of a spin glass:

There is no unique experiment which is able to definitely identify a sample as a spin glass. Some of the characteristic properties of spin glasses which will be discussed below also occur for other sorts of magnets, so in practice it is necessary to observe several characteristics before classifying any material as a spin glass. As an example, we present experimental data in Fig. 2 on the spin glass sample, $Eu_{0.40}Sr_{0.60}S$, which may be taken as a possible collection of defining properties:

(a) In the ac-susceptibility: A peak in $\chi'(T)$ at low magnetic fields. It defines the spin-glass temperature T_f, not necessarily the phase transition temperature T_c (if it exists at all) because T_f is often dependent on the measuring frequency.

(b) In the neutron diffraction spectrum: No magnetic Bragg peaks. That means, the spin "freezing" (associated with feature (a)) is accompanied with no periodic long-range order at $T \leq T_f$.

(c) In the magnetic specific heat: no anomaly in $C(T)$ at T_f. A broad peak exists at higher temperature (at about $1.3\ T_f$).

(d,e) In the magnetization: Below T_f severe history dependency (the magnetization measured after zero-field cooling, ZFC, is different from that in field cooling, FC), remanence (TRM measured after FC, IRM measured after ZFC) and slow (non-exponential) relaxation exist after magnetic perturbation (TRM denotes the thermoremanent magnetization, and IRM the isothermal remanent magnetization).

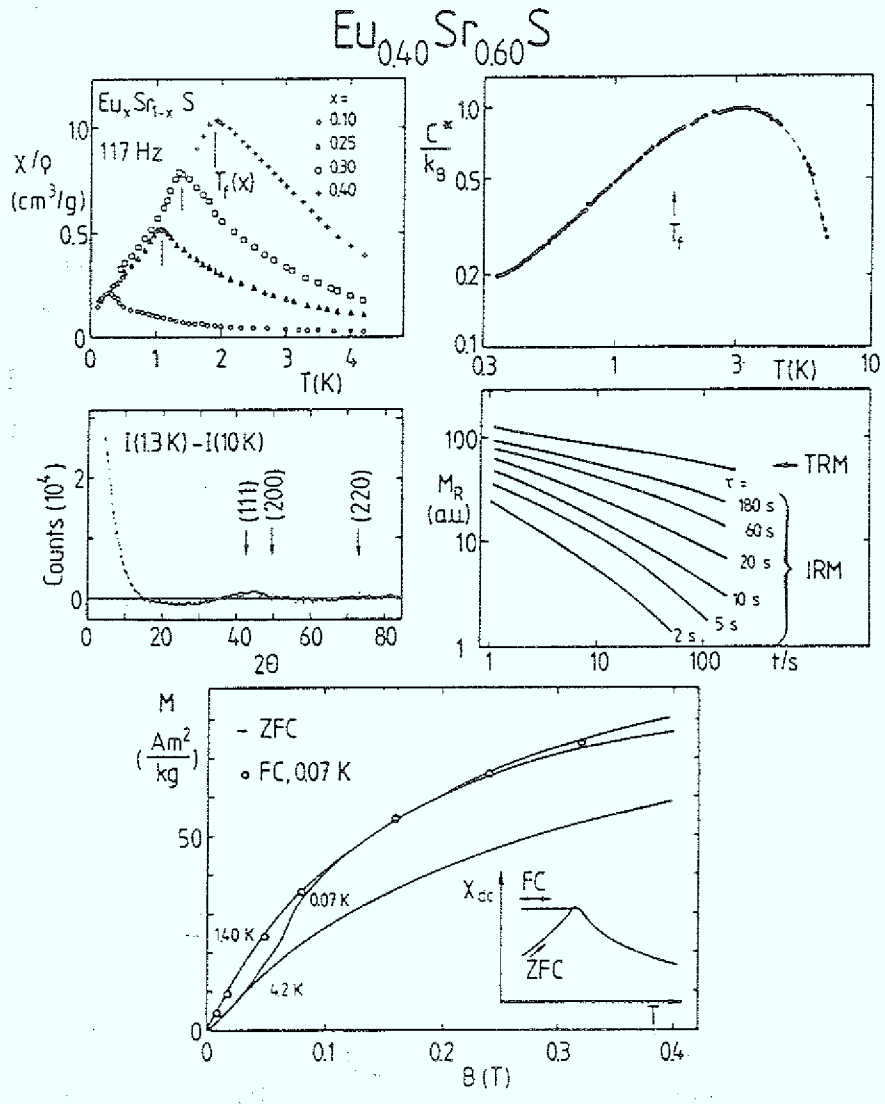

Fig. 2: Collection of defining properties of a spin-glass. Data of $Eu_{0.40}Sr_{0.60}S$ are taken from measurements of (a) ac-susceptibility $\chi(T)$ (Maletta and Felsch, 1979b), (b) neutron diffraction I(T = 1.3 K) - I(T = 10 K) (Maletta and Felsch, 1979b), (c) magnetic specific heat C(T) (Meschede et al., 1980), (d) slowly decaying remanent magnetizations, TRM and IRM, for different values of the acquisition time τ, as indicated, at T = 1.32 K and H = 40 Oe (Ferré et al., 1981), and (e) magnetizations M after field-cooling (FC) or zero-field-cooling (ZFC) (Maletta and Felsch, 1979b). The insert shows the corresponding dc-susceptibilities, $\lim_{H \to 0} dM/dH$.

2.2 Ingredients for a spin glass:

In order to answer the second question above, we compare the magnetic phase diagrams of two systems, $Eu_xSr_{1-x}O$ and $Eu_xSr_{1-x}S$ (see also Westerholt et al., 1977), displayed in Fig. 3. Both insulating systems are based upon a ferromagnet, EuO (T_c = 69 K) and EuS (T_c = 16.6 K), and are magnetically diluted with Sr. These two Eu-monochalcogenides are rather similar chemically, and crystallize in the NaCl structure. The magnetic moments at the divalent Eu ions are coupled via short-range exchange interactions to the first (J_1) and second (J_2) nearest Eu neighbors. Thus, in both dilution systems the percolation threshold (depending on the crystal structure and range of interaction only) is the same and equal to x_p = 0.13. It means that for Eu concentrations $x < x_p$ the system consists exclusively of independent finite magnetic clusters (superparamagnet), whereas from geometrical arguments within percolation theory long-range magnetic order may be possible for all $x > x_p$ (i.e. as long as there exist infinite continuous exchange paths joining magnetic Eu ions). Fig. 3 demonstrates, however, that the systems do not exhibit the same type of magnetic phase diagram.

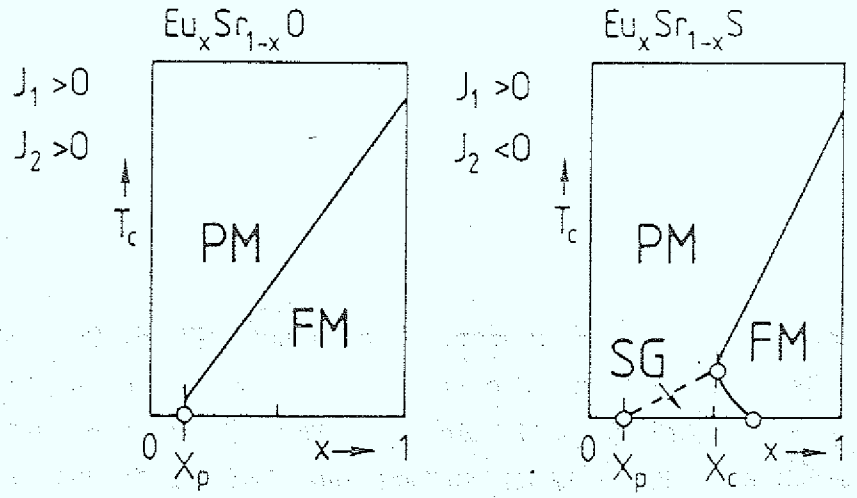

Fig. 3: Schematic magnetic phase diagrams for $Eu_xSr_{1-x}O$ and $Eu_xSr_{1-x}S$. PM = paramagnet; FM = ferromagnet; SG = spin glass. x_p = percolation threshold. The exchange interactions to the first (J_1) and second nearest neighbors (J_2) are of equal or of opposite sign in $Eu_xSr_{1-x}O$ or $Eu_xSr_{1-x}S$, respectively.

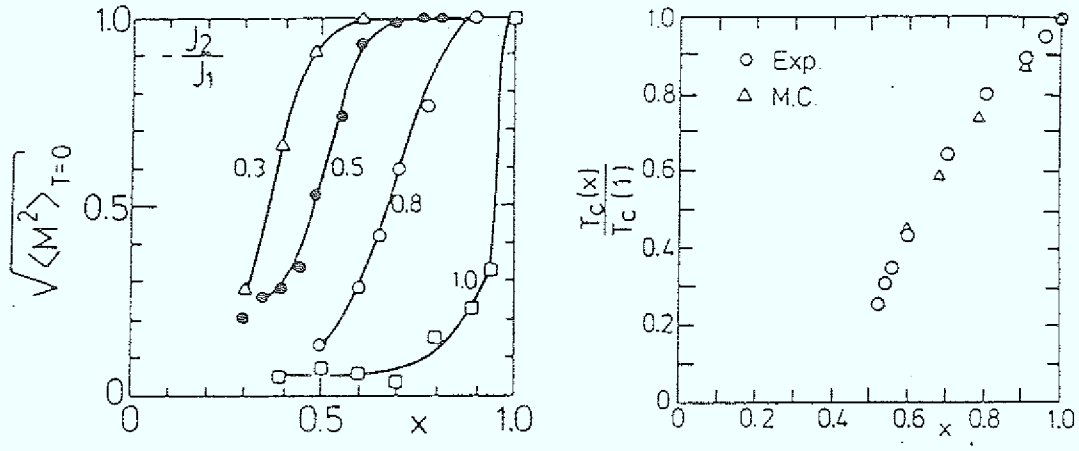

Fig. 4: (a) Simulated Curie temperatures T_c (triangles) of a fcc Heisenberg ferromagnet with $J_2/J_1 = -1/2$ plotted vs. concentration x of magnetic ions (Binder et al., 1980). Circles denote experimental data for $Eu_xSr_{1-x}S$ (Maletta and Convert, 1979a).

(b) Ground-state magnetization of a classical fcc Heisenberg ferromagnet as a function of concentration x for various ratios J_2/J_1 of exchange interactions, as obtained from Monte Carlo simulations (From Binder et al., 1979).

By dilution of a ferromagnet one expects the Curie temperature $T_c(x)$ first to decrease linearly with (1-x) due to the linear decrease in the effective exchange field, and, as x is further decreased, ferromagnetism to persist down to the critical concentration x_p where T_c has to go to zero. This happens in the dilution series $Eu_xSr_{1-x}O$. The origin of the fundamental difference in magnetic ordering observed in $Eu_xSr_{1-x}S$ has been proposed (Maletta and Convert, 1979) to lie in the presence of <u>competing</u> exchange interactions. Both exchange couplings, J_1 and J_2, are positive in EuO, whereas in EuS they are of opposite sign, with ratio $J_2/J_1 = -0.5$ (Zinn, 1976; Wachter, 1979). The important role played by the competing exchange is confirmed in Monte Carlo simulations by Binder et al.(1979, 1980). In a realistic

model for $Eu_xSr_{1-x}S$, considering an fcc lattice with $J_2/J_1 = -0.5$, they even find quantitative agreement with experimental results without adjustable parameters by calculating the concentration dependences of the Curie temperature $T_c(x)$ and the magnetization (Fig. 4). Obviously, the ferromagnetic state in EuS is unstable against dilution with SrS already at $x_c \simeq 0.50$, far above the percolation threshold $x_p = 0.13$.

To understand this behavior, we consider in Fig. 5 as a simple model the ground state of a diluted square lattice with $J_1 > 0$ and $J_2 < 0$.

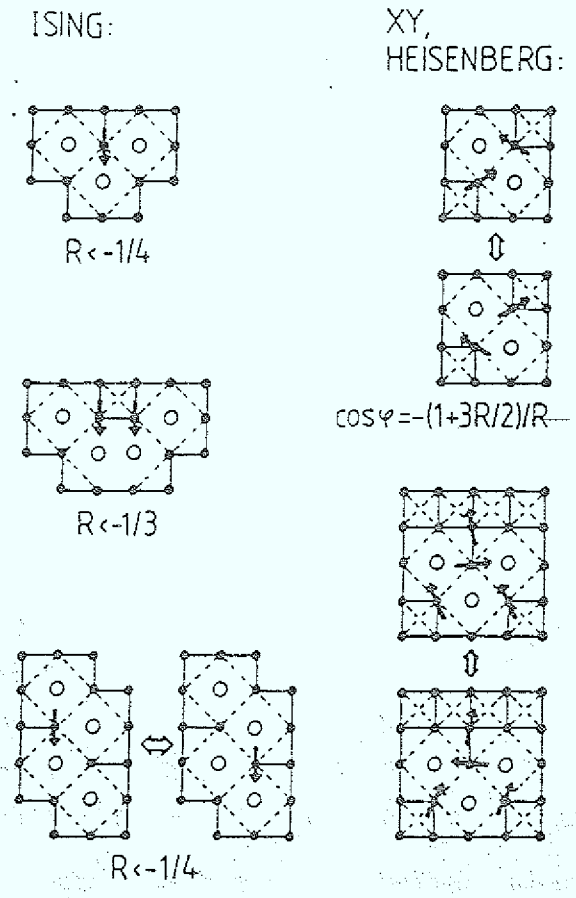

Fig. 5: Spin configurations near nonmagnetic atoms (circles) of a diluted ferromagnet with competing nearest (J_1) and next-nearest (J_2) neighbor interactions, $R = J_2/J_1 < 0$. Only the spins which are not aligned in the direction of the spontaneous magnetization (pointing upwards) are indicated by arrows. The most simple cases of both the Ising and XY or Heisenberg model are shown (From Maletta, 1981b).

Due to the competition between positive J_1 (full lines) and negative J_2 (broken lines) there occur spins or spin clusters near the non-magnetic atoms (open circles) which are aligned antiparallel to the ferromagnetic environment (in the Ising model), or which are turned away from the spontaneous magnetization direction by an angle φ (in the XY and Heisenberg model) which is dependent on the ratio of the exchange interactions $R = J_2/J_1$. Even more interesting is the behavior shown between the double arrows in Fig. 5. For instance in the lower left part it is favorable to have either one of two spins (in the middle) antiparallel to the ferromagnetic network but it is undecided which of them, and hence the states with these two spin configurations are degenerate. As a result, bulk magnetization is reduced, this two spin cluster is only weakly coupled to the ferromagnetic environment, in both states some interactions are unfavorable ("frustrated" bonds). Systems with frustration (Toulouse, 1977) cannot minimize simultaneously the energy because of competition between different requirements. This high ground state degeneracy due to frustration is a basic feature of spin glasses.

Similar frustration effects occur in XY- and Heisenberg-spin systems (Kinzel and Binder, 1981; Dunlop and Sherrington, 1985) as illustrated in Fig. 5. Thus, as dilution proceeds, we expect that more and more spins are effectively decoupled from the ferromagnetic alignment within the long-range ferromagnetic order, until ferromagnetism breaks down completely already above x_p, as observed experimentally in $Eu_xSr_{1-x}S$ (Maletta and Convert, 1979). A new type of order, the spin glass, occurs instead characterized by these two ingredients: disorder and frustration. Disorder in the Eu ions alone as induced in the dilution series by substitution with Sr will not destroy ferromagnetic order for $x > x_p$ ($Eu_xSr_{1-x}O$), unless competition in the exchange couplings comes into play ($Eu_xSr_{1-x}S$). On the other hand, frustration alone is also not sufficient to create a spin glass; for example a system on a triangular lattice with antiferromagnetic bonds to nearest neighbors, or the Mattis model (Mattis, 1976), both are frustrated systems but without disorder, i.e. no spin glasses.

3. Rare-earth spin-glasses

The basic requirements for any type of magnetic order in a solid are the existence of magnetic moments associated with unpaired electrons on the atoms, and interactions to couple them together.

3.1 Interactions:

In systems with lanthanides the 4f shell builts up a well-localized moment $g\mu_B S_i$ which may be coupled to neighboring moments by the isotropic Heisenberg exchange

$$\mathcal{H}_{ij} = -2J_{ij}\vec{S}_i \cdot \vec{S}_j \qquad (1)$$

where J_{ij} is the exchange parameter between spins at site i and site j. It is positive for ferromagnetic coupling and negative for antiferromagnetic coupling. The insulating Eu-monochalcogenides EuO and EuS are believed to be some of the most ideal realizations of the isotropic Heisenberg model of ferromagnetism (Zinn, 1976; Wachter, 1979).

In metallic systems with 4f atoms the most prominent source of long-range interaction between magnetic moments is the mechanism first described by Ruderman and Kittel (1954), Kasuya (1956) and Yosida (1957), which involves the conduction-electron sea as mediator of the interaction. Distinctive features of the RKKY-interactions are its long range and oscillatory nature:

$$J(R) = V_o \frac{\cos(2k_F R + \phi)}{(k_F R)^3} \quad , \quad k_F R \gg 1 \qquad (2)$$

The effective exchange parameter J between spins of distance R falls off as R^{-3} and oscillates in sign and magnitude with R, so the coupling can give ferro- as well as antiferromagnetic alignments. Here, k_F is the Fermi wave number, ϕ a phase factor, and V_o is proportional to J_{fs}^2 where J_{fs} is the exchange interaction between the localized f-electrons at the lanthanide and the conduction electrons of the host metal. The oscillations arise when the Fermi surface is sharply defined. For further discussions on the RKKY interactions in disordered

systems we refer to the literature (de Gennes, 1962; Kaneyoshi, 1975; de Châtel, 1981; Levy and Zhang, 1986).

3.2 Anisotropies:

The interactions discussed so far are isotropic in nature. Anisotropy, however, may influence the magnetic ordering substantially. Here, we are going to distinguish between three main sources of anisotropy:

(i) Magnetic dipolar interaction

$$\mathcal{H}_{ij}^{dip} = \frac{\vec{\mu}_i \cdot \vec{\mu}_j}{r_{ij}^3} - \frac{3(\vec{\mu}_i \cdot \vec{r}_{ij}) \cdot (\vec{\mu}_j \cdot \vec{r}_{ij})}{r_{ij}^5} \qquad (3)$$

tends to align the two moments $\vec{\mu}_i$ and $\vec{\mu}_j$ parallel, along the line joining their sites, $\vec{r}_{ij}$.

This anisotropy is of order 1 K only and probably not important for typical metallic spin glasses. It may be relevant for insulating spin glasses $Eu_xSr_{1-x}S$ (Binder and Kinzel, 1983).

(ii) Dzyaloshinskii-Moriya (DM) interaction (Dzyaloshinskii, 1958; Moriya, 1960):

$$\mathcal{H}_{ij}^{DM} = -\vec{D}_{ij} \cdot (\vec{S}_i \times \vec{S}_j) \qquad (4)$$

with vector $\vec{D}_{ij} = -\vec{D}_{ji}$. Here, a conduction electron of the host metal is first scattered by the spin $\vec{S}_i$, then via spin-orbit interaction by another (non-magnetic) impurity T (where D is proportional to the spin-orbit coupling constant), and finally by a second spin $\vec{S}_j$. The same mechanism, but without the process at T, leads to the RKKY interaction, thus the DM interaction is of third order in perturbation theory.

Fert and Levy (1980, 1981) propose this DM interaction to be responsible for observed anisotropy effects in metallic spin glasses. The anisotropy field D is randomly distributed (like the T atoms), i.e. there is no global anisotropy axis, but with eq. 4 one gets a macroscopic anisotropy energy of unidirectional character

$$E_{DM} = -K \cdot \cos \theta \qquad \text{with } K \sim D^2 \qquad (5)$$

E_{DM} is only dependent on the angle θ of spin rotation from any axis, there is no preferred direction. In this sense the DM interaction in spin glasses leads to an "isotropic anisotropy".

(iii) Single-ion anisotropy

$$\mathcal{H}_i^{si} = -D(S_i^z)^2 \qquad (6)$$

in uniaxial crystals where z being the easy-axis direction. This anisotropy is also related to the spin-orbit coupling which is rather strong in 4f atoms. It occurs in systems containing non-S state ions, mostly from interaction between the non-spherical electronic charge distribution and the local crystalline field created by the surroundings. Due to the uniaxial character of this type of anisotropy one expects to observe a preferred direction (z) in magnetic properties of such crystals.

3.3 Spin-glass systems:

Let us consider ingredients of typical systems out of the large variety of substances containing rare earths, for which some spin-glass properties have been reported (see also Durand and Poon, 1979).

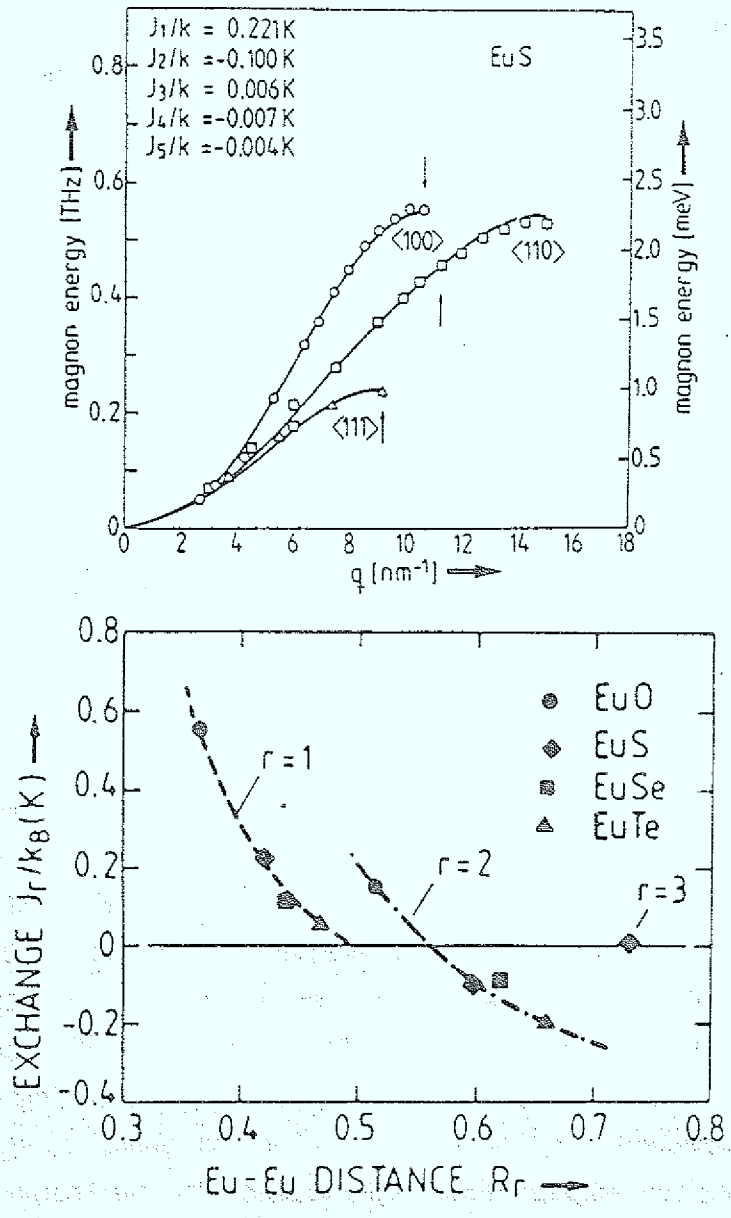

Fig. 6: (a) Spin-wave dispersion in EuS, measured by inelastic neutron scattering at T = 1.3 K(T_c = 16.6 K). The solid lines represent the best fit using up to fifth neighbors exchange interactions. The arrows indicate the boundary of the first Brillouin zone in the various symmetry directions (From Bohn et al., 1980).

(b) Dependence of the exchange interactions, J_1 and J_2, on the Eu-Eu distance R_r in the Eu-chalcogenides.

Insulating crystals: The system $Eu_xSr_{1-x}S$ has been studied in great detail in recent years (Maletta, 1982a) and is nowadays regarded as the standard system for spin-glass properties in insulating compounds. Its model character is due to the stable, well-localized, spin-only magnetic moment of $\mu_i = 2\,\mu_B S_i = 7\,\mu_B$ carried by the $4f^7 - {}^8S_{7/2}$ groundstate of the Eu^{2+} ion at a site i of the NaCl lattice of EuX, which is coupled to each of the z_r Eu spins S_r in the r-th neighbor shell by the isotropic Heisenberg interaction yielding the sum

$$\mathcal{H} = -\sum_{r=1}^{R} 2\, z_r\, J_r\, \vec{S}_i \cdot \vec{S}_r \quad . \qquad (7)$$

Recent detailed study of the spin-wave dispersion by Bohn et al. (1980) in a single crystal of EuS (enriched with ^{153}Eu) by inelastic neutron scattering technique (Fig. 6a) confirms previous assumption that the range of the exchange interactions is essentially limited to the second nearest neighbors: $J_1/k_B = 0.220$ K and $J_2/k_B = -0.100$ K, while the exchange interactions to more distant neighbors decrease to a few percent of J_2 only. The dependence of J_1 and J_2 on the Eu-Eu pair distance $R_r = a/\sqrt{2}$ (a = lattice parameter) for each of the four members of the EuX series is summarized in Fig. 6b. EuO with the shortest R_r values obviously is a special case where both J_1 and J_2 are positive, otherwise J_1 and J_2 are opposite in sign. Obviously, going from EuO to EuTe, i.e. in the direction of increasing lattice constants and covalent character of the chemical bond, J_r shifts to more negative (or smaller positive) values. In the theory of Kasuya (1973) the following exchange mechanisms for J_1 and J_2 are proposed:

- An Eu-Eu superexchange with virtual transfer of a 4f electron to the 5d-t_{2g} excited state of a Eu nearest neighbor (J_1; $z_1 = 12$).
- An indirect superexchange between Eu next-nearest neighbors involving the antibonding 5d-e_g orbitals of the Eu and the p orbitals of the anion(J_2; $z_2 = 6$).

For further discussions on EuX see Wachter (1979).

A careful analysis of the high-temperature susceptibility of $Eu_xSr_{1-x}S$ versus Eu concentration by Köbler and Binder (1980) has been used to search for possible deviations in the atomic arrangement from the ideal random mixing (see also Binder, 1982). No indication for chemical short-range order in $Eu_xSr_{1-x}S$ is found. The experimental data can be quantitatively understood over the whole Eu-concentration range by taking only into account the weak dependence of the exchange parameters on concentration and temperature via lattice expansion (EuS: a_o = 0.597 nm, SrS: a_o = 0.602 nm).

The presence of well-known competing exchange interactions of short range, J_1 and J_2, in $Eu_xSr_{1-x}S$ over the whole x-range has made this system a famous spin-glass material where the conditions for spin-glass behavior discussed above are realized very clearly. For this reason a lot of different experiments has been performed on this material, and experimental results on this rare-earth system will be somewhat emphasized in this review.

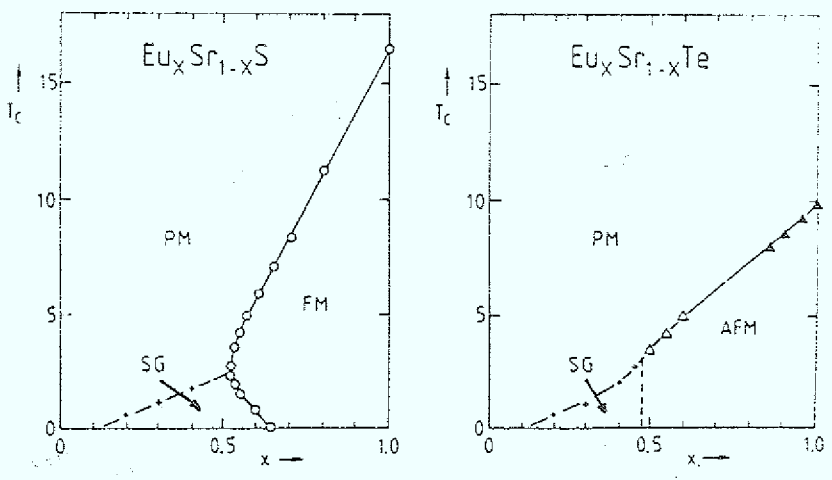

Fig. 7: Magnetic phase diagrams for the diluted ferromagnet $Eu_xSr_{1-x}S$ (Maletta and Felsch, 1979b) and the diluted antiferromagnet $Eu_xSr_{1-x}Te$ (Börgermann et al., 1986b). PM = paramagnet; FM = ferromagnet; AFM = antiferromagnet; SG = spin glass. Note that the boundary between SG and AFM in $Eu_xSr_{1-x}Te$ is not yet studied by neutron scattering technique.

In EuS the dominant interaction (J_1) leads to ferromagnetism, in EuTe the dominant interaction (J_2) to antiferromagnetism, both possessing competing exchange, J_1 and J_2. Thus, as expected from discussions above, spin-glass behavior is observed in both dilution systems, in the diluted ferromagnets $Eu_xSr_{1-x}S$ (Maletta and Felsch, 1979 b) and in the diluted antiferromagnets $Eu_xSr_{1-x}Te$ (Börgermann, Maletta and Zinn, 1986a, b). Their magnetic phase diagrams are displayed in Fig. 7).

Westerholt et al. (1981a,b) started by mixing the ferromagnet EuS with the metastable antiferromagnet EuSe together, EuS_ySe_{1-y}. From ac susceptibility and specific heat measurements they claim to obtain a narrow concentration regime around y = 0.10 with spin-glass or "mictomagnetic " properties (Fig. 8a). Theoretical work often predicts in such a phase diagram an intermediate region with mixed ferro- and antiferromagnetic order, instead (Fishman and Aharony, 1980). As long as neutron diffraction studies have not yet been performed, a finite decision on the type of magnetic order is still open in that case. The same authors proceed by diluting this system with

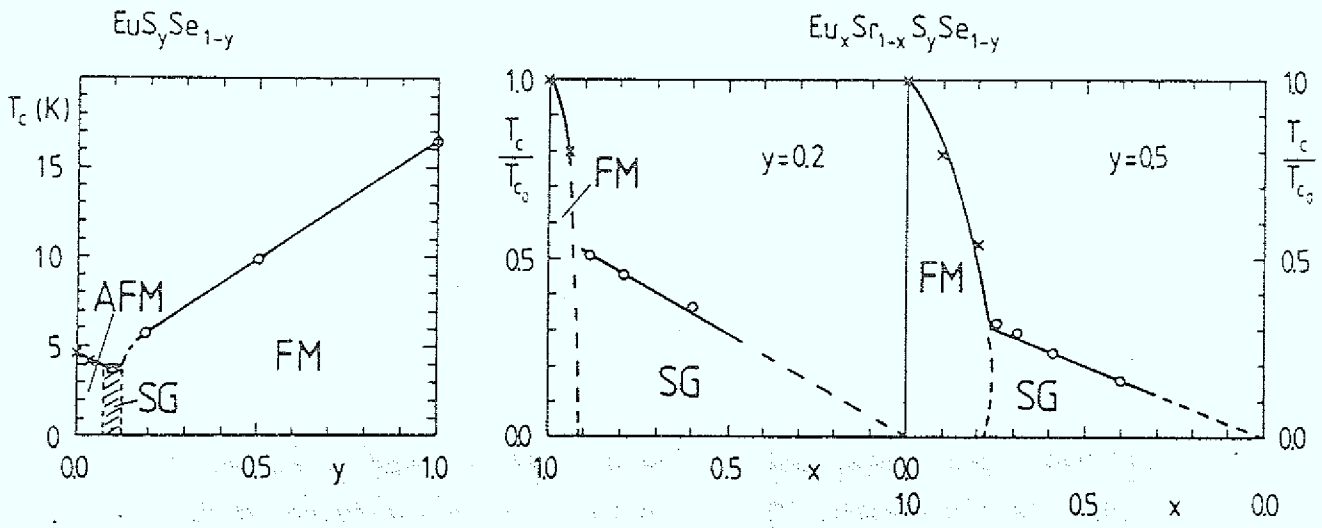

Fig. 8: Magnetic phase diagrams for EuS_ySe_{1-y} for $0 \leq y \leq 1$, and $Eu_xSr_{1-x}S_ySe_{1-y}$ with y = 0.2 and y = 0.5 for $0 \leq x \leq 1$. FM = ferromagnet; AFM = antiferromagnet; SG = spin glass (From Westerholt and Bach, 1981b).

Sr which stabilizes the spin-glass ordering, and broad spin-glass regimes versus Eu concentration are observed (Fig. 8b) in $Eu_xSr_{1-x}S_ySe_{1-y}$. It can be understood by systematically changing the ratio J_2/J_1 with concentration y, for instance they estimate $J_2/J_1 \approx -0.75$ for the system with y = 0.2, and $J_2/J_1 \approx -0.6$ for y = 0.5. This feature is in qualitative agreement with model calculations in 2 dimension by Binder et al. (1979) where just this behavior has been predicted.

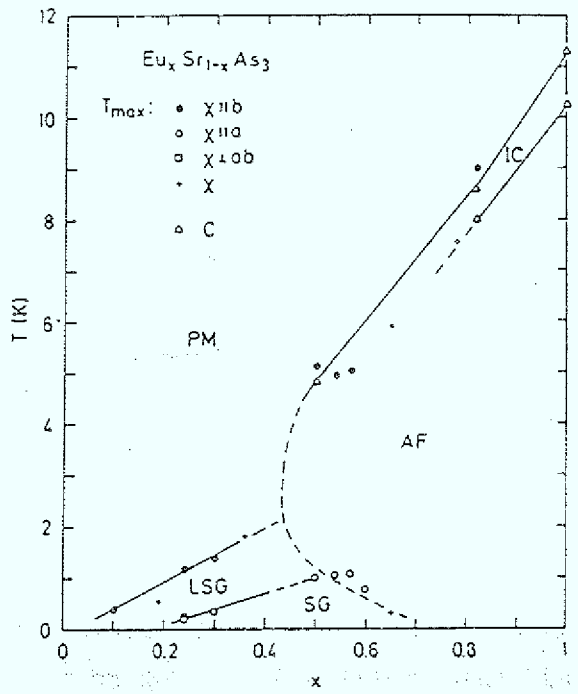

Fig. 9: Magnetic phase diagram for $Eu_xSr_{1-x}As_3$. PM = paramagnet; AF = antiferromagnet; IC = incommensurate antiferromagnet; LSG = longitudinal spin glass (freezing only for $\chi \| b$); SG = spin glass (additional freezing of transverse components). Triangles denote specific-heat results, other symbols denote the temperature of the maximum in the ac susceptibility χ. The crosses denote χ -measurements in unspecified directions. Note that the "re-entrant" phase boundary (dashed line) is only tentative, neutron-scattering studies are in preparation (From Schröder et al., 1986).

Semimetallic crystals: The next system being introduced in this section is the dilution system $Eu_xSr_{1-x}As_3$ based upon the semimetal $EuAs_3$. $EuAs_3$ and $SrAs_3$ are again isostructural, namely monoclinic, with nearly equal lattice parameters (Bauhofer et al., 1981). The antiferromagnet $EuAs_3$ undergoes two successive magnetic transitions (Bauhofer et al., 1985 and 1986; Chattopadhyay et al., 1986) at 11.2 K and 10.3 K. First, a transition to an incommensurate magnetic structure occurs which is followed by a lock-in transition to a commensurate antiferromagnetic phase at 10.3 K where the magnetic moments are oriented in the crystallographic b direction. Together with a careful neutron diffraction study, a detailed theoretical investigation of the incommensurate state has been performed (Thalmeier, 1986; Chattopadhyay et al., 1986), suggesting that there exist competing exchange interactions to the nearest and next-nearest Eu^{2+} neighbors.

Therefore, it is not astonishing that Lecomte et al. (1984, 1986a) observe a spin-glass regime in $Eu_xSr_{1-x}As_3$. Very recently, a study of the directional dependence of the ac susceptibility (Schröder et al., 1986) reveals anisotropic spin-glass behavior: By lowering the temperature longitudinal (i.e. for the ac driving field parallel to the b direction) and subsequently transverse freezing occurs at different temperatures. Fig. 9 shows the magnetic phase diagram of $Eu_xSr_{1-x}As_3$.

Metallic crystals: Metallic systems, like Fe impurities in Au, are often cited as "classical" spin glasses, referring to the pioneering experiment by Cannella and Mydosh (1972) where a "cusp" in the ac susceptibility, $\chi(T)$, in low magnetic fields is observed in these dilute alloys. In such systems, however, the interactions are rather complicated and not precisely known:

- Magnetism created by 3d electrons are not properly described by localized moments, at least for concentrations up to about 10 at% or even more, as often used in experiments. Modifications of the far too idealized RKKY interaction and additional direct overlap of the d electrons have to be included in realistic model calculations.
- The situation is even more complicated as sometimes an interplay with atomic short-range order occurs.

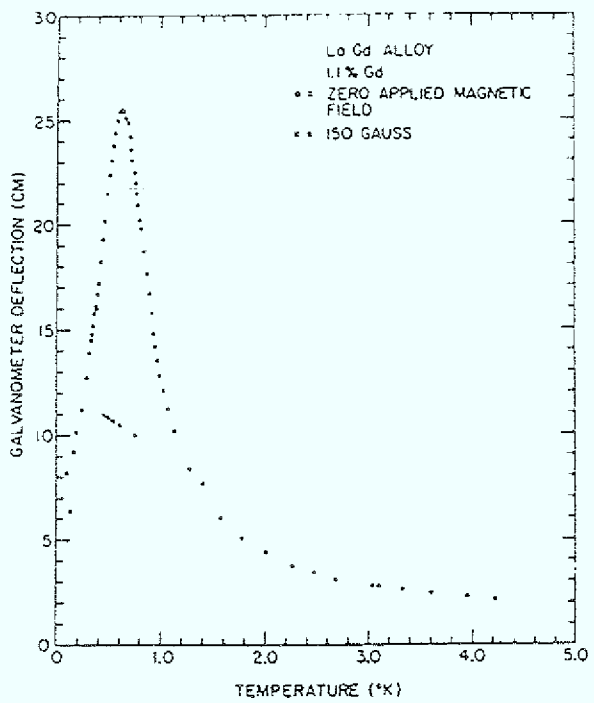

Fig. 10: Galvanometer deflection (proportional to the ac-susceptibility) in LaGd 1.1 at% as a function of temperature at H = 0 and H = 150 G (From Hein et al., 1959).

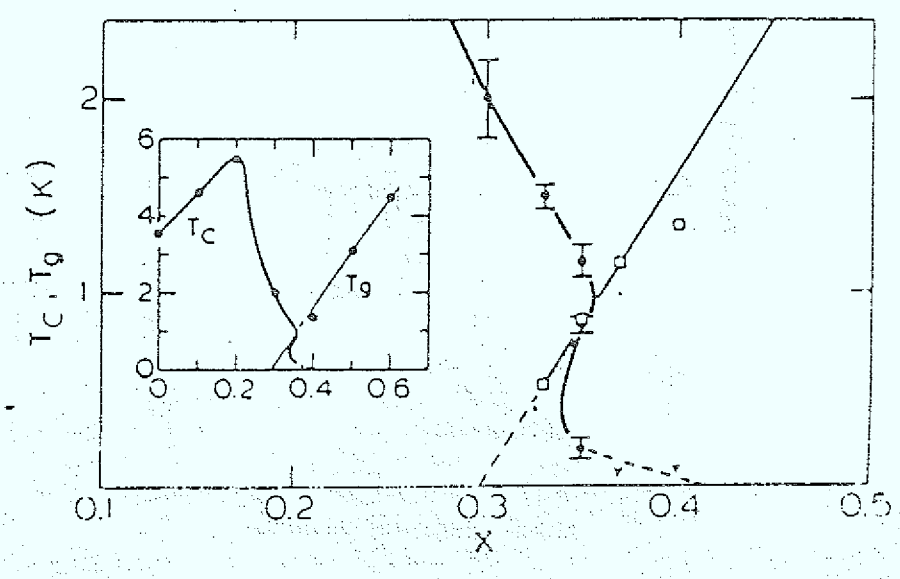

Fig. 11: Superconducting (T_c) and magnetic (T_g) phase diagram for $Th_{1-x}Nd_xRu_2$. The lines are a visual guide (From Hüser et al., 1983a).

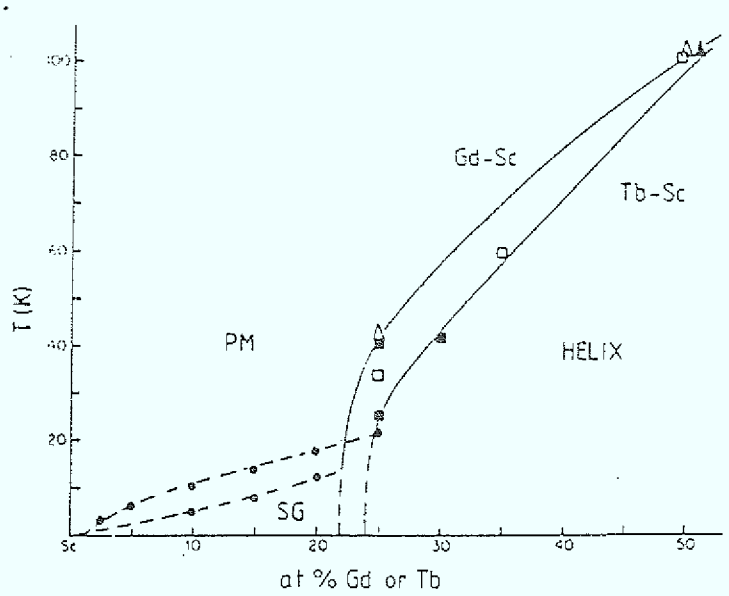

Fig. 12: Magnetic phase diagrams for Gd-Sc and Tb-Sc alloys. PM = paramagnet; HELIX = helical spin structure; SG = spin glass (From Sarkissian and Coles, 1976).

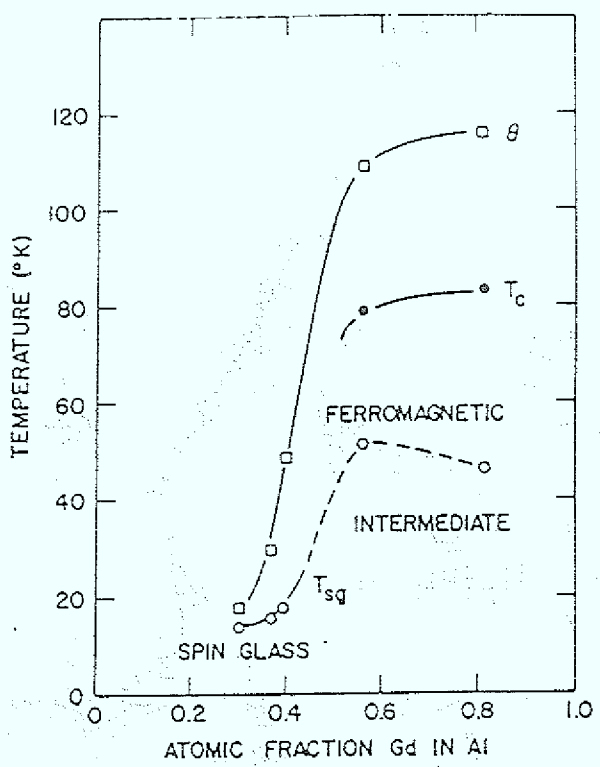

Fig. 13: Magnetic phase diagram for amorphous Gd-Al alloys showing temperatures for susceptibility peaks (T_{sg}), ferromagnetic Curie points (T_c), and paramagnetic θ values (From McGuire et al., 1978).

A careful analysis of the paramagnetic susceptibility by Morgownik and Mydosh (1983a,b) confirms both complications being present in 3d systems, e.g. in Cu, Au and Pt host-metals with even low ($\lesssim 8$ at %) Mn and Fe impurity concentrations. Nevertheless, there exist competing interactions which are responsible for the appearance of the spin-glass state in such systems.

Here we will concentrate an rare-earth systems which built up well-localized moments. In the class of dilute rare-earth metals and intermetallic compounds for which spin-glass behavior has been reported, one topic involves 4f-impurities in superconducting hosts. Already a small amount of paramagnetic impurities, as example 1 at% Gd in La, destroys superconductivity. Above this critical concentration Hein et al. (1959) have observed the first striking low-field susceptibility maxima (Fig. 10) already in 1959 which today we take as characteristic of spin-glass freezing (see also Finnemore et al., 1968, for an additional neutron diffraction study). In case of a very weak depression of the superconducting transition temperature T_c with magnetic impurity concentration x, as in $Nd_xTh_{1-x}Ru_2$, Hüser et al. (1983a) have given experimental evidence for even a coexistence of the spin-glass and superconducting state. Its phase diagram is shown in Fig. 11. For recent reviews on the competition between superconductivity and magnetic order, with more complete references on experimental systems studied, we refer to the literature (Maple, 1976; Roth, 1978).

Another subject class is concerned with diluted 4f metals. Sarkissian and Coles (1976) have tried to distinguish between spin-glass freezing and helical ordering in solid solutions of Gd, Tb and Dy in Y and Sc by means of resistivity and susceptibility measurements (Fig. 12). These materials have attracted recent interest again, because some are candidates for anisotropic spin glasses (Baberschke et al., 1984). It also turned out that spin-glass behavior in yttrium based alloys occurs at much lower concentrations than previously claimed.

Furthermore, diluted intermetallic compounds with 4f atoms also reveal spin-glass properties, for example (Gd, La)Al_2 (v. Löhneysen et al., 1978b), (Gd,Y)Al_2 (Besnus et al., 1980), (Gd, La)B_6 (Felsch, 1978), and (Er, Y)Al_2 (Bruss et al., 1979).

Amorphous alloys: This class of structural disorder contains for instance a-Gd_xAl_{1-x} where detailed studies provide evidence for spin-glass behavior in the concentration range $0.30 \lesssim x \lesssim 0.40$ (see phase diagram in Fig. 13; McGuire et al., 1978).

On the other hand, amorphous systems like a-DyCu whose magnetic orders are highly influenced by the random distribution of local anisotropy axes (due to single-ion anisotropy of non-S-state rare-earth atoms) will be called "speromagnets" (Moorjani and Coey, 1984) and not discussed here, but in section 9. Remember that we decided to adopt the term "spin glass" to denote disordered magnets whose magnetic properties are due to a broad distribution of positive and negative interactions.

4. Model calculations

To discuss this new type of ordered phase in spin glasses, one would like to have a microscopic model where the actual interactions and anisotropies are considered and the average over a realistic description of the site dilution disorder is performed. Clearly this is a difficult task and up to now no realistic model of a spin glass has been solved analytically. In addition, there exists another difficulty because a proper treatment of systems with quenched disorder like spin glasses involves averaging the free energy f rather than the partition function Z

$$f = \left[f\{x\} \right]_{av} = - \frac{k_B T}{N} \left[\ln Z \{x\} \right]_{av} \qquad (8)$$

where f depends on a large set of variables $\{x\}$ describing the randomness.

4.1 Edwards-Anderson model:

In 1975 Edwards and Anderson (EA) published a paper (Edwards and Anderson, 1975) which revolutionized the statistical mechanics of disordered spin systems. Stimulated by Cannella and Mydosh's observation of a cusp in the temperature dependence of the ac magnetic susceptibility of dilute alloys such as AuFe and CuMn (Cannella and Mydosh, 1972), EA propose a model to study this problem and a method of solving it. They consider the Hamiltonian

$$\mathcal{H} = - \sum_{ij} J_{ij} \vec{S}_i \vec{S}_j - g\mu_B \vec{H} \sum_i \vec{S}_i \qquad (9)$$

where classical spins $\vec{S}_i$ are put onto the sites of a regular lattice, and disorder is introduced by a suitable distribution $P(J_{ij})$ of exchange interactions. $\vec{H}$ is an external magnetic field. For instance a Gaussian distribution of the J_{ij} can be taken

$$P(J_{ij}) \propto \exp - \frac{(J_{ij} - J_o)^2}{2 \Delta J^2} \qquad (10)$$

For $|J_0| < \Delta J$ there are ferromagnetic ($J_{ij} > 0$) as well as antiferromagnetic ($J_{ij} < 0$) couplings.

EA present the following picture of a spin glass below the "freezing temperature": If one observes a given spin pointing in a certain direction, then there is a finite probability for a long period of time to find the spin pointing in the same direction. They propose a new type of order parameter which describes long-time correlations (instead of long-range spatial spin correlations)

$$q_{EA} = \lim_{t\to\infty} \left[\langle S_i(t) S_i(0) \rangle_T \right]_{av} \qquad (11)$$

where $\langle \ldots \rangle_T$ denotes a statistical mechanics average for a given set of interactions and $[\ldots]_{av}$ is an average over the distribution of interactions (=configurational average). It should be emphasized that what differentiates the spin-glass phase from the paramagnetic state is precisely the non-vanishing value of the local autocorrelation function in time. Thus a "memory" effect prevails in the spin-glass state.

In order to avoid averaging lnZ, EA use the so called replica trick, where one averages quantities such as Z^n when n is an integer. The relevance of averaging Z^n instead of lnZ lies in the relationship

$$\ln Z = \lim_{n\to 0} \frac{1}{n} (Z^n - 1) \qquad . \qquad (12)$$

Another way of getting around this difficulty is studying time-dependent phenomena in spin glasses (de Dominicis, 1978).

The EA model contains the two essential ingredients for a spin glass - disorder and competition as discussed above - but it is a crude approximation to real spin glasses. Therefore at the beginning we have to discuss how well this model reproduces spin-glass properties. Up to now there is no analytic solution available for the short-range EA model. Even modern methods like real space renormalization yield inconclusive results (Kinzel and Fischer, 1978; Tatsumi, 1978). Hence numerical methods like the Monte Carlo simulation have been applied to answer this question the results

of which will be briefly summarized now. Then the mean-field analysis of the EA model will be discussed, and finally the question about the existence of a phase transition in real spin glasses is taken up in the last part of this section. We restrict ourselves, however, to describing always some typical results only; further details of the model calculations are deferred to the following sections where they are presented in direct comparison with experimental data.

4.2 Monte Carlo simulations:

Extensive studies of the 2-dimensional EA-Ising model with Gaussian distributed nearest neighbor bonds by Monte Carlo simulations (Binder and Schröder, 1976; Kinzel, 1979; Kinzel and Binder, 1984) provide evidence that the EA model reproduces many experimental findings on real spin glasses remarkably well. For instance

- A peak in the time dependent susceptibility $\chi(T)$ at T_f (Fig. 14b).
- A broad maximum in the magnetic specific heat $C(T)$ above T_f (Fig. 14a).
- A plateau in the field-cooled magnetization $M(T)$ (Fig. 14c) and an S-shaped curve of $M_{ZFC}(H)$ (Fig. 14d).
- The existence of different remanences, TRM and IRM, and their dependence on temperature, field and time (Fig. 27).

Some of these results are shown in Fig. 14 and Fig. 27 which can be compared with Fig. 2.

4.3 Mean-field theory (Sherrington-Kirkpatrick model):

4.3.1 Ising spins: The infinite-range model of Sherrington and Kirkpatrick (SK) (1975) was originally introduced as a model for which the mean field analysis of EA would be exact. Here, each spin couples equally with every other spin in the system. One takes in eq. 10 the mean $[J_{ij}]_{av} = J_0/N$ and the variance $\Delta J = \tilde{J}/\sqrt{N}$ in order to get a non-trivial thermodynamic limit (N is the number of spins in the system).

But while the formulation of mean field theory e.g. for an infinite-range ferromagnet is rather trivial, the formulation for spin glasses has been a major challenge of theoretical physics. It has taken eight years to achieve an essentially complete understanding of the thermodynamics of this model. In fact, this model starts from an unphysical assumption, but equally as for conventional pure problems it has proven very instructive, and many experimental results are in remarkable qualitative agreement with the SK model's predictions.

It has been shown that the SK model has a true phase transition in thermal equilibrium at a finite temperature T_f, with a cusp both in the magnetic susceptibility $\chi(T)$ and the magnetic specific heat $C(T)$. The latter prediction is in serious disagreement with experimental specific heat data. In magnetic fields the cusp in $\chi(T)$ does get rounded, however the fields required for the rounding are approximately twenty times stronger than the ones observed experimentally.

In the original solution of this model by SK the low-temperature phase is characterized by a single order parameter, q_{SK}, defined by

$$q_{SK} = \left[\langle S_i \rangle_T^2 \right]_{av} \quad . \tag{13}$$

$q_{SK}(T)$ vanishes at T_f as $q_{SK} \propto 1-T/T_f$ and is unity at $T = 0$. The cusp in $\chi(T)$ at T_f is given by

$$\chi(T) = \frac{C}{T} (1-q_{SK}) \quad . \tag{14}$$

This solution was subsequently shown by de Almeida and Thouless (AT) (1978) to be unstable below a line in the H-T plane terminating at $T = T_f$ for $H = 0$, and varying for small fields as

$$\delta T_f(H)/\tilde{J} = (3/4)^{1/3} \cdot (H/\tilde{J})^{2/3} \tag{15}$$

with $\delta T_f = T_f(H = 0) - T_f(H)$.

It turned out that this instability is not an artifact of the method employed, but it represents an inherent difficulty of the spin-glass problem, and its study has pointed the way to the essential physics.

Below the AT line (at which the symmetry between replicas is broken) a single order parameter description is no longer correct, but a whole order parameter function $q(x)$ is necessary, monotonic in the range $0 \leq x \leq 1$, to describe the static properties (Parisi, 1979). The meaning of this function $q(x)$ was initially obscure. It has been obtained by the replica method together with a selfsimilar replica symmetry breaking (fractal structure; see e.g. de Dominicis, 1983), but $q(x)$ is also given by a dynamical formulation where the parameter x is related to a set of time scales (Sompolinsky and Zippelius, 1981). There have been various discussions of the relation between the two approaches (Houghton et al., 1983; de Dominicis and Young, 1983a). These considerations clarified the characteristics of the phase below the AT line in the SK model.

Sompolinsky (1981) shows that there are relaxation times which diverge exponentially in the thermodynamic limit ($N \to \infty$). This idea is connected with the fact that the mean-field equations of Thouless, Anderson and Palmer (TAP) (1977) which describe the magnetizations for a particular set of J_{ij}, have many solutions (Bray and Moore, 1980; de Dominicis et al., 1980): For a system of N spins the number of states metastable against single spin flip scales as $N_s(N) \propto \exp(\alpha(T) \cdot N)$ where $\alpha(T)$ is non-zero for T below the AT line. These minima in phase space ("valleys") are stable at finite temperatures if they are separated from each other by an energy barrier whose height diverges when $N \to \infty$. Sompolinsky's divergent times scales presumably correspond to the rare fluctuations over these barriers which can occur for finite N.

Thus spin-glass ordering is non-unique: there exists a large number of equivalent states with the same macroscopic properties but with different microscopic spin configurations - contrary to usual periodic order where only one state occurs (up to rotation or $S_i = \pm 1$ Ising symmetry). In Fig. 15 a schematic picture of the free energy is shown as function of one coordinate in phase space, with many "valleys" separated by high free energy barriers.

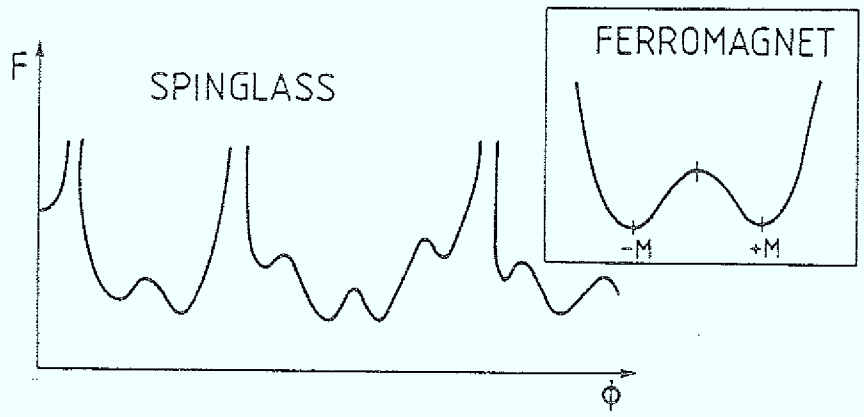

Fig. 15: Schematic plot of the free energy F of a spin glass as a function of a phase-space coordinate ϕ which measures the projection of the considered state on a particular ordered state. The insert shows the situation in an Ising ferromagnet for comparison.

Now the meaning of the order parameter function q(x) can be understood for instance in terms of dynamics: If one takes $N \to \infty$ before the time t tends to infinity, the system will stay in a single valley and one will measure q_{EA}. However, if we study the infinite time limit of a finite system then the system will move between different valleys in phase space and the time average will be equivalent to the average from equilibrium statistical mechanics, q:

$$q_{EA} = \lim_{t\to\infty} \lim_{N\to\infty} q(t) \qquad (16)$$

$$q = \lim_{\tilde{H}\to 0} \lim_{N\to\infty} \lim_{t\to\infty} q(t) \qquad (17)$$

Here in the time dependent autocorrelation function

$$q(t) = \left[\langle S_i(0)\, S_i(t) \rangle_{t'} \right]_{av} \qquad (18)$$

the time average $\langle \ldots \rangle_t$, is performed over the observation time. The canonical Gibbs average must be evaluated with a small field $\tilde{H}$ which breaks the spin reversal symmetry ($S_i \rightarrow -S_i$ for all i) and which is taken to zero after taking $N \rightarrow \infty$.

The parameter x labels a spectrum of relaxation times $\tau(x)$ where $\tau(x)$ decreases with x: The shortest time marked by $x = 1$ defines

$$q\ (x = 1) = q_{EA} \tag{19}$$

for which the system remains in a single valley, whereas the statistical mechanics order parameter q is associated with the longest time (marked by $x = 0$)

$$q\ (x = 0) = q \tag{20}$$

which leads to an average over all valleys.

From the monotonic increase of the lifetimes with N it follows that in the thermodynamic limit the SK model is <u>non-ergodic</u> (Palmer, 1982) below T_f (H): The time average of the order parameter q_{EA} does <u>not</u> agree with the ensemble average q. Monte Carlo simulations yield for the time average

$$1-q_{EA}(T) \propto T^2 \qquad \text{for } T \ll T_f \,. \tag{21}$$

$$\tilde{\chi}(T) = \frac{C}{T}\,(1-q_{EA}) \propto T$$

For the ensemble average one obtains

$$1-q(T) \propto T \tag{22}$$

$$\chi_{eq}(T) = \frac{C}{T}\cdot(1-q) = \text{const.}$$

These two limiting processes in $\chi(T)$ are sketched in Fig. 16.

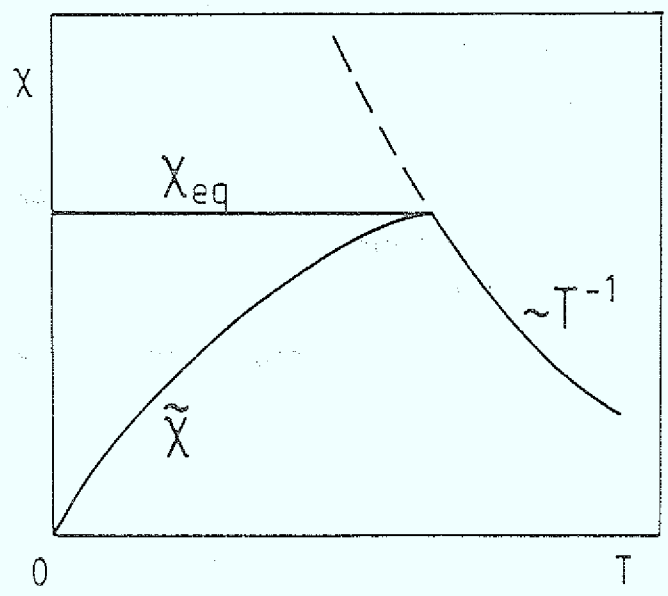

Fig. 16: Susceptibilities, eq. 21 and 22, vs. temperature as obtained for the SK model with infinite-range interactions.

The Parisi order parameter function $q(x)$ with $0 \leq x \leq 1$ is shown to be related to "overlap functions" between different valleys. Defining an overlap

$$q_{12} = \frac{1}{N} \sum_i \langle S_i^1 \rangle \langle S_i^2 \rangle \qquad (23)$$

between two states $\langle S_i^1 \rangle$ and $\langle S_i^2 \rangle$ (or two valleys), then the probability distribution $P(q)$ of phases having overlap equal to q is just the derivative of the inverse function $x(q)$:

$$P(q) = dx/dq \qquad (24)$$

(Parisi, 1983; Young, 1983b; de Dominicis and Young, 1983b).

Looking at overlaps between <u>three</u> valleys (Mézard et al., 1984) it turned out to ones surprise that there are restrictions on the values these overlaps can take: There is no probability associated with all three overlaps different. Such restrictions characterize an <u>ultrametric</u> space. Physically it arises from a hierarchical structure of "valleys within valleys within...".

Summarizing the theoretical picture of the SK model of a spin glass, there are many thermodynamic states below the phase transition at T_f which can be characterized by a whole order parameter function $q(x)$. In a single thermodynamic state ("valley") the order parameter is the largest value of the Parisi function, i.e. $q(x = 1) = q_{EA}$. The many valley structure of phase space leads to diverging relaxation times and to non-ergodic behavior. The freezing temperature T_f signals the onset of irreversibility (= replica symmetry breaking).

These properties are also found in an external magnetic field H below the AT line (see eq. 15 and Fig. 17). There is an analogous transition when $H = 0$ but the mean of the exchange distribution $J_0 > 0$: As shown in Fig. 18, then the AT line is the boundary between the ferromagnetic phase FM and a modified ferromagnetic phase F' with irreversibility (often called a "mixed" phase). The F'-SG phase boundary is vertical in the T-J_0 phase diagram in the Parisi theory.

4.3.2 Heisenberg spin glasses in magnetic field: Up to now we always considered Ising spins in the SK model. Let us now discuss very briefly the generalization to m component vector spin glasses ($m = 3$: Heisenberg spins) (Sherrington, 1983). It turned out that isotropic vector spin glasses within the SK model are rather similar to the Ising case. Interesting new features, however, occur in the presence of a magnetic field H, as first discussed by Gabay and Toulouse (1981) (see also Cragg et al., 1982a).

The EA-Hamiltonian in eq. 9 is now written for classical vector spins S_i with m components S_i^μ, $\mu = 1, \ldots, m$. The $\mu = 1$ component is defined to be parallel to the field H. The SG order parameter is then a tensor in spin space with

$$q_\parallel = \left[\langle S_i^1 \rangle_T^2 \right]_{av} \tag{25}$$

$$q_\perp = \left[\langle S_i^\mu \rangle_T^2 \right]_{av} \qquad \text{with } \mu = 2, \ldots, m. \tag{26}$$

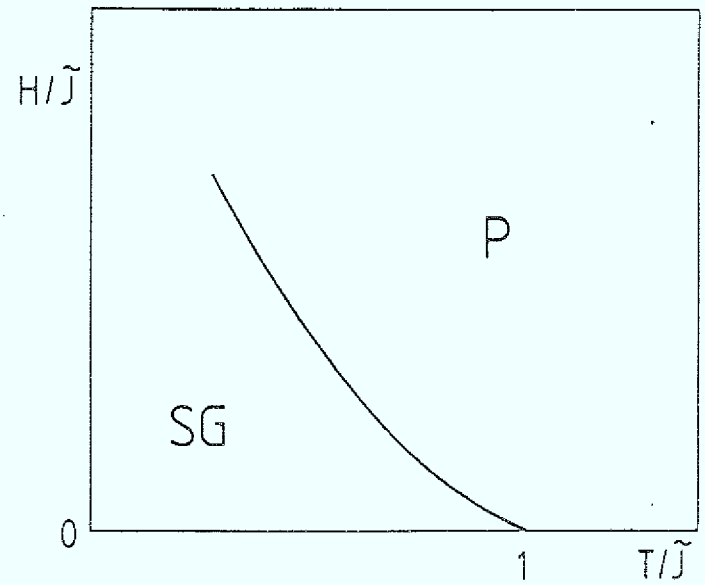

Fig. 17: Plot of the deAlmeida-Thouless (AT) line for the SK model (Ising spins) with $J_0 = 0$ (eq. 15). To the right of the AT line (P) the SK solution with a single order parameter is correct, while to the left of the AT line (SG) the Parisi's order-parameter function is believed exact. The AT line signals the onset of irreversibility.

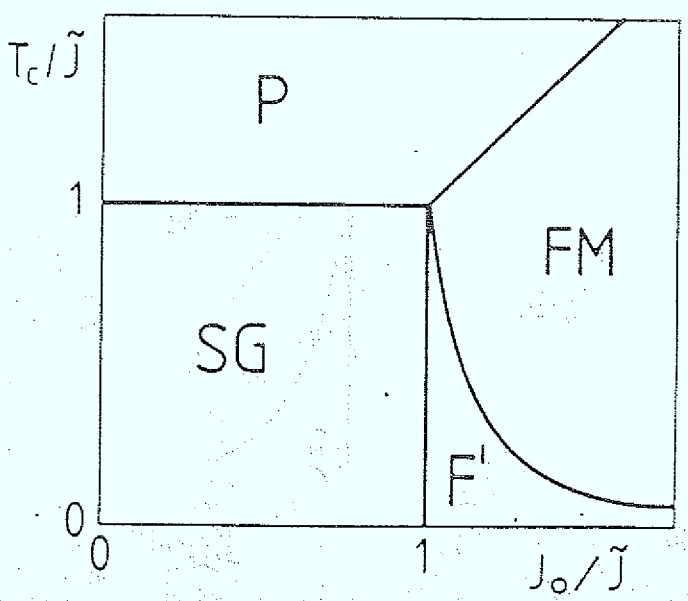

Fig. 18: Magnetic phase diagram for the SK model (EA) model for Ising spins with infinite range couplings). $\tilde{J}$ and J_0 denote the width and mean of the exchange distribution. P = paramagnet; FM = ferromagnet; SG = spin glass. F' is a ferromagnetic phase with replica symmetry breaking, i.e. irreversibility ("mixed phase") and is separated from FM by an AT line.

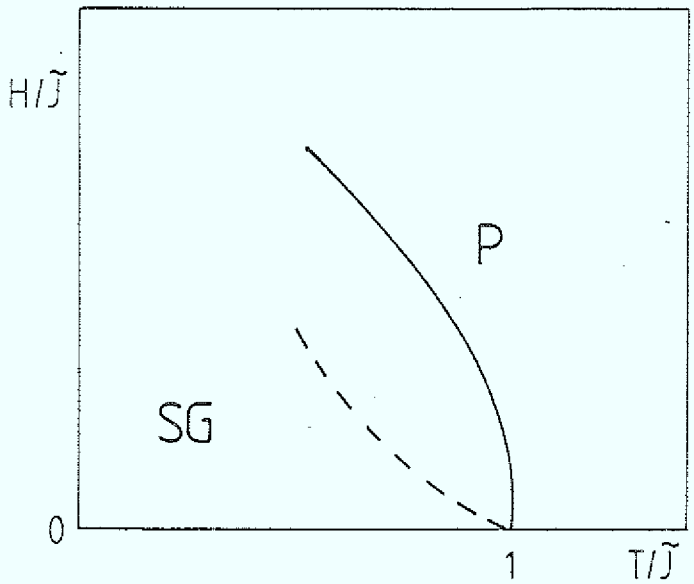

Fig. 19: Plot of the Gabay-Toulouse (GT) line (solid line) for an infinite-range vector-spin glass (eq. 27). The low-temperature phase (SG) has nonzero transverse spin-glass ordering. The deAlmeida-Thouless (AT) line (dashed line) strictly no longer occurs but there is a well-defined crossover region which follows a similar curve.

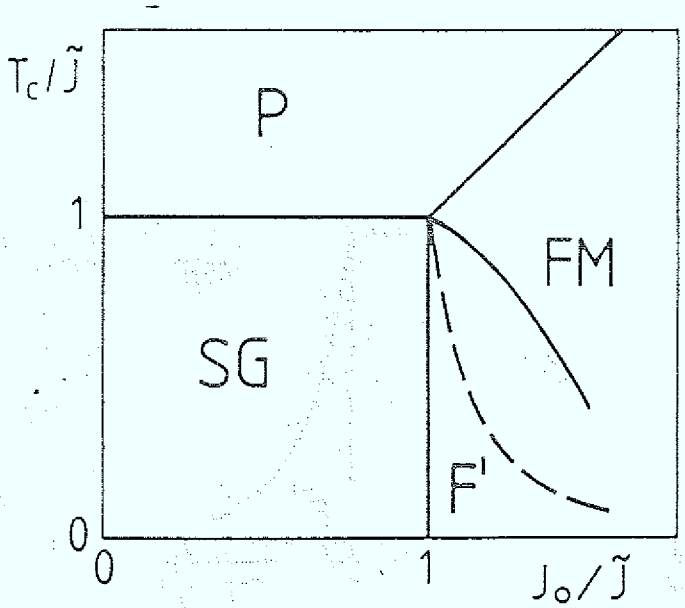

Fig. 20: Magnetic phase diagram for an infinite-range vector-spin glass with nonzero mean, J_0, in the exchange distribution. P = paramagnet; FM = ferromagnet; SG = spin glass. The "mixed phase" F' where ferromagnetism coexists with transverse spin-glass order is separated from FM by a GT line (solid line). The dashed line indicates a crossover region as in Fig. 19.

In the presence of a field one always have $M = \left[\langle S_i^1 \rangle_T \right]_{av} \neq 0$ and $q_{\parallel} \neq 0$, but Gabay and Toulouse (GT) predicted a transverse freezing, with $q_{\perp} \neq 0$, below the GT line (for small H):

$$\frac{\delta T_f(H)}{\tilde{J}} = \frac{m+4}{2(m+2)} \left(\frac{H}{\tilde{J}} \right)^2 . \qquad (27)$$

This feature is sketched in Fig. 19. Thus, a vector spin system in a field H within the SK model exhibits a phase with spin-glass order transverse to the field, reminiscent of a spin-flop phase of a pure antiferromagnet. Just below the GT line, only weak irreversibility occurs in the longitudinal component $q_{\parallel}$, but there is a crossover to strong irreversibility in $q_{\parallel}$ at a region which goes as $H^{2/3}$ like the AT line (indicated by the dashed line in Fig. 19).

Again we also report on the corresponding behavior in the $T-J_0$ phase diagram, as sketched in Fig. 20. There is an analogous GT-transition, when $H = 0$ but $J_0 > 0$, from a collinear ferromagnet FM to a "canted FM state" F', where the spins are not all parallel because $q_{\perp} \neq 0$ as well as $M \neq 0$. Thus, in vector spin glasses with $J_0 > 0$ a "mixed" phase F' is predicted in the SK model where ferromagnetism coexists with transverse spin-glass order. The F'-SG phase boundary is again vertical.

4.3.3 Anisotropic spin glasses: Now we turn to the effect of single-ion uniaxial anisotropy which in general leads to a preferred "easy" axis of magnetization. Recent mean-field calculations (Cragg and Sherrington, 1982b; Roberts and Bray, 1982) have predicted a rather rich magnetic phase diagram (Fig. 21) for such uniaxial anisotropic spin glasses. The Hamiltonian is given by

$$\mathcal{H} = -\sum_{ij} J_{ij} \vec{S}_i \vec{S}_j - D \cdot \sum_i (S_i^1)^2 \qquad (28)$$

where the anisotropy energy D is allowed any magnitude or sign. The

limiting models are (i) $D \to +\infty$, Ising; (ii) $D \longrightarrow -\infty$, planar XY; $D = 0$, Heisenberg. Let us consider the case $J_0 = H = 0$.

If the anisotropy $D > 0$ is weak compared to the exchange $\tilde{J}$, two successive transitions are expected (Fig. 21): As the temperature is decreased, spin components along the easy axis ("1"-direction) freeze at T_f (longitudinal spin-glass phase L-SG, with $q_{\parallel} \neq 0$ and $q_{\perp} = 0$). Then, at a lower critical temperature T_2 the transverse components freeze as well (LT - SG, with $q_{\parallel} \neq 0$ and $q_{\perp} \neq 0$). This second transition does not exist for sufficiently strong anisotropy. Corresponding features are found if $D < 0$ which favors transverse freezing (T - SG, with $q_{\perp} \neq 0$).

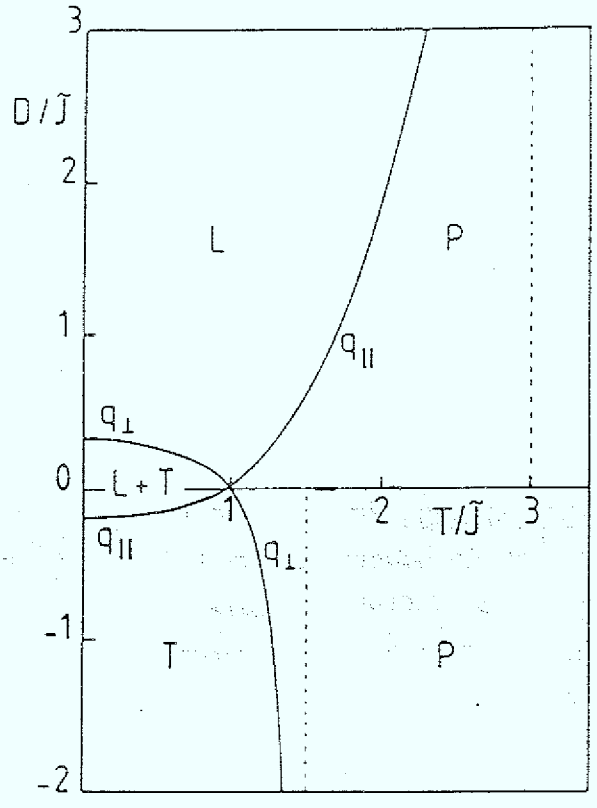

Fig. 21: Magnetic phase diagram for an infinite-range vector spin glass with uniaxial anisotropy D(Cragg and Sherrington, 1982b; Roberts and Bray, 1982). Longitudinal (L) and transverse (T) spin-glass order occur as well as both together (L + T).

4.3.4 Dynamics: The non-ergodicity of the spin glass as described by the SK model suggests that an understanding of spin-glass dynamics is essential. It has been studied for Ising spins in mean-field theory either in the Glauber model or in the "soft spin" version (in which the length of the spins is not fixed) (Kirkpatrick and Sherrington, 1978; Sompolinsky and Zippelius, 1981 and 1982). We have already discussed above the central feature of Sompolinsky's theory which introduces time-dependent order parameters and obtains a spectrum of timescales which diverge in the thermodynamic limit below the AT line.

For temperatures above T_f one has exponential decay of the spin correlations with a characteristic time τ and critical slowing down with a divergence of τ at T_f, as expected from dynamical scaling (Hohenberg and Halperin, 1977):

$$\tau \propto \xi^z \propto \left(\frac{T - T_f}{T_f} \right)^{-z\nu} \qquad \text{with } z\nu = 2. \qquad (29)$$

ξ is the correlation length and z the dynamic exponent.

Below T_f, however, the analysis predicts algebraic decay of the correlation function q(t) (see eq. 18)

$$q(t) \propto (t/\tau)^{-\nu} \qquad \text{for } T \leq T_f \ . \qquad (30)$$

That means one has a marginal spin-glass transition in the SK model (Bray and Moore, 1979), and the marginal stability of the spin-glass phase holds for all temperatures below T_f (Sompolinsky, 1981). Sompolinsky and Zippelius (1981 and 1982) obtain an exponent ν which decreases with temperature below T_f:

$$\nu(T) = \frac{1}{2} - \frac{1}{\pi} (1 - T/T_f) \qquad \text{for } T \leq T_f \ . \qquad (31)$$

Fischer and Kinzel (1984) calculate the dynamic susceptibility $\chi(\omega,T,H)$ near T_f and determine the crossover for low frequencies from the expected analytic behavior at high temperatures

$$\text{Im } \chi(\omega) \propto \omega \qquad \text{at } T > T_f \qquad (32)$$

to the behavior on the AT line:

$$\text{Im } \chi(\omega) \propto \omega^{1/2} \qquad \text{at } T = T_f \qquad (33)$$

which is consistent with the critical exponent $\nu = 1/2$ at T_f from eq. 31. The crossover relations also reproduce the sharp increase of Im $\chi(T)$ as measured in spin glasses.

4.4. Transition in real spin glasses:

We saw above that the SK model has a transition at $T_f > 0$ with a complicated ordered state below T_f. It is of great interest to know how many of these features of the mean-field theory are confirmed in real systems in three dimensions ($d = 3$). This will be discussed in the next sections where you will see that despite extensive experimental and theoretical studies several problems are still unsolved.

The question about the existence and nature of a spin-glass transition in $d = 3$ has remained controversial. The SK model does not answer the question since it is a mean-field theory, and the upper critical dimension d_u for spin glasses is $d_u = 6$ or for certain exponents even $d_u = 8$ (Fisher and Sompolinsky, 1985).

Suggestions for the lower critical dimension d_l for Ising spin glasses range from $d_l = 2$ (Southern and Young, 1977; Anderson and Pond, 1978) to $d_l = 4$ (Fisch and Harris, 1977; Sompolinsky and Zippelius, 1983). In pure systems d_l for Ising spins is known to be lower than that for Heisenberg spins ($d_l = 1$ for Ising ferromagnets; $d_l = 2$ for XY or Heisenberg ferromagnets). Below d_l no transition occurs at finite temperature due to thermal fluctuations, and for $d = d_l$ one expects e.g. a divergence of the exponent ν with $1/\nu = 0$.

The absence of a finite-temperature equilibrium transition of EA-Ising spin glasses in <u>two dimensions</u> has been inferred from transfer matrix calculations by Morgenstern and Binder (1979) which has been supported later by fitting the high-T Monte Carlo data (Young, 1983a; McMillan, 1983). Thus, Ising spin-glasses for d = 2 are now generally believed to have $T_f = 0$ and $1/\nu > 0$ (i.e. $d_l \neq 2$).

A similar concept of "T_f =0-freezing" has been assumed to be valid in <u>three dimensions</u> as well (Kinzel and Binder, 1983 and 1984; Binder and Young, 1984). More recently, however, finite-size scaling for "defect energies" for small lattices by Bray and Moore (1984 and 1985a), McMillan (1984a), and Bhatt and Young (1985) has been interpreted as an indication for a <u>finite</u> T_f in d = 3. Monte Carlo simulations on a very fast special-purpose computer by Ogielski and Morgenstern (1985) and Ogielski (1985) which exceed the previous ones by several orders of magnitude confirm the nonzero transition temperature for Ising spin glasses in d = 3. They obtain $T_f/\tilde{J} \approx 1.2$ and the following values of the critical exponents:

$\nu = 1.3 \pm 0.1$ for the correlation length $\xi \propto |T - T_f|^{-\nu}$.

$\gamma = 2.9 \pm 0.3$ for the non-linear susceptibility $\chi_{SG} \propto |T - T_f|^{-\gamma}$.

$\eta = -0.22 \pm 0.05$ for the decay of correlations (34)

$$G(r) = \left[\langle S_o S_r \rangle^2\right]_{av} \propto \xi^{-d+2-\eta} g(r/\xi).$$

$z\nu = 7.2 \pm 1$ for the correlation time $\tau \propto |T - T_f|^{-z\nu}$.

The exponential decay of spin correlations at high T changes to an algebraic (power-law) decay as the system goes through T_f. There is a divergence of ξ at T_f following the dynamical scaling hypothesis. The magnitude of critical exponents, and the rather unusual behavior of the spin-glass phase below T_f are not typical for a conventional phase transition to a state with long-range order. This suggests that d = 3 is close to the marginal dimension (i.e. $d_l \approx 3$). So far, the data are consistent with the hypothesis that the spin-glass phase is always critical at all $T \leq T_f$, i.e. that there is no true long-range order but rather that static and dynamic correlations decay algebraically (Bhatt and Young, 1985; Ogielski, 1985) - just as in the case of the Kosterlitz-Thouless (1973) transition in the two-dimensional XY ferromagnet. However, much greater lattice sizes and lower temperatures are required to clarify this last point.

5. Spin glasses at low temperatures

In this section characteristic properties of spin glasses at temperatures well below the freezing temperature T_f are discussed, T_f being determined e.g. by the maximum of the low-field, low-frequency ac-susceptibility. A number of fascinating phenomena are known to occur in spin glasses at low temperatures and they had been well documented in dilute alloys such as CuMn and AuFe (Owen et al., 1957; Schmitt and Jacobs, 1957; Kouvel, 1961; Tournier and Ishikawa, 1964) long before these systems became objects of such intense and systematic studies.

5.1 Irreversibilities:

In thermal equilibrium the magnetization of spin glasses is zero since the magnetic moments point into random directions (see e.g. property (b) in sec. 2.1.). However, there exists a finite magnetization, called remanent magnetization, M_r, after an external magnetic field has been switched off at low temperature. The M_r value and the magnetization M in small fields are found to be dependent on temperature, field, time and on the "magnetic history" of the sample. Observations of such irreversibilities provide potentially useful information on low-temperature properties of spin glasses which will be discussed now.

The two most commonly "magnetic histories" used in experiments are the following (Tholence and Tournier, 1974): The zero-field-cooled (ZFC) magnetization is obtained by cooling the sample to the measuring temperature $T^* < T_f$ in zero external field starting at high temperature $T > T_f$; then a field H is applied at T^* and M is measured (M_{ZFC}). After this ZFC procedure one can switch off the field H at T^* in order to obtain the so called isothermal remanent magnetization (IRM). The second, field-cooling (FC) procedure is to turn on the field H already above T_f and then to cool the sample in this field H down to the measuring temperature $T^* < T_f$ where one measures either the magnetization M_{FC} or, after switching off H, the so called thermo-remanent magnetization (TRM).

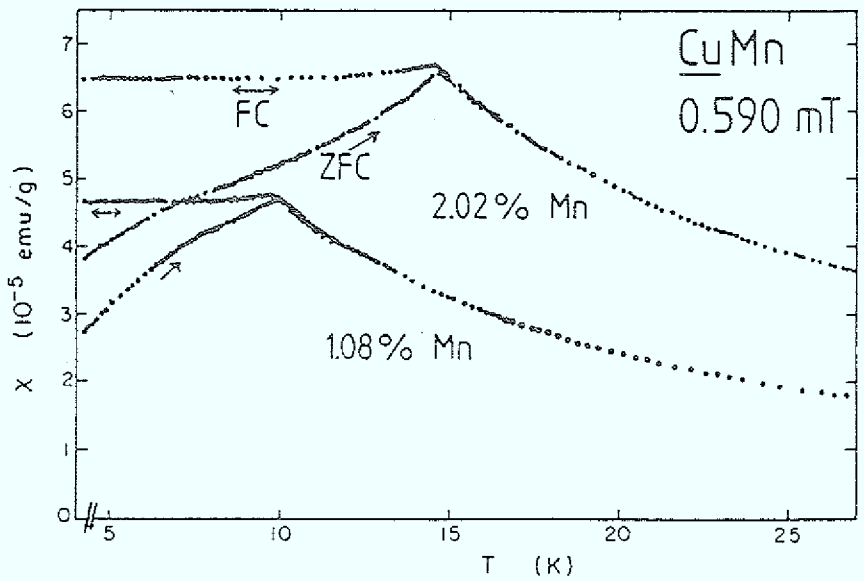

Fig. 22: Static susceptibilities M/H of CuMn spin glasses vs. temperature for 1.08 at% and 2.02 at% Mn. After zero-field cooling ($H \leq 5 \times 10^{-3}$ mT) the initial susceptibilities (ZFC) were taken for increasing temperature in a field of 0.590 mT. The field-cooling susceptibilities (FC) were obtained in the field of 0.590 mT which was applied above T_f before cooling the sample, and they are reversible (From Nagata et al., 1979).

Susceptibilities, M/H, deduced from such measurements in low field H are shown in Fig. 22 for two spin glasses $Cu_{1-x}Mn_x$ with concentration $x = 0.0108$ and 0.0202 (Nagata et al., 1979). One realizes that even in such a small field of H = 5.90 G, M_{FC} is different from M_{ZFC} (here the "zero" field is less than 0.05 G) below T_f. On heating, the FC-magnetization is reversible, whereas the ZFC-magnetization is not. If the ZFC-magnetization is cooled back down sufficiently below T_f, a reversible and relatively T-independent magnetization is obtained.

The field dependence of both sorts of magnetizations is displayed in Fig. 23, taking as example data of the spin glass $Eu_{0.30}Sr_{0.70}S$ at 70 mK (Maletta and Felsch, 1979b). The magnetization after ZFC exhibits a smaller slope versus H than M_{FC} (H) below T_f which is consistent with the findings at very low fields discussed above. An interesting feature is the S-shaped curvature of M_{ZFC} (H) with an inflection point which moves downward in H with increasing T and disappears at about T_f (see also: Knitter and Kouvel, 1980).

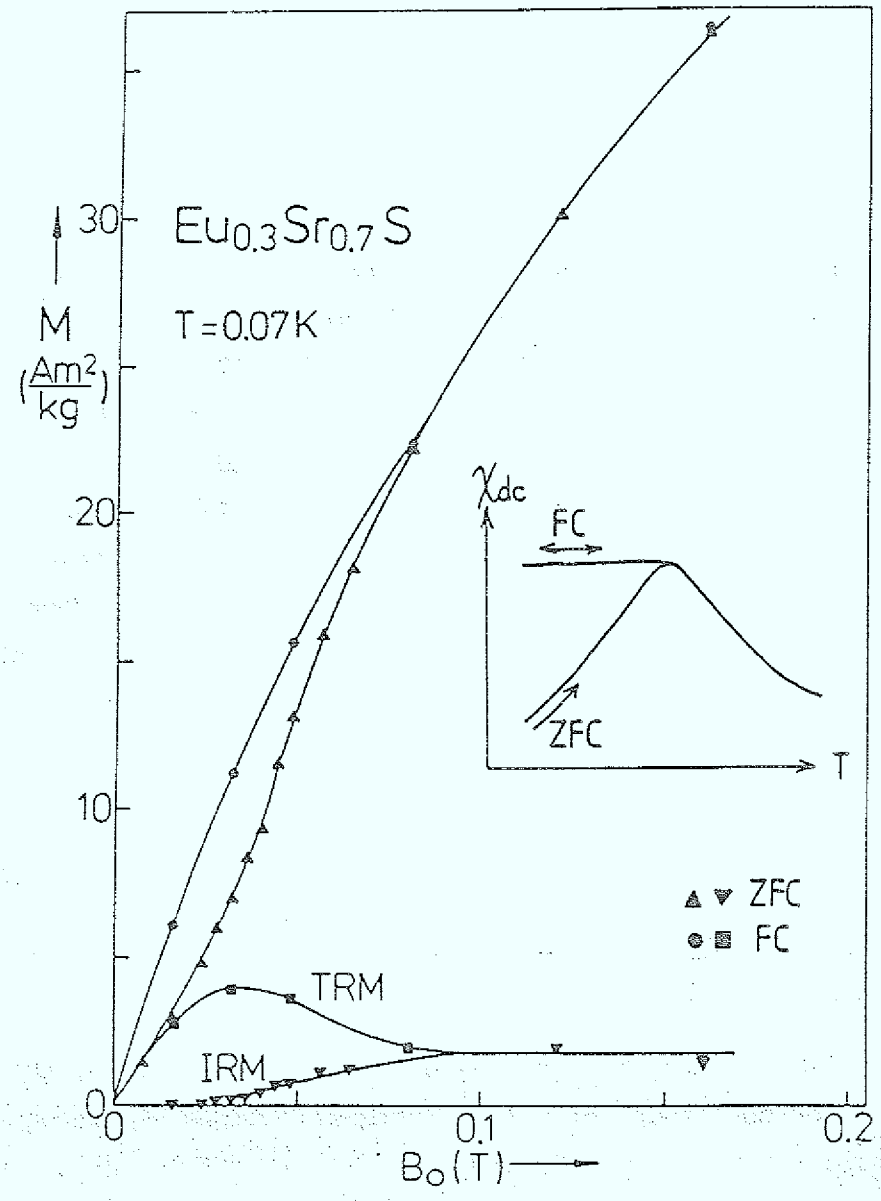

Fig. 23: Magnetization M of $Eu_{0.30}Sr_{0.70}S$ spin glass as function of the applied field at T = 0.07 K. Both the magnetization M_{ZFC} and isothermal remanent magnetization IRM, measured after zero-field cooling in increasing field, as well as the magnetization M_{FC} and thermoremanent magnetization TRM, measured after cooling in the field B_o, are shown. The insert displays schematically the corresponding ZFC- and FC-susceptibilities vs. temperature (From Maletta and Felsch, 1979b).

We now turn to the remanent magnetization which is only a small part of the total magnetization and is dependent on magnetic history, too, with

$$IRM\ (H,T) \quad < \quad TRM\ (H,T) \qquad \text{for small fields} \qquad (35)$$

as shown in Fig. 23. The TRM starts out linear with the field H at small H, while the field dependence of the IRM is quadratic. There is no indication of a threshold field down to 0.5 Oe (Ferré et al., 1981) below which no remanent magnetization is observed as claimed by some authors (Tholence and Tournier, 1974; Gray, 1979). In high enough fields, both IRM and TRM saturate to the same value M_{rs} for $H \geqslant H_{cr}$. The IRM approaches it in a monotonous way, while the TRM passes a maximum versus field. At fields exceeding H_{cr} (T) where IRM and TRM merge the history-dependence and hence irreversible effects are negligible. The total magnetization, however, does not saturate even in pulsed fields up to 40 Tesla (Smit et al., 1979 a and b; Rakoto et al., 1984). The temperature dependence of the saturated remanent magnetization obeys the relationship

$$M_{rs}(T) = M_0 \exp(-aT) \qquad (36)$$

except at very low temperature (just where the TRM is found to be larger than M_{rs}, see Fig. 23) as shown in Fig. 24.

It has been wellknown from the beginning of these studies that the ZFC-magnetization and both types of remanent magnetizations show long-time, non-exponential variation in time (Tournier and Ishikawa, 1964; Tholence and Tournier, 1974; Guy, 1975) typically of the form:

$$M(t) \backsim \ln t \qquad (37)$$

On the other hand, the FC-magnetization has been generally assumed to yield informations on the thermal equilibrium behavior of spin glasses because of its reversibility and time-independence (Malozemoff and Imry, 1981 b; Chamberlin et al., 1982; Monod and Bouchiat, 1982). Recently, several authors (Lundgren et al., 1982 and 1985; Wenger and Mydosh, 1984 a; Bouchiat and Mailly, 1985; Kinzel and Binder, 1984), however, question the validity of this assumption. We shall discuss this point in context with the time-dependent susceptibilities in sec. 6.1 .

As first suggested by Tholence and Tournier (1974) one can decompose the FC-susceptibility $\chi = \lim_{H \to 0} M_{FC}/H$ into a reversible and irreversible contribution at temperatures below T_f:

$$\chi_{rev}(T) + \chi_{irr}(T) = \chi(T_f) \qquad \text{for } T \leq T_f \qquad (38)$$

where the sum stays almost constant, and

$$\chi_{rev} = \lim_{H \to 0} dM_{ZFC}/dH \qquad (39)$$

$$\chi_{irr} = \lim_{H \to 0} dTRM/dH \quad . \qquad (40)$$

The ac-susceptibility as discussed later only measures the reversible part χ_{rev}. Equations (38) to (40) are consistent with the following relation (Maletta, 1980 c) between the magnetizations and remanent magnetizations measured after different magnetic histories, as is obvious from Fig. 23, too:

$$M_{ZFC}(H,T) = M_{FC}(H,T) - TRM(H,T) + IRM(H,T) \quad . \qquad (41)$$

Thus, the S-shaped curvature of the virgin magnetization, $M_{ZFC}(H)$, is directly connected to the field dependence of the remanences.

The shape of the TRM(H) curve is a consequence of the importance of the measuring time as shown by Ferré et al.(1981). They demonstrate that the maximum in TRM versus H results from an increase of the magnetization decay rate with field H which can compensate the higher initial TRM value at higher fields (Fig. 25).

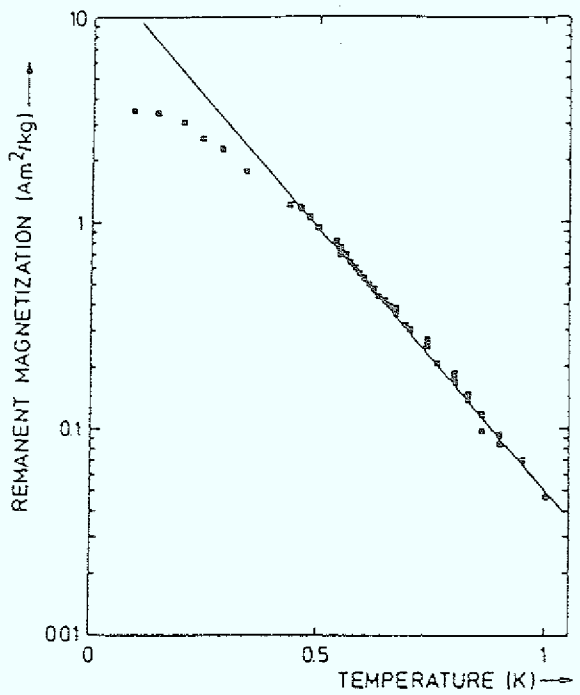

Fig. 24: Temperature dependence of the saturated remanent magnetization in $Eu_{0.40}Sr_{0.60}S$ (From Maletta and Felsch, 1979b).

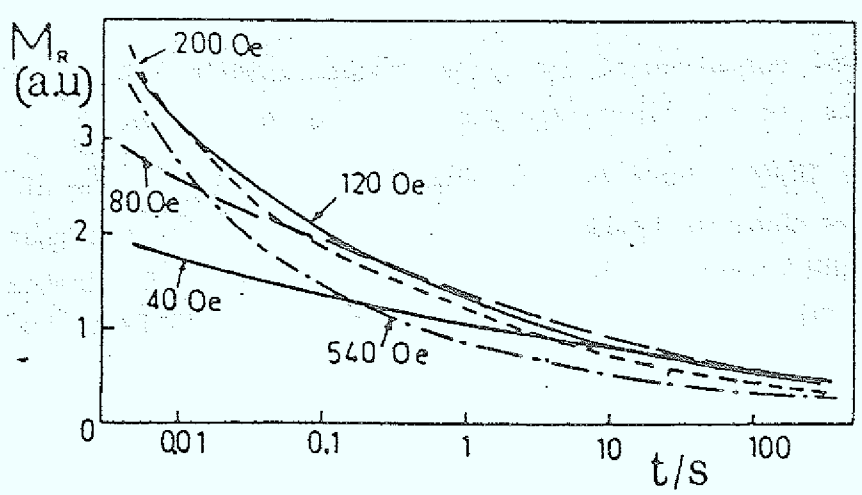

Fig. 25: Time decay of the TRM in $Eu_{0.40}Sr_{0.60}S$ for various fields at T = 1.32 K (From Ferré et al., 1981).

The time decay of the TRM in spin glasses has been studied in great detail. First it was described by a logarithmic law, as already mentioned in eq. 37:

$$TRM\ (t) \quad \propto \quad -S_{RM} \cdot \ln t \qquad (42)$$

where the coefficient S_{RM} is called "magnetic viscosity" (Guy, 1977 and 1978). An example is shown in Fig. 26: $M_{rs}(t)$ is displayed for the spin glass $(La_{0.98}Gd_{0.02})Al_2$ at various temperatures below T_f = 520 mK (v. Löhneysen and Tholence, 1979).

Measurements over two decades of time by Ferré et al. (1981) show that the data are better approximated by a power-law decay:

$$TRM(t) \quad \propto \quad t^{-a(T,H)} \quad . \qquad (43)$$

However, this power law fails for more than 3 decades of time, as already

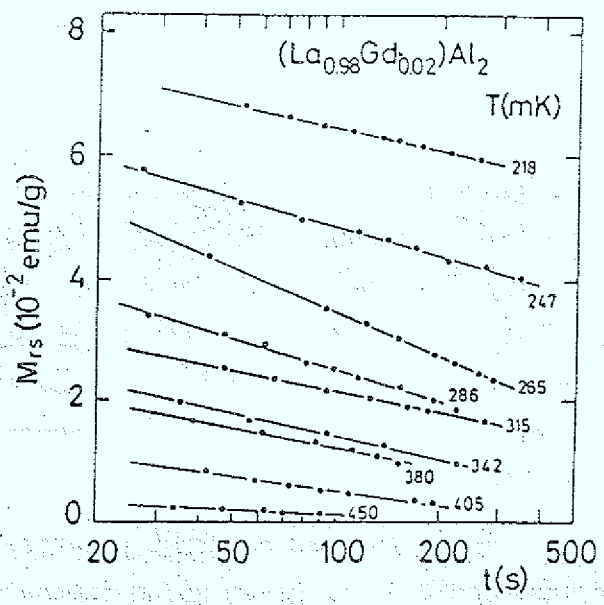

Fig. 26: Saturated remanent magnetization M_{rs} as a function of time (logarithmic) for $(La_{0.98}Gd_{0.02})Al_2$ at various temperatures (From v. Löhneysen and Tholence, 1979).

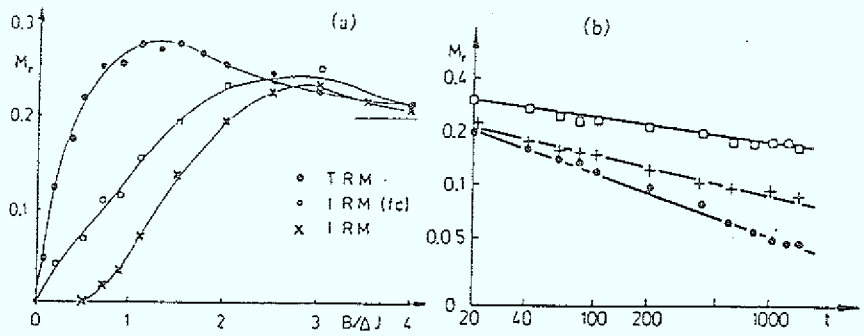

Fig. 27: Results from Monte Carlo simulations, like the data shown in Fig. 14:
(a) Remanent magnetization M_r obtained by cooling in a field (TRM) or shortly applying a field at constant temperature (IRM) as a function of the initially applied field. IRM (fc) is obtained by some mixed cooling procedure. M_r is measured at the temperature $T = \Delta J/4k_B$.
(b) Remanent magnetization M_r as a function of time. The squares (TRM, $B = \Delta J$) and dots (IRM, $B = 1.5 \cdot \Delta J$) have the same initial energy, the dots and crosses (TRM, $B = \infty$) have the same initial magnetization ($T = 0.5 \cdot \Delta J$) (From Kinzel, 1979).

mentioned in that paper. A power-law decay is proposed by Monte Carlo simulations of an EA spin glass (Binder and Schröder, 1976; Kinzel, 1979; see Fig. 27) which is nicely confirmed by the detailed Faraday-rotation measurements of $Eu_{0.40}Sr_{0.60}S$ by Ferré et al. (1981) as illustrated in Fig. 28. As additional information, the experiment reveals a drastic change in the dynamics very near $T_{fo} = 1.55$ K: there seems to be a divergence of the exponent a with T.

Very recently, Chamberlin (1985) pointed out that a better representation of his $M_r(t)$-data for AgMn and CuMn is given by an exponential function of time raised to a fractional power (a "stretched exponential"):

$$TRM(t) = M_r(0) \cdot \exp(-(t/\tau_p)^{1-n}) \qquad (44)$$

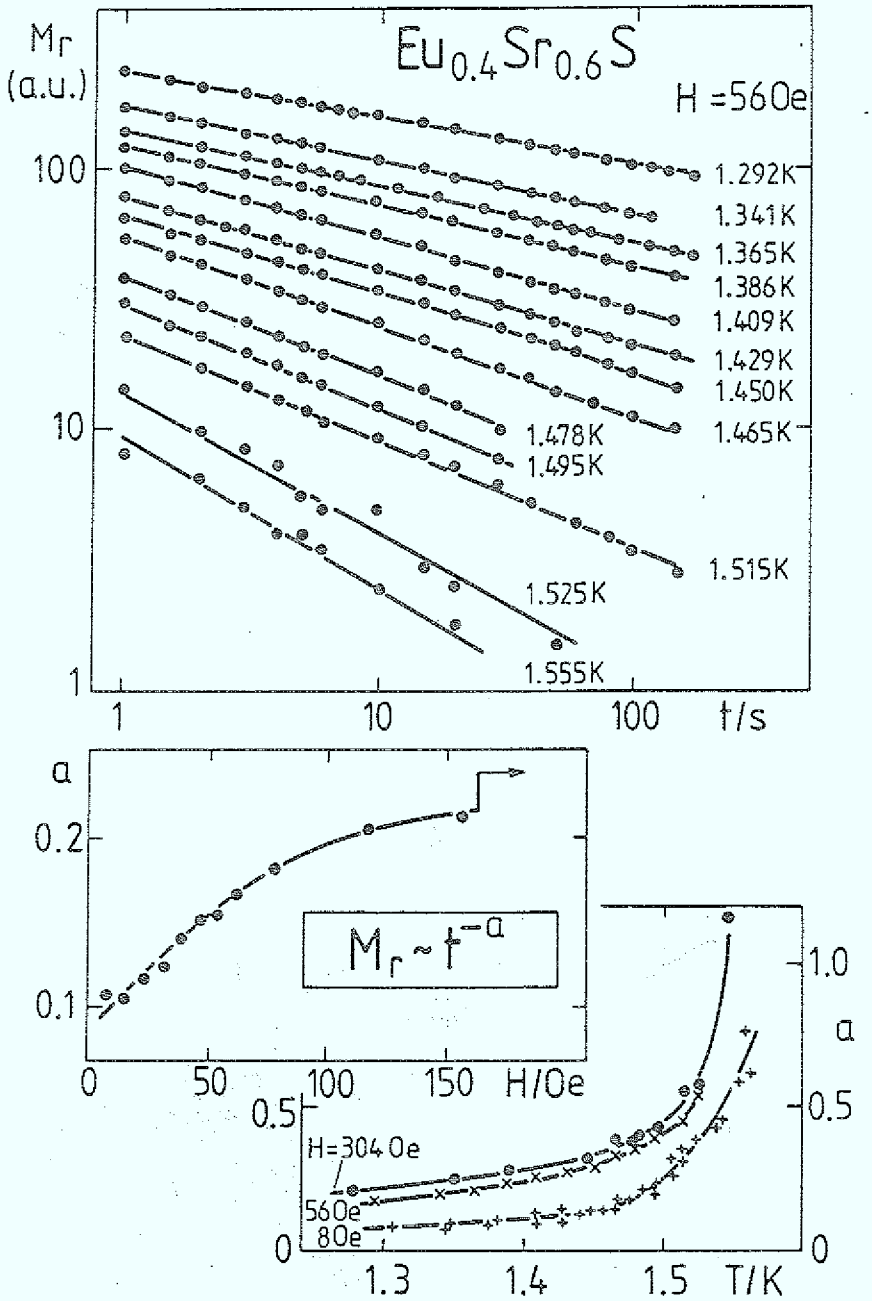

Fig. 28: Time decay of the TRM in $Eu_{0.40}Sr_{0.60}S$ spin glass close to T_f = 1.55 K (the initially applied field was H = 56 Oe), showing a power-law decay, t^{-a}, where the exponent a is dependent on the priviously applied field H and on temperature (From Rajchenbach et al., 1981, and Ferré et al., 1981).

with a characteristic mean relaxation time τ_p. New $M_r(t)$-data of $Eu_{0.40}Sr_{0.60}S$ over 5 decades of time (Ferré et al., 1986) and data of $Eu_{0.40}Sr_{0.60}Te$ (Börgermann et al., 1986b) can also be fitted by eq. 44. In $Eu_{0.40}Sr_{0.60}Te$ the time decay depends on the waiting time t_w spent during cooling the sample from T_f to the temperature of measurement, similar to other spin glasses (Lundgren et al., 1983; Chamberlin, 1985). Fig. 29 shows data of $Eu_{0.40}Sr_{0.60}Te$ at $T = 0.890\ T_f$ which follow eq. 44 with the fitting parameters $M_r(0) = 0.06\ M_{FC}$, $n = 0.80 \pm 0.02$, and the waiting-time dependent $\tau_p(t_w)$ as displayed in the insert. The functional form of the time decay in eq. 44 appears attractive to be checked experimentally because it is based on an universal relation used to describe relaxation phenomena in glasses, polymers, dielectrics, etc. (Ngai et al., 1984).

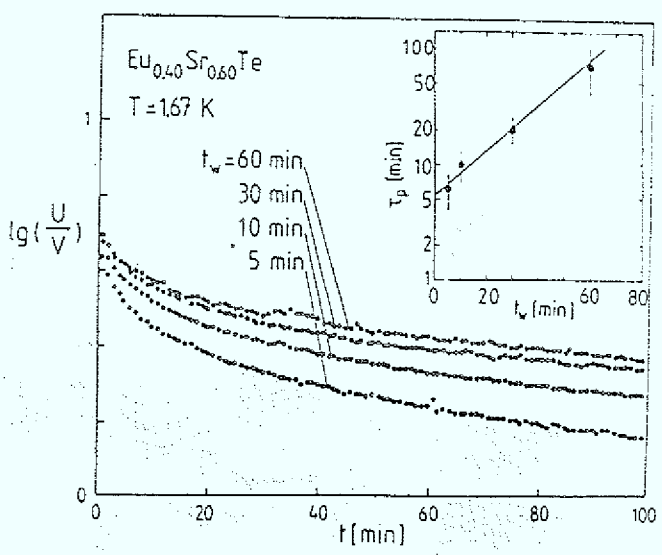

Fig. 29: Time dependence of the TRM in $Eu_{0.40}Sr_{0.60}Te$ spin glass as a function of the wait time t_w that the sample spent in the FC state at $T = 0.890\ T_f$ before the field of 1.0 mT was removed, for $t_w = 5, 10, 30$ and 60 min. $M_r(t = 0)$ is not a function of t_w but M_r relaxes more slowly for longer t_w. The best fits to the data by the "stretched exponential" (eq. 44) give a characteristic mean relaxation time τ_p which increases with t_w exponentially, as shown in the insert (From Börgermann et al., 1986b).

Recently, it has been predicted for glasses and spin glasses by Palmer et al. (1984) using models of hierarchically constrained dynamics and by de Dominicis et al. (1985) within the Parisi's model extended to a dynamic context. Eq. 44 holds only asymptotically for $t \gg \tau_p$. The problem, however, is the reliability of the three fitting parameters obtained with eq. 44, since they are generally rather correlated within the restricted time interval of the measurement.

One of the first phenomenological models to describe the irreversibilities in spin glasses is proposed by Tholence and Tournier (1974), following Néel's (1949) model for an ensemble of fine magnetic grains or particles. Their main assumption is the existence of well-defined "spin regions" or "spin clouds" in a spin glass which can relax between equilibrium orientations. For each cloud a potential barrier is determined by the dipolar anisotropy energy E_a which separates two easy orientations of its magnetization. Due to thermal fluctuations the magnetization can overcome the barrier within an average time τ given by the Arrhenius law

$$\tau = \tau_0 \exp(E_a/k_B T) \tag{45}$$

where τ_o is some intrinsic time constant (τ_o^{-1} = attempt frequency). This implies that a particular cloud is blocked at a temperature T_B for which the relaxation time τ becomes equal to or larger than the measuring time t_m. As a consequence there appears a maximum in the ac-$\chi(T)$ at the freezing or blocking temperature T_B which is dependent on the measuring frequency $\omega = 2\pi/t_m$:

$$T_B^{-1}(\omega) = -(k_B/E_a) \ln(\tau_o \omega) \quad . \tag{46}$$

Turning to the remanent magnetization M_r, this model provides a general relationship between the time and temperature dependence of M_r. Let $p(E_a)dE_a$ be the number of regions with an anisotropy energy between E_a and $E_a + dE_a$. Then the corresponding change of the remanent magnetization is

$$dM_r = -\frac{1}{2} M_g(E_a) p(E_a) dE_a \tag{47}$$

where $M_g(E_a)$ is the mean moment of those clouds and the factor $\frac{1}{2}$ takes into account the projection of M_g on the direction of field initially applied. By partial differentiation of M_r in eq. 47 with respect to lnt and T one obtains with eq. 45

$$\frac{\partial M_r}{\partial \ln t} = \frac{1}{\ln t - \ln \tau_o} \cdot T \cdot \frac{\partial M_r}{\partial T} \qquad (48)$$

For a number of years this concept of"spin clouds" has been very popular for analyzing experimental data of spin glasses (Tholence and Tournier, 1974; Wohlfarth, 1977; Prejean, 1978; v. Löhneysen and Tholence, 1979). As an example, Fig. 30 reproduces a plot according to eq. 48 for data of $(La_{0.98}Gd_{0.02})Al_2$ spin glass (with $\tau_o = 10^{-6}$ sec), which also follows eq. 36 and eq. 37 (Fig. 26). v. Löhneysen and Tholence (1979) claim that Fig. 30 gives support to the model of "spin clouds".

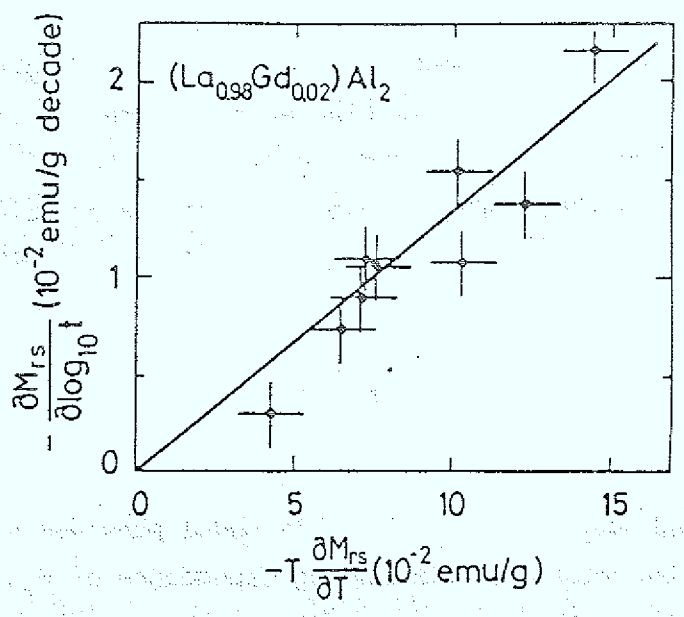

Fig. 30: Plot of the data from Fig. 26, M_{rs} (T,t), according to eq. 48 within the "spin cloud"-concept. The straight line yields $\tau_o = 10^{-6}$sec (From v. Löhneysen and Tholence, 1979).

Certainly, the "spin-cloud" model is based upon an oversimplified picture of spin glasses. It provides qualitative descriptions of several spin-glass properties, but thereby often unphysical fitting parameters are obtained. It is a correct, microscopic description of superparamagnetism, however in spin glasses no evidence for independent domain structure is available. Let us give some examples to these statements.

Superparamagnetic behavior of independent spin clusters can be studied experimentally in very dilute $Eu_xSr_{1-x}S$ with Eu concentrations x below the percolation threshold $x_p = 0.13$ (see discussion in sec. 2.2.), as demonstrated by Eiselt et al. (1979a,b). Counting the number of all small independent (since $x < x_p$) clusters by computer with calculation methods known from percolation theory and calculating energy barriers due to intracluster dipolar anisotropy energy one gets time-dependent susceptibility maxima at $T_B(t)$ similar to eq. 46 and in good agreement with experiment without adjustable parameters (Fig. 31). On the other hand, the frequency dependence of ac-susceptibility maxima $\chi(T)$ also observed in spin glasses, cannot be interpreted by means of the picture of blocking of superparamagnetic clouds, as done by v. Löhneysen et al. (1978a); a description with eq. 46 leads to unphysical fitting parameters (Maletta, 1980 a and c).

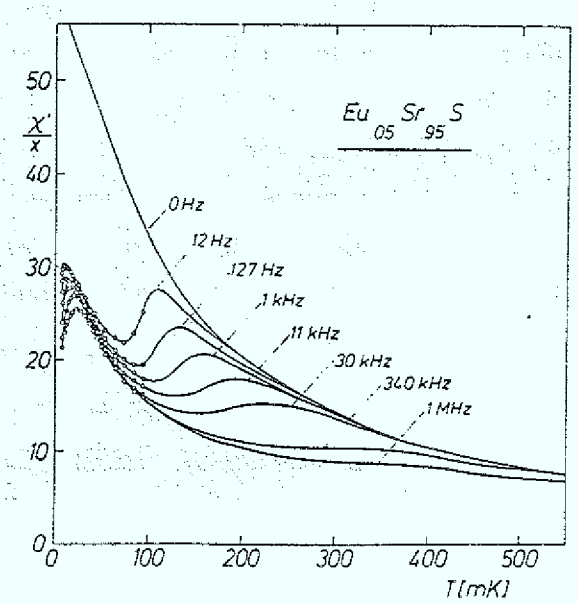

Fig. 31: Temperature dependence of the static (0 Hz) and ac susceptibilities of the superparamagnet $Eu_{0.05}Sr_{0.95}S$ for various measuring frequencies (From Eiselt et al., 1979a).

Experimental evidences for a distinction of spin-glass freezing from superparamagnetic blocking are collected by Maletta (1981b) from systematic studies and comparison of superparamagnetic compounds ($x < x_p$) and spin-glass compounds ($x > x_p$) in the dilution system $Eu_xSr_{1-x}S$. Hence, the interactions among spin clusters (which are partially frustrated) play an essential role in spin glasses.

Such a model of interacting spin clusters can be reduced to a model of EA-type by reasonable approximations, as has been emphasized by Binder already in 1977. Indeed, Monte Carlo simulations of the 2-dimensional EA-Ising model (Kinzel, 1979) yield reversible and irreversible susceptibilities and remanent magnetizations in excellent qualitative agreement with experimental data, as already mentioned in sec. 4.2 and shown in Fig. 14. In addition, a power-law decay of $M_r(t)$ and even details like the maximum of the TRM versus H are reproduced in the simulations (Fig. 27).

In this context one has also to report on a systematic experimental study by Bouchiat and Monod (1982) about the origin of the remanent magnetization in spin glasses. Analyzing data of AgMn spin glasses in the Mn concentration range 1% to 24% the authors come to the conclusion that remanent magnetizations are indeed an intrinsic property of the spin-glass state (and not some "parasitic" magnetic contribution). They show that the TRM and IRM data can be plotted on universal curves (independent of concentration) versus the reduced temperature T/T_f only, when they are normalized with $M_{rs}(T)$ and the field H is normalized with $H_{cr}(T)$. The same conclusion appears to hold in CuMn, AuFe, (LaGd)Al_2, and (Eu,Sr)S spin glasses. The authors argue that the mechanism responsible for the existence of a remanent magnetization in metallic spin glasses exclusively involves exchange interactions (without additional dipolar anisotropy).

Finally, we refer to work by Alloul (1979 a and b) on zero-field NMR on Cu in CuMn alloys (Mn concentrations from 0.4% to 4.7%) at low temperatures $T \lesssim 0.2\ T_f$, who finds no evidence for independent domain structure. The enhancement factor η of the rf-field and NMR signal intensity, associated

with the rotation of domain magnetization, is found roughly proportional to the remanent magnetization M_r and is negligible when the sample is ZFC. These results contradict the independent "spin cloud" model, for which η should be independent of M_r. A similar conclusion has also been reached from the square hysteresis loops observed well below T_f in CuMn (Monod et al., 1979) and is corroborated by computer simulations of CuMn alloys (Walker and Walstedt, 1980).

Thus, a large amount of experimental data shows the intrinsic feature of irreversibilities of spin glasses at low temperatures. These distinct properties are obviously due to their enormous number of equivalent states below T_f. Hence, the picture of free energy valleys in phase space (Fig. 15) is useful to explain the effects phenomenologically. In the FC procedure the system can go immediately into the lowest valley. On the other hand changing the field at fixed temperature below T_f gives rise to pronounced irreversibility. After ZFC the system can be trapped in a local minimum before it relaxes slowly into the lower minimum. More detailed theoretical work, however, would be desirable in order to understand the nature of the "frozen state" in spin glasses at low temperatures.

5.2 Anisotropy :

The very existence of a remanent magnetization, M_r, which keeps the direction of the cooling field is already a direct evidence of anisotropy in spin glasses (Alloul, 1983). This property turned out to be independent of crystallographic directions in classical spin glasses like CuMn and (Eu,Sr)S for which single-ion crystalline anisotropy can be neglected. First, these properties were again assumed to be linked with an inhomogeneous description of the spin system, subdivided into domains or spin clouds. Recent experiments, however, have provided evidence for a macroscopic character of the anisotropy in spin glasses. Even a microscopic origin of anisotropy in metallic spin glasses has been proposed.

Measurements of the transverse susceptibility $\chi_\perp$ (Alloul and Hippert, 1983) for instance allow the determination of the anisotropy energy $E_A(\theta)$ which keeps the remanent magnetization $\vec{M}_r$ aligned along the cooling field $\vec{H}_c$ ($\parallel \vec{z}$), θ being the angle $(\vec{M}_r, \vec{z})$. In the standard method after inducing the remanent magnetization M_r along z, the response $\chi_\perp$ of M_r to a small alternating field h_{ac} ($\lesssim 1$ G, $\parallel \vec{y}$) is measured in various static fields $\vec{H}_z \parallel \vec{z}$ (Fig. 32). In the most simple situation, assuming a collective response to a small field, one can define an anisotropy field

$$H_A = K/M_r \qquad (49)$$

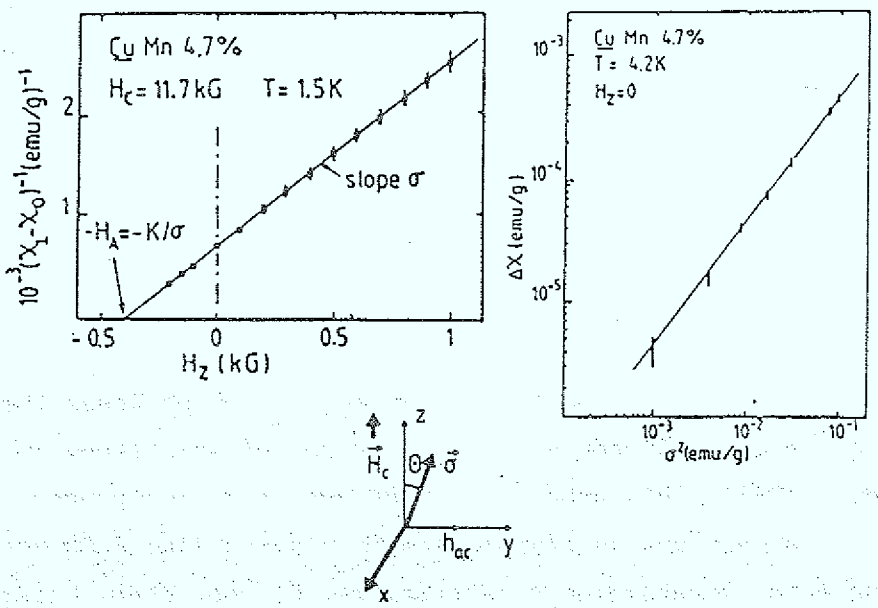

Fig. 32: Transverse susceptibility $\chi_\perp$:
(a) Typical $\chi_\perp$ data of CuMn 4.7%, obtained at 1.5 K in the cooling field H_c = 11.7 kG, showing perfect agreement with eq.50, the anisotropy field $H_A = K/M_r$ being the only parameter. The isotropic part χ_o is measured after ZFC, while M_r ($\equiv\sigma$) is measured independently on the same sample (From Alloul and Hippert, 1983).
(b) $\Delta\chi = \chi_\perp - \chi_o$ as measured for $H_z = 0$, plotted versus M_r^2 ($\equiv\sigma^2$) for various values of the remanence. The straight line with slope unity perfectly fits the data, which allows to conclude that $K = M_r^2/\Delta\chi$ from eq. 50 is independent of M_r (From Hippert and Alloul, 1982).

and the transverse susceptibility $\chi_\perp$

$$\chi_\perp - \chi_o = \frac{M_r}{H_z + H_A} \quad . \tag{50}$$

The decomposition of $\chi_\perp$ in eq. 50 into an isotropic part χ_o, measured after ZFC, and an anisotropic part is assumed to be reasonable since χ_o is not modified by the presence of M_r within the experimental accuracy. Measurements on CuMn spin glass show perfect agreement with this concept in eq. 50 as illustrated in Fig. 32. χ_o is obtained after ZFC, and M_r is measured independently on the same sample, hence the anisotropy field H_A is the only fitting parameter.

From the experimental definition of a unique anisotropy field by these $\chi_\perp$ measurements and from the result of an NMR analysis (Alloul, 1979a and b) that almost all local moments are involved in the magnetization rotation, Alloul and Hippert (1983) conclude that for $T \ll T_f$ small applied fields induce a macroscopic rotation of the spins in their metastable configuration. Further evidences for a macroscopic anisotropy in spin glasses are also found by ESR experiments (Monod and Berthier, 1980) and measurements of the magnetic hysteresis (Monod, Préjean and Tissier, 1979).

One has to point out, however, that the anisotropy of spin glasses is not induced by the field. Although H_A depends on the magnitude of M_r (eq. 49), K has been found to be rather well defined. Measurements of both M_r and H_A at a given temperature for various cooling conditions and therefore for a large range of M_r values give a straight line with slope unity in the plot $\ln (\chi_\perp - \chi_o)$ vs. $\ln M_r^2$, thus K is strictly independent of M_r for CuMn (Hippert and Alloul, 1982), as well as for an insulating spin glass (Velu et al., 1981). Not only is K independent of M_r, but it remains meaningful even in a zero-field cooled state where no remanence exists as clearly evidenced by a new ESR signal for $M_r = 0$ (Schultz et al., 1980).

Fig. 33 shows both ESR signals versus field corresponding to the large M_r (slope 1) and $M_r \to 0$ (slope 1/2) limits. In the presence of a large $M_r \gg \chi_o H_z$ and for small enough fields $H_z \lesssim 2 H_A$, a ferromagnetic like ESR mode is detected by Monod and Berthier (1980) at frequencies

$$\omega / \gamma = H_z + H_A \qquad \text{with } H_A = K/M_r \tag{51}$$

where H_A is found to be identical with that obtained from $\chi_\perp$ data (see eq. 50). Now even in a zero-field cooled state with $M_r = 0$ a second new ESR mode is predicted and found (Schultz et al., 1980) with frequency

$$\omega/\gamma = \frac{1}{2} \cdot (H_z + 2\,H_i) \qquad \text{with } H_i = \sqrt{K/\chi}$$
$$\rightarrow \sqrt{K/\chi_o} \qquad \text{for } H_z = 0 \quad . \tag{52}$$

Further ESR results are found in recent publications (Gullikson et al., 1983; Hoekstra et al., 1984) suggesting a breakdown of the rigid spin rotation at large field angles.

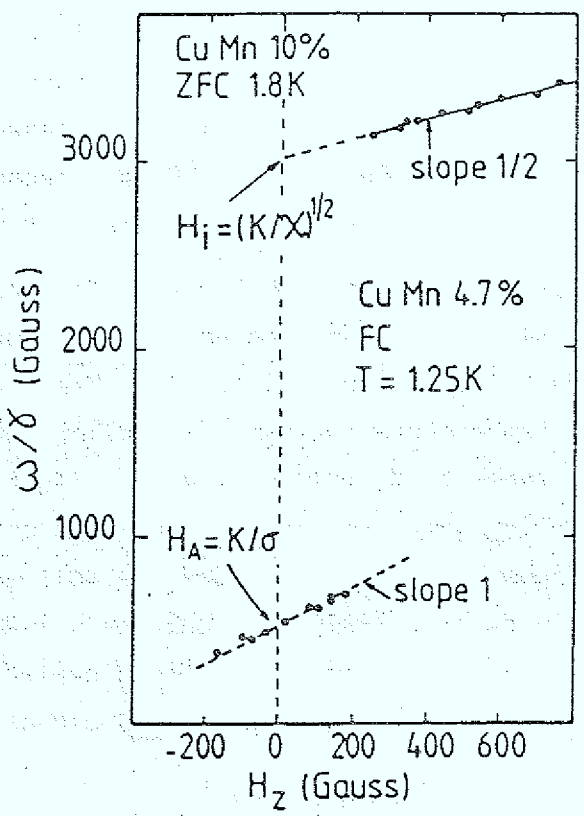

Fig. 33: ESR frequency in CuMn versus field in the two limiting cases of large M_r (slope 1) (Monod and Berthier, 1980) and $M_r = 0$ (Schultz et al., 1980)($M_r \equiv 6$).

Thus the anisotropy constant K and hence $E_A(\theta)$ is an intrinsic property of the spin glass state. It defines a macroscopic anisotropy. Any rigid rotation of the spin system with respect to the lattice costs some anisotropy energy. However, due to the overall isotropy of the state, this energy $E_A(\theta)$ will be the same whatever the axis of the rotation is. Often it is called an "isotropic anisotropy". Therefore, the spin-glass state has to be characterized by an anisotropy triad (Saslow, 1982) instead of an anisotropy axis.

The triadic character of the anisotropy shows up in an unidirectional angular dependence

$$E_A(\theta) = K_d(1-\cos\theta) \tag{53}$$

rather than in an uniaxial dependence

$$E_A(\theta) = \frac{K_{ax}}{2} \cdot \sin^2\theta \tag{54}$$

which would result from a vector anisotropy. In principle the difference between both types of anisotropy should be seen from hysteresis cycles. While in the first case (eq. 53) a reversible reversal of M_r should occur at $H_d = -K_d/M_r$, in the second one (eq. 54) a hysteresis cycle around $H = 0$ with half width $H_{ax} = K_{ax}/M_r$ should be observed. Experimental hysteresis cycles of CuMn show a mixture of these two features, but H_A-values deduced from eqs. 53, 54 are not in agreement with values from $\chi_\perp$-experiments.

Another experiment, however, demonstrates the purely unidirectional character of the anisotropy in CuMn spin glass. Hippert, Alloul and Fert (1982) note that $\chi_\perp$ is very sensitive to the ratio K_{ax}/K_d when being measured in the presence of a static field H_y applied in the direction of the susceptibility coil. The H_y dependence of $\chi_\perp$ is found to agree perfectly with $K_{ax} = 0$ (Fig. 34). The authors argue that the disagreement with the hysteresis experiment stems from the fact that a rigid-body rotation of the spin system can only be produced on a limited angular range (in CuMn for $\theta \lesssim 40°$). This is fulfilled in the $\chi_\perp$-experiment but not in the hysteresis.

The triadic character of E_A has been directly detected first by torque experiments (Fert and Hippert, 1982). The sequence of rotations of the anisotropy triad during the torque experiment can be followed in Fig. 35. After a rotation of π around x induced by rotating an applied field from z to -z in the yz-plane, the spin system does not have the same responses in the yz- and xz-planes (as would be the case for a vector anisotropy (Fig. 35)). Especially the torque $\Gamma_y = d_{EA}/d\varphi$ is found nearly zero for a further rotation of φ in the xz-plane, as the total rotation angle of the triad undertaken from the initial state is still π (the axis of rotation is different of course).

Microscopically, this type of anisotropy in metallic spin glasses is linked to the existence of Dzyaloshinsky-Moriya interactions (see sec. 3.2). This interpretation has been stimulated by hysteresis studies of ternary CuMn spin glasses by Prejean et al. (1980) where the third component is a nonmagnetic impurity of concentration x. Whereas M_r and T_f are found to be independent on x, the width of the hysteresis and hence the anisotropy constant K increases linearly with x (Fig. 36). By taking different impurities the authors demonstrate that the spin-orbit interaction is responsible for the anisotropy.

Many experimental results in spin glasses have demonstrated that for $T \ll T_f$ a macroscopic anisotropy energy can be defined even in ZFC spin glasses. The spin-glass state is characterized by a triad and E_A is only specified by the rotation angle of the triad, as long as a rigid spin rotation can be assumed; deviations are detected for large angle rotations and at increasing temperature. In metallic spin glasses this anisotropy is associated with DM-interactions between the spins. In insulating (Eu,Sr)S no study of this kind has been performed up to now.

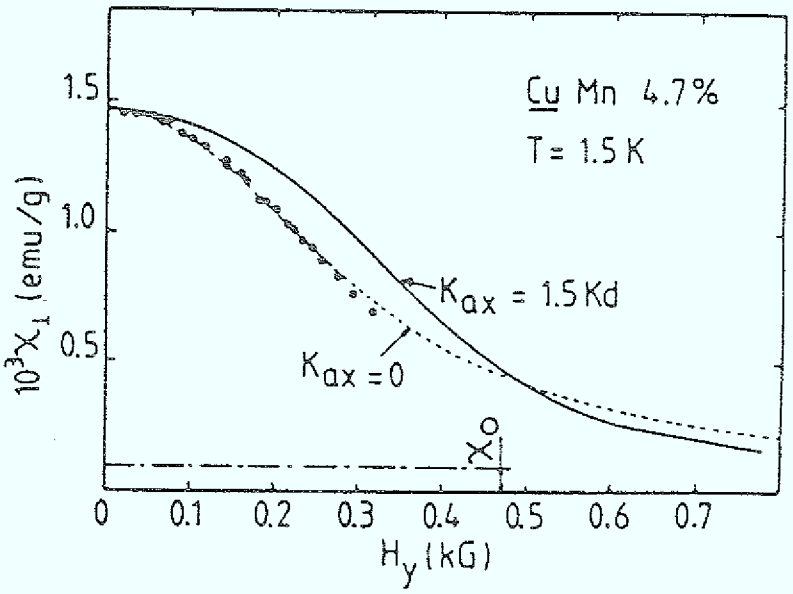

Fig. 34: Transverse susceptibility $\chi_\perp$ now measured versus H_y (compare with Fig. 32) in CuMn 4.7% for H_z = 0. Very good agreement is found with a purely unidirectional anisotropy energy (K_{ax} = 0, dotted line), while the data cannot be explained assuming the ratio K_{ax}/K_d given from $\chi_\perp$ experiments in the $\theta = 0$ and $\theta = \pi$ states (full line) (From Hippert, Alloul and Fert, 1982).

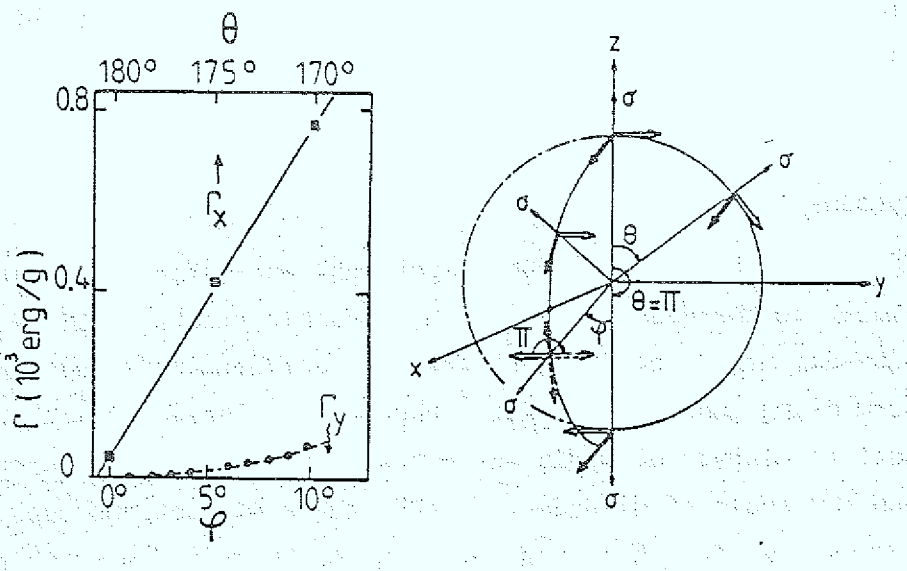

Fig. 35: Torque measurements in CuMn 20% at 1.5 K (Fert and Hippert, 1982). The torques Γ_x and Γ_y measured after a π rotation of $\vec{M}_r$ ($\equiv\vec{\delta}$) in the yz-plane are displayed. These two responses are quite different and point out the triad character of the anisotropy. The sequence of rotations during the torque experiment can be followed in the right part of the figure (From Alloul, 1983).

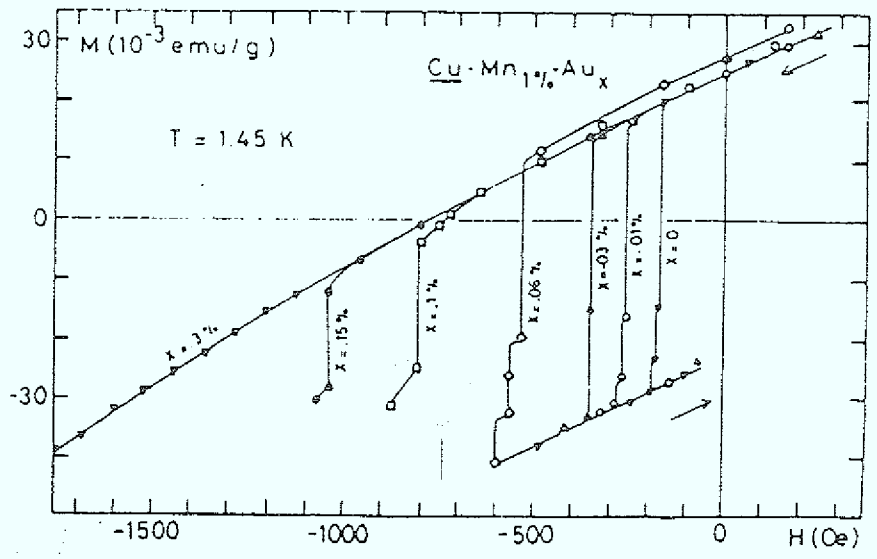

Fig. 36: Hysteresis cycles of various ternary CuMn 1%-Au_x spin glasses in low field. The remanent magnetization is obtained after removing a field of 18 kOe in which the sample was field-cooled down to 1.45 K. The time constants associated with the reversal increase with Au concentration x from ~1 sec for the more dilute to over hours for the most concentrated (From Prejean et al., 1980).

5.3 Excitations :

Here we focus attention to the low-temperature excitations in spin glasses and especially to the question about the possible existence of spin waves in spin glasses. Low-energy excitations in disordered materials in general are far from being understood. Waves (phonons in glasses) are expected to propagate in disordered media as long as their wavelength is much larger than the scale of disorder. However these excitations coexist at low temperature with other more or less localized modes which are still hard to characterize (two-level systems (Phillips, 1972; Anderson et al., 1972), fractons (Alexander et al., 1983)). In Heisenberg spin

glasses both magnons with a linear dispersion relation at long wavelengths (Halperin and Saslow, 1977) and diffusive modes (Dzyaloshinskii and Volovik, 1978) have been proposed from hydrodynamic approaches depending on the choice of order parameter and dissipative processes. The most sophisticated macroscopic theory is that of Fischer (1980); he uses both the hydrodynamic and gauge theory approaches and is able to calculate spin-wave damping. Walker and Walstedt (1980) and Walstedt (1981) present data from numerical simulations in a harmonic approximation for a dilute Heisenberg spin glass with RKKY interactions and obtain well defined oscillating modes within one of the many local energy minima. Most of these modes are fairly delocalized but not necessarily propagating. Sample-size limitations have further restricted the information from computer simulations especially at very low temperature.

Up to now the most meaningful tests of the validity of these approaches have come from comparison between measured and calculated values of the specific heat. From calculations of the density g(E) of spin excitations one can obtain the magnetic part $C_m(T)$ of the specific heat versus temperature at low T.

The magnetic specific heat, $C_m(T)$, of spin glasses exhibits three interesting features (see Fig. 2):

(i) A rather broad maximum at a temperature exceeding the spin-glass temperature T_f by about 30%. Typically, about one third of the total magnetic entropy is attained by the spin glass when $T = T_f$.

(ii) At temperatures below T_f, C_m varies approximately linear with T.

(iii) $C_m(T)$ is progressively reduced in a magnetic field.

These properties of $C_m(T)$ are observed in metallic (e.g. CuMn: Wenger and Keesom, 1976) as well as in insulating spin glasses ($Eu_xSr_{1-x}S$: Meschede et al., 1980), in spite of quite different types of magnetic couplings. The dependence (ii) at low T is not strictly linear. $C_m(T)$ can be represented as a power law in T with exponents ranging from 1.2 to 1.7 (Thomson and Thompson, 1981; Caudron et al., 1981), or alternatively several authors (Martin, 1979; Fogle et al., 1983; Sato and Miyako, 1982) suggest the relation $C_m(T) = c_1T + c_2T^2$ where c_1, c_2 are constants.

The occurence of a roughly linear T-term of $C_m(T)$ below T_f has been known for long, and in the early molecular-field theories was attributed to excitations of single spins submitted to essentially vanishing molecular fields (Wenger and Keesom, 1975). Convincing arguments that this can occur in Heisenberg spin-glasses with RKKY coupling have not been given. It reminds one to the linear specific heat of ordinary glasses which commonly is explained exclusively with the phenomenological concept of "two-level systems" introduced by Anderson et al. (1972) and Phillips (1972). Numerical studies by Walker and Walstedt (1977 and 1980) for classical spins and RKKY interactions demonstrate that in the cases of CuMn and AuFe spin glasses the linear term of $C_m(T)$ can be explained quantitatively (Fig. 37) by a high density of states of delocalized modes, i.e. magnon-like excitations of the spin system around either of its equilibrium configurations. For insulating spin glasses $Eu_xSr_{1-x}S$ the same conclusion is obtained by somewhat different numerical techniques of Krey (1980, 1981, 1982) and of Ching, Huber and Leung (1980). Hence, it is not necessary to refer to the speculation of "two-level centers" for an explanation of the linear specific heat of spin glasses, in contrast to ordinary glasses.

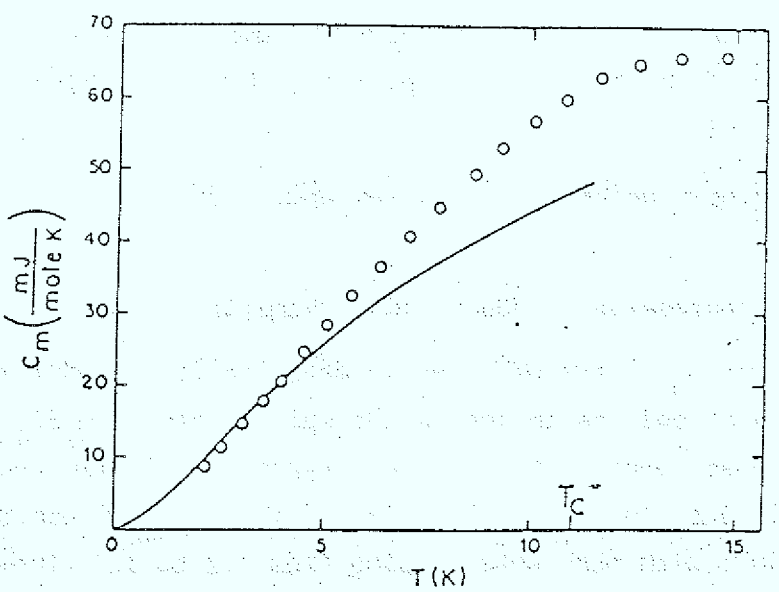

Fig. 37: Molar specific heat of a dilute RKKY-coupled spin-glass obtained by Walker and Walstedt (1977) by numerical simulations (solid curve). Circles are data for CuMn 1.2% spin glass from Wenger and Keesom (1976).

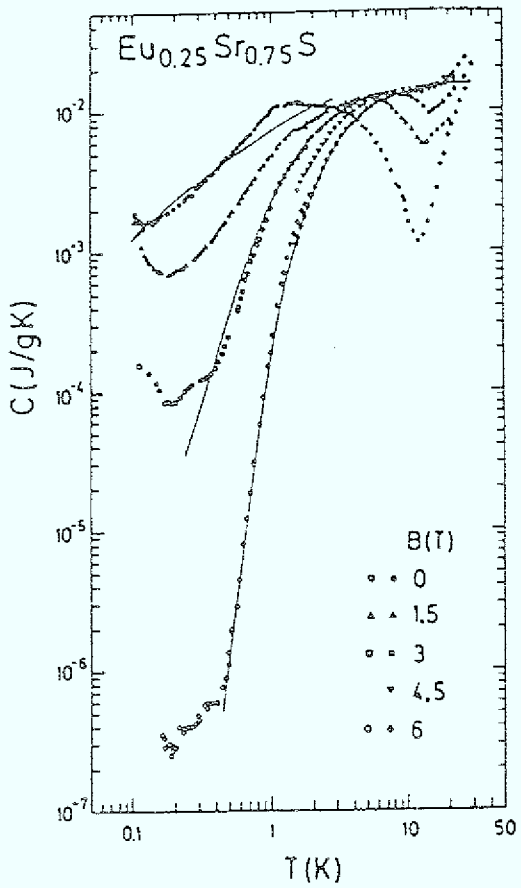

Fig. 38: Specific heat C of $Eu_{0.25}Sr_{0.75}S$ spin glass as a function of temperature T for various magnetic fields B between 0 and 6 T. Solid lines indicate the calculated specific heat by Krey for B = 0, 3, and 6 T (From Wosnitza et al., 1986).

In order to obtain further information about the magnetic excitations a comprehensive specific-heat study of $Eu_xSr_{1-x}S$ has been performed with x between 0.25 and 0.80 in magnetic fields up to 6 T (v. Löhneysen et al., 1985; Wosnitza et al., 1986). The experimental results agree quantitatively with recent numerical calculations by Krey (1985) who has extended his earlier calculations to high fields. Fig. 38 shows the specific heat C of the spin glass $Eu_{0.25}Sr_{0.75}S$ between 0.1 K and 30 K for various magnetic fields B between 0 and 6 T (Wosnitza et al., 1986) (The lattice contribution plays a negligible role at low T). A strong depression of C is found at lower temperatures, with a crossing-over towards higher T where C is increased in a magnetic field. The up-turn of C below 0.2 K towards low T is due to the nuclear specific heat contribution C_N arising from the hyperfine splitting of Eu^{151} and Eu^{153} nuclei (The apparent decrease of C_N with B is discussed by v. Löhneysen et al. (1985)).

The most interesting observation in Fig. 38 is the evidence for a gap in the excitation spectrum. The roughly linear T dependence of C in zero field below T_f = 0.8 K gradually turns steeper as the magnetic field is increased. For high fields, B > 3 T, however, the drop of C towards low T is quasi-exponential, indicating the opening of a gap (with energy ΔE) in the magnetic excitation spectrum at E = 0:

$$C_m(T) \propto \exp(-\Delta E/k_B T) \qquad (55)$$

$$E = g\mu_B(B - B_o(x)) \quad .$$

These data can be explained quantitatively, without any fit parameters (J_1 and J_2 are known), from a direct numerical calculation of the collective excitations of the system. In Krey's calculation (1985) the continued fraction method is used to obtain the density of magnon-like states, g(E), as displayed in Fig. 39 for various Eu concentrations at B = 6.6 T. The arrow denotes the Zeeman energy $E_B = g\mu_B B$. Treating the excitations as non-interacting bosons, i.e. in the RPA approximation, the magnetic specific heat C* per Eu atom is deduced from g(E) as

$$C^*/k_B = \int_0^\infty dE\, g(E) \left(\frac{E}{k_B T}\right)^2 \frac{e^{E/k_B T}}{(e^{E/k_B T}-1)^2} \quad . \qquad (56)$$

The solid lines in Fig. 38 represent some results of these calculations. The agreement with the experimental data is indeed excellent.

Three obvious trends of g(E) with Eu concentration x can be inferred from Fig. 39:

(i) With decreasing x, the energy range of g(E) shrinks, i.e. the upper band edge decreases.

(ii) Simultaneously, a pronounced peak appears around E_B.

(iii) Finally, the lower band edge is separated from E = 0 by an energy gap whose magnitude ΔE depends on B and x as found experimentally, eq. 55. The effective field $B_o(x)$ is negligible small for the ferromagnetic samples, $0.70 \leq x \leq 1.0$, whereas in the reentrant and spin-glass regimes, x 0.70, B_o increases with decreasing Eu concentration x.

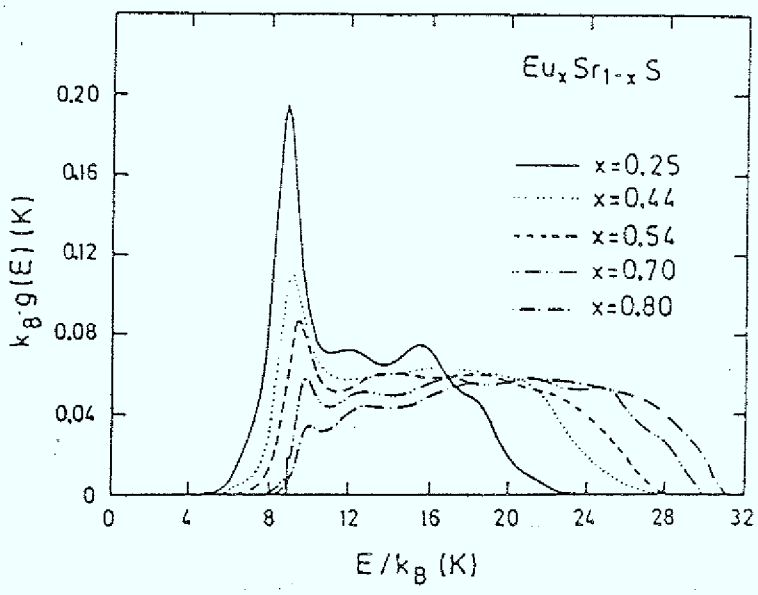

Fig. 39: Calculated spectral density of states g(E) per Eu atom for magnetic excitations in $Eu_xSr_{1-x}S$ for various concentrations x in a field of 6.6 T (Krey, 1985). The arrow indicates the Zeeman energy $E_B = g\mu_B B = k_B \cdot (8.87\ K)$ (From Wosnitza et al., 1986).

Hence, all these C_m data can be explained even quantitatively by dominant magnon-like excitations in (Eu,Sr)S spin glasses.

There have been other experimental attempts to study the nature of low-temperature excitations. Alloul and Mendels (1985) have recently measured the T dependence of the local magnetization in RKKY spin glasses (CuMn, AgMn and AuMn) for $T \lesssim 0.2\ T_f$, as obtained from the variation of the zero-field NMR frequency of Mn^{55}. It follows the T^2-dependence expected for magnon excitations with a linear dispersion relation, its spin-wave stiffness, however, does not agree with numerical estimates. Such an analysis implies, according to the authors, that the specific heat C(T) should be attributed to modes which do not contribute to the M(T) dependence. Obviously, more work is required to test this analysis and interpretation. Alloul et al. (1986) demonstrate that for $T \lesssim 0.1 \cdot T_f$ the T dependences of the local and macroscopic magnetization are quite identical within experimental accuracy, the latter being measured by the remanent magnetization M_r. The phenomena responsible for the time decay of M_r and its T dependence are shown to operate on completely different time scales. The authors speculate again on the nature of the excitations but the present data do not appear to be specific enough to distinguish between the various types of excitations.

Neutron scattering technique generally provides the most powerful probe of collective spin excitations. We recall that the cross section for magnetic neutron scattering from a system of N spins is given (Marshall and Lovesey, 1971) by

$$\frac{d^2\sigma}{d\Omega\, d\omega} = N\left(\frac{\gamma e^2}{mc^2}\right)^2 \frac{k'}{k_0}\left(S_s(q)\cdot\delta(\omega) + S_D(q,\omega)\right) \qquad (57)$$

where $S_s(q)$ is the static and $S_D(q,\omega)$ the dynamic structure factor, representing the elastic and inelastic/quasielastic scattering, respectively. The incident neutron beam with wavevector k_o is scattered to give a beam with wavevector k', with wavevector transfer $q = k_o - k'$ and energy transfer $\hbar\omega = \hbar^2/2m\cdot(k_o^2 - k'^2)$. The dynamic structure factor may be written in terms of the generalized susceptibility $\chi(q,\omega)$

$$S_D(q,\omega) \propto \frac{1}{1-\exp(-\hbar\omega/k_BT)} \cdot \mathrm{Im}\,\chi(q,\omega) \qquad (58)$$

which provides the information on spin dynamics. For a simple relaxational process with lifetime Γ^{-1} one measures a Lorentzian lineshape of the quasielastic line at $\omega = 0$ with

$$\mathrm{Im}\,\chi(q,\omega) \propto \frac{\omega\Gamma}{\omega^2+\Gamma^2} \quad , \qquad (59)$$

while for ferromagnetic ordering with propagating spin waves one obtaines two inelastic lines centered at $\omega = \pm\,\omega_q$ with the spectral shape function

$$\mathrm{Im}\,\chi(q,\omega) \propto \frac{\omega\Gamma}{(\omega-\omega_q)^2+\Gamma^2} + \frac{\omega\Gamma}{(\omega+\omega_q)^2+\Gamma^2} \qquad (60)$$

where Γ^{-1} is the lifetime of the spin waves, and the spin-wave dispersion is quadratic at low wavevectors q

$$\omega_q = D\cdot q^2 \quad . \qquad (61)$$

Neutron studies have been performed very extensively by Murani (see e.g. 1978b) on metallic spin glasses such as CuMn and reveal a distribution of relaxation times (see discussion in the next section). So far, no experimental evidence for spin-wave excitation exists in the typical metallic spin glasses. It is likely that in metals all modes are overdamped due to the strong Korringa relaxation of the spins to the conduction electron sea. In insulating spin glasses this mechanism is missing, and theories of the spin-glass dynamics might be more realistic.

In $Eu_xSr_{1-x}S$ considerable effort has been made in the seach for spin waves in spin glasses by neutron inelastic scattering technique (Maletta et al., 1981a; Maletta, 1982c). The idea in these experiments is to probe the dynamics of the spin-glass phase by studying the evolution of the spin waves from the ferromagnetic phase ($x \gtrsim 0.70$), where the dynamics are reasonably well understood, into the spin-glass phase. In a single crystal of pure EuS (enriched with ^{153}Eu to limit neutron absorption) the spin-wave dispersion over the whole Brillouin zone has been measured and analyzed by Bohn et al. (1980), the result is given in Fig. 6a. The anisotropy of the spin-wave energies in EuS, in spite of the high symmetry of the rocksalt crystal structure and the isotropic exchange interactions, stems from the fact that the predominant exchange interactions to the first (J_1) and second (J_2) nearest neighbors have opposite sign.

The measurements on $Eu_{0.70}Sr_{0.30}S$ (in powder form) which orders ferromagnetically below $T_c = 8.5$ K show well-defined spin-wave excitations at 4.5 K (Fig. 40a), and a quadratic form of the spin-wave dispersion at low q (eq. 61) similar to pure EuS. The stiffness constant D, related to the exchange constants in the non-diluted ferromagnet by the relation

$$D = 2a^2S\,(J_1 + J_2) \qquad (62)$$

is found to be $D = 1.1$ meV $\cdot$ Å^2 in $Eu_{0.70}Sr_{0.30}S$, as compared to $D = 2.5$ meV$\cdot$Å^2 in EuS at low temperatures (see insert in Fig. 40a). Thus, D decreases much faster than linearly with dilution. One should note that there is a non-negligible broadening of the inelastic line which is only partly due to powder averaging. Fig. 40a also demonstrates (see spectrum of $x = 0.70$ at $q = 0.6$ Å^{-1}) that one has to operate the spectrometer with a good energy resolution in order to resolve the inelastic line from the peak centered at $E = 0$.

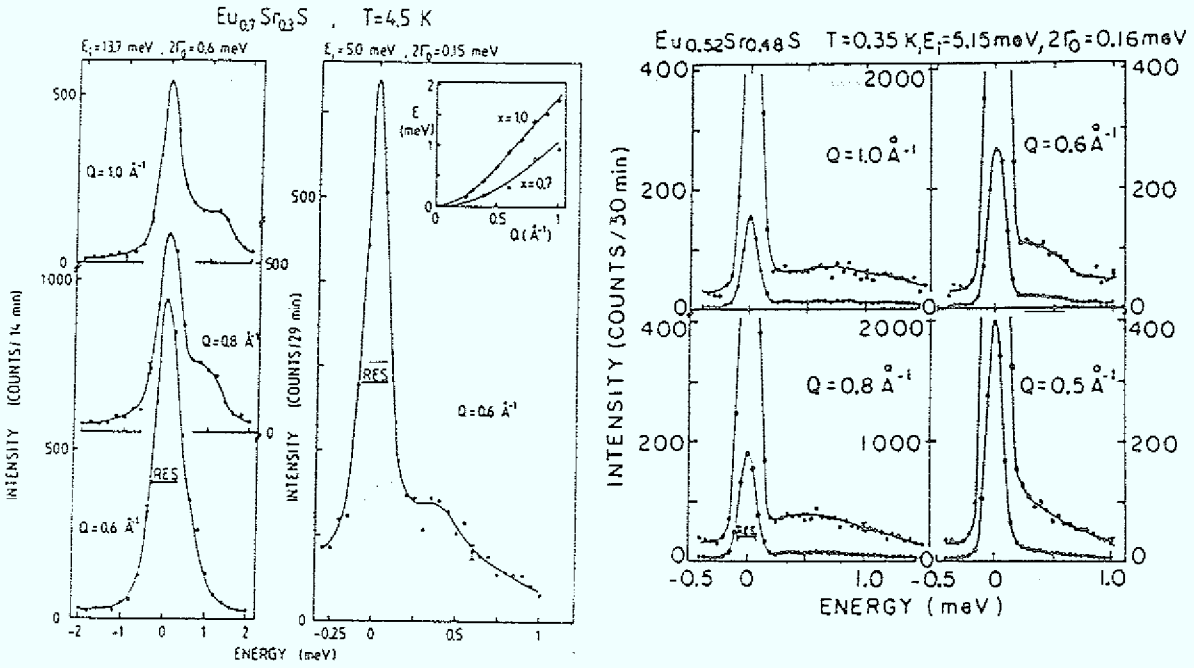

Fig. 40: Inelastic neutron spectra of $Eu_xSr_{1-x}S$ for various wave vectors q for (a) x = 0.70 at 4.5 K, and (b) x = 0.52 at 0.35 K. The insert in (a) shows the spin-wave dispersion E(q) for x = 1.0 and 0.70 (From Maletta, 1982c).

Fig. 40b displays spectra of $Eu_{0.52}Sr_{0.48}S$ measured for various wave vectors q at T = 0.35 K, i.e. in the spin-glass state. True inelastic scattering is present as evident by the asymmetry between the intensities for neutron energy gain ($E < 0$) and neutron energy loss ($E > 0$), i.e. the so-called detailed balance factor. As q decreases, the intensity shifts to lower energies consistent with the width of the distribution and position of the intensity maxima shifting to lower energies. At the same time, the intensity at E = 0 increases dramatically.

The difficulty in interpreting these data is deciding which form of Im $\chi(q,\omega)$ gives a better representation of the data. The physics implicit in the forms of eqs. 59 and 60 may be different but the spectra will look very similar at low temperatures: As described in eq. 58 the inelastic scattering intensity is proportional to Im $\chi(q,\omega)$ and to the Bose-Einstein factor, hence at low temperature if $\hbar\Gamma \gg k_B T$ the spectra will peak at a finite energy for <u>both</u> forms of Im $\chi(q,\omega)$ (eqs. 59 and 60). The authors convoluted the cross section using eq. 59 and 60 with the instrumental resolution function and performed a least-square fit to the data varying Γ, D and a normalization parameter. The χ^2 for the fit was slightly better using eq. 60. If one accepts the spin-wave like form for Im $\chi(q,\omega)$, a stiffness constant $D = 0.6 \pm 0.2$ meV $\cdot$ Å^2 for $x = 0.52$ is obtained formally, which is reasonable in magnitude compared with higher Eu concentrations. The line widths Γ obtained at high q are much broader than that expected for any powder broadening, and Γ decreases as q decreases. The additional strong intensity at $E = 0$ increases as q decreases. Only a small fraction of this is elastic incoherent scattering and background from the sample container and cryostat. Most of it is a true q dependent scattering with $E = 0$. Quite similar results are obtained with the spin-glass samples $x = 0.50$ and $x = 0.40$ at low temperatures where the inelastic scattering intensity is shifted to lower energies, thus the analysis is even more difficult.

The authors (Maletta et al., 1981a) prefer to attribute the inelastic lines to spin-wave like modes even in the spin-glass phase of (Eu, Sr)S. The accessible q-range, however, is restricted to large values $q \gtrsim 0.4$ Å^{-1} and the observed modes are highly damped. Probably these magnon-like excitations cannot be labelled by the quasi-momentum q, since one is dealing with a strongly disordered system. These modes are superposed by a quasielastic contribution centered at $E = 0$ with a high density of states attributed to diffusive modes of low energy. The results are in qualitative agreement with numerical model calculations by Krey (1981). As an example results for $x = 0.40$ for two directions of propagation are displayed in Fig. 41: the theoretical neutron spectra for [100] (and [110]) show a "ferromagnetic like" spin-wave dispersion, whereas there is no dispersion along [111]. See also the calculated spectral density of states g(E) for magnetic excitations in $Eu_xSr_{1-x}S$ in Fig. 39 and discussions there.

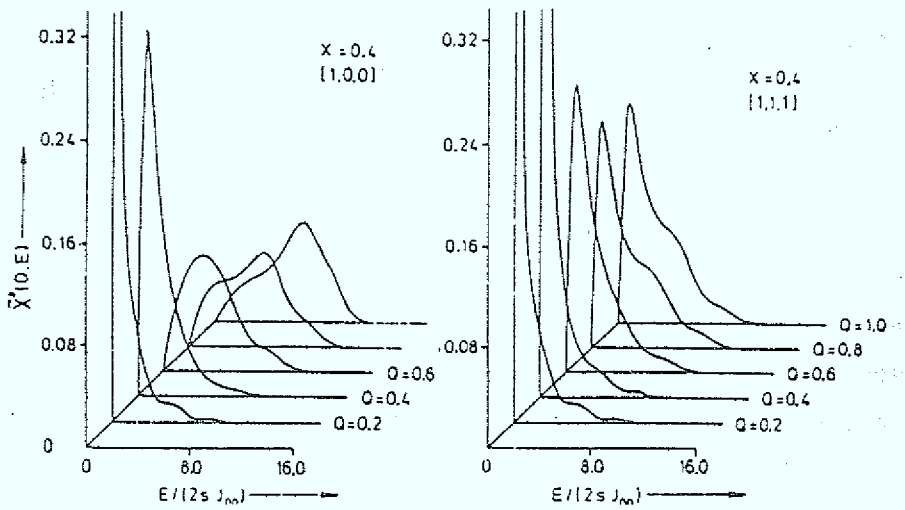

Fig. 41: Calculated neutron spectra for the $Eu_xSr_{1-x}S$ spin glass with $x = 0.40$ in two directions, $[100]$ and $[111]$ and for various wave vectors q at T = 0 K (From Krey, 1981).

6. Dynamics of spin-glass freezing

In spin glasses a freezing of spin motion occurs at low temperature in such a way that no conventional long-range magnetic order exists, as we have seen above. The upsurge of interest in spin-glass systems in the last decade appears to be related to two important events concerning this freezing process. First, the discovery by Cannella and Mydosh (1972) of a sharp maximum ("cusp") in the low-field, low-frequency ac-susceptibility of AuFe spin glasses at the spin-glass temperature T_f leads to the theoretical interpretation by Edwards and Anderson (1975) in terms of a new kind of phase transition in such disordered systems. The second event, the observation of a particularly complicated spin dynamics near T_f seems to contradict the concept of a phase transition. Experimental studies on the spin freezing reveal a wide spectral distribution of relaxation times (Murani and Heidemann, 1978c) extending even to macroscopic times around T_f (Maletta, Felsch and Tholence, 1978a; Maletta and Felsch, 1979b). At present, however, the lack of corresponding reliable analytic theories hampers the interpretation of these and similar experiments. In this section, we will present data from different experiments which in principle might provide detailed insight into the dynamics of spin-glass freezing. Subsequently in sec. 7 attempts to interpret data at the transition into the spin-glass state in terms of a phase transition will be discussed.

6.1 Time dependent susceptibilities:

One of the most prominent methods to study the onset of spin-glass freezing remains the low-field ac-susceptibility χ. Since the observation of a "sharp cusp" in $\chi(T)$ at T_f of AuFe alloys in 1972, an ac mutual inductance technique is commonly used to measure $\chi(T)$ and to determine T_f, with a very small driving field (< 1 Oe) and a rotation-frequency (normally < 100 Hz) which should be large enough to prevent the appearance of long-time metastable effects. Thus the reversible susceptibility (see eq. 38) is generally believed to be measured by this ac-χ method, due to the long-time scale of the irreversible behavior especially in small fields.

One often also describes the different susceptibilities (see sec. 5.1) phenomenologically by means of the picture of the many-valley structure of free energy in phase space (Fig. 15): The ac-χ measures the response of only one valley, whereas field-cooling is believed to correspond to averaging over all available states. These interpretations have to be taken with great precautions, as we will discuss below.

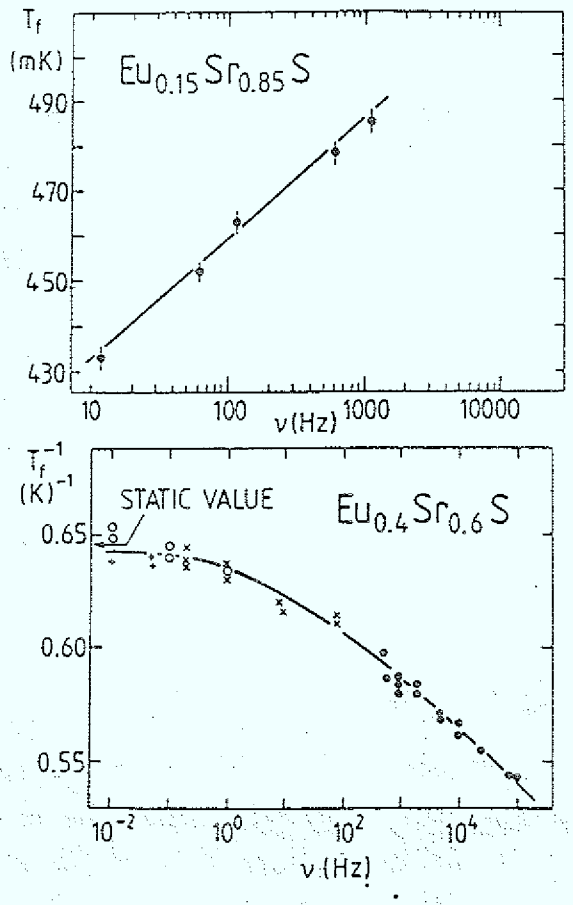

Fig. 42: Frequency dependence of the temperature T_f for the spin glasses $Eu_xSr_{1-x}S$ with x = 0.15 (Maletta and Felsch, 1978b) and x = 0.40 (Ferré et al., 1981). $T_f(\omega)$ is determined from ac-susceptibility measurements at various measuring frequencies ω.

In 1978 Maletta et al. (1978a, 1979b) discovered the frequency dependence of T_f in (Eu, Sr)S spin glasses measured in a series of ac-χ experiments with various measuring frequencies ω. As an example the result of $Eu_{0.15}Sr_{0.85}S$ is shown in Fig. 42a where a 15% increase of T_f is found by going from 10 Hz to 1000 Hz. Such a behavior is also observed in (LaGd)Al_2 spin glasses (v. Löhneysen et al., 1978a). It is less pronounced in other metallic spin glasses like CuMn (Tholence, 1980; Mulder et al., 1981), but up to now at least a small frequency shift of χ in the range 1 Hz to 1 kHz has been measured for most spin glasses.

The frequency dependence in spin glasses cannot be explained with the simple picture of thermal blocking of superparamagnetic clouds, eq. 46, as already discussed in sec. 5.1. Ferré et al. (1981) pursued the time effect on T_f over 7 decades of frequency in $Eu_{0.40}Sr_{0.60}S$ (Fig. 42b) by means of Faraday rotation measurements. One realizes in Fig. 42b that now over such a broad frequency range even a formal description of $T_f(\omega)$ with eq. 46 does not work. The data are also incompatible with the Vogel-Fulcher law where one substitutes $T_B(\omega)$ in eq. 46 by $(T_B(\omega) - T_o)$. The law is proposed by Tholence (1980b) to apply to $T_f(\omega)$ in spin glasses but the meaning of T_o remains unclear. This phenomenological relation has long been known in the literature devoted to viscous fluids and glasses.

It is quite interesting, however, that the pronounced $T_f(\omega)$-effect in insulating spin glasses can be used to determine the limits in concentration of the spin-glass regime of a dilution system, as already shown in $Eu_xSr_{1-x}S$ (Maletta, 1981b) where spin-glass freezing is distinguished experimentally from superparamagnetic blocking. Very recently, Börgermann et al. (1986a,b) established the phase diagram of $Eu_xSr_{1-x}Te$ (Fig. 7b) in a similar way. The frequency shift of T_f, $\delta T_f(\omega)$, within the spin-glass regime is found to be equal in both systems, $Eu_xSr_{1-x}S$ and $Eu_xSr_{1-x}Te$: It is independent of the Eu concentration x and even equal in magnitude, $\delta T_f(\omega) \simeq 30$ mK per ω-decade within the frequency range displayed in Fig. 43 (compare with Fig. 42).

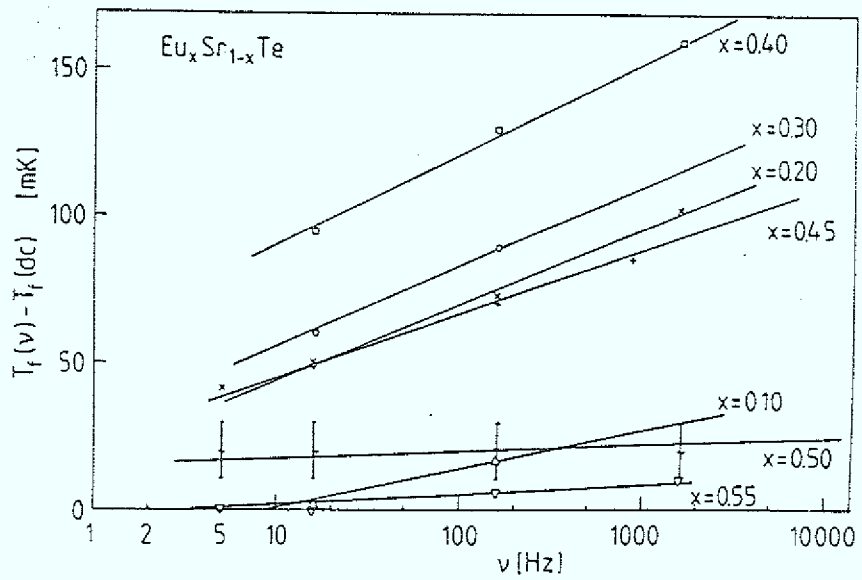

Fig. 43: Frequence dependence of T_f for $Eu_xSr_{1-x}Te$ with various Eu-concentrations x (From Börgermann et al., 1986b).

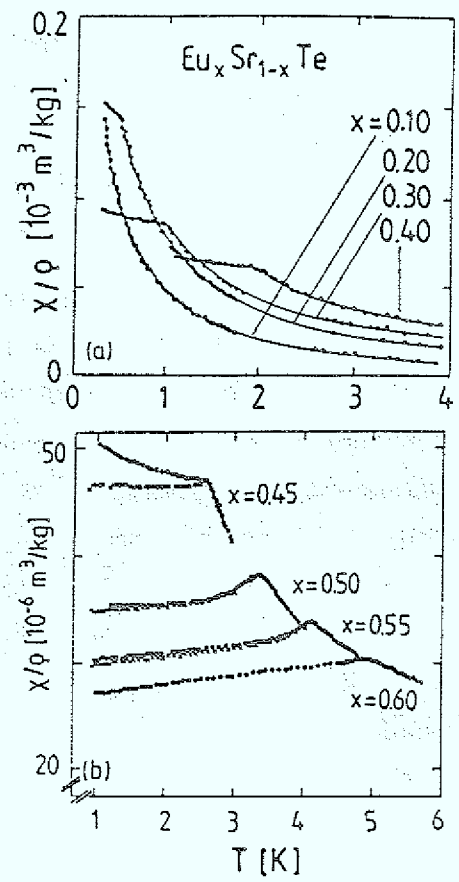

Fig. 44: Static susceptibility (χ = M/H) data vs. T for $Eu_xSr_{1-x}Te$ with various Eu-concentrations x: (a) Field-cooling χ in the earth's magnetic field (0.05 mT); (b) χ in 0.15 mT for "ZFC" (X: after cooling in 0.05 mT) and for FC (● : in 0.15 mT). The "ZFC" and FC curves coincide for x = 0.60 (From Börgermann et al., 1986a).

For Eu concentrations x above 0.50, $Eu_xSr_{1-x}Te$ shows $\delta T_f(\omega) \simeq 0$ (Fig. 43) which coincides with the disappearance of irreversibilities (FC- and ZFC-magnetizations) as can be seen in Fig. 44. Obviously these samples order antiferromagnetically. At low Eu concentrations, i.e. below the percolation threshold $x_p = 0.13$, the x = 0.10 compound for example exhibits no anomaly in dc-M(T) (the lowest temperature of measurement was 20 mK) but an ac-χ(T) maximum at 150 mK for 5 Hz with a smaller $\delta T_f(\omega)$ compared to the spin-glass regime, which now can be explained quantitatively with eq. 46 similar to the $Eu_xSr_{1-x}S$ superparamagnetic compounds below $x_p = 0.13$ (Eiselt et al., 1979). Such type of experiments obviously provides evidence for the collective character of spin-glass freezing around T_f (Maletta, 1981b).

The unique properties of $\delta T_f(\omega)$ described above are a challenge to get more insight into the dynamics of spin-glass freezing. At present, however, no theory is available to be compared with. Nevertheless the data already demonstrate the essential role played by the competing exchange interactions (frustrations) in producing the $\delta T_f(\omega)$ of spin glasses, because $Eu_xSr_{1-x}Te$ is based on the antiferromagnet EuTe (with $J_2/J_1 \simeq -2/1$) and $Eu_xSr_{1-x}S$ on the ferromagnet EuS (with $J_2/J_1 = -1/2$). Thus, it is misleading to consider $T_f(\omega)$ as a "cluster property" (Fischer, 1985) since clusters are expected to be x-dependent and different in diluted ferro- and antiferromagnets. Apparently, the competing exchange interactions within the infinitely connected network of magnetic moments at the Eu ions create a constant frustration effect on spin dynamics in dilution systems above the percolation threshold, independent of concentration x as long as J_2/J_1 stays constant. The only necessary condition is a sufficiently high disorder (together with the frustration effects) in order to destroy long-range periodic magnetic order (Note that the competition of J_1 and J_2 has no essential influence on magnetic ordering in the pure systems, x = 1). Obviously, both dilution series, $Eu_xSr_{1-x}S$ and $Eu_xSr_{1-x}Te$, exhibit an even quantitatively comparable behavior due to the same magnitude of competition relative to the different dominating exchange $J_1 (> 0)$ and J_2 (< 0), respectively. It seems to us that competition in the exchange interactions is generally weaker in metallic spin glasses, consistent with a smaller frequency dependence of T_f.

Particularly valuable information on the dynamics of spin-glass freezing has recently been gained by experiments where both the real and imaginary component (χ', χ'') of the complex susceptibility $\chi(T,\omega)$ have been measured accurately. As regards metallic spin glasses, eddy currents in the material easily obscure an accurate observation of χ''. Such measurements, however, have been possible mainly for insulating spin glasses (Lundgren et al., 1981; Hüser et al., 1983b; Paulsen et al., 1984; Rajchenbach and Bontemps, 1983; Baumann et al., 1984; Wenger, 1983; Paulsen et al., 1986a and b).

The magnitude of the imaginary part χ'' of the complex susceptibility only amounts to a few percent of χ', but χ'' is directly indicative of the spectral distribution of relaxation processes because it singles out processes with relaxation times around the measurement time $\tau_m = 1/\omega$. In contrast, the real part χ' integrates over all relaxation processes which are fast compared with $\tau_m = 1/\omega$ and, therefore, is rather inconspicuous.

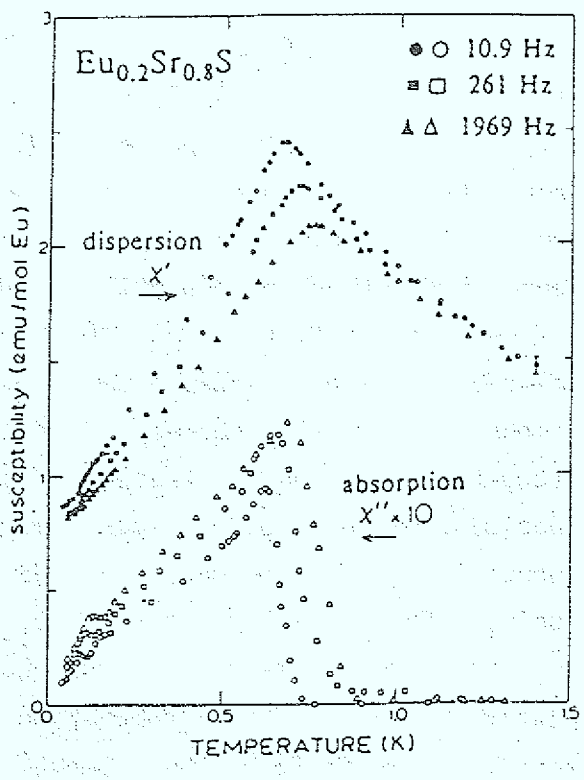

Fig. 45: Temperature dependence of the real (χ') and imaginary (χ'') part of the ac-susceptibility for $Eu_{0.20}Sr_{0.80}S$ spin glass with various frequencies (From Hüser et al., 1983b).

The complex susceptibility, $\chi(T,\omega)$, of the $Eu_{0.20}Sr_{0.80}S$ spin glass is shown in Fig. 45 as function of temperature for three different frequencies (Hüser et al., 1983b). At the highest temperatures, $T \gtrsim 1$ K, no difference is observed in the dispersion (χ') for the various measuring frequencies within the experimental accuracy. This feature plus the absence of any absorption (χ'') indicates the measured χ' is the isothermal susceptibility, χ_T, i.e. the spin system is in thermodynamic equilibrium. On cooling one observes a nonzero absorption signal starting at the higher frequencies. Similarly, deviations in the dispersion signal from χ_T are evidenced. We also note that the temperature of the inflection point of $\chi''(T)$ corresponds to the temperature T_f of the $\chi'(T)$ maximum for each measuring frequency. Both features shift to higher temperatures with increasing frequency.

If the magnetization would relax with a single relaxation time τ, the frequency dependences of χ' and χ'' could be expressed by the Casimir and du Pré (1938) equations:

$$\chi'(\omega) = \chi_s + \frac{\chi_T - \chi_s}{1+\omega^2\tau^2}$$

$$\chi''(\omega) = \omega\tau\,\frac{\chi_T - \chi_s}{1+\omega^2\tau^2} \qquad (63)$$

where χ_T is the isothermal susceptibility in the limit $\omega \to 0$ and χ_s the adiabatic one in the limit $\omega \to \infty$. Already from the results described above, however, one expects the relaxation of the magnetization in spin glasses to be governed by a distribution of relaxation times rather than a single one. Then, following Lundgren et al. (1981) the equations (63) are generalized and one obtains for instance

$$\chi''(\omega) = \frac{1}{h_o}\int_{\tau_{min}}^{\tau_{max}} \frac{m_o(\tau)\,\omega\tau}{1+\omega^2\tau^2}\, g(\tau)\, d\ln\tau \qquad (64)$$

which reduces in the spin-glass state ($\tau_{min} \ll 1/\omega \ll \tau_{max}$) to

$$\chi''(\omega) \approx -\frac{\pi}{2} \cdot \frac{m_o(1/\omega)}{h_o} g(1/\omega). \qquad (65)$$

$m_o(\tau)$ is the magnetization of the magnetic entities with relaxation time τ in the field h_o and in the limit $t \to \infty$; $g(\tau)$ their spectral distribution function and $m_o(\tau)g(\tau)$ their spectral weight. In order to reduce eq. 64 to eq. 65 one has to assume that

$$m_o(\tau)g(\tau) \approx \text{const} \qquad (66)$$

around the measuring frequency $\omega = 1/\tau$. Hence, in this approximation $\chi''(\omega)$ is directly proportional to the spectral weight of relaxation processes with relaxation times $\tau = 1/\omega$ (eq. 65). In a more complete treatment and using the same assumption, Lundgren et al. (1981) also obtain

$$\chi'' \approx -\frac{\pi}{2} \cdot \frac{\partial \chi'}{\partial \ln \omega} \quad . \qquad (67)$$

Relation (67) can be used to test the applicability of the approximation in eq. 65, and indeed good agreement is obtained with various samples (Lundgren et al., 1981; van Duyneveldt and Mulder, 1982; Baumann et al., 1984; Paulsen et al., 1986a and b). We will come back to this point in sec. 7.1.

Thus, the absorption data $\chi''(T,\omega)$ provide important information about the relaxation spectrum of the freezing process in spin glasses. In Fig. 46 such data of the $Eu_{0.46}Sr_{0.54}S$ spin glass are compiled in dependence of temperature and frequency on a logarithmic scale (Baumann et al., 1984). The measurements were performed in the frequency range 10 Hz to 50 MHz, the earth's magnetic field was compensated; however the results were not corrected for demagnetization effects which should have been done. At high temperatures, $T > T_f = 2$ K, the main part of the spectral

weight is concentrated in the high-frequency relaxations. On cooling these relaxations shift to lower frequencies, their spectral weight function decreases and seems to broaden. Low-frequency relaxations suddenly appear in a narrow temperature interval on approaching T_f from above. Obviously, at least these low-frequency relaxations are incompatible with an Arrhenius-type description (eq. 45). It is reasonable to assume that their appearance around T_f is due to the collective nature of the freezing process.

In summary, the relaxation time spectrum in spin glasses is broad already above T_f, and it dramatically broadens at T_f, extending even to macroscopic times. This seems to occur in all spin glasses which have been studied by this technique so far. Hüser et al. (1983) and Wenger (1983) try to analyze their data quantitatively via a plot of χ'' versus χ' with ω as a parameter which is a generalization of the "Cole-Cole plot" or the "Argand diagram" but no more informations could be deduced as already described above by means of Fig. 46 and eq. 65.

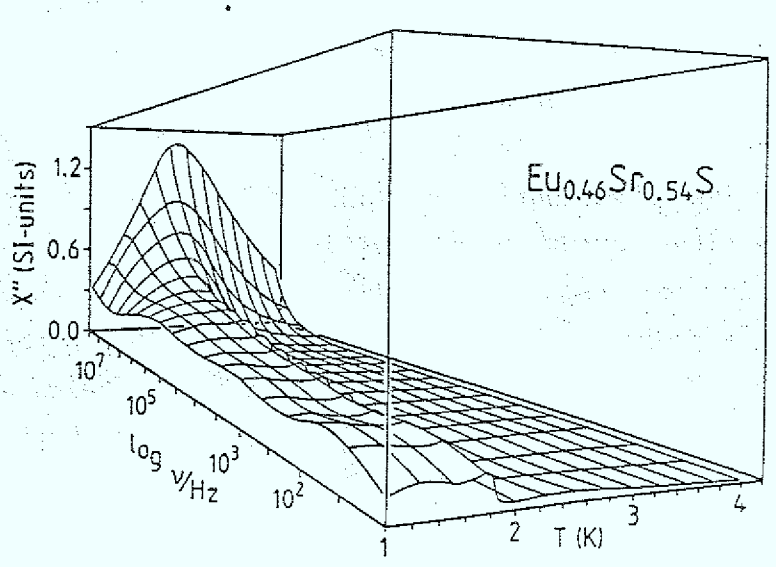

Fig. 46: Absorption χ'' in dependence of temperature and frequency, obtained from a fit to the measured data of the spin glass $Eu_{0.46}S_{0.54}S$ (From Baumann et al., 1984).

6.2 Inelastic neutron scattering :

In the study of spin-glass phenomena during the last years neutron scattering measurements have made important contributions to our knowledge of spin glasses. First of all, elastic neutron scattering is an invaluable tool for asserting that conventional periodic long-range order in the spin system is really absent (see point (b) of the defining properties of a spin glass in sec. 2.1). Inelastic magnetic neutron scattering techniques provide information about elementary spin excitations (see sec. 5.3) or via the quasielastic line $S(q,\omega)$ around $\omega = 0$ (eq. 58, 59) about spin relaxations. Typical results from this latter method will be presented now, and we emphasize that in the limit $q \to 0$ $\chi(q,\omega)$ in the cross-section eq. 58 reduces to the dynamic susceptibility discussed just above. Finally, measurements on the neutron spin-echo spectrometer will be reviewed where one measures directly the time correlation function.

Results of a detailed neutron scattering study of the metallic spin glass CuMn 8% by Murani and Tholence (1977) are given in Fig. 47. Spectra at four different temperatures are shown for various wave vectors q ($\mathring{A}^{-1}$) obtained on a time-of-flight spectrometer using a constant-q interpolation technique. Neutrons of incident energy 3.0 meV ($\lambda = 5.14$ $\mathring{A}$) were selected by a multichopper system with an elastic energy resolution (FWHM) of 230 μeV. The spectra consist of a strong elastic line superposed over a broad quasielastic structure as shown on the reduced scale. The solid lines through the data points in Fig. 47a represent the Lorentzian fits (eq. 59) to the quasielastic scattering intensity. Using the results of these fits the integrated elastic and quasielastic cross-section as well as their sum (given as total cross-section) have been determined as shown in Fig. 47b. Note that the elastic scattering begins to increase markedly with decreasing temperature below about 75 K, where simultaneously the quasielastic cross-section begins to diminish. In comparison, the temperature of the ac susceptibility peak is $T_f = 39$ K.

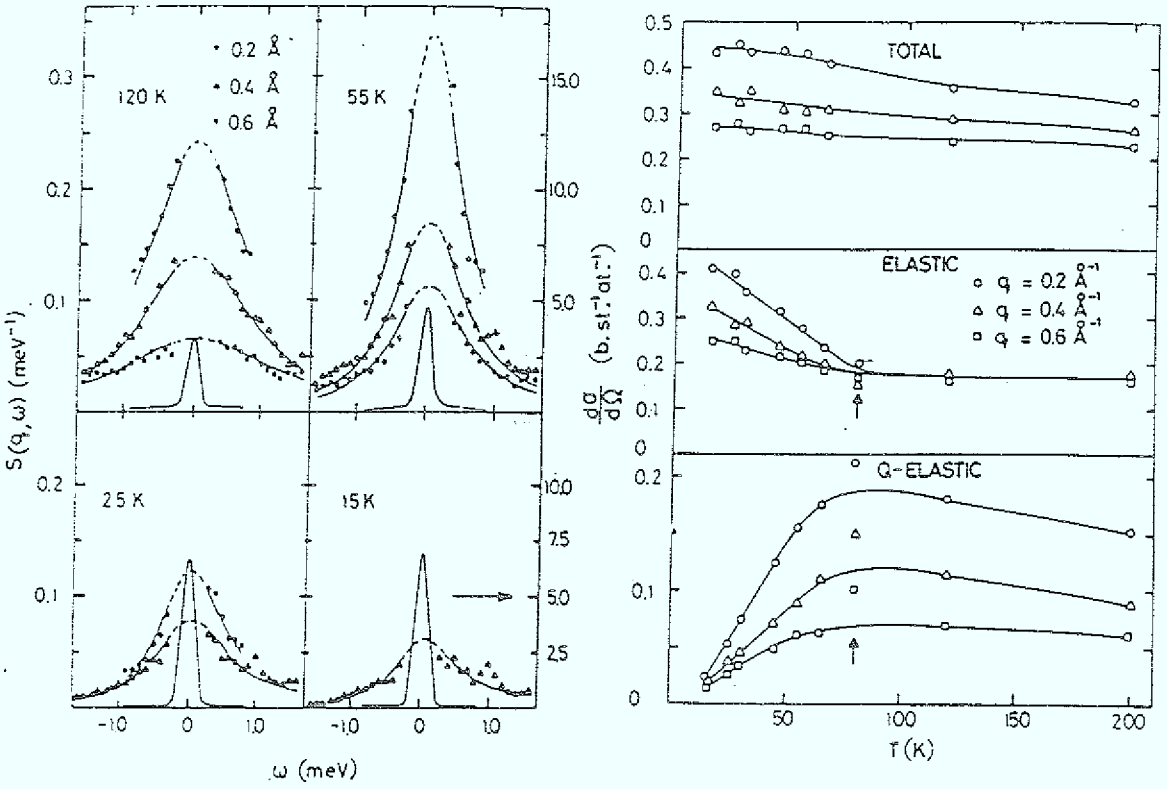

Fig. 47: Neutron scattering data of CuMn 8at%: (a) Spectra $S(q,\omega)$ vs. energy $\hbar\omega$ for various q_0-values at four different temperatures. The solid lines through the data points represent the Lorentzian fits to be quasielastic scattering. (b) The scattering cross-section, $d\sigma/d\Omega$, as a function of temperature is given for the total, the elastic, and the quasielastic scattering from data in (a). The vertical arrows indicate the temperature where marked changes in the cross-sections become evident (From Murani and Tholence, 1977).

Two essential remarks, however, should be added to this analysis which are related to each other. We have seen above in sec. 6.1 that with decreasing temperature a whole spectrum of relaxation times develops. Therefore, fitting the quasielastic line by a simple Lorentzian becomes inadequate near T_f. Indeed, this has been demonstrated by Murani (1978a) who measured CuMn spin glasses of various Mn concentrations over a much broader energy range. Examples for a small $q = 0.08\ \text{Å}^{-1}$ in Fig. 48 clearly reveal strong deviations from a

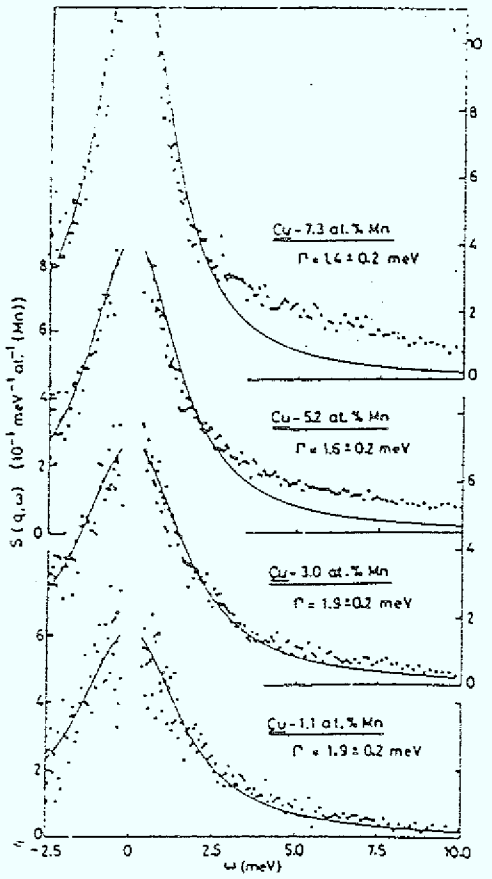

Fig. 48: Neutron scattering spectra, $S(q,\omega)$, vs. energy $\hbar\omega$ for q = 0.08 $\mathring{A}^{-1}$ at T = 300 K, for CuMn alloys with Mn concentrations as indicated. The data points for elastic scattering are not shown in the figure. The continuous curves represent the best fits to the data using the Lorentzian form. Note the progressive narrowing of the spectra accompanied by increasing deviation from the fits in the high-energy wings with increasing concentration (From Murani, 1978a).

simple Lorentzian spectral function already at high temperature, T = 300 K. The only exception is the spectrum for the 1.1 at% Mn alloy where obviously the description with a single relaxation time works at high temperature. The problem of a proper description of the spin relaxation spectrum is even worse in metallic spin glasses where the Korringa relaxation of isolated spins mediated via their exchange coupling with the conduction electrons overlaps in an unknown fashion with the relaxation spectrum due to the solute-solute

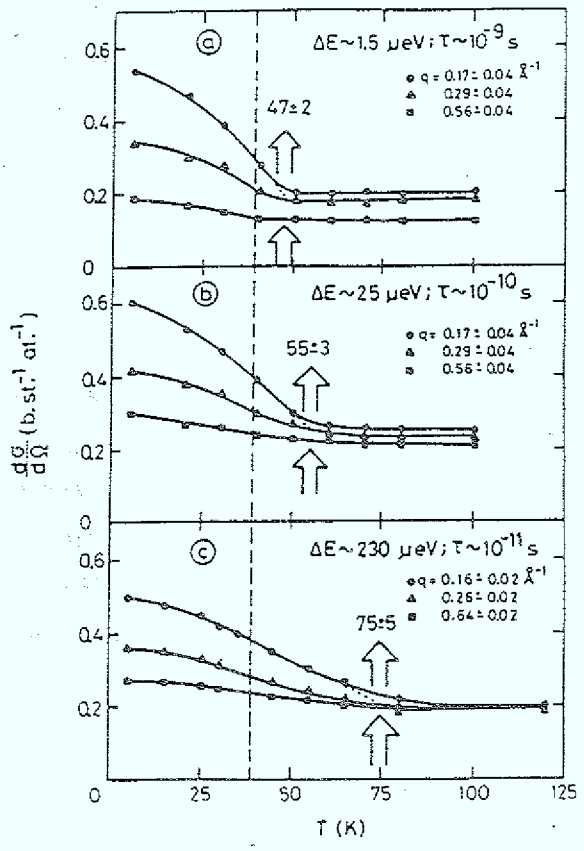

Fig. 49: "Elastic" scattering cross-section vs. temperature for various q-values in CuMn 8at%, employing different energy resolutions: (a) Results from IN10 meausrements with elastic energy resolution $\Delta E \sim 1.5$ μeV. (b) Total intensity within an energy window $\Delta E \sim 25$ μeV centered about $\omega = 0$ in the IN10 measurements. (c) Results from the IN5 time-of-flight measurements with elastic energy resolution $\Delta E \sim 230$ μeV. The arrows indicate the temperatures where marked increases in the cross-sections begin. The dashed line marks the temperature of the ac susceptibility peak, measured with a time constant $\tau \sim 10^{-2}$ sec. The statistical errors are smaller than the size of the data points and the curves are drawn to guide the eye (From Murani and Heidemann, 1978c).

exchange interactions (Murani, 1978 a and b). The first mechanism if separated leads to a Lorentzian form, eq. 59, with a single q-independent relaxation time $\tau = h/\Gamma$.

The second severe difficulty in the analysis of neutron spectra of spin glasses is the separation of the elastic scattering from the inelastic/quasielastic scattering contribution, which is limited by the finite instrumental energy resolution. This has special relevance for spin glasses where with the evolution of correlations in the spin system with decreasing temperature a whole spectrum of relaxation times develops. A neutron spectrometer with energy resolution ΔE_0 can only resolve processes with the longest relaxation times τ_0 given by $\tau_0 = h/\Delta E_0$, the rest with times longer than this would be indistinguishable from the truly elastic processes. It is obvious therefore that the apparent "elastic" scattering cross-section will depend on the instrumental energy resolution. This is clearly borne out by measurements of Murani and Heidemann (1978c) as shown in Fig. 49. The temperatures, indicated by arrows in the figure, where the marked increase of the elastic scattering cross-section occurs depend strongly on the energy resolutions (ΔE) employed and hence on the measurement time constant $\tau = h/\Delta E$. All these temperatures, however, are systematically higher than the temperature T_f of the maximum of the ac-χ (time constant $\tau = 10^{-2}$s) shown by the dashed vertical line in Fig. 49.

In conclusion these measurements again have indirectly shown the presence of a wide spectrum of relaxation times near the spin-glass temperature (Murani, 1981). The elastic magnetic scattering in the cross-section, eq. 57, of neutron scattering is formally related to the Edwards-Anderson order parameter q_{EA}

$$q_{EA} = \left[\langle S_i \rangle_T^2 \right]_{av} = \frac{1}{N} \sum_q \left(S_S(q)/2F^2(q) \right) \qquad (68)$$

where F(q) is the magnetic form factor. Due to the finite measurement-time constant of any spectrometer, however, q_{EA} is not accessible (Murani and Heidemann, 1978c), i.e. a decision about the existence of an equilibrium spin-glass state with this type of order parameter is impossible by these techniques.

The neutron-spin-echo (NSE) spectrometer invented by Mezei in 1971 detects the velocity change of the neutrons through the sample (inelastic scattering) by measuring the angle of the polarized neutron spins Larmor precessed around the external field. This spin-echo technique was used to decouple the energy resolution from the momentum resolution. Thus, one can look at much longer times, down to 5×10^{-9} sec (higher energy resolution), without the loss of intensity inherent in conventional neutron techniques. The NSE-machine also has the advantage of measuring the spin auto-correlation function directly in the time domain which is the Fourier transform of $S(q,\omega)$ measured in conventional neutron spectroscopy:

$$s(q,t) = \int_{-\infty}^{\infty} \frac{S(q,\omega)\cos\omega t}{S(q)} \, d\omega \qquad (69)$$

Here $S(q) = \int_{-\infty}^{\infty} S(q,\omega)\, d\omega$ reflects the short-range order. By definition $s(q,t=0) = 1$. This technique gives also information (in contrast to μSR) on the spatial correlations (Mezei, 1983)

$$S(q,t) = S(q)\cdot s(q,t) \quad . \qquad (70)$$

It has been shown that the ac susceptibility and the function in eq. 70 are related in a good approximation for relaxation type dynamics by the equation (Mezei, 1981):

$$\chi(\omega) \propto \lim_{q\to 0} \frac{1}{kT} S(q)\cdot(1-s(q,t)) \qquad (71)$$

where $t = 0.7/\omega$. This equation has a simple physical meaning: $(1-s(q,t))$ is the fraction of the magnetic moments which can respond to an external field within time t.

Up to now it has been applied to three different spin glasses: CuMn with 1 % and 5 % (Mezei and Murani, 1979; Mezei, 1982), $La_{0.7}Er_{0.3}Al_2$ (Mezei, Murani and Tholence, 1983), and $Eu_xSr_{1-x}S$ with $x = 0.40$ and $x = 0.54$ (Shapiro, Maletta and Mezei, 1985).

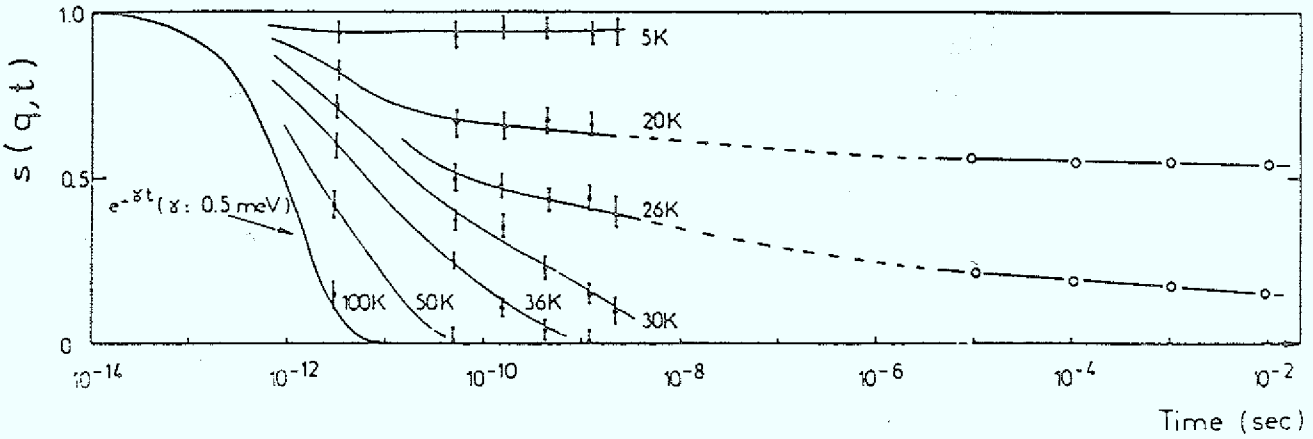

Fig. 50: Spin relaxation in Cu Mn 5at% spin glass at various temperatures. Data points at times shorter than 10^{-8} sec were directly measured by neutron-spin-echo technique at q = 0.093 $\mathring{A}^{-1}$ (Mezei and Murani, 1979), those beyond 10^{-6} sec were calculated from ac susceptibility results (Tholence, 1980). The lines are guides to the eye only (From Mezei, 1983).

Fig. 50 shows the result for the spin glass CuMn 5 % ($T_f \approx 27$ K) by Mezei and Murani (1979) where the time-dependent correlation function s(q,t) is plotted on a logarithmic scale. The thick continuous curve represents a simple exponential decay function, exp $(-\Gamma t)$ for Γ = 0.5 meV, whereas the thinner lines are drawn to indicate the trend of the points. The data are found to be independent of q in the measured range 0.04 $\mathring{A}^{-1} < q < 0.4$ $\mathring{A}^{-1}$, thus the results in Fig. 50 indeed represent the spin autocorrelation function $\zeta(t) = s(q,t)$. Data points beyond 10^{-6}s were calculated from ac-χ measurements. It is remarkable that at $T_f \approx 27$ K (from ac-χ measurement) at least half the spectral component has relaxation times below 10^{-9} sec and that this fraction decreases slowly below T_f. The time-decay is distinctly slower than exponential already above and below T_f, indicating again a broad distribution of relaxation times which extend progressively to longer times with decreasing temperature. (It should be noted that on such a diagram a simple exponential function always maintains the same shape being only replaced laterally for different values of Γ). At longer times the data can be approximated by a straight line in the plot which corresponds to

$$\zeta(t) \propto \text{const} - \ln t \qquad . \qquad (72)$$

The authors of this experiment (Murani, 1981; Mezei, 1983) interpret their results as a clear evidence that the freezing in spin glasses is a purely dynamical gradual process, without any static phase transition.

In contrast, Heffner et al. (1984) argue that the same data (Fig.50) can as well be fitted to the form

$$\xi(t) \propto \text{const} + t^{-\nu} \qquad (73)$$

where the exponent $\nu \approx 1/4$ near T_f, and $\nu \approx 1/2$ for $T < T_f$. Curiously, the neutron-spin-echo data on the other sample, CuMn 1%, still yield $\nu \approx 1/2$ near T_f. The constant in this form (73) is non-zero only below T_f and thus would imply a truly static ordering.

Results from neutron spin-echo measurements on the insulating $Eu_xSr_{1-x}S$ compounds will be described briefly in sec. 8.

Remember that simulations of the nearest-neighbor two-dimensional Ising spin glass (Binder and Schröder, 1976) yield logarithmic time-decay of the spin auto-correlation function while for the infinite-range three dimensional Ising spin glass Kirkpatrick and Sherrington (1978) find a power-law decay with an exponent $\nu = 1/2$. Sompolinsky and Zippelius (1981 and 1982) also obtain a power-law decay for the Heisenberg spin glass with infinite-range random exchange interactions at and below T_f (see eq. 31).

Very recently, Murani (1985) again started the attempt to study the spin auto-correlation function and to see whether the infinite-range mean-field model may have direct application to relaxation dynamics in real spin-glass systems. He measured the CuMn 3 % spin-glass alloy using unpolarized neutron-scattering techniques, namely the conventional time-of-flight spectrometer and the more sophisticated backscattering spectrometer. Both these techniques permit measurements over a wide q-range. The slight disadvantage of the shorter time range covered by these "classical" techniques (8.8×10^{-9}s) compared to the neutron spin-echo method (5×10^{-9}s) is compensated by the greater statistical accuracy of the data, due to the higher neutron intensity using un-

polarized neutrons and due to integrating over this wide q-range in order to obtain the correlation function. Murani shows in the paper that within a reasonable approximation for spin glasses the time correlation function $\xi(t)$ can be determined by these techniques from the "elastic" component using various energy resolutions ΔE. There is a direct relationship between the "elastic" scattering contribution, measured with finite resolution ΔE, and the local or auto-correlation function $\xi(t)$ at time $t = 1/\Delta E$. Including ac-χ measurements on the same sample he finds a power-law decay

$$\xi(t) \propto t^{-\nu} \qquad (74)$$

with $\nu \approx 0.25$ at $T/T_f = 1.25$ (T_f is determined by ac-χ at 10 Hz), but $\nu = 0.1 \pm 0.02$ at and just below T_f. At lower temperatures ($T/T_f \approx 0.75$) $\xi(t)$ is best expressed as

$$\xi(t) \propto t^{-\nu} + \log t \qquad \text{with} \quad \nu = 0.4 \pm 0.1 \ . \qquad (75)$$

At still lower temperatures ($T/T_f \lesssim 0.5$) $\xi(t)$ can be expressed again as a power law with a value of $\nu = 0.5$ which is consistent with the theoretical predictions. The anomalously low value of ν close to T_f (see eq. 74 and 73), also found in muon spin relaxation measurements (Heffner et al., 1984), is still unexplained and calls for further theoretical investigation.

6.3 Muon spin relaxation :

Another new microscopic technique which can determine in principle $S(q,t)$ in spin glasses is the measurement of muon spin relaxation (μSR). Here the q dependences are not tunable as in the NSE method (eq.70) but are broadly averaged over all q. The "window" of relaxation times seen by μSR spans the 10^{-11}s to 10^{-5}s regime, and hence partly overlaps with that of the neutron techniques (10^{-12}s to 10^{-8}s).

This technique was first applied to CuMn and AuFe spin glasses by Murnick et al. (1976), who observed the spin precession of μ^+ around the applied transverse magnetic fields (transverse-field μSR) and found a rapid increase of muon-spin depolarization rate on cooling towards T_f. Similar TF-μSR measurements were performed later in CuMn (Emmerich and Schwink, 1981) and AgMn (Brown et al., 1981). It was not possible, however, to distinguish the effects of static inhomogeneous random fields from those of fluctuating dynamic fields since the TF-μSR experiment corresponds to the T_2-measurement of magnetic resonance. This difficulty also limited the information obtained from previous linewidth measurements in NMR (Mac Laughlin and Alloul, 1976;, Levitt and Walstedt, 1977) and ESR (Dahlberg et al., 1979; Salamon, 1979; Wu et al., 1985; Baberschke et al., 1986). Furthermore, such experiments with external magnetic fields are not quite suitable for probing spin glasses in which the "cusp" of $\chi(T)$ is substantially rounded by a small H.

To overcome these difficulties Uemura et al. (1980 and 1981) have applied the zero-field μSR (ZF-μSR) to spin glasses. They have also made measurements on CuMn in finite longitudinal magnetic fields (LF-μSR) to separate the static and dynamic effects (Uemura and Yamazaki, 1982). A review of these studies is given by Uemura et al. (1985).

In ZF-μSR the longitudinal muon spin relaxation function $G_z(t)$ is directly deduced from the time-differential measurement of the forward/backward muon decay asymmetry, without any disturbance of the spin-glass system by an external field. (No depolarization of the muon spin means $G_z = 1$, complete depolarization $G_z = 0$). The observed time evoluation $G_z(t)$ of muon-spin polarization reflects amplitudes, randomness, and fluctuations of local magnetic fields at muon sites in the specimen. There appear two essential problems in analyzing μSR experiments on spin glasses: (i) One has to make model assumptions about the shape of $G_z(t)$; (ii) Any relaxation slover than 10^{-5} sec appears as a "static" component in μSR (lifetime of the muon is $\tau_\mu = 2.2 \times 10^{-6}$sec).

In the early stage of such studies on spin glasses (Uemura, 1981) one assumed a simple exponential decay of spin correlation at all temperatures above and below T_f. With recent high-statistics data, as shown in Fig. 51, Uemura et al. (1985) include a stochastic theory

of spin relaxation to analyze the ZF-μSR data on CuMn spin glasses. Assuming a simplified autocorrelation function of the impurity spins (which is not in accordance with the experimental findings described above)

$$\left[\langle S(t)S(0)\rangle / \langle S(0)\rangle^2\right]_{av} = (1-Q_{EA})\exp(-\nu t) + Q_{EA} \qquad (76)$$

the authors calculate $G_z(t)$ analytically. Best-fit curves to this form of $G_z(t)$ are shown in Fig. 51 as solid lines. This ansatz leads to distinguish between "static" and dynamic random local fields at the muon site which are involved in $G_z(t)$. For the purely dynamic case where the averaged amplitude a_s of the "static" random fields is zero and $Q_{EA} = 0$, the $G_z(t)$ function exhibits a "root-exponential" decay, $G_z(t) = \exp(-\sqrt{\lambda_d t})$, similar to the ansatz in the early work (Uemura, 1981). Here λ_d is the dynamic muon-spin depolarization rate which is proportional to the correlation time $\tau_c = 1/\nu$ above T_f. The "static" effect is reflected in the quick initial decay of $G_z(t)$ followed by the "$\frac{1}{3}$ tail" (for $a_s \neq 0$, $\lambda_d = 0$, $Q_{EA} = 1$). The only fitting parameters in Fig. 51 are a_s and λ_d which are displayed in Fig. 52. It turns out that a_s exhibits non-zero values only below T_f of each specimen. The λ_d value increases rapidly when T_f is approached both from higher and lower temperatures. The spin correlation time

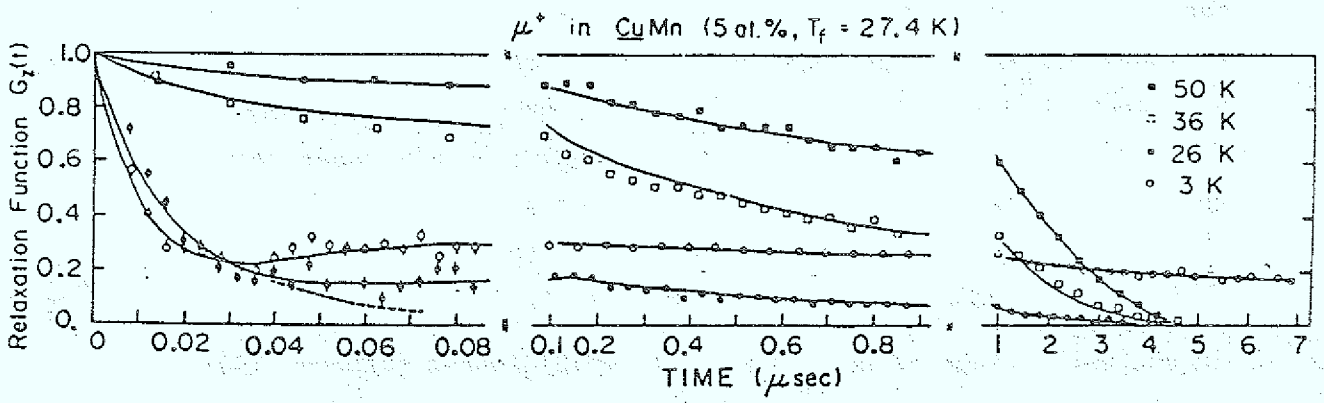

Fig. 51: Zero-field muon-spin-relaxation function, $G_z(t)$, observed in the spin glass CuMn 5at% (T_f = 27.4 K) at various temperatures. The solid lines represent the best-fit curves for eq. 76 with the values of a_s and λ_d given in Fig. 52 (From Uemura et al., 1984).

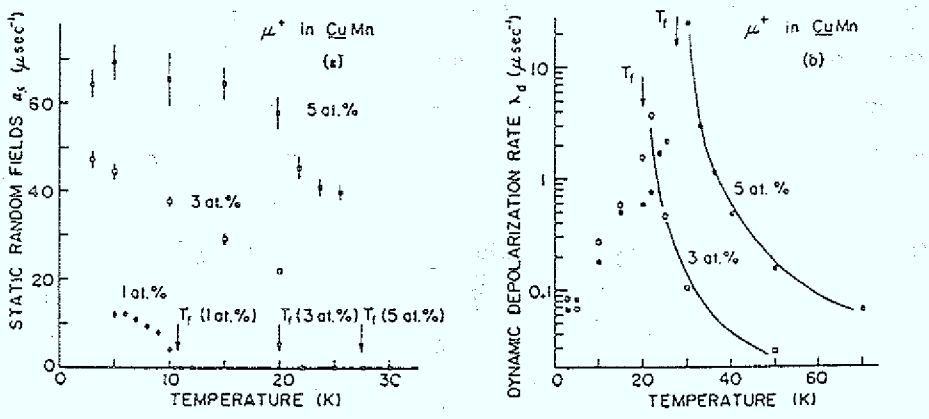

Fig. 52: Parameters from the best-fit curves in Fig. 51: (a) Averaged amplitude a_s of static random local field at the muon site, and (b) the dynamic muon-spin depolarization rate λ_d. The solid lines of (b) correspond to the fit of λ_d to the power-law behavior of critical slowing down, eq. 77 (From Uemura et al., 1984).

τ_c deduced from λ_d shows a rapid change from $\tau_c \approx 10^{-12}$ sec at $T \gtrsim 2T_f$ towards $\tau_c \approx 10^{-9}$ sec at $T \approx T_f$ in all the specimens. Comparing λ_d or τ_c with the power law behavior of critical slowing down

$$\tau_c = \tau_0 \, (T/(T-T_f))^z \qquad \text{for } T \gtrsim T_f \qquad (77)$$

the authors obtain values of z = 2.9 for CuMn 5% and z = 2.6 for CuMn 3% from the corresponding fit to λ_d, shown by the solid lines in Fig. 52b. Below T_f "static" and dynamic effects are found to coexists. The broken line at 26 K in Fig. 51 illustrates the decay of G_z (t) assuming $a_s = 0$ (but assuming still only a single relaxation rate and eq. 76). By the way, this kind of coexistence has also been found by LF-μSR below T_f (Uemura et al. 1985). The values of the "average" relaxation time fitted to the CuMn 5% by μSR roughly agree with NSE above and below T_f. The authors also argue that they can rule out the extremely inhomogeneous spin freezing (where for example 10 spins out of 100 are completely frozen ($Q_{EA} = 1$) while the remaining 90 spins are paramagnetic ($Q_{EA} = 0$)) (see also Emmerich et al., 1985).

The use of a single relaxation time and the ansatz, eq. 76, for the spin autocorrelation function in random systems like spin glasses is, of course, a very crude approximation, but Uemura et al. (1985) discuss that point and state, that "it is difficult to calculate $G_z(t)$ when the correlation times of impurity moments have a distribution in a more microscopic way", and hence, "it is difficult for μSR to directly determine the shape of $\xi(t)$". Nevertheless, a recent attempt is made in this direction by MacLaughlin et al. (1983) and Heffner et al. (1984) with LF-μSR in AgMn spin glasses applying high external fields up to H_L = 5 kOe. The spectral distribution of the fluctuating field below T_f is "gated" by the Zeeman level $\omega = \gamma_\mu H_L$, and the authors claim to have evidence for an algebraic time dependence of $\xi(t)$ with $\nu = 0.24 \pm 0.02$ for $T/T_f = 0.92$, and $\nu = 0.54 \pm 0.05$ for $0.3 \leq T/T_f \leq 0.66$ (see eqs. 73, 74; NSE data). However, the studied time region is very limited, and, in addition, the influence of the applied fields on the spin dynamics cannot be excluded.

6.4 1/f magnetic noise :

Very recently two groups succeeded in observing equilibrium magnetic fluctuations or 1/f magnetic noise spectra (as distinguished from so-called Barkhausen noise) in various insulating spin glasses (Ocio et al., 1985 and 1986; Reim et al., 1986), mainly due to the existence of relaxation times down to very low frequencies in such disordered spin systems and the lack of contributions from eddy current noise (as for metallic samples). Here we present results obtained near the spin-glass temperature whereas effects of magnetic field and waiting time on the magnetic noise spectrum will be discussed in the next section (sec. 7.1).

Fig. 53a displays typical noise power spectra of the $Eu_{0.40}Sr_{0.60}S$ spin glass at two different temperatures above and below T_f = 1.54 K, compared to the noise of the detection system alone (Reim et al., 1986). While the empty-system noise is white above 1 Hz and shows some $1/\omega$ component below 1 Hz, the noise level of the sample is up to three orders of magnitude larger and displays a $1/\omega^n$ behavior in the whole frequency range with $n \leq 1$. The noise magnitude of the

spin glass is obtained after subtracting the noise of the empty system at each temperature, the result is plotted versus temperature at five different frequencies in Fig. 53b. Below 2 K, the amplitude of the magnetic fluctuations increases rapidly and levels off around $T \simeq 1.6$ K(near T_f).

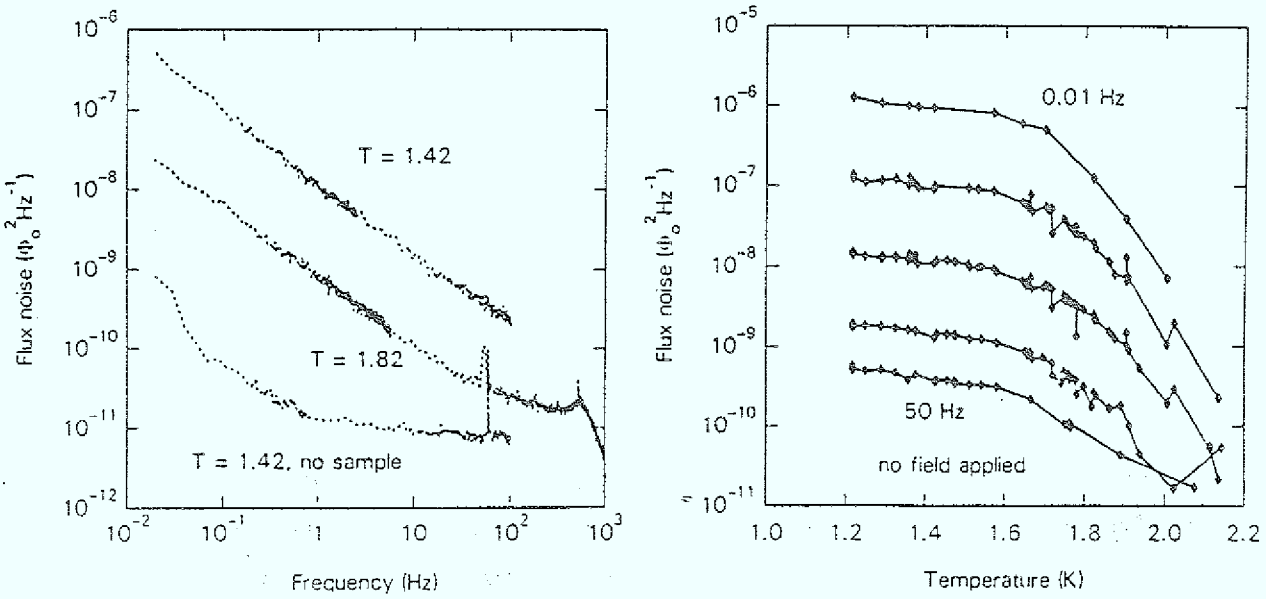

Fig. 53: Magnetic noise for the spin glass $Eu_{0.40}Sr_{0.60}S$ (a) as function of frequency at two different temperatures above and below T_f = 1.54 K, and (b) as function of temperature at five different frequencies 0.01, 0.1, 1, 10, and 50 Hz (at zero applied field). The data in (b) are obtained after subtracting the noise of the empty system at each temperature (the one at T = 1.42 K is shown in (a)) (From Reim et al., 1986).

The fluctuation dissipation theorem states (Kubo, 1966) a general relationship between the response of a given system to an external disturbance and the internal fluctuations in the absence of the disturbance at thermal equilibrium. Applied to magnetic equilibrium fluctuations $S(\omega)$ this reads (Ocio et al., 1985):

$$S(\omega) = \alpha \chi''(\omega) 4k_B T/\omega \qquad (78)$$

where α is a geometry dependent conversion factor. Reim et al. (1986) prove unambiguously by measuring the noise spectrum $S(\omega)$ and the imaginary part $\chi''(\omega)$ of the ac-χ simultaneously, that the fluctuation dissipation theorem is as accurately obeyed by the magnetic fluctuations below as above T_f. This is important because recent theories suggest that the spin-glass phase below T_f could be non-ergodic (see sec. 4.3).

Given the validity of eq. 78, measurements of the noise spectrum offer an alternative way to measure χ''. Two experimental advantages important in spin-glass research are that the noise measurement is done at zero field and conveniently as a function of frequency in the low-frequency regime. Therefore, Reim et al. (1986) studied the low-frequency dynamics of the $Eu_{0.40}Sr_{0.60}S$ spin glass near T_f. Fig. 54 shows the temperature dependence of the noise exponent $n(T)$ in $S(\omega) \propto \omega^{-n}$ at five frequencies. The data exhibit a maximum slope in the vicinity of T_f, with the magnitude of the logarithmic slope decreasing both above and below T_f. Most important, the slope at a fixed temperature is <u>frequency</u> dependent even at T_f. This second fact implies that it is not possible to describe the noise power or the imaginary part of the susceptibility by a simple power law, $\chi''(\omega) \propto \omega^{1-n}$, as derived in mean-field theory by Fischer and Kinzel (1984) (see eq.33). The intriguing experimental result may be explained by the recent prediction (Fisher and Huse, 1986) of a 1/f noise up to logarithmic corrections.

As another direct consequence of this finding, the time exponent of the magnetization decay M(t) is expected to be also time dependent, an effect which should be noticeable already at $t \sim 1$ sec. For instance a fit of M(t) with the commonly used stretched exponential form (eq.44) may lead to in some sense "<u>averaged</u>" values for the exponent n(T). Indeed, Ferré et al. (1986) find for $Eu_{0.40}Sr_{0.60}S$ from Faraday rotation measurements of M(t) and a fit with eq. 44 in the 10^{-3} to 10^{2} sec time-interval an "averaged" exponent $n(T_f) = 0.9$, compared to the values of 1.0 at 0.01 Hz and 0.8 at 50 Hz in Fig. 54.

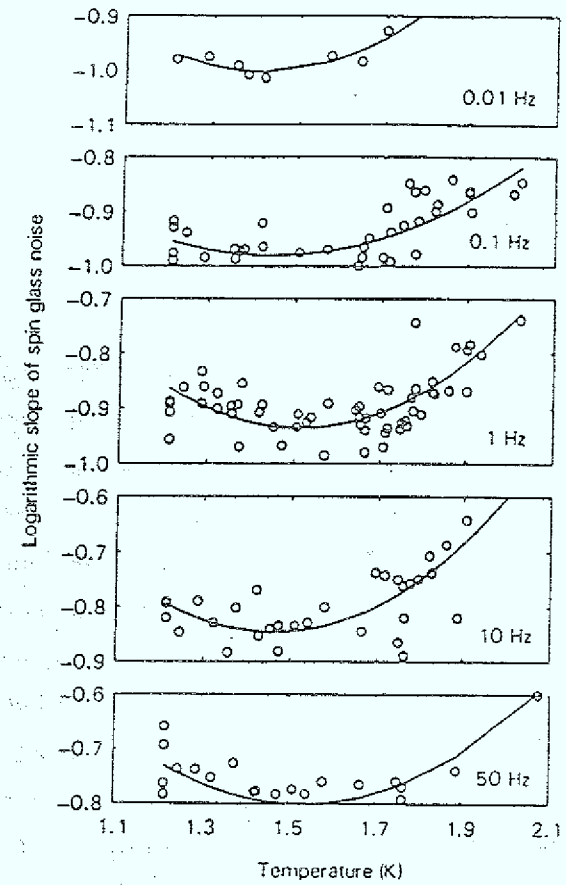

Fig. 54: Logarithmic slope of the noise power spectra (from Fig. 53) versus temperature near T_f at five different frequencies. The solid curves show polynomial fits as guides for the eyes (From Reim et al., 1986).

7. Spin-glass transition

Let us now proceed to discuss the nature of the transition into the spin-glass state by reviewing experimental studies which have been devoted to analyzing the data in terms of a phase transition and to look for a static T_f. Hence, this section is intimately related to the results and discussions presented above.

7.1 Search for a static T_f :

First we turn our attention to the field-cooled magnetization, M_{FC}, measured in a small field which has been applied already above T_f. Most important $M_{FC}(T)$ of the spin glass is often assumed to be the equilibrium magnetization (Malozemoff and Imry, 1981b; Chamberlin et al., 1982; Monod and Bouchiat, 1982) because it does not seem to depend on time and is reversible as one moves up and down in temperature, as long as H_{FC} remains constant below T_f. In addition, $M_{FC}(T)$ usually develops a plateau below T_f, and a small "bump" ($\approx$ 10%) occurs around T_f for CuMn and AgMn spin glasses (Chamberlin et al., 1982), but for many other spin glasses there is a rather large peak in M_{FC} in the region of T_f. In spin glasses with dominating antiferromagnetic couplings $M_{FC}(T)$ still increases below T_f on cooling but with a pronounced change in slope at T_f,as can be seen for instance in Fig. 44a for $Eu_xSr_{1-x}Te$ spin glasses (Börgermann et al., 1986a and b). The field dependence of M_{FC} near T_f is often related to the mean-field prediction which gives M_{FC} independent of T below T_f (Parisi and Toulouse, 1980; Sompolinsky, 1981) as will be discussed below.

Recently, Lundgren et al. (1982, 1985) however questioned the validity of the assumption that the measured FC-susceptibility is the thermodynamic susceptibility of a spin glass. They study the time variation of the relaxation rate in spin glasses by ac-χ measurements and show that the time range can be extended to considerably longer times

utilizing ZFC-χ measurements, too. In this method a set of ZFC-χ curves is recorded each of which is obtained after various waiting periods t_w at constant temperature before the external field is applied. Figure 55 shows such ZFC-χ curves for the CuMn 4% spin glass at $T/T_f = 0.9$. In Fig. 55a the curves are represented in a relative diagram with $\Delta\chi(t)$ arbitrarily displaced along the vertical axis. A relative change of the total χ of 1 % is indicated. Figure 55b

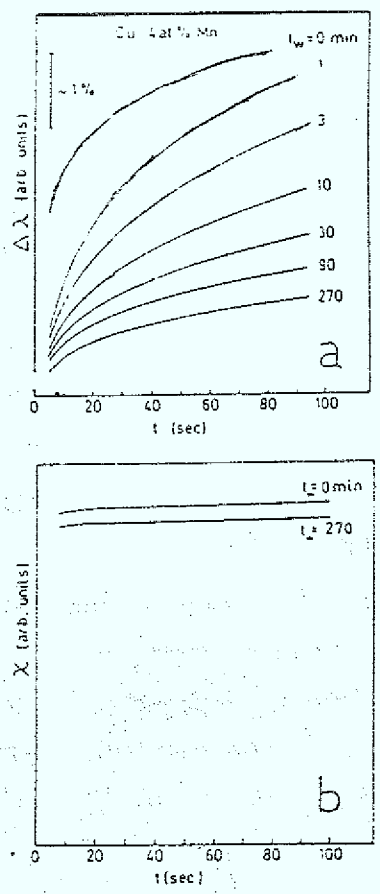

Fig. 55: Time dependence of the ZFC susceptibility for CuMn 4at% at $T = 0.9 \cdot T_f$ (T_f = 26 K), obtained after different waiting times t_w before the external field is applied (at t = 0). Part (a) of the figure shows the curves arbitrarily displaced on the vertical axis, part (b) on an absolute scale. The estimated equilibrium χ coincides with the upper horizontal line of the frame of the figure (From Lundgren et al., 1985).

shows two curves $\chi(t)$ for $t_w = 0$ and $t_N = 270$ min in an absolute diagram. The data demonstrate that at a certain observation time t both the relaxation rate, S, and the time-dependent susceptibility, $\chi(t)$, markedly depend on the waiting time t_w at a constant temperature. Both are related to the ac-χ via

$$S(t) = (1/H)\,\Delta M(t) / \Delta \ln t \approx -(2/\pi)\,\chi''(\omega)$$
$$\chi(t) = (1/H)\,M(t) \approx \chi'(\omega) \qquad (79)$$

if $t = 1/\omega$. In a logt diagram these ZFC-χ curves display an inflection point at an observation time comparable to t_w at constant temperature. Although the experimental data only cover a limited range in observation time ($< 10^3$ sec) and waiting time ($< 10^4$ sec), the authors construct a diagram describing the evolution of $\chi(t)$ towards equilibrium. They claim that, independent of t_w, the time-dependent susceptibility attains equilibrium at the same observation time t_{eq} (T). For example, for CuMn 4% at $T/T_f = 0.9$ (see Fig. 55) they estimate $t_{eq} \approx 10^{15}$sec, or that the cusp of $\chi(t)$ coincides with the equilibrium susceptibility at T_f at an observation time of about 10^5 sec. For shorter times, the data are interpreted as nonequilibrium or aging phenomena in the zero-field state of the spin glass.

The aging of the ZFC-state will be shown up analogously in the thermoremanent magnetization. For instance, these authors (Nordblad et al., 1986b) demonstrate that the t_w-dependence of the TRM-decay described by Chamberlin (1985) with the stretched-exponential form (eq.44, where $\tau_p(t_w)$) is only an artifact caused by the influence of an aging process of the spin-glass state on the relaxation of the magnetization. Hence, according to Nordblad et al. (1986b) a stretched exponential only describes the relaxation in a specific time interval and does not accurately describe the total relaxation of the remanent magnetization. In contrast, Hoogerbeets et al. (1986) present new data of the temperature- and field-dependence of the TRM-decay which they analyze in "remarkable agreement" with predictions of de Dominicis et al. (1985) within the infinite-range mean-field model (eq. 44). (See also the results obtained from magnetic noise measurements as described in sec. 6.4).

Following Nordblad et al. (1986a) further, they argue that the closely similar wait-time dependence of the TRM-decay to the ZFC-magnetization implies that a corresponding aging process also occurs in the field-cooled spin-glass state. The time effects, however, are drastically weaker in the $M_{FC}(t)$, as illustrated in Fig. 56 (Note the striking feature of an inflection point at $t \approx t_w$ of the $M_{ZFC}(t)$ in the M-logt plot). According to these authors all the magnetizations measured in spin glasses below T_f probe the non-equilibrium state.

Similar time dependencies are observed in low-frequency magnetic noise measurements of the insulating spin glass $CsNiFeF_6$ at 4.2 K (T_f = 5.4 K) by Ocio et al. (1986). In the frequency range below 10^{-1} Hz the amplitude of the noise power strongly depends on the time t_w elapsed after cooling the sample (no field is applied!). The noise power measured for example at 3×10^{-3} Hz in the first five hours is 10 times above its value measured after 50 h. There seems to exist a characteristic frequency (which decreases with t_w), above which the $1/\omega$ noise spectrum is observed, but below which the spectrum presents a $1/\omega^x$ dependence with $1.5 < x < 2$. Spectra recorded for waiting times longer than 70 h are stationary and present a $1/\omega$ dependence between 2×10^{-4} Hz and 2×10^{2} Hz.

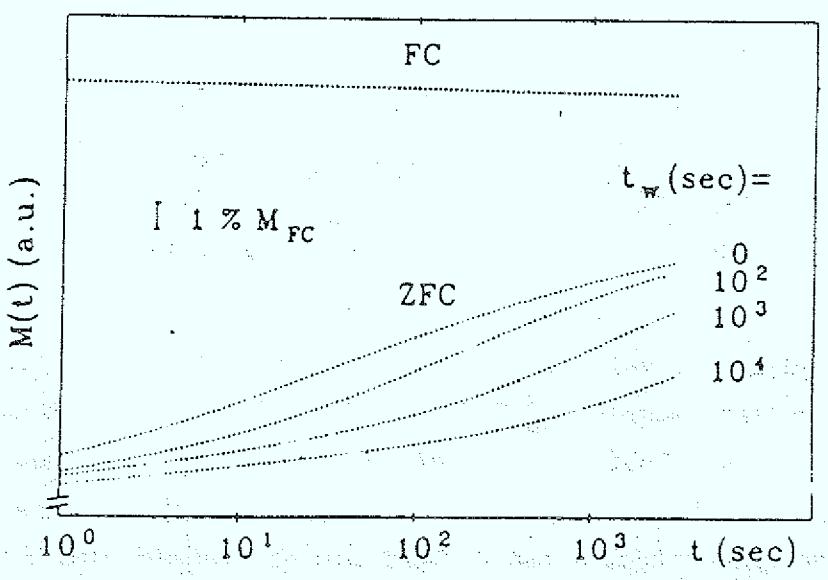

Fig. 56: ZFC magnetization of CuMn 5at% in H = 1 G after different wait-times t_w at $T = 0.9\ T_f$(T_f = 28.0 K) plotted vs. log t. The FC magnetization is also shown. 1% of the FC-magnetization value is indicated in the figure (From Nordblad et al., 1986a).

Noise measurements were also performed in the presence of a small magnetic field of 0.3 Oe by Ocio et al. (1986). "Aging effects" are again observed in the ZFC state, but not after FC.

The "aging process" is possibly due to continuous rearrangements of the spin configuration caused by frustration phenomena. Very recently, Binder and Young (1986) argue that it is not absolutely certain that the findings described above really prove the non-equilibrium character of the spin-glass state. If states with spin-glass order exist as thermal equilibrium states, they are certainly highly degenerate (i.e. there are many order-parameter components). On cooling the system through its transition temperature one would expect that locally the system starts to form ordered regions of its various possible order-parameter components. As these regions grow there is misfit at their walls, and hence the growth of the domains might be extremely slow.

Several authors believe that in field-cooling experiments and using "very slow" cooling rates one measures the equilibrium susceptibility, or at least there is no time dependence observable in χ and on T_f when deduced from such FC-measurements. For instance, this tacit assumption is made in many experiments described in the following sections. Time effects on M_{FC} after slow cooling are generally tiny, and Chamberlin (1984) even speculates that any observed time dependence of M_{FC} may be a consequence of the fact that the sample is not cooled in a constant local field, due to a small temperature dependence of M_{FC} and the resulting corrections to the local field. Hence, it is important to establish whether there exists a static freezing temperature T_f.

Malozemoff and Imry (1981b) were one of the first who demonstrated with two spin-glass samples, CuMn 4.6 % (with $T_f \approx 27$ K) and a-AlGd 37% (with $T_f \approx 17$ K), that no shift of the peak position of dc-$\chi(T)$ (defined by M_{FC}/H at a field of 4.5 Oe) can be detected over a long range of time delays from 6 min to 2400 min per temperature change $\Delta T = 0.2$ K. Further below the peak temperature, however, it is more difficult to achieve time-independence of M_{FC} in spin glasses. Results from recent experiments by Matsui et al. (1985) are displayed in Fig. 57. The data on a-AlGd 37% in Fig. 57a indicate that even at

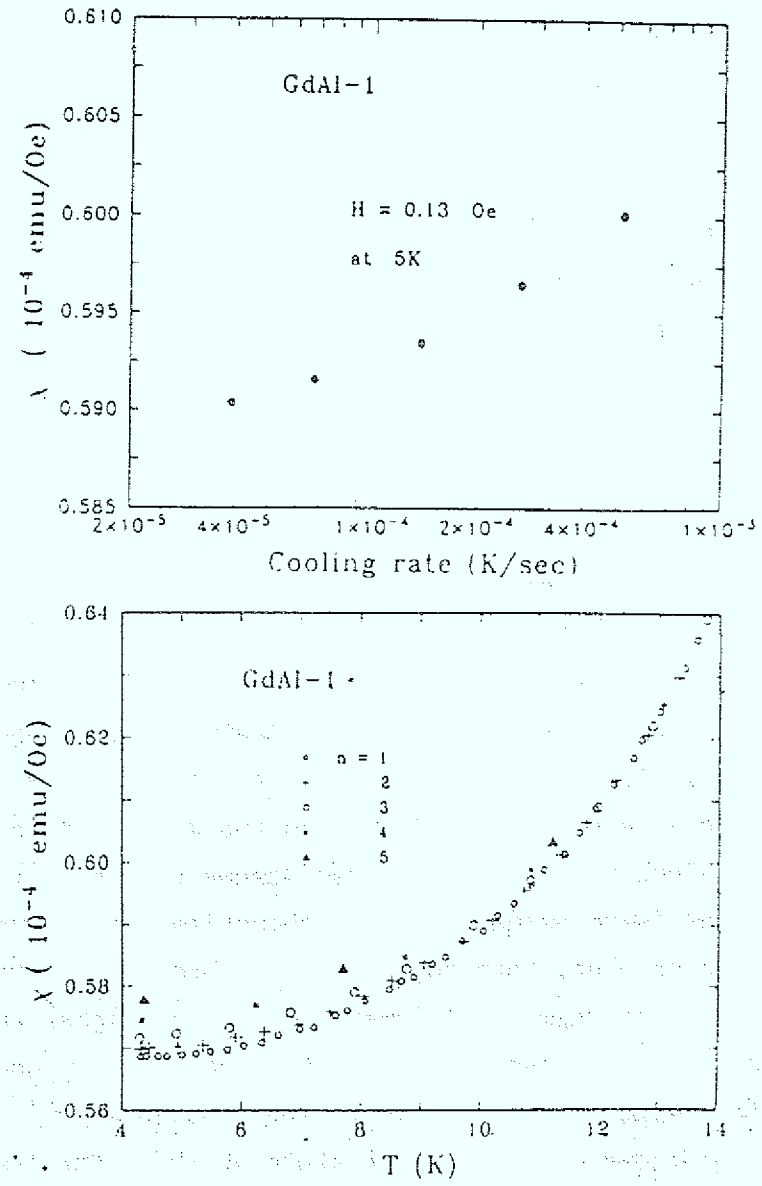

Fig. 57: Susceptibility, $\chi = M_{FC}/H$ at H = 0.13 Oe, of a-AlGd 37% spin glass (T_f = 17 K) after cooling from 23.5 K at different rates: (a) χ at T = 5 K; (b) χ at various T measured after different cooling rates; n = 1 ...5 correspond to 4×10^{-5}, 7×10^{-5}, 1.4×10^{-4}, 2.6×10^{-4}, 5×10^{-4} K/sec (From Matsui et al., 1985).

the lowest cooling rate applied χ (= M_{FC}/H at 0.13 Oe) seems to be not yet independent of the cooling rate at the low temperature of 5 K (compared to T_f = 17 K). Nevertheless, the authors interpret the curve $\chi(T)$ in Fig. 57b measured at this lowest cooling rate of 4×10^{-5} K/sec as the "equilibrium curve" since at higher temperatures it is "common for all the other cooling rates." By means of this working definition one can determine a characteristic temperature T_{ne} at which a given curve in Fig. 57b "peels away" from the common curve. Then, a slower cooling rate determines a lower value of T_{ne}. The authors interpret T_{ne} as the lowest temperature for measuring an equilibrium susceptibility in field-cooling at a given cooling rate. For example, data of Fig. 57 are in equilibrium for a cooling rate of 1.4×10^{-4} K/sec down to 12 K (i.e. 5 K below T_f) when cooling in 0.13 Oe, and down to 11.5 K for 10 Oe.

Detailed dc-magnetization measurements on the spin-glass YEr 1%, presented by Bouchiat and Mailly (1985), also reveal the existence of long-time relaxations of the FC-magnetization which, however, is not incompatible with the existence of a well-defined temperature, characteristic of the occurrence of thermal hysteresis, independent of the cooling rate. Figure 58 illustrates these findings: Below T_f = 0.59 K strong irreversibility occurs in the magnetization when measured at 10 G along the c-axis (one can assume that the Er magnetic moments behave like Ising spins), the ZFC-magnetization differs from the FC one. As can be seen, both magnetizations measured at the warming or cooling rate of 0.15 mK/min are lower than at the higher rate of 10 mK/min, however the onset of hysteresis occurs at T_f independent of the rate. This temperature is defined with an accuracy of better than 0.5 % and coincides with the temperature at which the system deviates from the Curie law.

A completely different behavior is found in a cobalt aluminosilicate glass, $Al_2O_3 \cdot SiO_2 \cdot CoO$, by Wenger and Mydosh (1984a). A higher FC-magnetization is observed at a slower cooling rate (Fig. 59), but apparently inconsistent with that, the magnetization stays constant at 4.4 K when monitored over a period of 8×10^4 sec. They interpret the data as result of a "supercooling" effect, strongly analogous to the formation of ordinary glasses.

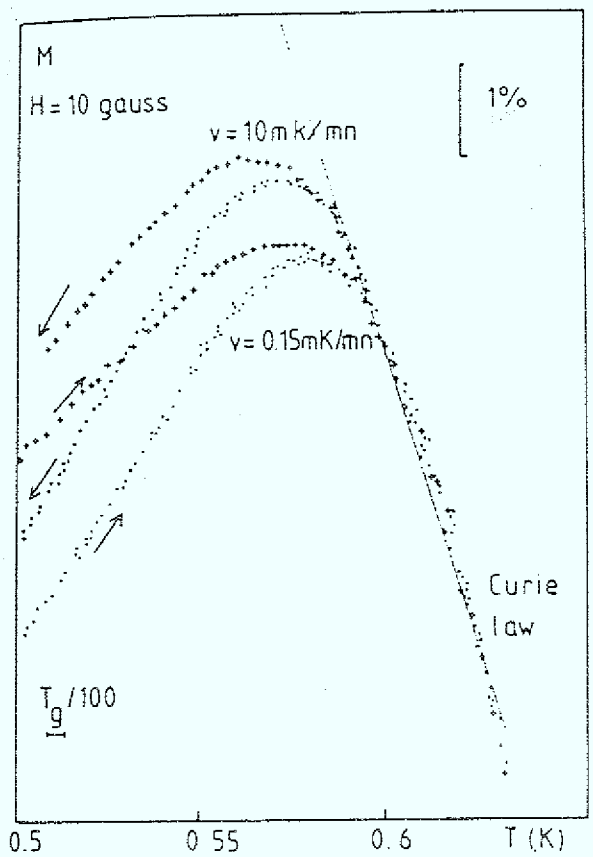

Fig. 58: Thermal hysteresis loops for YEr 1 at% obtained by cooling the sample from 0.7 K to 0.4 K and warming it under a field of 10 G with a constant speed equal to 10 mK/min (+) or 0.15 mK/min (●) (From Bouchiat and Mailly, 1985).

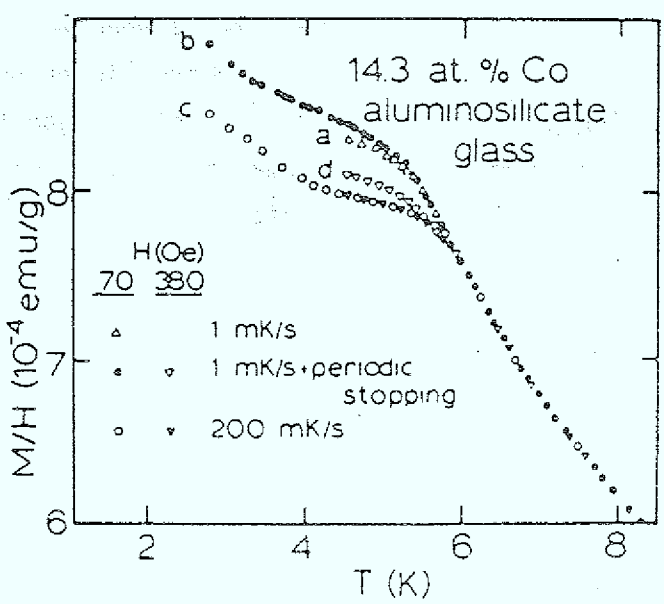

Fig. 59: Field-cooled susceptibility, M/H, of cobalt (14.3 at%)-aluminosilicate glass versus temperature for various cooling rates and magnetic fields (From Wenger and Mydosh, 1984a).

Guy and Park (1983) conclude that the FC-magnetization in CuMn 0.25 % is in thermal equilibrium since the thermodynamic (Maxwell) relations are fulfilled for their magnetization data together with data from magneto-caloric and specific heat measurements. Duffield and Guy (1985) propose on the basis of a similar analysis where CuMn and (La,Gd) Al_2 spin glasses are compared that the equilibrium phenomenon is often obscured by secondary but large irreversible effects. They show that (La,Gd) Al_2 is an extremely reversible system that exhibits a relatively large amount of adiabatic cooling below T_f and very little irreversibility. On the other hand, CuMn is much more irreversible and a definite observation of adiabatic cooling has not been made.

Another procedure to search for a static T_f is applied in the $Eu_xSr_{1-x}S$ spin glass with $x = 0.40$ where Ferré et al. (1981) observe a pronounced frequency dependence of the ac-$\chi(T)$ maximum, as shown in Fig. 42b. $T_f(\omega)$ seems to saturate for low frequencies at a constant value near the temperature determined by static magnetization measurement. In order to obtain evidence that $T_f(\omega)$ for an infinite observation time really saturates at a nonzero temperature Paulsen et al. (1986b) propose the following extrapolation of the data to $\omega = 0$: First, careful measurements of the real (χ') and imaginary (χ'') part of $\chi(T,\omega)$ are performed in the frequency range $7\ \text{Hz} \leq \omega \leq 5\ \text{kHz}$. It is shown that the relation in eq. 67 between χ' and χ'' holds in zero and finite fields (examined up to 15 Oe). This is remarkable when one considers that the peak in χ' of $Eu_{0.40}Sr_{0.60}S$ shifts toward higher temperatures in moderate H while the χ'' response is moved toward lower temperatures in fields (Maletta and Felsch, 1979b; Paulsen et al., 1986a). Then, the authors generalize the mean-field relation $\chi'' \propto \omega^{\nu}$ (eq. 33) via eq. 67 to obtain the functional form of $\chi(T,\omega)$:

$$\chi(T,\omega) = \chi' + i\chi'' = \chi_0 + (2A/\pi\nu)\omega^{\nu} + iA\omega^{\nu} \qquad (80)$$

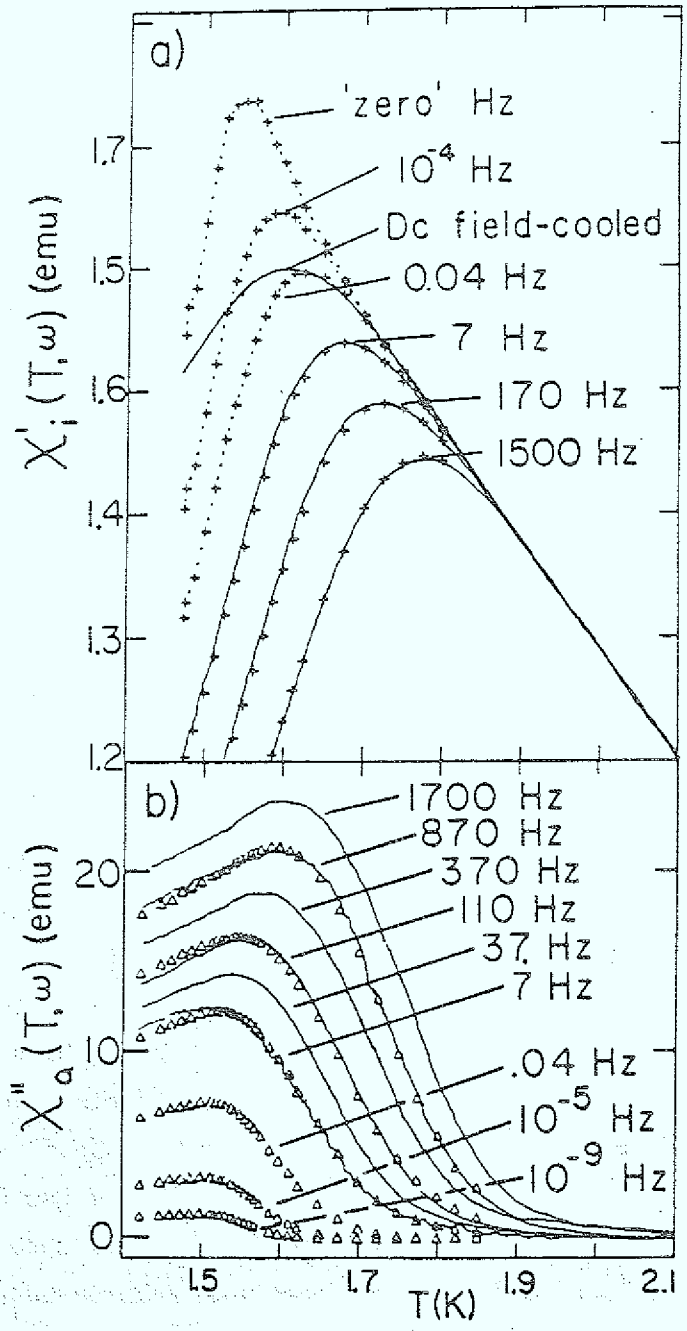

Fig. 60: Real and imaginary part of the ac susceptibility as measured in $Eu_{0.40}Sr_{0.60}S$ spin glass for various frequencies, shown by solid lines in part (a) and (b). Eq. 80 describes the data quite well (crosses and triangles), obtaining the parameters $\nu(T)$ and A(T) as shown in Fig. 61. Then, χ' (crosses) and χ'' (triangles) can be predicted in the very low frequency-range down to 0 Hz using these parameters and eq. 80. In addition, the dc susceptibility (M_{FC}/H at H = 0.5 Oe) is shown for comparison (From Paulsen et al., 1986b).

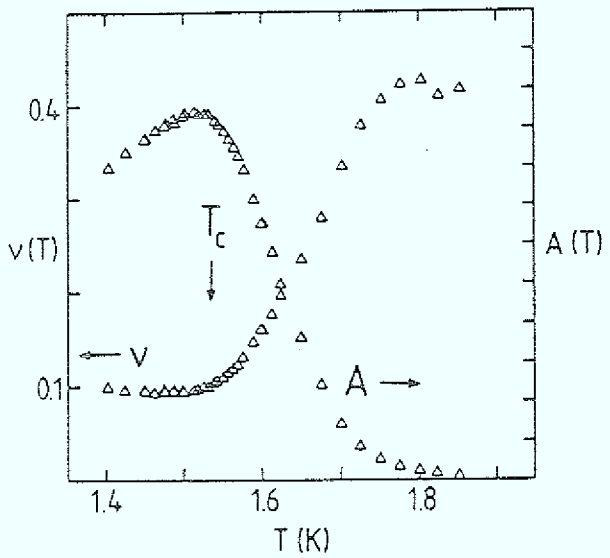

Fig. 61: The temperature dependence of the parameters $\nu(T)$ and A(T) extracted from least-squares fits to the data, shown and described in Fig. 60 (From Paulsen et al., 1986b).

where A(T) and $\nu(T)$, are shown to describe the data for the $Eu_{0.40}Sr_{0.60}S$ spin glass quite well at low frequencies near $T_f(\omega)$. Least-squares fits to the data of χ' and χ'', as illustrated in Fig. 60 for a few representative frequencies determine the parameters A(T) and $\nu(T)$ displayed in Fig. 61. Finally, eq. 80 and these parameters are used to calculate $\chi(T,\omega)$ in the limit $\omega \to 0$. The "static" limit is approached very slowly in Fig. 60, with the peak in $\chi'(T)$ sharpening as it shifts toward lower temperatures. Also shown is the conventional dc susceptibility obtained by cooling the sample at a rate of $\sim$0.2 K per 10 min in a field of 0.5 Oe. The departure from paramagnetic behavior above T_f is similar to that of the ac-χ for a frequency of 0.04 Hz, which is not inconsistent with the rate of field cooling. The zero-frequency behavior suggests that a phase transition occurs at $T_f(\omega = 0) = T_c = 1.54$ K for this sample. T_c is even somewhat below T_f(dc), but it is interesting to note that the exponent $\nu(T)$ levels off just at T_c(Fig. 61). As this limit is approached in the extrapolation, χ'' decreases toward zero but at 10^{-9} Hz still has a small finite value (Fig. 60).

7.2 H-T phase diagram: role of anisotropy :

AT-like lines: The mean-field theory of spin glasses predicts for Ising spins one and for Heisenberg spins two critical lines in the magnetic field-temperature plane (see sec. 4, eqs.15 and 27). De Almeida and Thouless (AT) (1978) obtain in the mean-field Ising model of SK a transition line $H_f(T)$ below which the system becomes non-ergodic. This AT-line, separating the spin-glass phase from the paramagnetic phase (Parisi and Toulouse, 1980), ends for $H \Rightarrow 0$ at the freezing temperature T_f. Later on, the instability line is suggested to be also a critical line for the disappearance of macroscopic irreversibility (Sompolinsky, 1981).

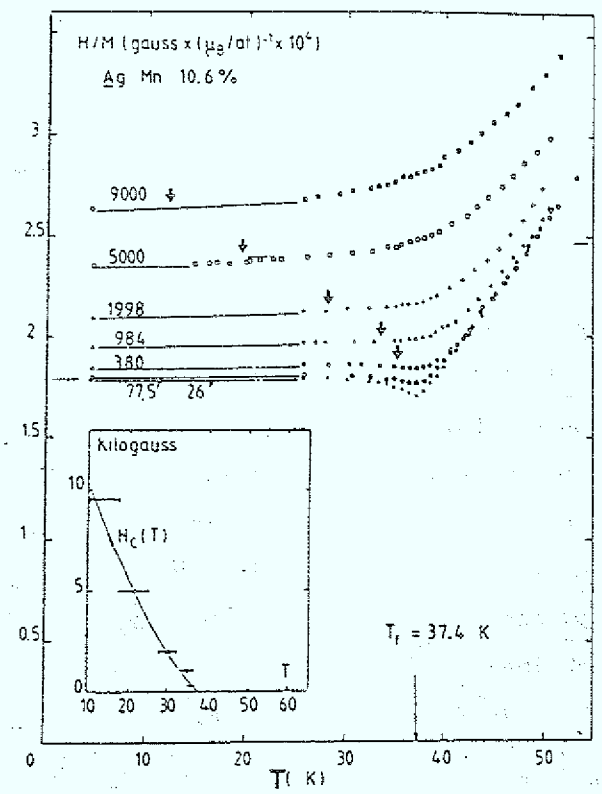

Fig. 62: Inverse of the susceptibility, $\chi^{-1} = H/M$, of AgMn 10.6 at% as a function of temperature for various magnetic fields (indicated on each curve in G). Data points were obtained by slow cooling in constant field H. The onset of the plateau (marked by arrows) is defined arbitrarily by the point of the M(T) curve departing by 3% from its low-temperature value. The resulting boundary for the spin-glass phase $H_c(T)$ is shown as an insert (From Monod and Bouchiat, 1982).

It is thus very tempting to test this issue of the mean-field theory. Monod and Bouchiat (1982) perform measurements of the "equilibrium" magnetization in AgMn 10.6 % by slow field cooling as function of temperature and magnetic field. Their data in Fig. 62 reveal a deviation from the low-temperature plateau of M(T,H) shifting to lower temperature with increasing field. The temperature of its onset, however, is experimentally ill defined, nevertheless by means of an (arbitrary) working criterion qualitative agreement of $T_f(H)$ with the AT-line (eq. 15) is obtained (see insert of Fig. 62).

Chamberlin et al. (1982) present high-resolution SQUID measurements of the dc magnetization of two AgMn spin glasses containing 2.6 and 4.0 at% Mn. They use the temperature derivative, dM(H,T)/dT, of the ZFC-curve near T_f for the identification of several characteristic temperatures associated with the paramagnetic to spin-glass transition in the presence of an external field. Only the temperature which defines the change of the slope dM/dT yields a power law with an exponent similar to the AT-line.

Berton et al. (1982) use the magnetocaloric effect to determine the H-T diagram of a CuMn 0.25% spin glass. Here, the variation of the temperature of an adiabatically isolated substance with external magnetic field is measured which is directly related to the magnetization via the Maxwell relation. Their result suggests the presence of two lines: the spin-glass to paramagnetic boundary line $H_c(T)$ and a cross-over line $H_m(T)$ separating a pure Curie paramagnet from a non-Curie paramagnet. The critical field $H_c(T)$, defined rather arbitrarily in the paper, is associated with the AT-line.

As already mentioned above, $T_f(H)$ is also predicted to be seen by the disappearance of irreversibility. Salamon and Tholence (1982) explore this possibility by examining the relaxation of the magnetization of zero-field-cooled samples (CuMn 0.24 % and a-$Fe_{10}Ni_{70}P_{20}$) following the application of a step increase in magnetic field. They show that the magnetic viscosity S(H,T) = dM(t)/dlnt first increases with field at a fixed temperature, reaches a maximum at $H_m(T)$ and then tends toward zero at large fields. The values of $H_m(T)$ vary similar to

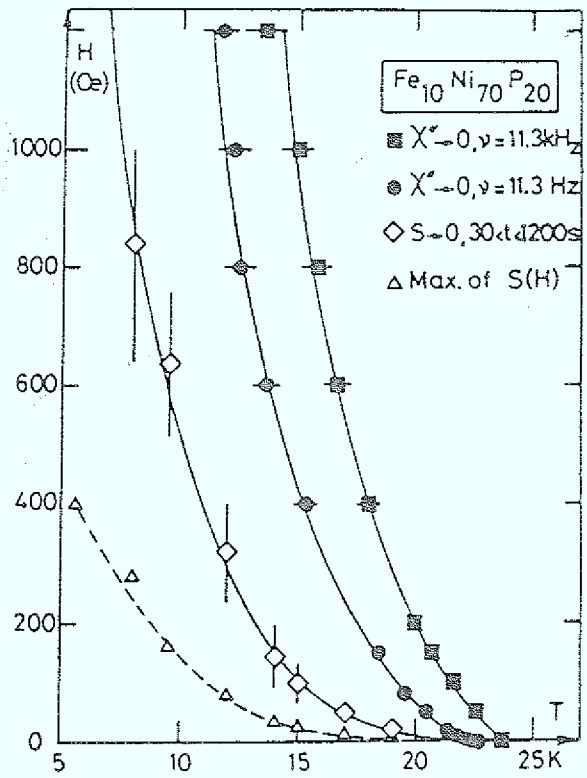

Fig. 63: Critical fields $H_c(T,\omega)$ (or $H_c(T,t)$) for a-$Fe_{10}Ni_{70}P_{20}$ spin glass, as defined by the disappearance if irreversibility (on different time scales) from different experiments. The dashed line represents the maximum of S(H) for 30 sec < t < 1200 sec (From Salamon and Tholence, 1983).

the AT line, $\delta T_f \propto H^{\eta}$ with $\eta = 0.66$ and 0.55 for CuMn and a-FeNiP, respectively, but the amplitude of the field is much smaller than expected. Salomon and Tholence (1983) use as another criterion for a critical line in the H-T plane the disappearance of the dissipative part of the ac-susceptibility, $\chi''(\omega,T,H)$, in a-$Fe_{10}Ni_{70}P_{20}$ for two frequencies, 11.3 Hz and 11.3 kHz. Of course, such lines depend on the time scale of the measurement, and each of these arbitrary definitions defines a separate curve. Figure 63 summarizes these results, including the line for $S \to 0$. The characteristic field increases strongly with the frequency of the measurement, and the functional form changes. The exponent of T in $H_c(T)$ changes from 1.8 for the long-time data to 1.3 for 11.3 kHz, and the prefactor from 250 Oe to 3 kOe.

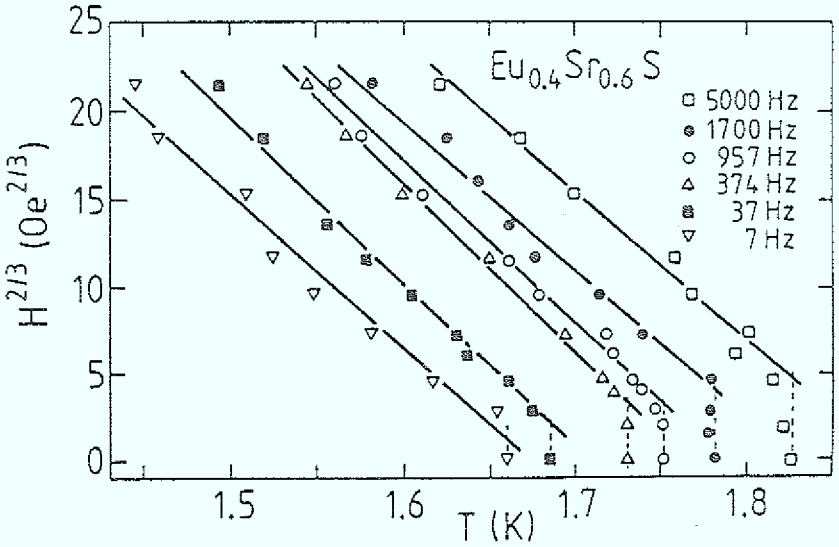

Fig. 64: Critical magnetic field (raised to the 2/3 power to check for the AT-behavior) plotted versus temperature for $Eu_{0.40}Sr_{0.60}S$, determined from the imaginary part $\chi''(T,H,\omega)$ of the complex susceptibility at various frequencies (From Paulsen et al., 1984).

For the insulating spin glass $Eu_{0.40}Sr_{0.60}S$ characteristic $H_c(T)$ lines are obtained from the decay of the magnetization after a small field change (superimposed on a larger constant field) $\Delta M(T,H,t_m)$ for fixed time scales t_m, 1 msec $< t_m <$ 1 sec (Bontemps et al., 1983), and from the imaginary part $\chi''(T,H,\omega)$ of the complex susceptibility at different frequencies (Paulsen et al., 1984; Rajchenbach et al., 1984). Again, similarity with the AT-line is observed, but in the latter experiments a different structure at weak fields is detected, as illustrated in Fig. 64: the $T_f(H)$ curves exhibit for higher frequency a low-field behavior of T_f nearly independent of H. The dynamic theory of the SK model (Fischer, 1983b) confirms this crossover for lines of constant average relaxation time from analytic behavior for high frequencies, $\delta T_f \propto H^2$, to AT-like behavior for $\omega \to 0$, $\delta T_f \propto H^{2/3}$.

To summarize these few examples, the experimental data exhibit a fairly similar behavior to the AT-line of the mean-field theory, in spite of some arbitrariness in the determination of the transition from the data. Nevertheless, two questions arise:

(i) Can one interpret the data only by assuming a nonzero transition temperature?

(ii) Why do experiments often show AT-like behavior rather than GT-lines, although most spin glasses are more Heisenberg-like than Ising-like?

The first question has been studied by computer simulations (Kinzel and Binder, 1984). Even the two-dimensional EA-Ising model with a Gaussian distribution of nearest-neighbor interactions reproduces several experiments described above qualitatively in surprising many details (see also sec. 4.2). Since this 2d-model has a spin-glass transition at $T_f = 0$, the "$T_f = 0$ - hypothesis" (Binder and Young, 1984) has been used to describe even 3-dimensional Ising spin-glasses. We will discuss some examples here and also later in this section. These Monte Carlo simulations yield a temperature-independent plateau (Fig. 14c) in the FC-susceptibility, M/H, which diverges for small fields as $H^{-1/\Delta}$ with $1/\Delta = 0.28$ (Fig. 14d). The critical field, $H_{eq}(T)$, as determined from the onset of the plateau tends to zero as T^{Δ} (Fig. 65). Both data are consistent with the scaling description for a static phase transition at $T_f = 0$:

$$\frac{M(T,H)}{H} = \frac{1}{T} \cdot g\left(\frac{H}{T^{\Delta}}\right) \quad . \qquad (81)$$

The existence of the plateau appears as an effect of the non-linear susceptibility. Since the model has a zero-temperature, transition, the linear equilibrium susceptibility should follow a Curie law ($\propto 1/T$) for all temperatures. Magnetizations measured after ZFC deviate from the plateau-value at low temperatures (Fig. 14c). For a given field H and observation time t those ZFC curves merge with the equilibrium-plateaus at a temperature $T_f(H,t)$. This defines a line $T_f(H)$ below which for a given time scale t irreversible behavior is observed. $T_f(H)$ is shown in Fig. 65 for different times t, and one can see in Fig. 66 that the scaled curves, $T_f(H)/T_f(H = 0)$, are similar to the AT-line in mean-field theory. However, this line should vanish for $t \to \infty$ (since $T_f = 0$).

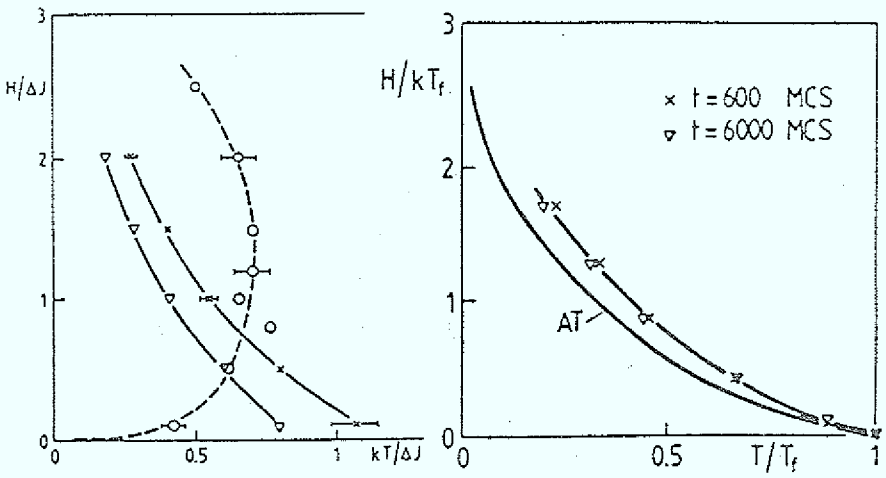

Fig. 65: Results from Monte Carlo simulations deduced from Fig. 14c: Static critical field H_c^{eq} (T) (open circles) and dynamic critical fields $H_c(t)$ for t = 600 Monte-Carlo steps per spin (MCS) (crosses) and t = 6000 MCS (triangles) plotted versus temperature (From Kinzel and Binder, 1984).

Fig. 66: Normalized dynamical critical fields, taken from Fig. 65, where $T_f(t)$ is obtained from extrapolating $H_c(t)$ to H = 0, compared with the AT-phase boundary of the mean-field theory (SK) (From Kinzel and Binder, 1984).

Now, if one tries to interpret the FC-plateaus of AgMn in Fig. 62 by means of this concept, one finds a rather different exponent, $1/\Delta = 0.03$, i.e. ten-times smaller than in the simulations for d = 2. This may well be taken as evidence for $d_1 \leq 3$ (see sec. 4.4).

The static critical fields, $H_{eq}(T)$, which separate the region of plateaus from the region of non-constant magnetizations behave quite different from the "dynamical" AT-line in the 2d-Monte Carlo-simulations (Fig. 65): $H_{eq}(T) \propto T^{\Delta}$. Binder and Kinzel (1983) suggest that the experimental data on a-AlGd 37% (Barbara and Malozomoff, 1983) shown in Fig. 67 can possibly be interpreted similarly, but a fit

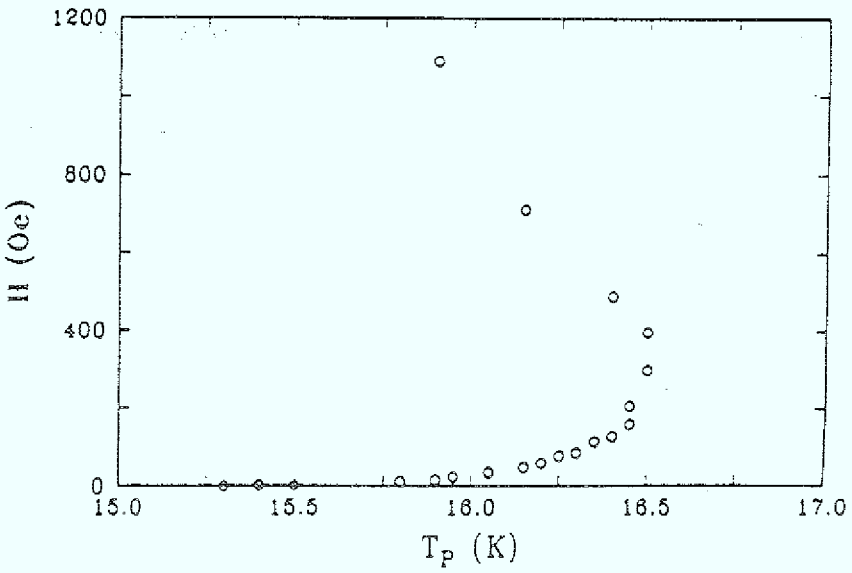

Fig. 67: Temperature $T_p(H)$ of a-AlGd 37at% where the field-cooled magnetization has its maximum. It shows a vertical tangent at H = 250 Oe and $T - T_f = 0.07 \cdot T_f$ (From Barbara and Malozemoff, 1983).

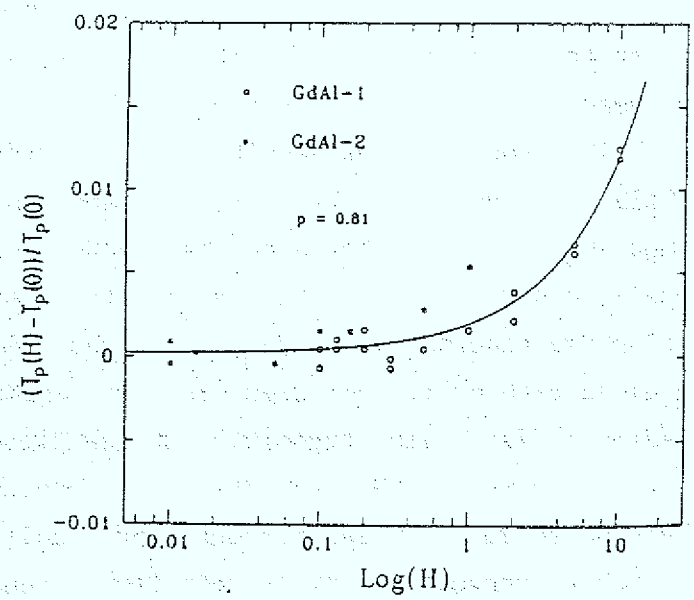

Fig. 68: Normalized peak-temperature, $t_p = (T_p(H) - T_p(0))/T_p(0)$ versus field H for two a-AlGd 37at% samples. $T_p(0)$ was determined as the zero-field limit of a fit to eq. 82, shown by the solid line, which gives the exponent p = 0.81 (From Matsui et al., 1985).

then again implies a large value, $\Delta = 10^2$, which either means $T_f > 0$ or $d_l = 3$. Matsui et al. (1985) extended recently these FC-measurements down to 0.01 Oe, using very slow cooling rates (see Fig. 57). The new, more precise data (Fig. 68) rule out the $T_f = 0$ assumption since at very low fields no shift is observed in the position $T_p(H)$ of the maximum of the FC-$\chi(T)$. Thus, a fit to a nonzero-temperature transition

$$t_p = (T_p(H) - T_p(0))/T_p(0) \propto H^p \qquad (82)$$

with $p = 0.8$ is very satisfactory, as shown by the solid line in Fig. 68.

Now we turn to the second question about the observation of AT-like lines even for typical Heisenberg systems. To reconcile this result with the mean-field predictions of Gabay and Toulouse (1981) (see sec. 4.3.2 and eq. 27), it has been argued that most of experimental methods are weakly sensitive to transverse freezing and can detect only the crossover to strong irreversibility. However, AT-like lines have also been found recently by measurements of the transverse susceptibility which is supposed to be sensitive to transverse freezing (Ketelson and Salamon, 1984). An alternative explanation comes from Kotliar and Sompolinsky (1984). They show that random anisotropy forces, even small, can mix the longitudinal and transverse components and hence the GT-phase diagram is changed. By a mean-field treatment of the SK spin glass with additional Dzyaloskinskii-Moriya interactions the authors predict an Ising-like transition at low fields; high enough fields (relative to the DM-interaction) restore the behavior expected for Heisenberg spin glasses without random anisotropy. Some indications of such a crossover behavior come from torque measurements (Campbell et al., 1983 and 1984; de Courtenay et al., 1984), in which a nearly field-independent irreversibility line is observed. Further work for a clear verification of the GT-line is certainly necessary.

Anisotropic spin glasses: Anisotropy plays a crucial role in the freezing of real spin glasses. Isotropic Heisenberg spin systems are expected to show no spin-glass phase in three dimensions. Monte Carlo simulations on RKKY Heisenberg spin glasses by Walstedt and Walker (1981) suggest that (at least weak) microscopic anisotropy is necessary in order to obtain a cusp in the magnetic susceptibility $\chi(T)$.

The effect of single-ion anisotropy can be studied systematically in rare-earth spin-glasses (Baberschke et al., 1984). Those experiments with uniaxial anisotropic spin-glasses have attracted recent interest, and we will show how far the results can be compared with the magnetic phase diagram in Fig. 21 (sec. 4.3.3) predicted within mean-field theory (eq. 28) by Cragg and Sherrington (1982b) and Roberts and Bray (1982). Finally the behavior in applied magnetic fields will be discussed briefly.

Baberschke et al. (1984) report on magnetization measurements on single crystals of Y and Sc containing Gd, Tb, Dy, and Er impurities. The crystal-field parameters are wellknown. YEr and ScEr are expected to be Ising-like systems (longitudinal freezing for $D > 0$) while the alloys with Dy and Tb are expected to be XY-like (transverse freezing for $D < 0$). The ratio $D/\tilde{J}$ can be changed by varying the rare-earth concentration, which enables one to go from the Ising or XY limit at low concentrations to the most interesting intermediate situations at higher concentrations where at sufficiently small values of $/D//\tilde{J}$ the successive freezing of the two components at different temperatures is predicted; see the phases L, T and LT in Fig. 21. For YGd and ScGd, D is very small ($\sim 4 \times 10^{-3}$K); their magnetic properties appear to be almost isotropic (Wendler et al., 1984).

In Fig. 69 the experimental results are compiled in a plot of $D/\tilde{J}$ versus $T_f/\tilde{J}$ which can be compared directly to the theoretical phase diagram in Fig. 21. The values of $D/\tilde{J}$ are calculated as explained in the paper (Baberschke et al., 1984), and T_f is chosen as the low-field limit of the temperature at which the FC-$\chi(T)$ curve departs from the ZFC curve. Typical experimental data of the Heisenberg-spin system ScGd 15% (Wendler et al., 1984) and of the XY-spin system YDy 3% (Baberschke et al., 1984) are shown in Fig. 70 and 71, respectively.

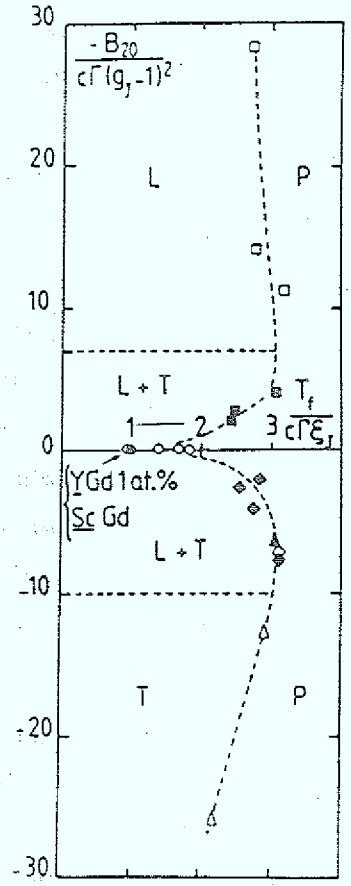

Fig. 69: Experimental phase diagram for Sc- and Y-based alloys (to be compared to the theoretical phase diagram of Fig. 21). $-B_2^0/[c\,\Gamma\,(g_J-1)^2] \equiv D/\tilde{J}$ versus $T_f/(c\,\Gamma\,\tilde{\xi}_j) = T_f/J$. The experimental data correspond to YEr (□), ScEr (■), YDy (◇), ScDy (◆), YTb (△), ScTb (▲), YGd (○), and ScGd (●) alloys (From Baberschke et al., 1984).

The most remarkable agreement of Fig. 69 with Fig.21 is for the ratio of about 3 between the values of $T_f/\tilde{J}$ in the Ising ($D/\tilde{J} \gg 1$) and Heisenberg ($D/\tilde{J} = 0$) limits. In contrast, the ratio between the experimental values of $T_f/\tilde{J}$ in the XY and Heisenberg limits is definitely larger than the value 1.5 predicted by theory. At large values of $/D//\tilde{J}$ (=open symbols in Fig. 69) irreversibility effects are observed only for longitudinal (or transverse) fields (see Fig. 71). At small values of $/D//\tilde{J}$ (=full symbols in Fig. 69) irreversibilities are observed in both directions below the same temperature (see Fig. 70). Thus the two-stage freezing predicted by the theory (Fig. 21) cannot be identified here.

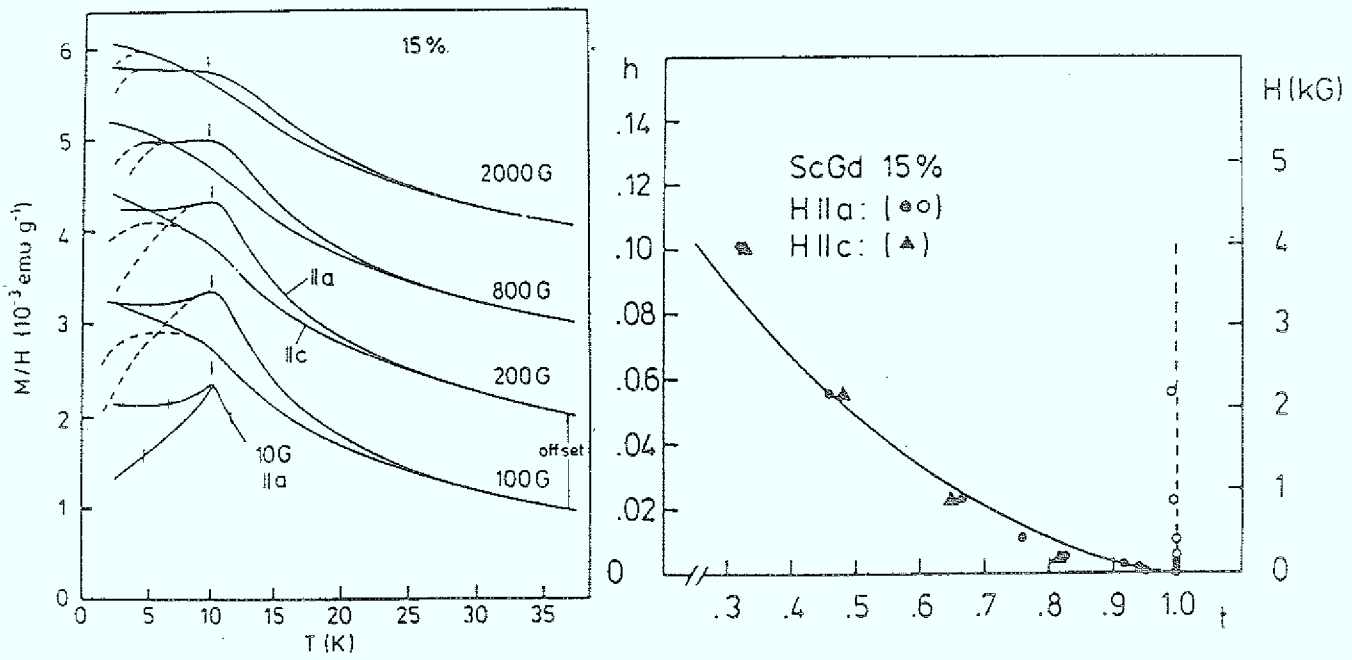

Fig. 70: (a) ZFC (dashed line) and FC (solid line) susceptibility, M/H, of ScGd 15at% for $\parallel \vec{a}$ and $\parallel \vec{c}$. The curve for 100 G corresponds to the scale of the vertical axis, the other curves are shown with the indicated offset. In the 10 G experiment the experimental error bars are indicated by vertical lines. The arrows indicate the cusp temperature. (b) Full symbols show the onset of irreversibility (T_f^{irr}), open symbols the temperature of the cusp (T_f^{χ}) versus $h = g\mu_B(S(S+1)/m)^{1/2}\cdot(kT_{fo})^{-1}$. The temperatures are scaled with $T_{fo} = T_f^{irr}$ (10 G) = T_f^{χ}(10 G). The solid curve is the AT line (eq. 15), with a scaling factor 1/12, and the dashed one the GT line (eq. 27) (From Wendler et al., 1984).

Very recently, Schröder et al. (1986) have succeeded in observing an anisotropic behavior with subsequent longitudinal and transverse freezing at different temperatures in a new anisotropic spin glass $Eu_xSr_{1-x}As_3$ whose phase diagram is displayed in Fig. 9 (see sec. 3.3). The ac susceptibility $\chi(T)$ at 380 Hz of the x = 0.24 compound (Fig. 72) exhibits a strong difference in $\chi_{\parallel}$(= ac driving field

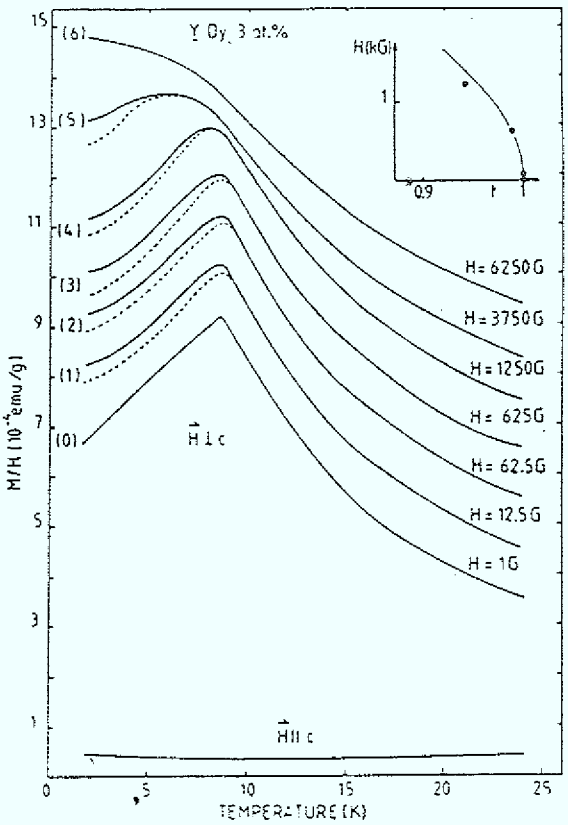

Fig. 71: ZFC (dashed line) and FC (solid line) susceptibility, M/H, of YDy 3at% for $\vec{H} \perp \vec{c}$ and $\vec{H} \parallel \vec{c}$. Insert: Field H vs. $t = T_f^{irr}/T_f$, where T_f^{irr} is defined as the temperature where the ZFC curve departs from the FC one. The full line corresponds to $H^2 \sim 1-t$ (From Baberschke et al., 1984).

parallel to the b direction) and $\chi_\perp$, the longitudinal spin components freeze at $T_f^{\parallel} = 1.17$ K, while $\chi_\perp$ continues to rise towards lower temperatures and shows a maximum at $T_f^{\perp} = 0.20$ K. The peaks in $\chi(T)$ at both temperatures are frequency dependent (see inserts of Fig. 72). The interactions in this system are predominantly short-ranged, and there are Eu^{2+} ions in an S-state where crystal-field effects are absent to lowest order. Probably a weak anisotropic contribution to the exchange interactions

is the origin of the behavior of $\chi(T)$ shown in Fig. 72. In this context it is interesting to note that Thalmeier (1986) proposes a realistic exchange Hamiltonian for pure $EuAs_3$ which is shown to lead to a proper incommensurate modulation of the spin order (see sec. 3.3) if the exchange interactions are sufficiently anisotropic.

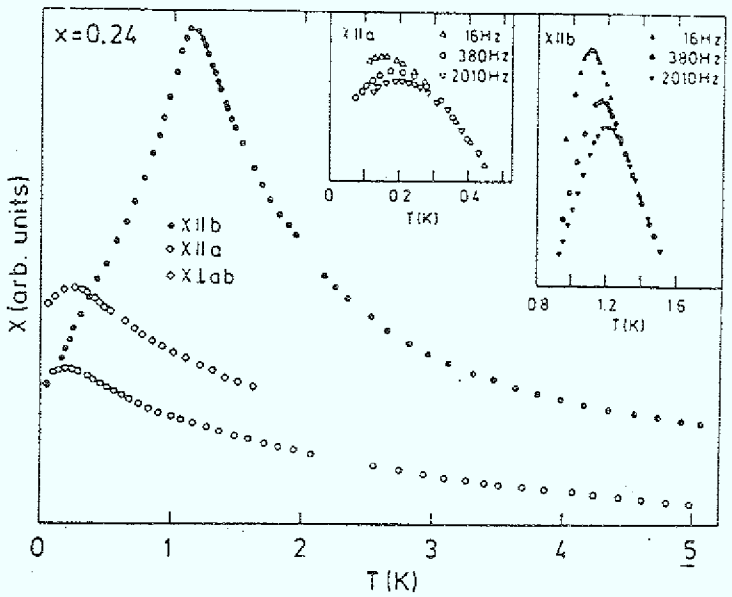

Fig. 72: Ac susceptibility χ(at 380 Hz) of $Eu_{0.24}Sr_{0.76}As_3$ in different crystallographic directions. Inserts show the frequency dependence of χ (From Schröder et al., 1986).

Let us return to Figs. 70, 71 in order to discuss the field dependencies of T_f. If one defines T_f^{irr} as the temperature where the ZFC-susceptibility departs from the FC one, Baberschke et al. (1984) find $\delta T_f^{irr}(H) \propto H^2$ for XY spin-glasses like YDy (Fig. 71 and insert), in agreement with what is expected for the GT-line. In addition, a general feature observed for all XY-like alloys is that T_f^{irr} is always higher than the temperature T_f^{χ} of the maximum of the ZFC susceptibility (Fig.71). Both properties observed in the XY-like systems apparently follow the behavior predicted for Heisenberg-spin glasses on the basis of the SK Hamiltonian (Sherrington, 1983).

On the other hand, the also studied Ising-like ScEr and YEr alloys follow the behavior expected for Ising-spin glasses, with a splitting between the FC and ZFC susceptibility at the same temperature T_f^{irr} as T_f^{χ} , and with $\delta T_f^{irr}(H) \propto H^{2/3}$.

But surprisingly, Wendler et al. (1984) observe in the Heisenberg-like spin glass ScGd (Fig. 70) the characteristic temperature T_f^{irr} to be shifted to lower temperatures in the field with $\delta T_f^{irr}(H) \propto H^{2/3}$, while $T_f^{\chi}(H)$ stays constant ($\geq T_f^{irr}$). Thus, it is difficult to understand why the behavior predicted for Heisenberg-spin glasses should be observed in XY-spin glasses and not in ScGd or in the classical Heisenberg-spin glasses such as CuMn, AgMn, etc.

Summarizing this subsection, there are extensive efforts in the comparing of experimental results with mean-field theory of spin glasses. Indeed, a great deal of theoretical information about the spin-glass transition has been provided by the mean-field theory but one has to keep in mind that it is only valid in high dimension. Even if in real three-dimensional systems the spin-glass freezing is a static phase transition, one should not expect that one can describe it quantitatively by mean-field theory. Fisher and Sompolinsky (1985) argue that several mean-field results for spin glasses apply only for $d \geq 8$. They show that for $d < 6$ in particular the exponent ψ of the finite-field transition lines, $\delta T_f \propto H^{\psi}$, if they exist, should be equal for both Ising and Heisenberg spins in short-range spin-glasses and different from the mean-field exponents $\psi_{AT} = 2/3$ and $\psi_{GT} = 2$, respectively. Recent numerical estimates for a three-dimensional Ising-spin glass by Bhatt and Young (1985) and Ogielsky (1985) yield $\psi = 2/3.7 = 0.54$ and $\psi = 2/3.4 = 0.59$, respectively, thus the apparent agreement (see above) between the measured exponent ψ and the AT-mean-field exponent $\psi_{AT} = 2/3$ is accidental, as already suggested by Malozemoff et al. in 1983.

Clearly there is need for spin-glass theories beyond mean-field. One approach in this direction is presented by Malozemoff et al. (1983, 1985). They propose a critical fractal cluster model of spin glasses which is able to describe the essential features of the phenomena

occurring near the spin-glass transition and to account for the static critical exponents. The basic assumption of this fractal model is the existence of a temperature- and magnetic-field-dependent characteristic cluster size s_ξ on which all relevant physical quantities depend and which diverges at the transition temperature T_f. It is related to the correlation length ξ and the cluster fractal dimension D by $s_\xi \propto \xi^D$. Very recently, Continentino and Malozemoff (1986) extend this model to describe several aspects of spin-glass dynamics: stretched exponential relaxation, magnetic noise, and scaling above $T_f(H)$.

7.3 Evidences for a phase transition :

In spin glasses critical behavior near T_f is not expected in the linear term χ_o of the susceptibility M/H, but in the nonlinear susceptibility χ_{nl}. This is known from mean-field theory of spin glasses (Suzuki, 1977) where the order parameter is not the magnetization but the quantity $q = \sum_i [\langle S_i \rangle^2]_{av}$ as suggested by Edwards and Anderson in 1975(see sec. 4). Then, the field conjugate to the order parameter q is H^2 in spin glasses (instead of H which is coupled to the order parameter M in a ferromagnet). Above T_f this transition shows up in the susceptibility $\chi_{EA} \propto \sum_i [\langle S_i S_j \rangle_T^2]_{av}$ which diverges at T_f as

$$\chi_{EA} \propto t^{-\gamma} , \quad \gamma = 1 \qquad (83)$$

where $t := |T-T_f|/T_f$. Furthermore, the magnetic field dependence of the susceptibility at T_f may be associated with the critical exponent δ (Chalupa, 1977)

$$q(T_f,H) \propto (H^2)^{1/\delta} . \qquad (84)$$

The nonlinear susceptibility is defined by the expansion of the magnetization with respect to an external field as

$$M/H = \chi_o(T) - \chi_{nl}(T) \cdot H^2 + o(H^4) . \qquad (85)$$

The critical parts of χ_{nl} and of χ_{EA} are proportional (Binder, 1982), for symmetric models we have simply

$$\chi_{nl}(T) = T^{-3}(\chi_{EA}(T)-2/3) \quad . \qquad (86)$$

Hence, the nonlinear χ of spin glasses is one of the most important physical quantities characterizing the spin-glass transition, if it exists at all in the thermodynamic sense, and we will discuss experimental efforts in this direction now.

In spite of problems as discussed above to locate the static T_f in zero field, numerous attempts have been made to estimate critical exponents for spin glasses. Table 1 contains a list of values for critical exponents obtained from measurements on various spin glasses either directly or via scaling relations. Monod and Bouchiat (1982) show in Fig. 73 that their field-cooled magnetization data of the spin glass AgMn 10.6 % (with T_f = 37.4 K) indeed exhibit a quadratic variation of M/H in H above T_f, thus $\chi_{nl}(T)$ is defined according to eq. 85.

Note the general feature and hence difficulty in this analysis that the field extension allowing a reasonable fit of the nonlinear susceptibility decreases rapidly when approaching T_f. The authors conclude that the resulting χ_{nl} is consistent with a power-law divergence

$$\chi_{nl}(T) \propto t^{-\gamma} \qquad (87)$$

with a critical exponent γ of $1<\gamma<2$ as displayed in the insert of Fig. 73.

Barbara et al. (1981) analyze their data by taking a free exponent a(T) of the nonlinear term, $H^{a(T)}$, instead of the quadratic term in the expansion of eq. 85. Starting with a(T) = 2 at high temperatures they find a continuous decrease of a(T) already in the paramagnetic regime (which does not fulfill the general law that the free energy has to be analytic in H) and a pronounced minimum of $a(T_f) \approx 0.7$ as well as a divergence of $\chi_{nl}(T)$ at T_f(eq. 87).

Table 1: Critical exponents obtained for various spin-glass systems. Some of the values are deduced from scaling laws (e.g. specific heat with = 2 - - 2β).

	δ	γ	β	ϕ	α	Range of T: $\Delta T/T_f$	Range of H: M_{nl}^{max}/M	Remarks	Reference
AgMn(0.4,0.5,0.7,20.5%)	3.1±0.2	2.2±0.2	1.0±0.1	3.2±0.1	-2.2	0.1	0.1	not s.-c.	Bouchiat, 1986
AgMn (10.6%)		1.5±0.5				0.4	0.1		Monod and Bouchiat, 1982
AgMn (150 ppm)	6.6	3.8	0.7	4.5	-3.2			not s.-c.	Novak et al., 1986
CuMn (1%)	4.4	3.25±0.10	0.75±0.25	4.2	-2.7	2	0.5		Omari et al., 1983
CuMn (0.25%)	4.5	3.6±0.3	1	4.5	-3.6	0.7			Berton et al., 1982
CuMn(4.6%)	4.15±0.15	3.8±0.5	1.2	5.0±0.5	-4.1	1	0.5	not s.-c.	Barbara et al., 1981
CuMn(2%)	1.5±0.3						0.02	AC	Mulder et al., 1981
AuFe (1.5%)	2.0±0.2	1.1±0.2	0.9	2.0	-1	0.1	0.01	AC	Taniguchi et al., 1983
$Eu_xSr_{1-x}S$(X=0.15,0.25, 0.3,0.4)	4.1							AC	Maletta et al., 1979b
a-AlGd (37%)	6.1±0.2	3.4±0.4	0.7	4.0±0.5	-2.8	1	0.6	not s.-c.	Barbara et al., 1981
a-AlGd (37%)	5.7±0.2	2.7±0.1	0.9/0.6	3.3±0.4	-2.1	0.16	0.3		Malozemoff et al.,1982
a-$Fe_{10}Ni_{70}P_{20}$	5.2±0.5	2.3±0.2	0.55	2.9	-1.4	0.3	0.15	AC	Taniguchi et al.,1985
a-AlMnSi	5±1	0.9	0.2	1.1±0.2	+0.7			AC, not s.-c.	Beauvillain et al.,1984a
a-AlMnSi	3.2	3.1±0.1	1.4±0.1	4.5	-3.9	0.4	0.05	AC	Beauvillain et al.,1984b
a-AlMnSi	3.4	3.4±0.1	1.4±0.1	4.8	-4.2			AC	Beauvillain et al.,1986
a-FMnP	5.5	3.6±0.15	0.8±0.1	4.4	-3.2			AC	Beauvillain et al.,1986
a-FMnP	5.5	3.6±0.2	0.8±0.1	4.4	-3.2				Beauvillain et al.,1986

AC = ac-technique

not s.-c. = treatment not self-consistent, as described in the text.

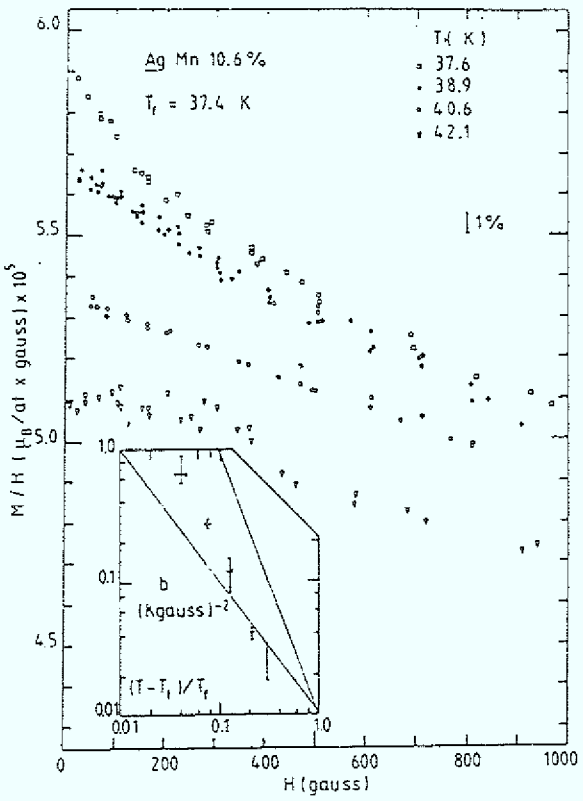

Fig. 73: Susceptibility, M/H, plotted vs. magnetic field H in AgMn 10.6at% at four temperatures above T_f as indicated. Insert shows a log-log plot of the nonlinear susceptibility χ_{nl} vs. the reduced temperature $t = (T-T_f)/T_f$. Straight lines indicate variations $\chi_{nl} = t^{-\gamma}$ with $\gamma = 1$ and $\gamma = 2$, respectively (From Monod and Bouchiat, 1982).

Chikazawa et al. (1983) analyze ac susceptibility data (80 Hz) of AuFe 0.97 % and claim that $\chi_{nl}(T)$ exhibits a logarithmic behavior rather than a power law (eq. 87). But after improving the signal-to-noise ratio in the ac-technique (discussing also the contributions of 3ω- and 5ω-terms induced by the ac-field amplitude $h=h_0 \cdot \sin\omega t$), the same group (Taniguchi et al., 1983) also obtains a critical power-law behavior for χ_{nl} (T) in AuFe 1.5 % with $\gamma = 1.1 \pm 0.2$. Taniguchi et al. (1985) recently studied the a-$Fe_{10}Ni_{70}P_{20}$ spin glass by the same method which shows $\gamma = 2.3 \pm 0.2$.

Most other work yield somewhat higher values of γ (Berton et al., 1982; Barbara et al., 1981). Careful ac and dc susceptibility measurements were performed on the amorphous manganese aluminosilicate spin glass with 15at% Mn by Beauvillain et al. (1984b). The ac susceptibility data are fitted with a series expansion in even powers of an applied static field up to the forth term in order to obtain $\chi_{nl}(T)$, resulting in $\gamma = 3.1 \pm 0.1$ and $\beta = 1.4 \pm 0.1$.

Fairly strong evidence in favor of the existence of a nonzero transition is provided by the measurement of the magnetic equation of state at $T > T_f$, as done with CuMn 1% by Omari et al. (1983). They analyze their static magnetization data in the ranges $T_f < T < 4T_f$ and $0 < H < 7T$ in terms of an expansion including higher-order nonlinear terms:

$$\frac{M}{\chi_0 H} = a_1 - \frac{1}{15} a_3 \cdot \left(\frac{\mu H}{kT} \right)^2 + \frac{2}{305} a_5 \cdot \left(\frac{\mu H}{kT} \right)^4 + \ldots \qquad (88)$$

where the expansion coefficients a_1, a_2, a_3 are related to the critical exponents β and γ by

$$a_1 = 1$$
$$a_m = \left(\frac{T - T_f}{T} \right)^{-n(\beta+\gamma)+\beta} \qquad \text{for } m = 2n + 1 > 1 \qquad (89)$$

and are all normalized to 1 for $T \to \infty$. Note that Omari et al. use the nonlinear variable $(T-T_f)/T$ instead of t. The values of the parameters a_1, a_2, and a_3, obtained in a fit with eq. 88 for various temperatures above $T_f = 10.05$ K, are displayed in Fig. 74b. While a_1 stays constant (=1) representing the non-interacting paramagnetic contribution, the other parameters, a_3 and a_5, vary by 3 and 7 orders of magnitude, respectively, between $4T_f$ and $1.1\ T_f$ and seem to diverge both at the same temperature T_f. Assuming $T_f = 0$, a power-law divergence of a_3 in T does not describe the $a_3(T)$ data (see insert of Fig. 74b). Both coefficients are found to be related to each other by

$$a_5 \approx a_3^{2.25 \pm 0.05} \qquad \text{for } T \geq 1.1\ T_f \qquad (90)$$

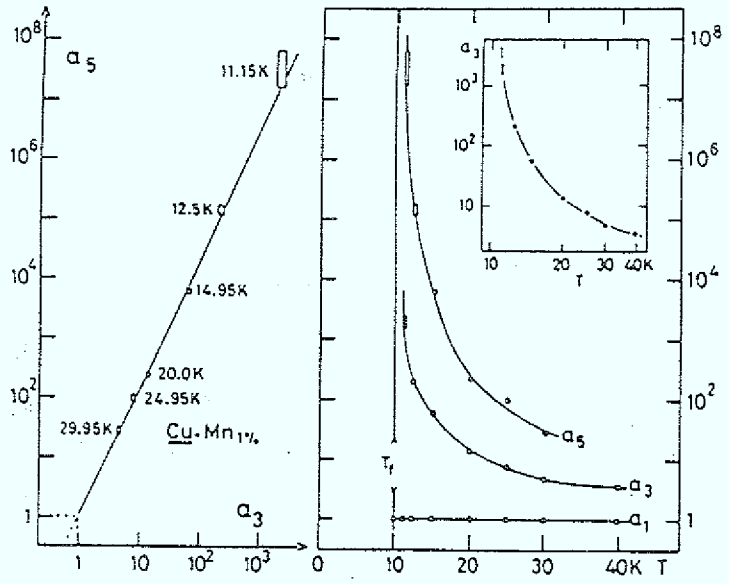

Fig. 74: The coefficients a_1, a_3, a_5 involved in the series expansion of the magnetization (eq. 88) for CuMn 1at% are displayed vs. temperature in a semi-log plot on the right-hand-side (part b) of the figure. On the left-hand-side (part a), log a_5 is plotted vs. log a_3 at the same temperatures. Note that the data extrapolate to a point where both a_3 and a_5 are equal to unity, which should be associated to the high-temperature paramagnetic limit. The straight line in part a of the figure yields the slope 2.25 ± 0.05 (eq. 90). The log a_3 vs. log T plot shown in the insert stresses the failure of any attempt to describe the data with a power law in T ($T_f = 0$ - hypothesis) (From Omari et al., 1983).

shown in Fig. 74a. The fact that $a_5 \neq (a_3)^2$ implies that two exponents, γ and β, are necessary to describe the transition with eq. 88. This eliminates the possibility of a transition occuring at $T_f = 0$. The divergence of both a_3 and a_5 can be described over the whole T range by the power law in $T/(T-T_f)$ with the exponents 3.25 ± 0.05 and 7.25 ± 0.05, respectively. Using eq. 89 implies $\gamma = 3.25 \pm 0.10$ and $\beta = 0.75 \pm 0.25$.

Very recently Bouchiat (1986) performed magnetization measurements on AgMn spin glasses in a wide concentration range, 0.4 % < c < 24%, by means of an experimental set-up where the linear part of M is compensated in situ by a small coil mounted on the sample holder in order to increase the accuracy of the so directly measured nonlinear part $\Delta M/H$ ($=M_{nl}/H$). A typical set of curves $\Delta M/H$ as function of H^2 in AgMn 20% is shown in Fig. 75 for various temperatures above T_f = 68.5 K. The initial slope of each curve yields $\chi_{nl}(T)$ of the H^2-term in eq. 85, which is well described by a power law divergence (eq. 87) with $\gamma = 2.3 \pm 0.1$ for this sample with 20 at% Mn in the temperature range between T_f and 1.1 T_f ($\gamma = 2.1 \pm 0.1$ for the 0.5 at% sample). An apparently higher value of $\gamma_{eff} = 3$ is obtained in an extended T-range between 1.1 and 1.5 T_f.

Turning over to the determination of the critical exponent δ (table 1), one of the first experimental attempts is performed for $Eu_xSr_{1-x}S$ spin glasses with x = 0.15, 0.25, 0.30 and 0.40 (Maletta and Felsch, 1979b). They measure the dependence of the ac-χ-maxima (with 117 Hz) on a superposed static field up to 0.1 T. The normalized data, $\chi_{max}(H)/\chi_{max}$

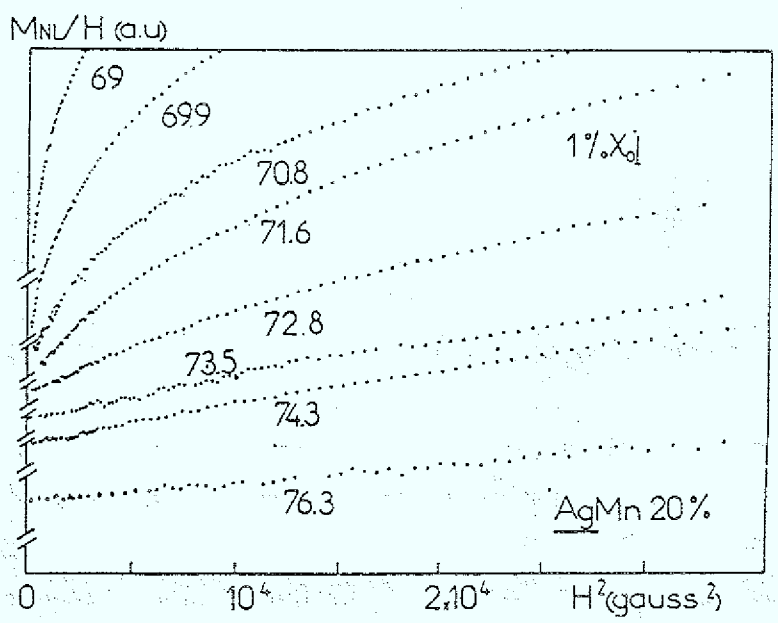

Fig. 75: Typical set of curves, $\Delta M/H$ as a function of H^2, in AgMn 20 at% for various temperatures above T_f (From Bouchiat, 1986).

(H=0), fairly independent of concentration are associated with the putative order parameter q by the relation

$$q(T_f,H) \propto 1-\chi_{max}(H)/\chi_{max}(H=0) \qquad (91)$$

and are indeed compatible with eq. 84 (Fig. 76a), which gives an exponent δ = 4.1. Moreover, good agreement is found (Fig. 76b) with numerical simulations of the EA-order parameter at T_f by Stauffer and Binder (1978) yielding δ= 4.0 in three dimensions.

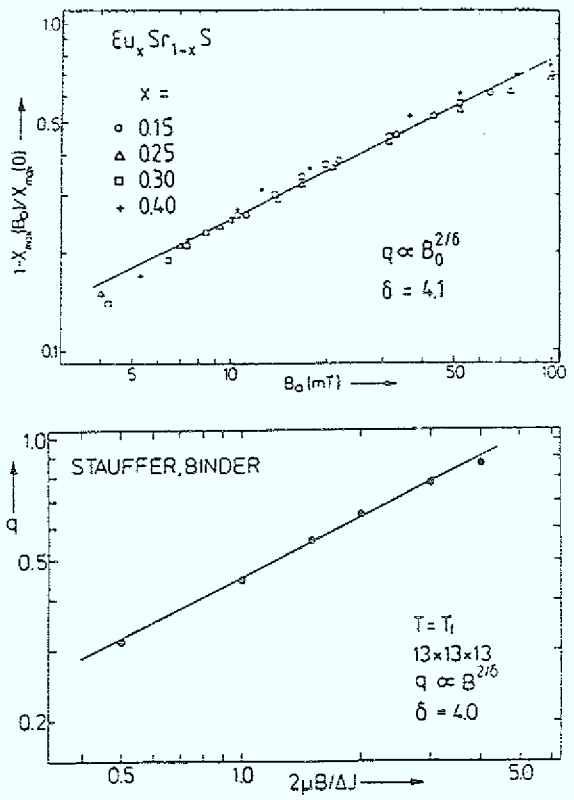

Fig. 76: (a) Depression of χ at the maximum of the ac-χ(ω= 117 Hz) in $Eu_xSr_{1-x}S$ spin glasses as function of the external field, measured for various Eu-concentrations x as indicated. Straight line on this log-log plot gives an exponent δ = 4.1 (From Maletta and Felsch, 1979b). (b) Field dependence of the EA order-parameter at T_f, calculated from Monte Carlo simulations of a simple cubic Ising model with nearest-neighbor exchange distributed according to a Gaussian of width ΔJ. Data points are based on observations of 2000 MCS (From Stauffer and Binder, 1978).

Similar measurements of ac-χ (332 Hz) on CuMn 2% by Mulder et al. (1981) yield an anomalously small value of $\delta = 1.5 \pm 0.3$. Taniguchi et al. (1985) obtain $\delta = 5.2 \pm 0.5$ in a-$Fe_{10}Ni_{70}P_{20}$.

Bouchiat (1986) determines δ from the M_{nl} measurements. At the transition temperature T_f the data of AgMn 0.5% can be well fitted between 10 G and 400 G (where $M_{nl}/M < 0.1$) by a power law

$$M_{nl}/H \propto H^{2/\delta} \qquad (92)$$

yielding $\delta = 3.1 \pm 0.1$ (independent of concentration) as shown in Fig. 77. Deviations towards apparently higher values of δ occur at higher fields (see Fig. 77).

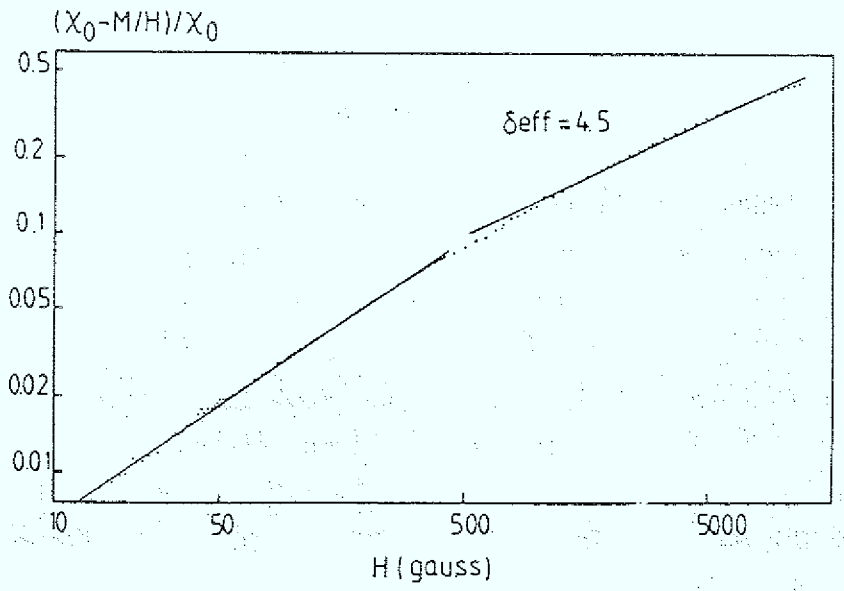

Fig. 77: Nonlinear magnetization versus magnetic field at T_f (log-log plot) for AgMn 0.5 at% in the range of magnetic field where $M_{nl}/M < 0.5$. Note deviations towards apparent values of δ ($\delta_{eff} = 4.5$) which are higher than the value ($\delta = 3.1$) deduced when the analysis is restricted to the range of field where $M_{nl}/M < 0.1$ (From Bouchiat, 1986).

If a phase transition at a nonzero temperature T_f exists in spin glasses, one expects that the nonlinear susceptibility should satisfy a static scaling law:

$$1-\frac{M}{\chi_0 H} = t^{\beta}\cdot\tilde{M}\left\{\left(\frac{H}{T}\right)^2\cdot t^{-\phi}\right\} \qquad (93)$$

where $t = (T-T_f)/T_f$, $\tilde{M}$ being the appropriate scaling function with

$$\begin{aligned}\tilde{M}(x) &\propto x && \text{for } x \to 0\\ \tilde{M}(x) &\propto x^{1/\delta} && \text{for } x \to \infty\end{aligned} \qquad (94)$$

and scaling relations for the crossover exponent ϕ

$$\begin{aligned}\phi &= \beta + \gamma\\ \phi &= \gamma\delta/(\delta-1) = \beta\delta.\end{aligned} \qquad (95)$$

Barbara et al. (1981) presented the first experimental demonstration of scaling in both field and temperature for the spin-glass susceptibility in CuMn 4.6 % and a-AlGd 37%. This first treatment is not self-consistent because they determine χ_0 from an expansion in H with a varying term $H^{a(T)}$ (as described above) which does not agree with eq. 93. The same criticism holds for the recent papers by Beauvillain et al. (1984a) and Novak et al. (1986). A self-consistent scaling analysis is performed by Malozemoff et al. (1982) of magnetization data on a-AlGd 37%, the results of such a fit give $\phi = 3.3 \pm 0.4$, $\gamma = 2.7 \pm 0.1$, $\beta = 0.93 \pm 0.04$, and $\delta = 5.7 \pm 0.2$. They argue that the critical region extends from $T_f = 15.5$ K to about 22 K and in field up to about 15 kOe. Not all scaling relations for the various critical exponents are nicely satisfied, and low-field upturns fail to be described by the scaling. The authors suggest transition broadening due to sample inhomogeneity as a possible cause.

Beauvillain et al. (1986) measured the dc- and ac-susceptibility (69 Hz) of two insulating spin glasses, the amorphous manganese aluminosilicate (a-AlMnSi) with $T_f = 2.95$ K and the amorphous manganese fluorophosphate (a-FMnP) with $T_f = 2.80$ K in the field range up to 600 Oe near the freezing temperature. The nonlinear parts of the ac-χ are well described by the series expansion up to the H^6-term,

yielding the exponents $\gamma = 3.4 \pm 0.1$, $\beta = 1.4 \pm 0.1$ in a-AlMnSi and $\gamma = 3.6 \pm 0.15$, $\beta = 0.8 \pm 0.1$ in a-FMnP. Using these values of γ and β, all data in the whole field range fall onto a universal curve in a scaling plot with eq. 93. These results are in remarkable agreement with the scaling analysis of the static low-field magnetization measured on the same a-FMnP spin glass which gives identical values for γ and β.

Omari et al. (1983) present an impressive scaling plot as shown in Fig. 78. All the data of CuMn 1% within the anomalous wide range $1.1\ T_f < T < 4\ T_f$ in fields up to 7 T superimpose to fit a unique function of the scaling variable with $\gamma = 3.25$ and $\beta = 0.75$ as deduced from the temperature dependence of a_3 and a_5 (eq. 88) in the $H \to 0$ limit (which is already described above). An even improved scaling is obtained with $\beta = 0.95$ (which yield $\delta = 4.4$). These values of the exponents are consistent with those deduced on the same spin glass, CuMn 0.25 %, by a completely different technique using the magnetocaloric effect (Berton et al., 1982).

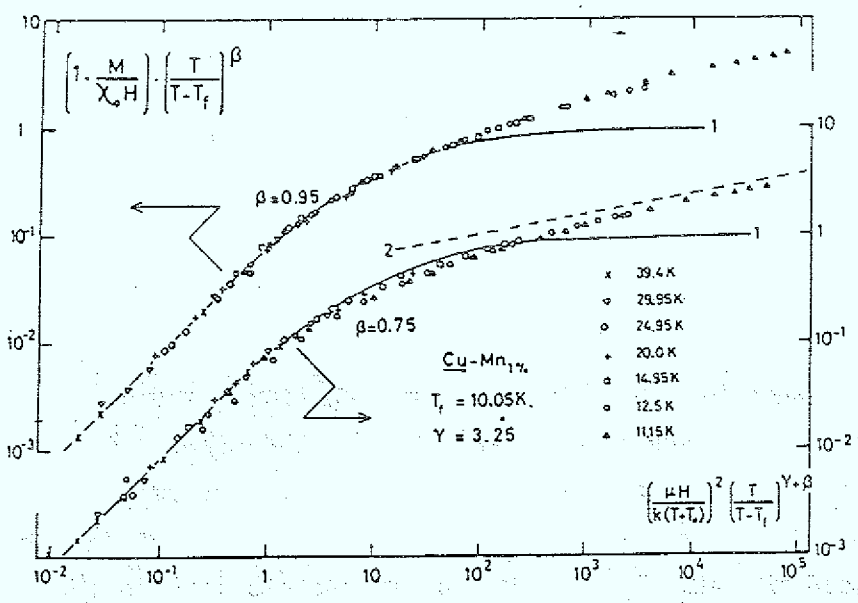

Fig. 78: Scaling plot of the magnetization data for CuMn 1at% using eqs. 88 and 89 for two choices of the exponent β (as indicated) and for $\gamma = 3.25$. Data at H up to 70 kOe and T up to 4 T_f are included (From Omari et al., 1983).

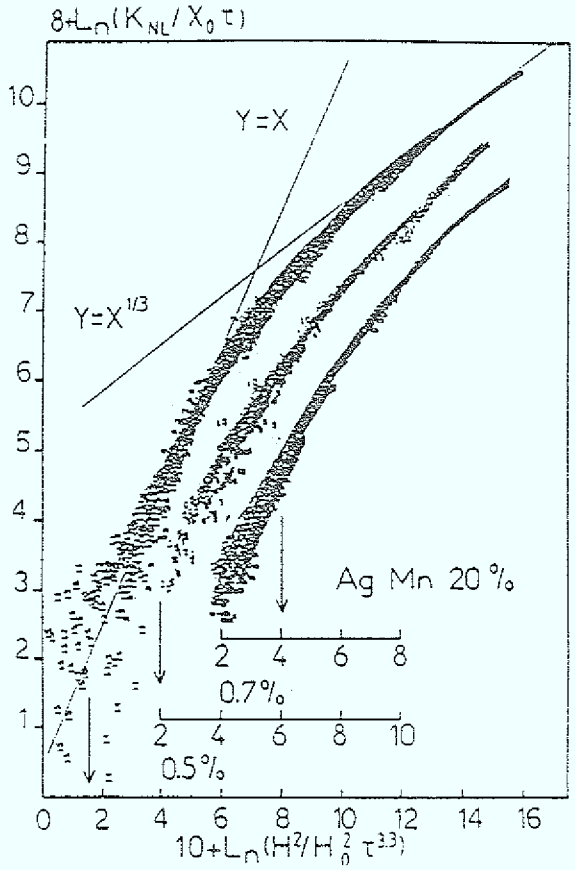

Fig. 79: Scaling of the nonlinear magnetization (eq. 93-95) for 15 different values of temperature between T_f and 1.1 T_f (τ denotes the reduced temperature t) and 200 values of magnetic field for which $M_{nl}/M < 0.1$. Note the shifted origins on the abszissa for the three alloys of AgMn with 0.5, 0.7, and 20 at% Mn concentration (From Bouchiat, 1986).

In a very careful work by Bouchiat (1986) the nonlinear magnetization of various AgMn spin glasses is also analyzed in the framework of a phase transition. The transition temperature T_f is determined by three methods which give the same value within $\pm$ 0.5 %: ac-χ maximum (30 Hz); low-field magnetization; onset of irreversibility in the low-field magnetization (FC, ZFC). Then, Bouchiat uses three independent experimental criteria to determine the critical exponents among which two only are independent, assuming the T_f-value from above. When

the analysis is restricted to the reduced temperature and magnetic field range where $(T-T_f)/T_f < 0.1$ and $M_{nl}/M < 0.1$, Bouchiat finds $\gamma = 2.2 \pm 0.2$, $\beta = 1.0 \pm 0.1$, and $\delta = 3.0 \pm 0.2$. (The determination of γ and δ was already discussed above). It is also possible to describe all the data with a universal scaling function (eq. 93), as illustrated in Fig. 79. The best fit is obtained for $\phi = 3.2 \pm 0.1$ and $\beta = 1.0 \pm 0.1$ independent of the Mn concentration. Note that the crossover exponent ϕ verifies the scaling relations $\phi = \beta + \gamma$. The asymptotic forms of the scaling function $\tilde{M}(x)$ (eq. 94) can also be checked in Fig.79 as indicated by the two straight lines. The three independent determinations of the critical exponents also verify the scaling relations in eq. 95. Extending the "critical range" leads to apparently higher values of the exponents as shown above (Fig. 77), but the possibility of a real physical crossover occuring at $t > 0.1$ cannot be excluded. The different ranges of the critical region used in the various attempts to deduce critical exponents for spin glasses may explain the discrepancies existing between the different values obtained so far (see table 1).

Finally, let us consider the spin dynamics near T_f. Nonexponential decay of the dynamic correlation function and the rapid growth of correlation times on approaching T_f from above have been clearly established in spin glasses, as discussed in sec. 6. At present experiments, however, do not permit the determination of the exact shape of the dynamic correlation function. On the other hand the temperature dependence of the correlation times is analyzed very carefully by Bontemps et al. (1984, 1986) within the framework of <u>critical slowing down</u> applying two different dynamical scaling models:

(i) The <u>standard dynamic scaling</u> near the spin-glass temperature $T_c > 0$ which is considered as a second-order phase transition gives for the relaxation time τ and the correlation length ξ the relations

$$\tau/\tau_0 \propto \xi^z \propto t^{-z\nu} \qquad (96)$$

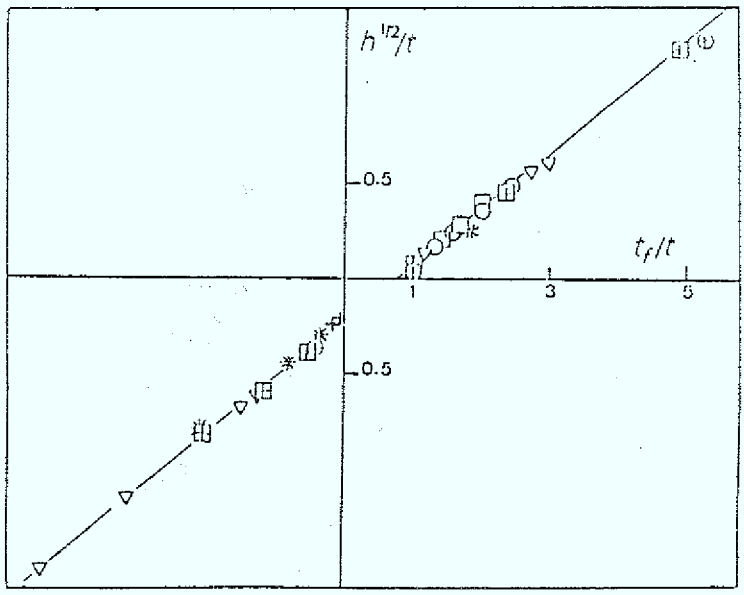

Fig. 80: Dynamic scaling of the $T_f(H,\omega$ or $t_m)$ lines for $Eu_{0.40}Sr_{0.60}S$ in the case of a nonzero-temperature transition (T_c = 1.50 K). Data are taken from χ-phase (1 Hz$<\omega<10^4$ Hz) and remanent-magnetization (10 msec $< t_m <$ 25 sec) measurements (From Bontemps et al., 1986).

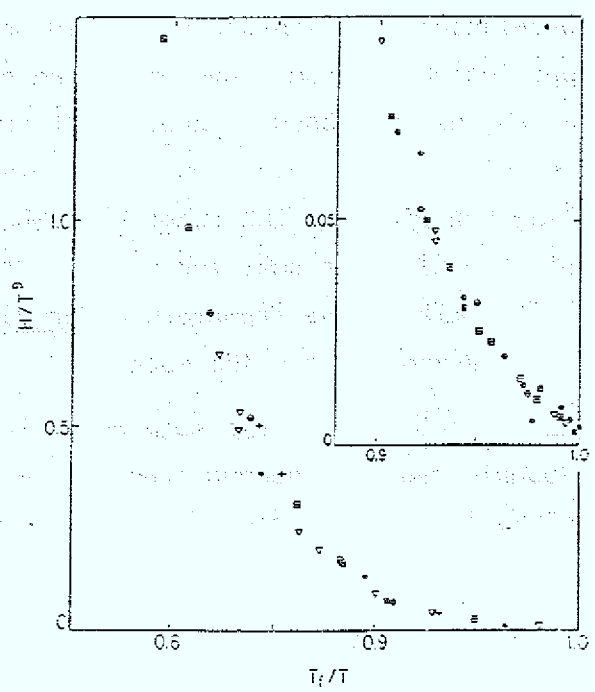

Fig. 81: "Logarithmic" dynamic scaling of the T_f $(H,\omega$ or $t_m)$ lines for the same data as in Fig. 80, but now in the case of a zero-temperature transition (T_c = 0). The insert shows the low-field points with an extended scale (From Bontemps et al., 1986).

where z is the dynamic exponent (Hohenberg and Halperin, 1977). The field dependence of ξ generates the field dependence of τ :

$$\tau / \tau_0 \propto t^{-z\nu} \cdot \tilde{\tau}(h^2/t^{\beta+\gamma}) \qquad (97)$$

$\tilde{\tau}$ being an appropriate scaling function.

(ii) The alternative picture of logarithmic scaling near a $T_c = 0$ phase transition (Binder and Young, 1984) (see also eq. 81 and discussion there) assumes that thermal activation processes over free energy barriers ΔF controlled by $\xi(T)$ are important, hence

$$\ln(\tau/\tau_0) \propto \Delta F(\xi)/T \propto \xi^{z-1/\nu} /T \propto T^{-z\nu} \qquad (98)$$

and similarly:

$$\ln(\tau/\tau_0) \propto T^{-z\nu} \cdot \tilde{\tau}(h /T^{\Delta}) \quad \text{with } \Delta=(\beta+\gamma)/2 \ . \qquad (99)$$

Bontemps et al. (1984, 1986) study $T_f(\omega,H)$ lines of the $Eu_{0.40}Sr_{0.60}S$ spin glass for frequencies 10^4 Hz $< \omega <$ 10^{-2} Hz by means of Faraday rotation and SQUID measurements. In addition measurements of the remanent magnetization are performed by optical means in the 10 msec-1 sec and 500 msec - 25 sec time ranges. Large demagnetizing-field corrections have to be made due to the platelet-shaped sample. The authors establish a dynamical criterion in order to extract a characteristic response time from the $\chi(\omega,T,H)$ data. Taking the response of a system in terms of a complex susceptibility $\tilde{\chi}(\omega) = \chi e^{i\phi}$, they define the zero-field freezing temperature T_f as the temperature where $\tan\phi = \varphi(\omega\tau)$ takes a given phase angle ϕ_0. The value of ϕ_0 has to be chosen as independent of ω and small but clearly above the noise of the signal. This defines $\tau = A/\omega$.

Table 2:

Parameters obtained for the spin glass $Eu_{0.40}Sr_{0.60}S$ from two dynamic scaling models, eq. 97 with T_c = 1.50 K and eq. 99 with T_c = 0 (From Bontemps et al., 1986).

T_c=1.50 K:	$\tau_0 \simeq 3\times10^{-12}$ sec	$z\nu = 8.2\pm0.5$	$(\beta+\gamma) = 4$
T_c=0 :	$\tau_0 \simeq 10^{-8}$ sec	$z\nu = 9 \pm 1$	$\Delta = (\beta+\gamma)/2 = 9$

Bontemps et al. (1986) can fit the data with both scaling models, eqs. 97 and 99, as shown in Figs. 80 and 81, respectively. The generalized reduced temperatures are $t = (T-T_c)/T$ and $t_f = (T_f-T_c)/T_f$ (following Omari et al., 1983) and the reduced field is $h = g\mu_B \sqrt{S(S+1)/3}\, H/kT$. They obtain the parameters summarized in table 2. Both fits are of comparable quality, which shows how difficult it is in practice to distinguish the two possibilities, but the parameters provide a strong support for the model of a nonzero-temperature transition in this insulating spin glass:

- T_c = 1.50 K is consistent with the value of 1.51 K determined by dc-magnetization measurement on the same sample.
- $\tau_0 \simeq 3\times10^{-12}$ sec compares very well with $\hbar/kT_c \simeq 4\times10^{-12}$ sec.
- $z\nu$ = 8.2 is comparable to computer simulations by Ogielski (1985) which yield $z\nu = 7.2 \pm 1$ (see eq. 34).
- $(\beta+\gamma)$ = 4 is in good agreement with the values found in other spin glasses experimentally and by simulations. For instance, Bouchiat (1986) obtains $(\beta+\gamma) \simeq 1.0 + 2.2 = 3.2$ (see table 1); Bhatt and Young (1985) $(\beta+\gamma) \simeq 0.5 + 3.2 = 3.7$; and Ogielski (1985) $(\beta+\gamma) \simeq 0.5 + 2.9 = 3.4$ (see eq. 34).

As consequence the scaling with eq. 97 leads to a divergence of the relaxation time along an "AT-line", $\delta T_f \propto H^{\Psi}$, with $\Psi = 2/(\beta+\gamma) = 1/2$ in $Eu_{0.40}Sr_{0.60}S$ (see discussion at the end of sec. 7.2 and in sec. 10).

Summarizing, the fairly convincing experimental demonstrations of static and dynamic scaling at a nonzero spin-glass temperature as reviewed above provide strong evidence for a nonzero phase-transition temperature in spin glasses, in good agreement with recent numerical results (see sec. 4.4).

8. Crossover to long-range periodic order

So far we have discussed the ordering behavior of diluted magnetic systems with competing ferro- and antiferromagnetic interactions which exhibit a transition from the paramagnetic to the spin-glass phase on lowering the temperature. By increasing the concentration of magnetic atoms (less dilution), the exchange couplings become stronger at the cost of less frustrated bonds between the magnetic moments on the average, thus one expects the evolution of long-range ferro- or antiferromagnetic order out of the spin-glass phase at a critical concentration x_c. Here, we are interested in the crossover regime which may be influenced by the interplay between spin-glass and long-range periodic order phenomena.

8.1 Reentrant behavior:

One of the most fascinating aspects of these investigations has been the discovery of reentrant spin glasses. It has been claimed that within a small concentration regime a ferromagnetic-like state occurs at temperatures higher than the spin-glass state (see e.g. Maletta, 1983b). This is an unusual property since ordered ferromagnetic states generally have a lower free energy than manifestly disordered states. Nevertheless, many different systems are supposed to show such a behavior, the first studied examples are: Al-Fe (Shull et al., 1976), Pd-Fe-Mn (Verbeek et al., 1978), Au-Fe (Verbeek and Mydosh, 1978; Crane and Claus, 1981), Cr-Fe (Fincher et al., 1980), (Eu,Sr)S (Maletta and Convert, 1979a; Maletta, 1979c), and a-(Fe,Mn)PBAl (Yeshurun et al., 1980). The interpretation of the various experiments, however, are still highly controversial (Coles, 1984).

Sherrington and Kirkpatrick (1975) were the first to predict a similar phenomenon of Ising spins for $J_o/\tilde{J} \geq 1$ within mean-field theory. It turned out, however, that one needs the Parisi solution (Vannimenus, Toulouse, and Parisi, 1981) of the SK model to get the exact solution at low-temperature. But then, reentrant spin-glass behavior does not occur (see Fig. 18 and discussion in sec 4.3): With decreasing

temperatures, the system becomes first ferromagnetic (FM) with a spontaneous magnetization $M_0 \neq 0$ and subsequently goes into a "mixed phase" (F') with $M_0 \neq 0$ and with irreversibility (= a modified FM with SG-like features); the second transition is quite analogous to the AT-line of SG in a field. For Heisenberg spins, the mean-field theory (Toulouse, 1980; Gabay and Toulouse, 1981; Cragg, Sherrington and Gabay, 1982a) predicts at the second transition (a GT-like line) a change from a collinear ferromagnet to a "canted ferromagnetic state" with $M_0 \neq 0$ and transverse-spin freezing (Fig. 20). Thus, in both cases within the SK model the low-temperature state is a "mixed phase" where FM and SG orders coexist.

To date, bulk measurements like the magnetization and ac-susceptibility have mostly been performed in order to identify a second transition and a reentrant spin-glass (RSG) phase. This low-temperature transition at T_f manifests itself in a number of ways: drop of the demagnetization-limited ac susceptibility (Fig. 82) (Verbeek et al., 1978; Coles et al., 1978; Maletta and Felsch, 1980d); field-dependent peak in the ac-susceptibility measured in the presence of a dc-field (Fig. 83)(Maletta, 1979c; Geohegan and Bhagat, 1981); vanishing of the spontaneous magnetization (Fig. 84)(Manheimer, Bhagat and Chen, 1983; Crane and Claus, 1981); onset of magnetic viscosity (Yeshurun and Salamon, 1981); onset of history-dependent effects (Carnegie and Claus, 1979; Yeshurun and Sompolinsky, 1982); change of hysteresis loop (Senoussi, 1984).

Since all these experiments are performed in finite field and the sensitivity to the applied H is remarkable (see Figs. 83 and 84) one has to work in really low fields and has to introduce a reliable extrapolation procedure in order to obtain the spontaneous magnetization and to locate the temperature T_f. At first sight, one would expect only fields of the order of (kT_f/μ_B) or (kT_c/μ_B) to give significant effects, but the applied fields are several orders of magnitude smaller. For the a-$(Fe_xMn_{1-x})_{75}P_{16}B_6Al_3$ alloy with $x = 0.80$, for instance, Manheimer et al. (1983) locate $T_f(H \to 0)$ at 28 K, but an applied field of 10 Oe already suppresses to below 4 K any evidence of the low-T downturn of M(T).

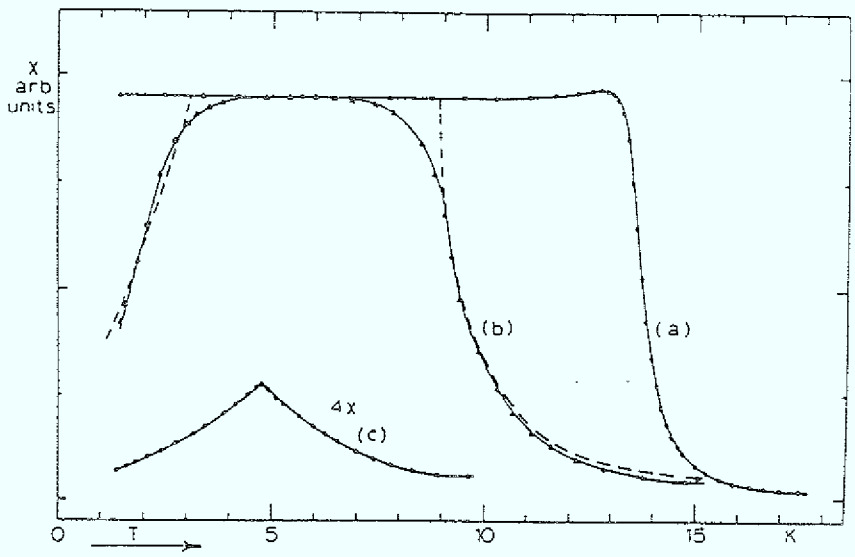

Fig. 82: Temperature dependence of the ac susceptibility for $(Pd_{0.9965}Fe_{0.0035})_{1-x}Mn_x$. Curve a: x = 0.01; curve b: x = 0.05; curve c: x = 0.065 (From Verbeek et al., 1978).

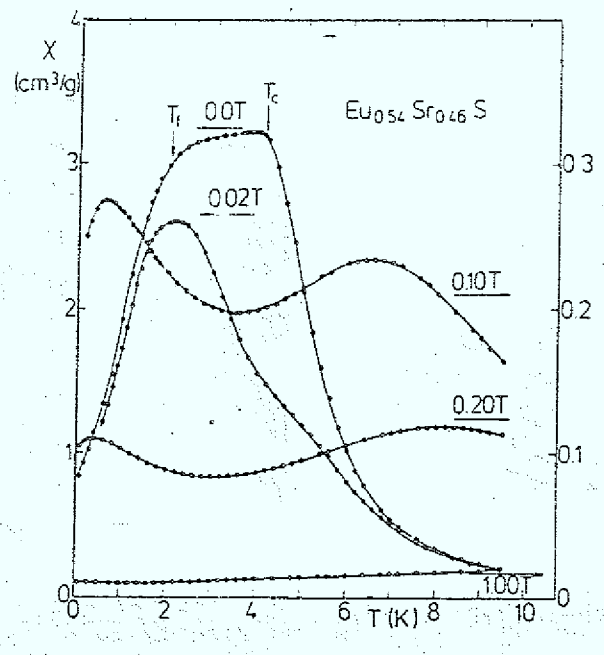

Fig. 83: Temperature dependence of the ac susceptibility (at 117 Hz) for $Eu_{0.54}Sr_{0.46}S$ in various magnetic fields. Note the change of scale between B = 0.02 T and 0.10 T (From Maletta and Felsch, 1980d).

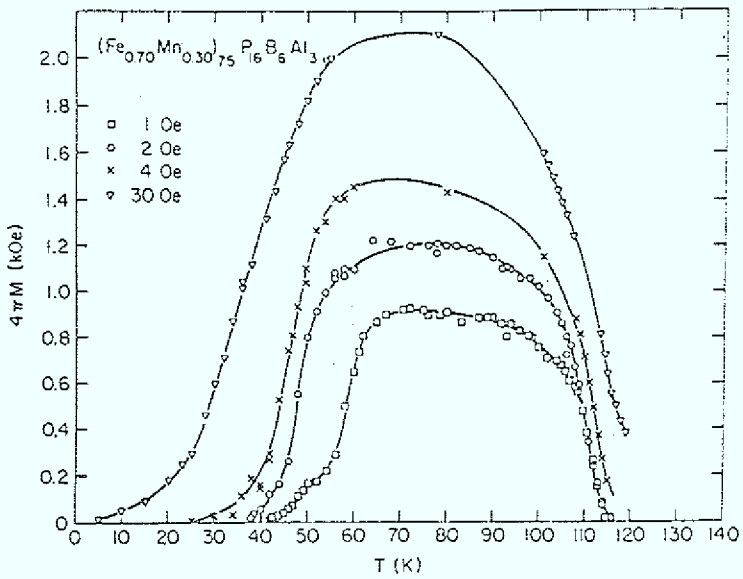

Fig. 84: Reversible magnetization as a function of temperature for amorphous $(Fe_{0.70}Mn_{0.30})_{75}P_{16}B_6Al_3$ at various applied fields (From Manheimer et al.,1983).

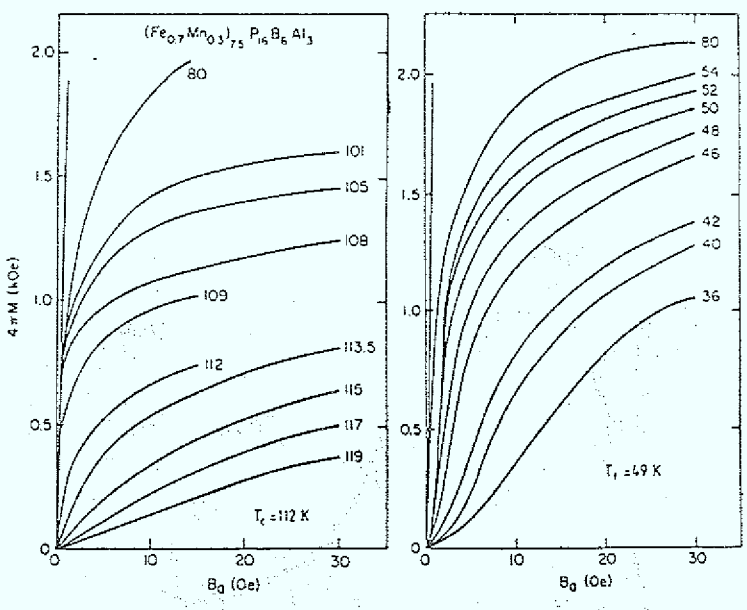

Fig. 85: Magnetic isotherms for a-$(Fe_{0.70}Mn_{0.30})_{75}P_{16}B_6Al_3$ in the vicinity of T_c = 112 K and T_f = 49 K. The left most (highest slope) line marks the demagnetization limit. The number labelling each curve is the temperature in K. Note that the role of temperature is reversed near T_c and T_f (From Manheimer et al., 1983).

Manheimer et al. (1983) report such low-field dc magnetization measurements on a-$(Fe_xMn_{1-x})_{75}P_{16}B_6Al_3$ in the SG-FM crossover regime (x = 0.65, 0.70 and 0.80) at fields below 30 Oe. By reversing the field H and comparing field cooled and zero-field cooled states at low T they separate out the reversible (M) and irreversible (M_i) contributions to the magnetization. M is defined as that part of the measured magnetization which changes sign when the applied field H is reversed. Fig. 84 shows the reversible (M) magnetization of the x = 0.70 alloy for various applied fields H: the system apparently exhibits reentrant behavior, one can define two characteristic temperatures in Fig. 84: an effective freezing temperature T_f^* (H) by extrapolating the linear part of the drop in M at low T to obtain T_f^* (H) as the M = 0 intercept, and an effective Curie temperature T_c(H) for the onset of the large increase of M. Increasing the applied field H favors the FM state, i.e. the rise in M near T_c shifts to higher T while the drop in M near T_f^* moves to lower T (Fig. 84, see also Fig. 83). T_f^* (H) reduces as $\delta T_f^* \propto H^{1/2}$, thus by extrapolation the value of $T_f = T_f^*$ (H = 0) can be determined (T_f = 49 K). The Curie temperature T_c is found by means of an Arrott plot; the applied fields have to be corrected for demagnetization (T_c = 112 K).

Here we want to call attention to the large magnitude of M measured at such low applied fields in the FM phase (Fig. 84). For instance, the authors cite ferromagnetic resonance data taken at 3-10 kOe applied fields which give M values only about 50% higher than those at 30 Oe in Fig. 84.

Fig. 85a,b summarizes the magnetic isotherms of the x = 0.70 alloy in the neighborhood of T_c and T_f, respectively. As expected, the curves in Fig. 85a resemble those obtained near a PM ⇒ FM transition (T_c = 112 K), while in Fig. 85b a similar behavior is observed except that now the role of temperature is reversed (i.e. the low-T data show less curvature). The authors demonstrate that the reversible part(M) of the magnetization can be described by the usual scaling laws for critical magnetic behavior

$$M = t^{\beta} \cdot \tilde{M}(H/t^{(\beta+\gamma)}) \qquad (100)$$

not only at T_c but also at the FM⇒SG transition temperature T_f, yielding exponents as summarized in table 3. We note that a much smaller value of T_f($\sim$ 30% lower) is obtained by a similar scaling analysis of high-field measurements (0.1 kG $\lesssim H \lesssim$ 15 kG) by Salamon et al. (1981).

Below T_f no reversible magnetization M is left when extrapolating to H⇒0. The irreversible part (= frozen magnetization) M_i measured after field cooling is nonzero below T_f and vanishes approximately at T_f. Thus, relying on the separation (M, M_i) and extrapolation (H⇒0) procedures Manheimer et al. (1983) provide experimental evidence for the existence of a RSG phase in a-(Fe-Mn)PBAl alloys.

Table 3:

Critical exponents obtained from a scaling analysis (eq. 100) of low-field magnetization data of amorphous $(Fe_{0.70}Mn_{0.30})_{75}P_{16}B_6Al_3$ at the PM-FM transition (T_c = 112 K) and at the FM-SG transition (T_f = 49 K) temperature (From Manheimer et al., 1983).

T_c = 112 K:	β = 0.47	γ = 1.42	δ = 4.0
T_f = 49 K:	β^*= 0.37	γ^* = 1.36	δ^* = 4.7

The main problem in studying the RSG phenomenon remains the enormous sensitivity to applied fields, as illustrated in Fig. 84. In order to really support the picture of a RSG with no spontaneous magnetization, a zero-field technique has to be applied. While neutron diffraction experiments do not share the resolution of bulk magnetization measurements, they can be performed in zero applied field and give microscopic information, for instance on the spatial spin correlations. Consequently, Maletta et al. (Maletta and Convert, 1979a; Maletta and Felsch, 1980d; Maletta, Aeppli and Shapiro, 1983a) have carried out detailed neutron diffraction studies of $Eu_xSr_{1-x}S$ which will be discussed now.

This insulating dilution system has been studied in great deal in the spin-glass regime, $0.13 \lesssim x \lesssim 0.51$, as described above. Early ac susceptibility measurements (Maletta and Felsch, 1980d) displayed

in Fig. 86 can be taken as a first hint at a RSG behavior of the compounds with Eu concentrations $0.51 \leq x \lesssim 0.65$. Note that the different plateau values in Fig. 86 are only due to different sample geometries in the various measurements, which is checked experimentally.

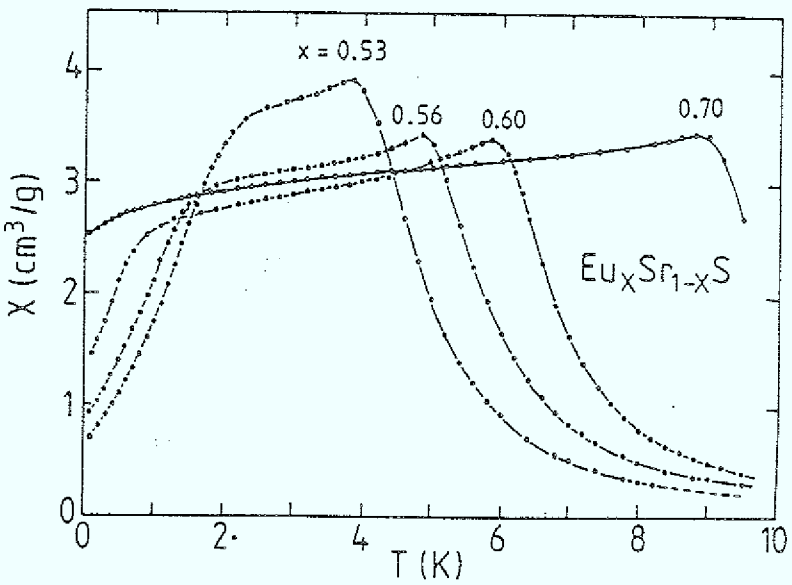

Fig. 86: Temperature dependence of the ac susceptibility for $Eu_xSr_{1-x}S$ with various Eu concentrations x, as indicated (From Maletta et al., 1980b).

Turning now to the neutron diffraction measurements of $Eu_xSr_{1-x}S$ with $x = 0.52$ (Maletta et al., 1982b), typical data of elastic scans through the (002) reflection are shown in Fig. 87a for three temperatures: $T = 6.0$ K in the PM regime, $T = 2.5$ K in the FM regime, and $T = 1.0$ K in the RSG regime. These results immediately suggest the existence of some unusual magnetic state. At high temperatures, the scattering consists of only the nuclear Bragg scattering centered at $q = 0$. As T is lowered, diffuse scattering appears whose width is a measure of the size of the ferromagnetically correlated regions. The diffuse scattering is seen to be very temperature dependent and exhibits even a broadening at the lowest temperature. Fig. 88 shows the temperature

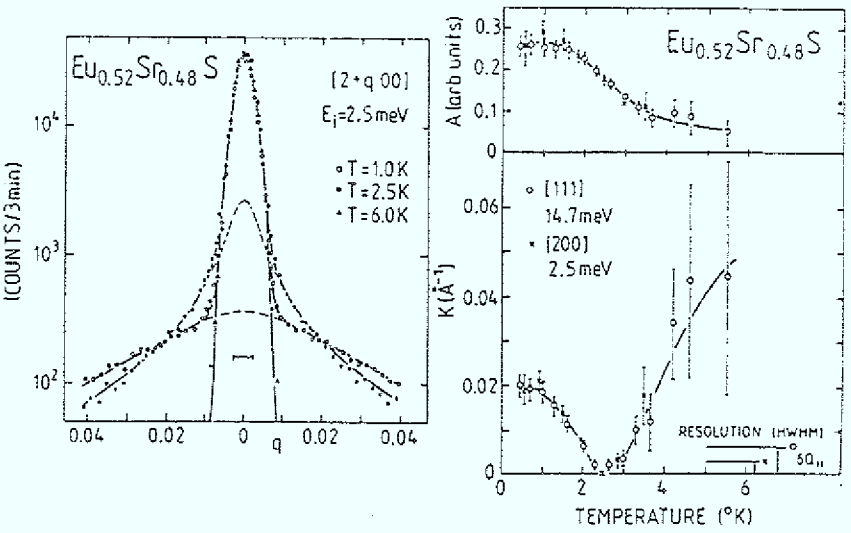

Fig. 87: Neutron-diffraction measurements of $Eu_{0.52}Sr_{0.48}S$ single crystal: (a) Elastic scans measured at (2-q, 0,0). The curve through the T = 6 K data is a resolution-limited Gaussian. For T < 6 K the solid line represents fits to the data using eq. 101, and the dashed line indicates the Lorentzian (non-Bragg) part of the scattering. (b) Temperature dependence of Lorentzian amplitude A and halfwidth κ obtained from the fits shown in part (a). The limits of instrumental resolution in q are indicated (From Maletta et al., 1982b).

dependence of the peak intensity of the (111) Bragg peak with various momentum resolutions. The following features of the data are especially important since they are in strict contrast with normal FM-ordering: (i) the magnetic signal normalized to the nuclear background decreases as the instrumental resolution is improved; (ii) the onset of the intensity increase shifts to lower temperatures with improved resolution; and (iii) the magnetic scattering is largest not at T = 0 but at the intermediate temperature T = 2.5 K. These observations indicate that the magnetic intensity is due primarily to diffuse scattering and not to the Bragg scattering which would arise if long-range FM order were present. As the instrumental resolution is improved different volumes of reciprocal space are sampled and the magnetic diffuse intensity will be decreased relative to the nuclear intensity.

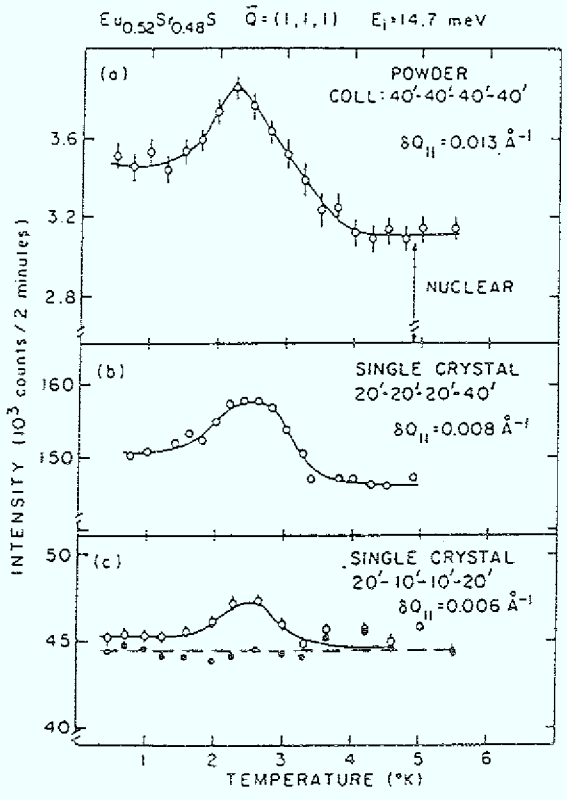

Fig. 88: Temperature dependence of (111) peak intensity (open circles) observed for $Eu_{0.52}Sr_{0.48}S$ for various experimental configurations. Filled circles in (c) represent Bragg intensity corrected for magnetic diffuse scattering (From Maletta et al., 1982b).

The data can be described more quantitatively by assuming the following form for the scattering cross section:

$$S(\vec{Q}) = A/\left[(\vec{Q}-\vec{\tau})^2 + \kappa^2 \right]^{1-\eta/2} + B \cdot \delta(\vec{Q}-\vec{\tau}). \qquad (101)$$

The Lorentzian-like and δ-function terms represent the diffuse and Bragg scattering, respectively. τ is a reciprocal lattice vector and κ is the inverse correlation length ($\kappa = 1/\xi$). The solid lines in Fig. 87a are the result of the least-squares fit to eq. 101 with $\eta = 0$ (= pure Lorentzian) after folding eq. 101 with the instrumental resolution function. The temperature dependence of A and κ are shown in Fig. 87b. The amplitude A increases with decreasing T, which indicates that an increasing number of spins are becoming correlated. The Lorentzian

linewidth κ becomes indistinguishable from zero around 2.5 K, and then increases again at lower T (the authors place a lower limit of 400 Å on the FM correlation length at 2.5 K, estimated from the high-resolution data).

These results contrast sharply with a normal Heisenberg FM where the correlation length remains infinite for all temperatures below T_c. In addition, the diffuse scattering below T_c would be almost entirely associated with the spin waves. In $Eu_xSr_{1-x}S$, the scattering is elastic on the scale of the instrumental energy resolution (30 μeV). Much higher resolution studies performed by the neutron spin echo technique (Shapiro et al., 1985) have shown that at low temperatures relaxation times are greater than 10^{-8} sec. Since also the Bragg amplitude B stays constant at the nuclear level at low temperatures, the authors conclude that the state in $Eu_xSr_{1-x}S$ with x = 0.52 at the lowest T is a spin-glass phase, without a coexisting FM component.

The intermediate T regime where the correlation length diverges is studied (Maletta et al., 1983a) in detail in $Eu_xSr_{1-x}S$ with x = 0.54, since it is more extended here: 2 K $\lesssim$ T $\lesssim$ 4 K. Line-profile analyses using eq. 103 reveal the same results as described for the x = 0.52-compound, except that now at intermediate temperatures the scattering profile shows clear deviations from the standard Lorentzian form (the maximum value of $|\eta|$ is η = -0.6 at 2.3 K; eq. 103) (see also: Maletta and Felsch, 1980d). The magnetic Bragg scattering contribution (B_m) is weak (or even zero), as long as $\kappa \simeq 0$, and it vanishes at the lowest T where again κ becomes larger than the instrumental resolution width.

Due to the high amount of magnetic diffuse scattering the intermediate T regime with $\kappa \simeq 0$ is suggested to be called a "frustrated FM" state. Now it is plausible that such a highly distorted FM state (near the reentrancy point at x_c = 0.51) can change into a spin-glass state (RSG) at lower temperature. The authors don't observe the "mixed phase" at the lowest T, as predicted in the mean-field model. Stimulated by these experimental data they present a phenomenological description of RSG systems (Maletta et al., 1983a; Aeppli et al., 1984), based upon the competition between two different ordering phenomena. Within

the crossover regime, i.e. in $Eu_xSr_{1-x}S$ at Eu-concentrations just above $x_c = 0.51$, frustration leads to an effective decomposition of the spin system into a spin-glass-like and a ferromagnetic network (see also discussion in sec. 2.2). If the continuous network of "decoupled" spins undergoes a freezing transition, the frozen spins will impose a <u>random field</u> on the FM network through the exchange bonds also responsible for frustration. Hence, the order-parameter scattering, $B_m \cdot \delta(q)$, is converted into the sum of a Lorentzian and its square, similar to the structure factor with $\eta<0$ in eq. 101, and finally the FM state is destroyed (see e.g. a recent review on random-field studies by Birgeneau et al., 1986).

This two-network model accounts for both the statics and dynamics of RSG systems, as observed in $Eu_xSr_{1-x}S$, Fe_xCr_{1-x}, Fe_xAl_{1-x} and $a\text{-}(Fe_xMn_{1-x})_{75}P_{16}B_6Al_3$ (Aeppli et al., 1984; Shapiro et al., 1986). Fig. 89 is a schematic rendition of how the model describes the dynamics. At high T (frame (a)), the dotted and dashed lines represent the spin-wave spectrum for the related FM network and the relaxation spectrum for the SG spins, respectively. It is useful to think of the <u>time-varying random field</u> imposed on the FM spins at high T as an additional noise term, $\eta(t)$, in the semiclassical equations of motion for spin waves. The noise $\eta(\omega)$ has the property that its net weight, $\int |\eta(\omega)|^2 d\omega$, is weakly temperature dependent, while its bandwidth, γ, given by the inverse correlation time for the SG spins, can be a strong function of T. The primary effect of decreasing T will be to decrease γ, which initially will increase $|\eta(\omega)|^2$ at frequencies on the order of the spin-wave energies. Consequently, reducing T in such a RSG system above T_f has the same effect as increasing T in an ordinary FM: the occupation of the spin-wave modes increases, which leads to a decrease of M and a concomitant decrease in spin-wave stiffness D (see e.g. Fincher et al., 1980). The solid line in Fig. 89a represents the net result of this process for T much larger than the temperature T_f where freezing occurs and $\gamma \to 0$.

For $T \ll T_f$ (Fig. 89c), the SG network is entirely frozen, and a delta function at $\hbar\omega = 0$ exhausts most of the spectral weight of $\eta(\omega)$. Then, the SG network produces a static random field acting on the FM network and a pure RSG state is left. As consequence, the delta function domain scattering will coexist with weak sidebands (solid line in Fig. 89c) associated with heavily damped spin waves "propagating" through a medium of static scattering centers. For intermediate T (Fig. 89b), both the enhanced occupation of spin-wave modes and the domains commonly induced by static random fields must be taken into account.

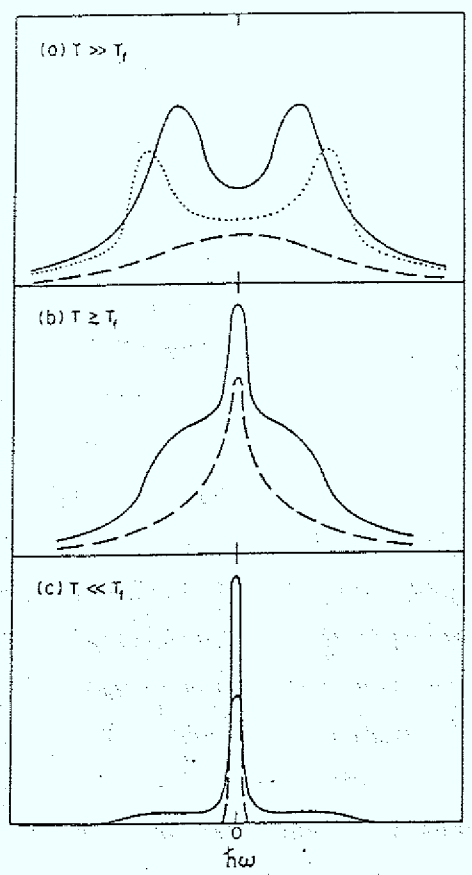

Fig. 89: Schematic constant-Q spectra of the magnetic response for the reentrant spin-glass problem. Dotted line represents spin-wave spectrum when the coupling between FM and SG network vanishes; dashed line represents spectrum for SG network, and solid line corresponds to spectra for FM network when it is coupled to SG spins (From Shapiro et al., 1986).

Recently, the same group (Aeppli et al., 1986) started to study neutron diffraction of the reentrant system $Eu_{0.54}Sr_{0.46}S$ in magnetic fields $H \lesssim 60$ mT. Such magnitudes of H can easily induce some alignment of the Eu spins at the expense of the defective regions responsible for the magnetic diffuse scattering (Fig. 90). That is observed in both FM and SG regimes, but while the net magnetization, monitored using the extinction-limited Bragg intensity, is history-dependent in both regimes, remanence effects at microscopic length scales (i.e. history dependences of the diffuse scattering) exist only in the SG regime (Fig. 91). Thus, the authors have found a new distinction between FM and SG regimes in RSG systems. The latter effect is very dramatic: cooling to 0.5 K in a 41 mT field and then setting H = 0 results in a magnetic fluctuation length of less than 65 Å, well below the zero-field cooled value of 140 Å.

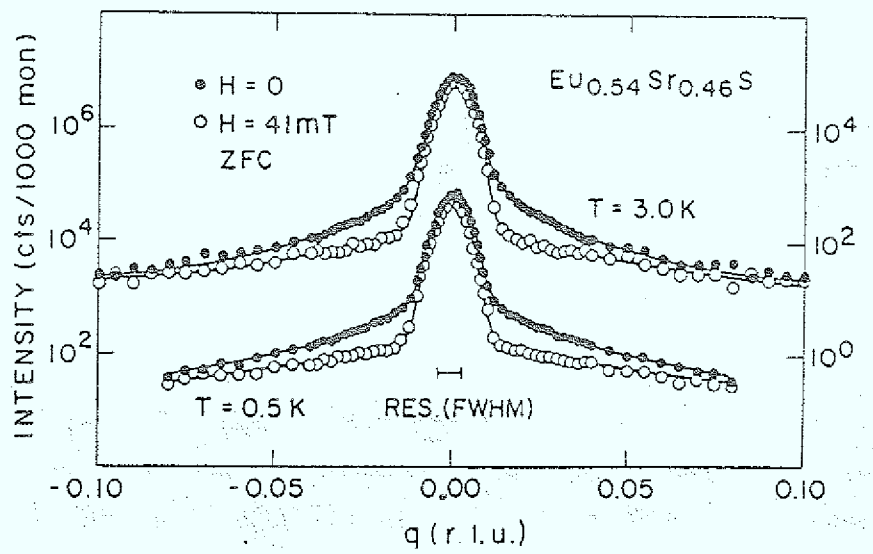

Fig. 90: Neutron scattering intensity of $Eu_{0.54}Sr_{0.46}S$ measured after zero-field cooling plotted as function of momentum transfer $(q,0,0) = Q - Q_0$ where $Q_0 = (2,0,0)$. Spectra at H = 0 and H = 41 mT are shown, each at a temperature in the FM-regime (T = 3.0 K) and in the RSG-regime (T = 0.5 K). The right- and left-hand vertical scales are for the 3 K (upper curves) and 0.5 K (lower curves) data, respectively. Solid curves correspond to eq. 101 (From Aeppli et al., 1986).

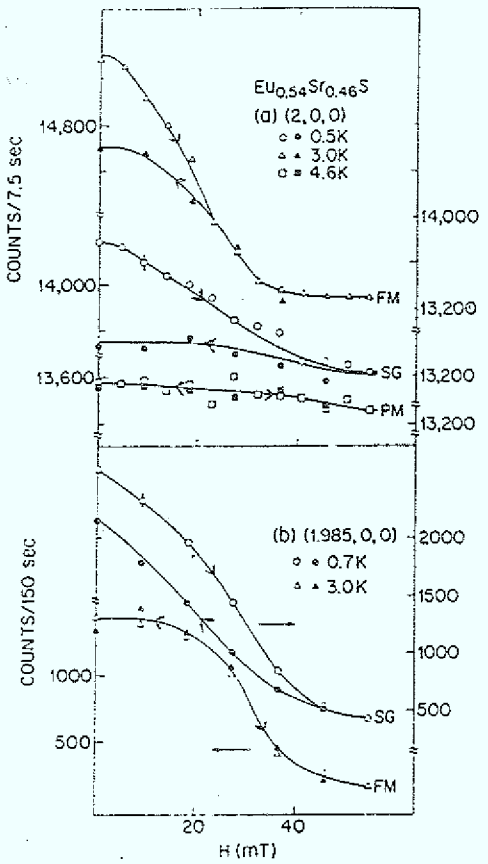

Fig. 91: Field dependence of (2, 0, 0) and (1.985, 0,0) intensities for $Eu_{0.54}Sr_{0.46}S$ at fixed temperatures in the paramagnetic (4.6 K), ferromagnetic (3.0 K), and spin-glass (0.5 K and 0.7 K) regimes. Solid lines are guides to the eye (From Aeppli et al., 1986).

Shapiro et al. (1985) have performed neutron-spin-echo (NSE) experiments in $Eu_xSr_{1-x}S$ with $x = 0.40$ and $x = 0.54$ in order to further study the double transition PM → FM and FM → SG in $x = 0.54$. They observe no depolarization of the neutron beam for the SG sample ($x = 0.40$), but in the RSG sample ($x = 0.54$) the beam partly depolarizes near T_c. It becomes more depolarized on cooling further into the FM phase but less depolarized in the SG state. The incomplete depolarization of the scattered beam confirms the absence of true long-range FM order below T_c. Thus, there is sufficient neutron polarization of the incident beam to perform the experiment at all temperatures.

The NSE method (see sec. 6.2 and Fig. 50 for the SG CuMn) measures directly the time dependence of spin correlations, $S(q,t)$, for times between 0.03 nsec $\lesssim t \lesssim$ 5 nsec. Fig. 92 compares $S(q,t)$ in the SG sample ($x = 0.40$) with that in the RSG sample ($x = 0.54$), measured for $q = 0.072$ $\mathring{A}^{-1}$ at various temperatures. Both samples show similar behavior at low temperatures, the data in Fig. 92 follow a straight line, i.e. $S(q,t) \propto A \cdot \ln t$, which implies that the spin correlations decay much slower than exponentially, typically for spin glasses. On heating the relaxation decay gets smoothly more rapid but no dramatic change of behavior is observable within our time interval of measurement at T_f in both samples. Similar behavior is observed in CuMn, except that the time spectrum for the decay in the insulating compounds is shifted towards (at least one order of magnitude) longer relaxation times compared to the metallic SG CuMn (see also Fig. 50).

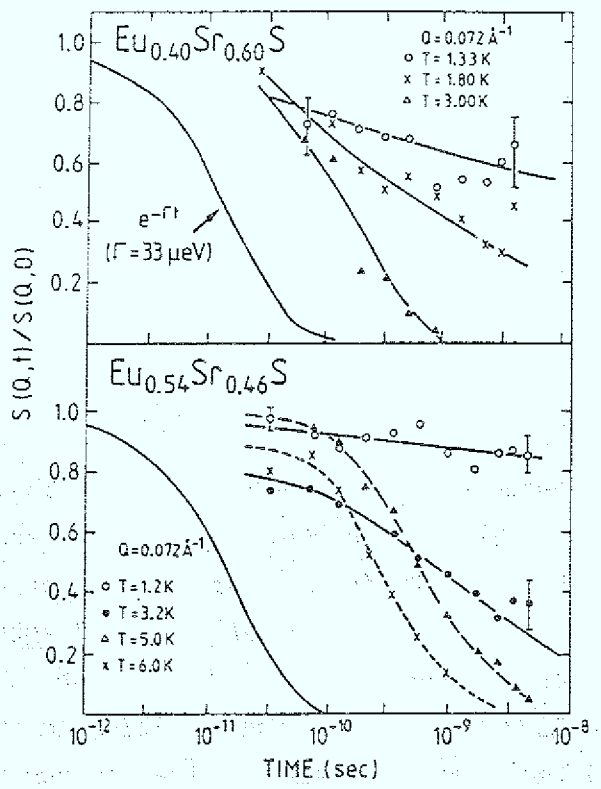

Fig. 92: Time correlation function, $S(q,t)/S(q,0)$, for $Eu_xSr_{1-x}S$ as measured for the SG compound ($x = 0.40$) and the RSG compound ($x=0.54$) for $q = 0.072$ $\mathring{A}^{-1}$ at various temperatures by the neutron spin-echo technique (From Shapiro et al., 1985).

On further heating the RSG sample ($x = 0.54$) into the range of the Curie temperature T_c, $S(q,t)$ changes into an exponential form (Fig.92b): $S(q,t) \propto \exp(-\Gamma \cdot t)$. It is interesting to mention the also observed q dependencies. Relaxation effects in ordered magnets generally are q dependent, and indeed near T_c of the $x = 0.54$ sample the measurements are consistent with the behavior $\Gamma = D \cdot q^2$. Near T_f of both samples, however, the decay is nearly q independent. This lack of kinematical slowing down near T_f may be interpreted by dipolar effects at the freezing process.

In conclusion, neutron scattering has played an important role in advancing our understanding of the magnetic behavior in RSG systems. The interpretation of some neutron experiments, however, is still controversial. From inelastic neutron scattering Fincher et al. (1980) find a spin-wave stiffness D in the RSG system $Cr_{1-x}Fe_x$ which after the usual increase below T_c decreases again within the intermediate FM regime and practically goes to zero in the RSG regime. In contrast, Hennion et al. (1983, 1984) and Murani (1983) observe more or less resolved spin waves in $Ni_{0.784}Mn_{0.216}$ and AuFe down to the lowest temperatures ($T < T_f$). The result on the constant D also depends on the ambiguity in choosing the proper spectral form for analyzing the spin-wave line (using either the "double Lorentzian" or the "damped harmonic oscillator" form). We want to emphasize, however, that contrary to their assertion the observation of well-defined spin waves at finite wave vectors does not demonstrate the existence of long-range FM order.

Among many other experiments which have been performed in order to elucidate the nature of RSG systems, two other microscopic techniques in addition to neutron scattering studies, ESR and Mössbauer effect, should be mentioned in this context. A careful study of the electron spin resonance (ESR) should provide valuable information about RSG systems, but one has to keep in mind the high resonance fields in this method. To date, many uncertainties remain already in the interpretation of experiments on SG samples near T_f. The origin of the dramatical change in the field for resonance (or g-shift) and linewidth while decreasing the temperature towards T_f is unclear. Very recently, Monod et al. (1986) have studied ESR in $Eu_xSr_{1-x}S$ for $0.01 < x < 1$ in the high-T regime (also

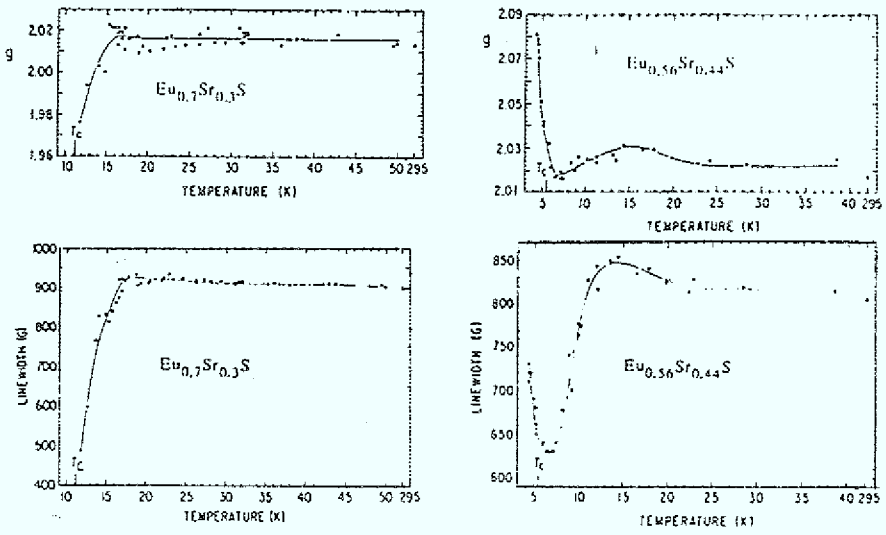

Fig. 93: Temperature variation of g-value and linewidth in $Eu_xSr_{1-x}S$ from ESR measurements. The left-hand-side (parts a1 and a2) shows the results for the FM compound with x = 0.70, the right-hand-side (parts b1 and b2) for the RSG compound with x = 0.56 (From Mehran et al., 1984).

as function of frequency). They observe an exchange narrowed dipolar linewidth (proportional to $\sqrt{x}$), as proposed by Levy and Raghavan (1986), with a Lorentzian line shape (Deville et al., 1981 a, b). For $x > 0.1$ the linewidth decreases when the resonance frequency increases.

Mehran et al. (1984) present an ESR study (at 9 GHz) of the RSG system $Eu_xSr_{1-x}S$ with x = 0.56 by comparing the data to measurements of a FM-sample (x = 0.70) (see Fig. 93) and a SG-sample (x = 0.40: Deville et al., 1981 a, b). In the FM-sample (x = 0.70) they find a sharp narrowing of the line near 2 T_c (Fig. 93, a2) and a g-shift to lower values (Fig. 93, a1). Below T_c the ESR spectrum breaks up into several asymmetric lines, probably due to disorder. These findings are in contrast with those reported for the SG-sample (x = 0.40) where both g-value and linewidth are found to increase as T is lowered towards T_f. The behavior of the RSG-sample (x = 0.56) is qualitatively different from both others, as shown in Fig. 93 b. Although the linewidth in the PM phase narrows

T is decreased no substantial asymmetry is detected in the x = 0.56 sample. For temperatures just above T_c the line starts to broaden and shifts to higher g-values. This broadening and shifting continue into the FM phase to the lowest temperatures measured (Fig. 93, b1 and b2), as the FM ⇒ SG transition is approached (Similar variations have been observed in an a-FeMn RSG system by Rosenbaum et al., 1982). Probably, the line broadening and shift observed in the x = 0.56 sample near T_f in the intermediate FM regime as well as in the x = 0.40 sample just above T_f have the same origin. A detailed analysis of these data has not yet been published.

Now, considering Mössbauer effect studies on RSG systems, Lauer and Keune (1982) show in their pioneering ^{57}Fe Mössbauer effect measurements on AuFe 16.8 % at H_{ext} = 20 kOe, that while essentially all the Fe spins are aligned parallel to H_{ext} below T_c (= 165 K), the magnetic state below T_f (≃ 45 K) is no longer collinear: the average $\langle \sin^2\Theta \rangle$ increases from zero below T_f where Θ is the angle between the magnetic Fe moment and the external field H_{ext}. This is deduced from the observation that the absorption lines with numbers 2 and 5 of the magnetic hyperfine pattern of ^{57}Fe (i.e., the $\Delta m = 0$ nuclear transitions) disappear in the FM state (only since all spins are aligned parallel to the γ-ray direction!), but become finite at lower T (below T_f), all spectra are measured at 20 kOe (see lower part of Fig. 94). They also find at $H_{ext} = 0$ that the average hyperfine field $\bar{H}$ increases below T_f somewhat faster than in the (collinear) FM phase (see upper part of Fig. 94), which is related to an increase in the average magnetic moment $\bar{S}$ in the RSG state. These two results are summarized by the authors in the canting model: In the FM phase, all moments are parallel to the external field H_{ext}. Spin components transverse to H_{ext} are free to rotate and do not contribute to the moment S (thermally averaged spin). At T_f, these components freeze out, canting the moment out of the direction of H_{ext}, and increasing its magnitude.

The analysis yields distribution functions of the hyperfine field, $P(H_{hf})$, with a double-peak structure in $P(H_{hf})$ at low T, as shown in Fig. 95. The external field has little effect on $P(H_{hf})$ below T_f, but strongly suppresses the low hyperfine fields which appear above T_f (Brand et al., 1983). The interpretation of such Mössbauer spectra of AuFe has

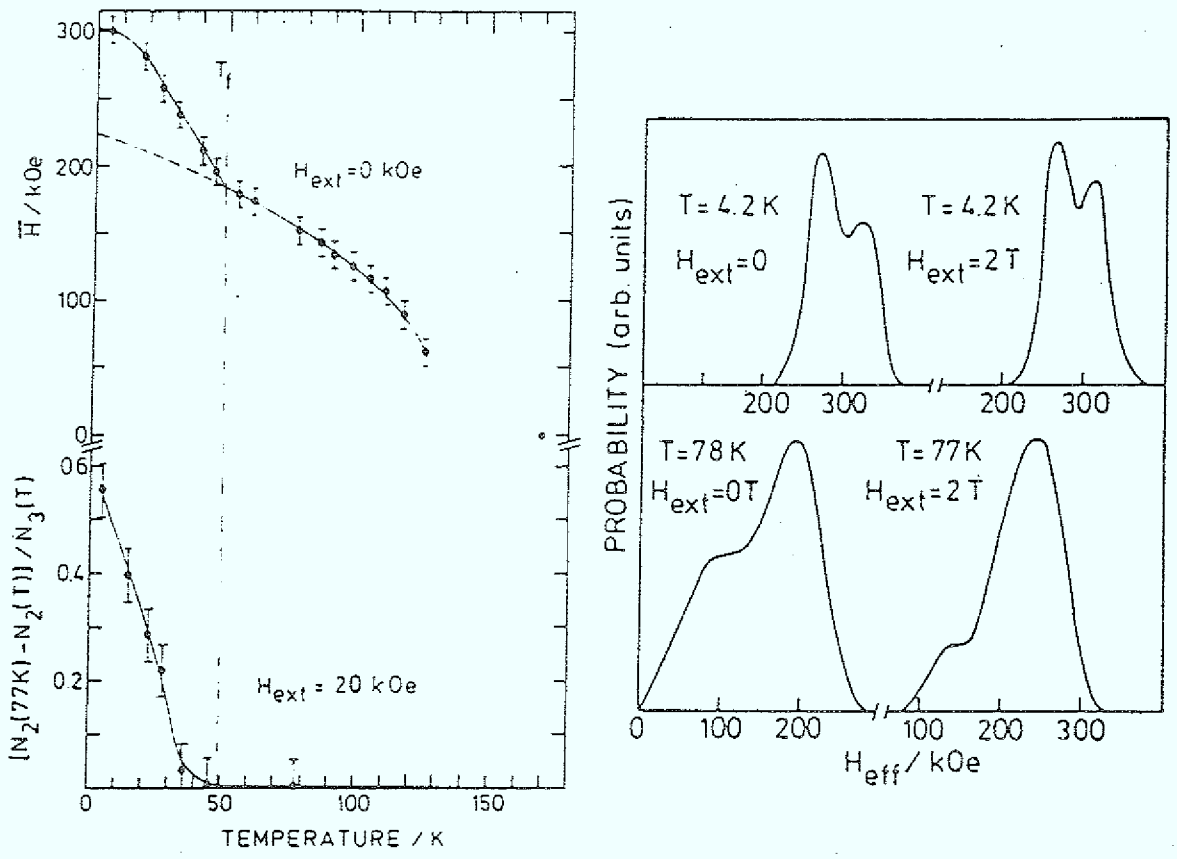

Fig. 94: Results from Mössbauer effect studies on the RSG system AuFe 16.8 at %. Top: Average hyperfine field $\bar{H}(T)$ at zero applied field H_{ext}. Bottom: Peak-intensity ratio versus temperature measured at H_{ext} = 20 kOe (see text) (From Lauer and Keune, 1982).

Fig. 95: Hyperfine-field distribution functions for AuFe 16.8 at% in the SG-state at 4.2 K (upper part of the figure) and in the FM-state at 78 K(lower part), both shown at H_{ext} = 0 and 20 kOe (From Brand et al., 1983).

led to some controversy due to the known chemical short-range order (SRO) (Dartyge et al., 1982). The simple two-"phase" model proposed by Violet and Borg (1983, 1984), where SRO leads to phase segregation into Fe-rich platelets and remaining solid solution, is both erroneous and

misleading as argued by Monod and Campbell (1984) and Brand and Keune (1984). The alloys seem to be magnetically homogeneous in the sense that $H_{hf}(T)$ disappears at one (x dependent) temperature within the resolution of Mössbauer spectroscopy, hence the magnetic correlation length is expected to be larger than the SRO-range.

Another severe problem is involved in the Mössbauer method itself since this "spin canting" can only be observed experimentally in the presence of a sufficiently high external field. Otherwise one cannot associate the variation of the line intensities (numbers 2 and 5) with "transverse spin freezing". Note that at zero external field the hyperfine patterns of a FM and a SG are quite similar (see e.g. the recent detailed discussion on the Mössbauer effect analysis of the spin glass AuFe 3 % by Meyer et al., 1985; or: Maletta and Crecelius, 1976). As an illustration, one may question the conclusion by Varret et al. (1982) from similar experiments on AuFe 19 % at a somewhat lower field of 6 kOe, that "spin canting" is already weak below T_c. Recently, Brand, Lauer and Keune (1985) attempt to analyze the spectra in zero external field by taking into account that the electric quadrupole hyperfine interaction defines locally an axis, and the orientation of the magnetic moments with respect to this local axis influences the spectrum line positions and profile. However, it is not convincing to us that by these means they can decide between a "canted" or collinear state at intermediate temperatures (FM phase).

In our opinion, Mössbauer effect measurements (as well as the ESR data presented above) reveal the existence of two different states in RSG systems, where the low-T state is hard to be aligned by external fields as is wellknown for spin glasses. As long as there is no experimental evidence for "spin canting" in zero field, we prefer this much simpler interpretation of the spectra. In any case, the Mössbauer method is a local one, thus global properties cannot be obtained easily such as the coexistence of transverse freezing with long-range FM order, as predicted for the zero-field GT state in mean-field theory at the lowest temperatures. We don't see any contradiction of the Mössbauer data to the model presented above in order to interpret the low-field magnetization and neutron-scattering data.

Very recently, Viana and Bray (1985) have proposed a dilute infinite-ranged SG model which can have such a RSG transition. Wolff and Zittartz (1985) present the phase diagram of the random-bond Ising model which quite generally exhibits reentrant behavior whenever there is a competition between a ferromagnetic coupling and a weaker antiferromagnetic one (or vice versa).

8.2. Coexistence of spin-glass and Ising antiferromagnetic orders:

Now we present experimental results of an Ising-type dilute antiferromagnet $Fe_{0.55}Mg_{0.45}Cl_2$ which give clear evidence for the coexistence of longitudinal spin-glass and antiferromagnetic orders (Wong et al., 1985a,b), as predicted by mean-field theory.

Pure $FeCl_2$ is an antiferromagnet (T_N = 24 K) with a strong uniaxial anisotropy (D = 17 K) which aligns the moments along the hexagonal c axis. There are ferromagnetic a-b planes that stack antiferromagnetically along the c axis. By dilution with Mg^{2+} ions, Bertrand et al. (1982, 1984) observe spin-glass behavior beyond 50 % dilution as shown in Fig. 96. The low-field dc-magnetization data measured along the c axis suggest a reentrant behavior in $Fe_{0.55}Mg_{0.45}Cl_2$, because the susceptibility shows a peak near $T_N \approx 8$ K and history-dependent behavior below $T_f \simeq 3$ K (Fig. 96). However, there are reservations with this interpretation because the applied field in the measurements produces site-random staggered fields which can also cause similar irreversibilities (see e.g. Birgeneau et al., 1986). Nevertheless, ac-susceptibility measurements by Wong et al. (1985b) confirm the existence of a spin-glass transition at $T_f \approx 3.0$ K: as displayed in Fig. 97, a frequency-dependence gradually appears in $\chi'_{\parallel}$ below 5 K, with a corresponding onset of the imaginary part $\chi''_{\parallel}$. Below 3.0 K, $\chi'_{\parallel}$ shows a drop and $\chi''_{\parallel}$ rises rapidly, and simultaneously the frequency dependence becomes much stronger.

In order to decide between reentrance or coexistence, Wong et al. (1985a) carried out neutron-diffraction experiments. We recall that because the system is antiferromagnetic, the magnetic and nuclear Bragg peaks are separated in reciprocal (q-) space, and this allows one to study the magnetic order with little ambiguity. The scattering near the reciprocal lattice point (0,0,3), which in principle gives information about

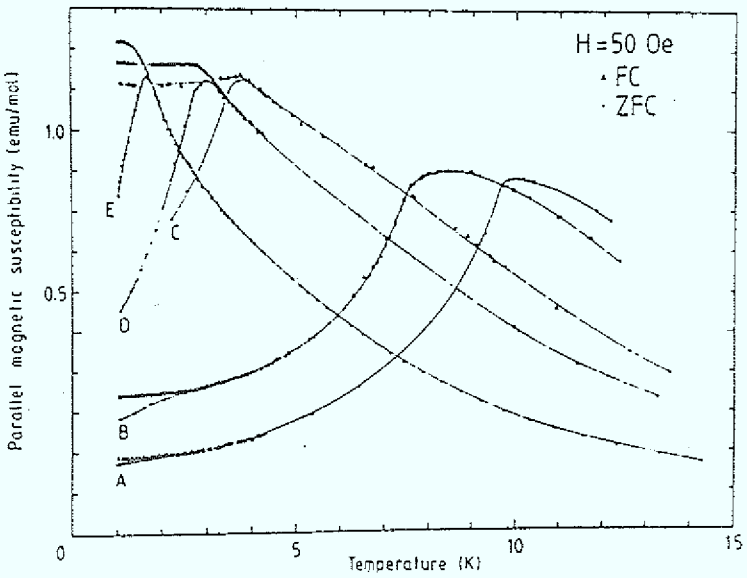

Fig. 96: ZFC- and FC-susceptibilities, M/H at H = 50 Oe, for $Fe_xMg_{1-x}Cl_2$ with the following Fe concentrations x: A: 0.610; B: 0.552; C:0.495; D:0.413; E: 0.286. The curves through the experimental data are guides to the eye (From Bertrand et al., 1984).

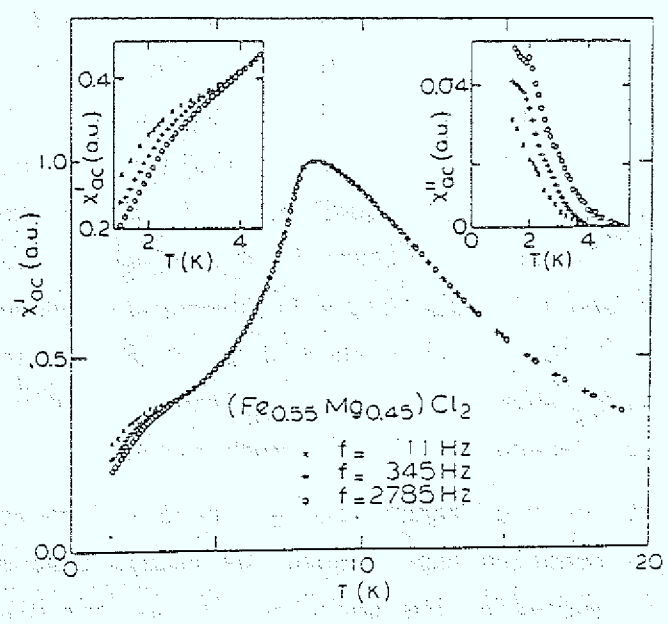

Fig. 97: Temperature dependence of the ac susceptibility $\chi'_{\parallel}$ for $Fe_{0.55}Mg_{0.45}Cl_2$ measured parallel to the easy axis at three different frequencies. Detail of χ' and χ'' at low temperatures are displayed in the inserts (From Wong et al., 1985b).

the transverse spin component, is found to be independent of both T and q which implies no transverse components. Thus only a longitudinal component is present, and this is measured at $(1,0,\bar{1})$. The temperature dependence of the peak intensity $I(1,0,\bar{1})$ and the diffuse scattering $I(0.98,0,\bar{1})$ slightly off the peak (Fig. 98) indicates a well-defined Néel transition at T_N = 7.5 K, but remarkably there are no obvious signs for a SG transition at T_f = 3 K. In particular, $I(1,0,\bar{1})$ increases smoothly down to 1.2 K, suggesting that the AFM order persists below T_f (in contrast to the behavior shown in Fig. 88). However, the diffuse scattering is much higher than the background at low temperatures, which implies that not all the spins are antiferromagnetically ordered as T ⇒ 0. Analyzing the line widths and

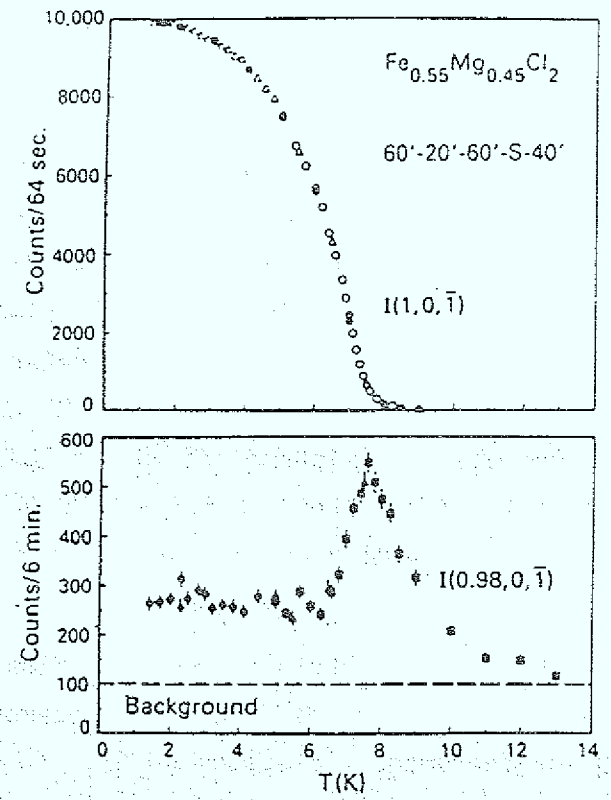

Fig. 98: Temperature dependence of the magnetic Bragg scattering at $(1,0,\bar{1})$ and magnetic diffuse scattering at $(0.98, 0,\bar{1})$ for $Fe_{0.55}Mg_{0.45}Cl_2$. The open and solid symbols denote data taken on cooling and warming the sample, respectively (From Wong et al., 1985a).

shape, it turns out that the AFM order is of long range ($> 10^3$ Å) below T_N and unaffected by the SG transition (obtained from the Bragg line), but simultaneously a Lorentzian magnetic diffuse peak appears underneath the Bragg peak whose width and amplitude are constant below 6.0 K. This frozen short-range correlation of approximately 10 Å is most likely the origin of the SG behavior observed in the ac and dc susceptibility experiments. There is no indication of atomic clustering in the sample.

In summary, the magnetic Bragg scattering demonstrates directly that the long-range AFM order is not destroyed by the SG transition, i.e. $Fe_{0.55}Mg_{0.45}Cl_2$ does not reenter into a disordered phase. Instead, combining all observations, the authors (Wong et al., 1985b) conclude that the low-T phase of the system consists of both SG and long-range AFM orders.

It is natural to question why coexistence is observed in a dilute Ising antiferromagnet like $Fe_{0.55}Mg_{0.45}Cl_2$, but not in a dilute Heisenberg ferromagnet such as $Eu_{0.52}Sr_{0.48}S$ (see sec. 8.1). Since there is no existing theory that explains this difference the authors offer several conjectures. In any case, both observations are consistent with the phenomenological model of intrinsic random fields (Maletta et al., 1983a) described in sec. 8.1: The effect of random fields is to raise the lower critical dimension from 2 to 4 for Heisenberg systems, but only from 1 to 2 for Ising systems (see e.g. Birgeneau et al., 1986). As consequence, one expects a coexistence of SG and long-range periodic order in 3-dimensional Ising systems, but a destruction of long-range periodic order, i.e. reentrancy, in 3-dimensional Heisenberg systems.

In order to further test this model of intrinsic random fields in the crossover regime to SG order, neutron diffraction experiments on the diluted Heisenberg antiferromagnetic system $Eu_xSr_{1-x}Te$ are underway (see its preliminary magnetic phase diagram in Fig. 7b). As described in sec. 6.1, the borderline between SG and AFM behavior in $Eu_xSr_{1-x}Te$ has been determined up to now (Börgermann et al., 1986a,b) only from bulk measurements: disappearance of the frequency shift of the ac-susceptibility-maximum (Fig. 43) and of the irreversibilities (FC, ZFC : Fig. 44).

Westerholt and Bach (1985) have studied magnetic ordering in $Eu_xSr_{1-x}Se$ by ac-χ and specific heat experiments. EuSe is a Heisenberg antiferromagnet with rather complex magnetic behavior (see e.g. Wachter, 1979), since the exchange interactions J_1 and J_2 are nearly equal in magnitude, but opposite in sign. It shows at H = 0 a first-order transition to AFM ordering at T_N = 4.64 K. The metamagnetic transitions in an applied field (from AFM to ferrimagnetic order and finally to FM alignment), mostly studied in M(H) experiments, can also conveniently be observed by measuring the field dependence of the ac susceptibility ($\Rightarrow$ maxima in ac-χ(H)). Dilution of EuSe with SrSe leads to spin-glass behavior for $x \lesssim 0.70$, established by a frequency dependence of the ac-χ maximum and a broad maximum of the specific heat C(T) at an even higher temperature. Compounds with $x \gtrsim 0.85$ are definitely different: no frequency shift of the susceptibility, and the Néel temperature as derived from the position of the broadened maximum of the specific heat (see also Scherzberg et al., 1981) coincides with the maximum of $d\chi/dT$, as in normal antiferromagnets. The authors claim to have found evidence for the coexistence of SG effects and AFM order for the intermediate concentration range around x = 0.80 for $Eu_xSr_{1-x}Se$. This compound (x = 0.80) with a frequency shift of the χ-peak has a structure in the ac-χ(H) which resembles the response of metamagnetic transitions. There is a maximum in ac-χ versus field at finite H (similar to the more concentrated compounds), while for $x < 0.70$ (only shown for x = 0.50) the susceptibility decreases continuously with H similar to other spin glasses. Since a metamagnetic transition is a collective phenomenon of a large number of spins coupled rigidly, Westerholt and Bach (1985) argue that these experimental results indicate a coexistence of long-range AFM order and SG order. Again, neutron-diffraction studies would give more direct information on the behavior in the crossover regime.

Hiraoka et al. (1986) have found the onset of spin-glass order at the dilution concentration $(1-x) \approx 0.11$ in similar compounds of the diluted antiferromagnetic system, $Eu_xYb_{1-x}Se$, by measurements of ac-χ and ^{153}Eu-NMR.

8.3. Crossover via modulated spin structures:

Competing exchange interactions not only induce spin-glass ordering, but are also responsible for modulated spin structures as is wellknown for rare-earth metals (see e.g. Koehler, 1972; Elliott, 1961). Dilution of heavy rare earths with yttrium or scandium stabilizes the antiferromagnetic spiral structure at the expense of any ferromagnetic component or phase present in the rare earth (Child and Cable, 1969). The Néel temperature T_N decreases smoothly with dilution, while the interplanar turn angle ω of the helical structure increases (ω is also temperature dependent). Thus, one can expect to observe the crossover to spin-glass freezing upon further dilution.

An early study by Sarkissian and Coles (1976) has tried to find the boundary concentrations between helical antiferromagnetic spin ordering and a spin-glass state in Y and Sc based alloys with 4f magnetic impurities. By measuring the ac susceptibility and resistivity, they propose a critical rare-earth concentration of 2.6 at. % for YGd and YDy alloys, 5 at. % for YTb, and about 23 at. % for Sc based alloys with Gd, Tb and Dy. In recent years there have been further attempts to distinguish experimentally between both types of magnetic ordering, which will be reviewed now. The studies reveal that spin-glass behavior in Y based alloys occurs probably at lower concentrations than previously believed.

Magnetization data (Wendler et al., 1984) of single crystals of ScGd (5 and 15 at. %) and YGd (1, 2 and 3 at. %) demonstrate different types of magnetic ordering. The ScGd system shows all the experimental features of a spin glass (Fig. 70) (see also specific-heat data by Caudron et al., 1981), while YGd even at a Gd concentration as small as 1 at. % exhibits some kind of long-range antiferromagnetic order (Fig. 99). Surprisingly both Gd systems are definitely anisotropic.

Fig. 99a displays the dc susceptibility M/H as a function of temperature for the 1 at. % and 3 at. % GdY single crystals. The applied field ranges from H = 10 G to 15 kG and is applied in both directions parallel

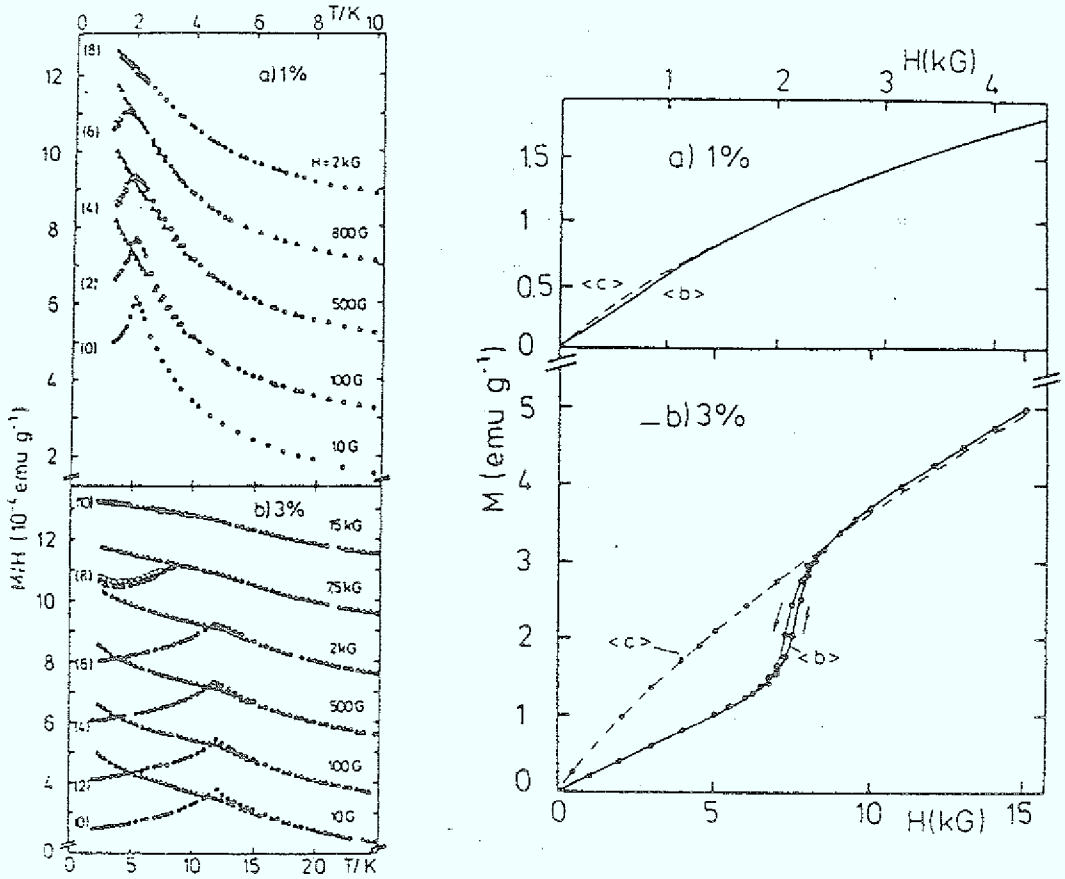

Fig. 99: (a) Susceptibility, M/H, at various fields H for two YGd single crystals, ● ○ $\parallel \vec{c}$, ▲ △ $\parallel \vec{a}$. Full symbols are ZFC, open symbols FC. In most cases the open and full symbols coincide. The curves are displaced vertically as indicated in brackets.

(b) Magnetization of YGd at T= 1.5 K. For $\vec{H} \parallel \vec{b}$ in YGd 3 at% a small magnetic hysteresis in M(H) is observed, the direction of the field scan is indicated by the arrows (From Wendler et al., 1984).

and perpendicular to the hexagonal c axis. When the field is perpendicular to the c axis, the susceptibility shows a cusp at a temperature T_c. For parallel fields only clear deviations from Curie-Weiss behavior are measured at low T. Important features of all these curves are the absence of "FC-ZFC" irreversibility effects, normally observed in spin glasses (see e.g. ScGd: Fig. 70). In addition, a spin-flop tran-

sition is observed for $\vec{H} \perp \vec{c}$ in YGd 2 % and 3 % (Fig. 99b). This observation is consistent with features shown in Fig. 99a: Below 7.5 kG there are large differences for $M_{\parallel}$ and $M_{\perp}$ of YGd 3 %, while M is independent of the orientation of the crystal at higher fields. Similar effects are detected for the 2 at. % sample, but for the 1 at. % sample lower temperatures (< 1.4 K) would be needed to establish the effect. The small magnetic hysteresis in M(H) at the spin-flop transition (Fig. 99b) also appears in the M(T)-curves of Fig. 99a as a small difference between ZFC and FC at the spin-flop field (7.5 kG). These experiments rule out the existence of a spin-glass state in the YGd alloys down to 1 at. % Gd and strongly suggest the occurrence of an antiferromagnetic ordering with the Gd moments lying in the basal plane.

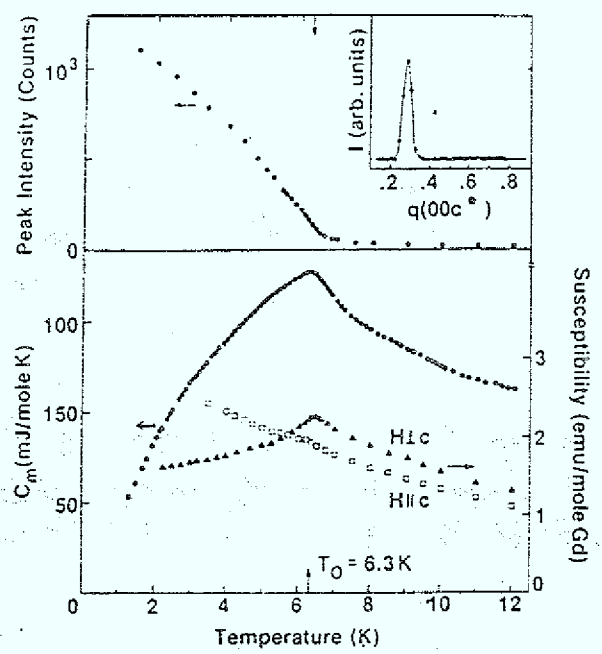

Fig.100: The temperature dependence of the magnetic neutron scattering intensity at the satellite peak (0,0,0.28), the ac susceptibility, and the magnetic specific heat for $Y_{0.978}Gd_{0.022}$. Inset: The scattered neutron intensity for a scan along the (0,0,1) line at T = 4.5 K (From Wenger et al., 1986).

Neutron diffraction measurements confirm the existence of long-range magnetic helical order in dilute YGd alloys for Gd concentrations of 2 and 3 at. % (Brown et al., 1985) and 1.5 to 4.4 at. % (Wenger et al., 1986). For all Gd concentrations, the diffraction patterns reveal magnetic satellites at positions $(0,0,1\pm\delta)$ where $\delta = 0.28c^*$ is the wave vector of the incommensurate periodic order (c^* is the reciprocal lattice vector). They correspond to a modulated spin state of about 20 Å wavelength with the Gd moment directions in the basal plane of the hexagonal structure (or very close to it) and the propagation wave vector along the c axis. The observed widths of the magnetic diffraction peaks are resolution limited, indicating that the scattering originates from a long-range ordered state. Below the ordering temperature, no shift in the position of the satellite peaks nor change in their width is measured. Fig. 100 displays the temperature dependence of the satellite peak intensity (its position is shown in the insert) for the YGd 2.2 at. % single crystal as well as its ac susceptibilities and magnetic specific heat (Wenger et al., 1986).

The existence of such a long-range ordered magnetic structure down to at least 1.5 at. % Gd in YGd alloys implies a driving mechanism due to the electronic structure of the yttrium matrix. It has been proposed (Sarkissian and Coles, 1976; Wenger and Mydosh, 1984b) that the rare-earth moments stabilize the spin density wave (SDW) (Overhauser, 1959 and 1960) in the matrix. A somewhat different mechanism, first suggested by Freeman (1972) to explain the AFM ordering in 4f-metals, considers the nesting properties of the Fermi surface of the rare earths as giving a maximum to the electron gas susceptibility at a given ("nesting") vector $\vec{q}_o$. These result in a RKKY exchange integral $J(\vec{q}_o)$ which can explain the observed helical spin structures. The 4d conduction electrons of the Y matrix are expected to participate in both mechanisms of magnetic coupling. More accurate measurements of the Gd form factor are required in order to reveal a possible contribution of delocalized electrons.

Additional support for the SDW approach is obtained by Wenger et al. (1984b and 1986). They present a quantitative interpretation of their specific heat data, also measured in applied fields, within a mean-field model of the SDW mechanism for AFM ordering. Note that already the bare data of $C_m(T)$ shown in Fig. 100 demonstrate the non-SG like behavior of the YGd alloy: The semicusp-like peak of the specific heat $C_m(T)$ appears at the temperature T_N of the $d(T\chi)/dT$ maximum, as common in antiferromagnets (in contrast to spin glasses where a very broad maximum occurs at a temperature far above T_f).

Alloys of Y or Sc with small concentrations of non-S-state ions, like Tb, Dy or Er, are expected to exhibit an anisotropic ordering behavior strongly influenced by the low-symmetry crystal-field acting on the highly asymmetric 4f electron cloud of the magnetic impurity (see also sec. 7.2). A comparison between ScGd and ScTb alloys is given by Sarkissian (1977), reporting on static and ac-susceptibility measurements. At present there is some ambiguity of interpreting several bulk measurements either in terms of SG or long-range AFM ordering, as will be discussed now:

In the case of YTb alloys, Ketelsen and Salamon (1985) observe small differences between the FC- and ZFC-magnetization at H = 20 Oe for Tb concentrations of 5 at. % and 3 at. %. Using neutron diffraction in addition, they demonstrate that YTb 5 % is a helical antiferromagnet (similar as described above for the YGd alloys), despite the "SG-like" history dependence of its magnetization. In the other alloy YTb 3 %, no magnetic satellites are found in the neutron-diffraction pattern. Hence, the authors conclude that only YTb 3 % is a SG. They emphasize that irreversibility alone cannot be used to characterize the SG state. The same system has also been studied by Rainford et al. (1985). Their neutron-diffraction measurements on six single crystals of YTb with Tb concentrations of 2, 3, 4, 5, 6 and 7 at. % show the existence of long-range helical AFM for all the measured samples, in contradiction to the result above. Extrapolation of the Néel temperatures versus concentration would indicate a critical concentration for the disappearance of long-range AFM order near or below 1 at. % Tb in Y.

In the case of YDy alloys, a similar confusion exists in interpreting the data. Lecomte et al. (1986b) have studied three samples of Y based alloys with Dy concentrations of 2.5, 3.5 and 4.5 at. %. For all three alloys the characteristic temperatures deduced from the maximum in the specific heat, the dc and the ac susceptibilities coincide within experimental error. This behavior is not characteristic of a spin glass. In addition, the specific heat data can be used to estimate the entropy change between 0 K and T_N, which agrees to within 5 % with the theoretical value of $Nk_B \ln (2J+1)$ for $J = 15/2$. Hence, the authors rule out a SG freezing in these samples and suggest long- range AFM ordering. They also argue that the early experiments with YDy 2 % by Wenger (1978) are probably not properly analyzed who found the ac-χ maximum even at a higher temperature than the maximum of the specific heat.

The finding by Lecomte et al. (1986b) is consistent with results from neutron-diffraction measurements on YDy 3 % by Rathmann and Touborg (1977) which reveal helical AFM ordering of the Dy moments below $T_N = 9$ K (again very similar to the YTb and YGd alloys). In contrast, Baberschke et al. (1984) measure on a similar sample YDy 3 % differences in the ZFC- and FC-magnetization (see Fig. 71) below $T_f = 9.2$ K and field dependences of the remanences (IRM and TRM), very similar to features in spin glasses.

YEr alloys have been studied by Fert et al. (1982), Wendler et al. (1983), Baberschke et al. (1984), Bonjour et al. (1984), and Bouchiat et al., (1985).

Much more work is still needed to clarify the question about the crossover to the spin-glass state by dilution of rare-earth metals. It is wellknown for long that Y and Sc based rare-earth alloys behave quite different. This has been explained by different spin-density wave effects: in Sc the congruence of the band structure with that of the 4f elements is weaker (Sarkissian and Coles, 1976; Touborg, 1977). Baberschke et al. (1984) estimate the ratio, $|D|/\tilde{J}$, between anisotropy D and exchange variance $\tilde{J}$ to be systematically smaller

in the Sc- than in the Y-based alloys. Rare-earth impurities in the Sc host seem to behave as "good" spin glasses, while there is a strong tendency in the Y host to form a helical or modulated magnetic structure. It could be that the strong SDW effect in Y-based alloys induces some kind of mixed state with long-range AFM correlations and SG irreversibilities (as directly observed in the diluted Ising AFM $(Fe, Mg)Cl_2$, see sec. 8.2).

So far we have considered 4f systems but in principle similar effects may be expected in diluted 3d metals, too. Cable et al. (1984) have performed neutron measurements on CuMn single crystals containing

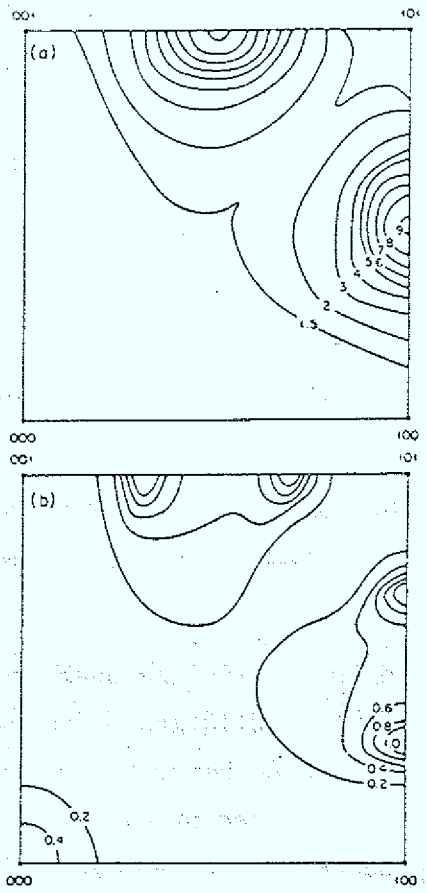

Fig. 101: Results from neutron-polarization analysis in CuMn 25 at% at T = 10 K. The non-spin-flip or nuclear (in part a) and the spin-flip or magnetic (in part b) cross sections are displayed (From Cable et al., 1984).

5, 10, 15 and 25 at. % Mn. Indeed, the results show the presence of a spin modulation with a period that varies continuously in terms of the edge of the fcc crystal cell from 6 a_o at 5 at. % Mn to about 3 a_o at 25 at. % Mn. For illustration, the intensity contours from nuclear and magnetic scattering are compared in Fig. 101 for CuMn 25 % at 10 K. In these systems, however, the correlation length associated with the modulation is of finite range (about 6 a_o) at all Mn concentrations. There are smaller regions of atomic short-range order in coexistence, which have net ferromagnetic moments, and which complicates the studies because both effects are not independent from each other (see also a similar work by Gotaas et al., 1985).

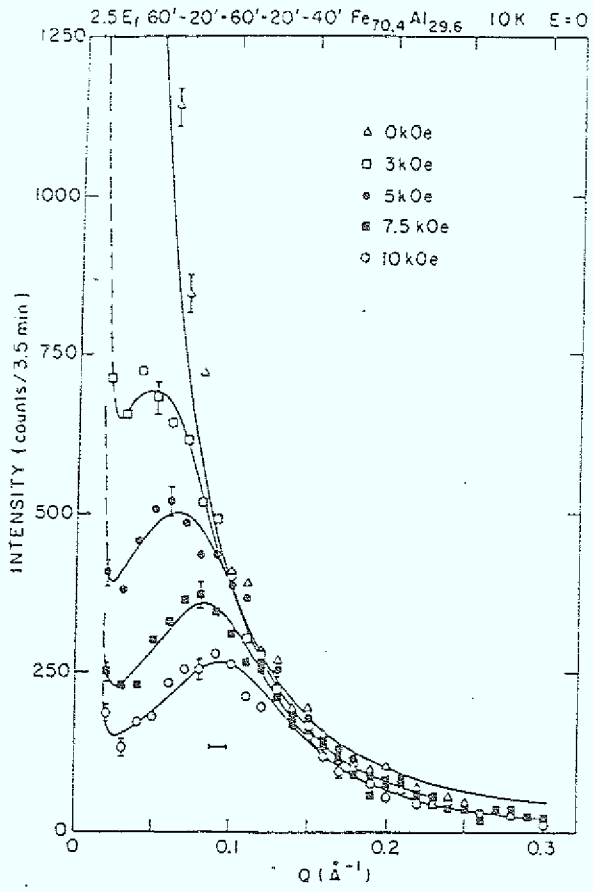

Fig. 102: Magnetic field dependence of the elastic scattering intensity for $Fe_{70.4}Al_{29.6}$ at 10 K. Note the very good Q-resolution ($\sim$0.01 Å^{-1}, represented by the bar) as indicated by the steep increase of the intensity near Q = 0 (From Böni et al., 1986).

In this context it is interesting to mention the very recent work by Böni et al. (1986). They have studied the reentrant spin-glass system $Fe_{70.4}Al_{29.6}$ in applied fields by neutron scattering technique. In zero field the elastic scattering peaks at $Q = 0$ in the low-temperature RSG phase, whereas for an applied field parallel or perpendicular to Q the intensity peaks at finite Q (Fig. 102). The peak position is field and temperature dependent and suggests a field-induced modulated spin structure within a finite correlation range of about 20 Å. This work opens a wide field of studying the field-dependence in other high-concentrated SG systems, which may help in further understanding the magnetic ordering in the crossover regime from SG to long-range FM or AFM order.

9. Systems with random anisotropy axis

Spin glasses are only one part in the issue of recent studies concerned with "frozen-in" disordered magnetic states. Random fields or random anisotropies also may destroy long-range ferro- or antiferromagnetic order. While it has been shown above that amorphous Gd-Al alloys (e.g. a-$Gd_{0.37}Al_{0.63}$, see Fig. 13) are typical spin glasses like crystalline CuMn or (Eu,Sr)S, due to competing exchange interactions, amorphous alloys with non-S-state ions are characterized by single-ion anisotropy axes (eq. 6) which are distributed randomly in space.
In this last section we shall discuss briefly recent research concerning magnetic order in amorphous materials with significant local random anisotropy, emphasizing their similarities to spin glasses (see also Moorjani and Coey, 1984). We shall use the term speromagnet to denote spin-glass-like magnetic structures that result from single-ion anisotropy to distinguish them from spin glasses which occur due to competing exchange interactions.

9.1 RAM-model :

In order to describe the magnetic order behavior of amorphous intermetallic compounds containing rare-earth atoms with nonzero orbital momentum such as a-$TbFe_2$, Harris, Plischke and Zuckermann (1973) have introduced a model (RAM) defined by the Hamiltonian

$$\mathcal{H} = -\sum_{ij} J_{ij} \vec{S}_i \vec{S}_j - D \sum_i (\vec{n}_i \cdot \vec{S}_i)^2 \qquad (102)$$

where $\vec{S}_i$ is the total angular momentum at site i, and J_{ij} are the ferromagnetic exchange interactions of any range. The second term with a constant second-order anisotropy parameter D represents the local anisotropy where the unit vectors $\vec{n}_i$ point in random easy-axis directions. The properties of this model are still controversial.

The mean-field treatment of the RAM-model (eq. 102) with interactions $J_{ij} = J_0/N$ between all pairs $\vec{S}_i$, $\vec{S}_j$ predicts for all ratios D/J_0 a ferromagnetic state below T_c (see e.g. Derrida and Vannimenus, 1980). But there is clearly a competition between the "aligning" effects of ferromagnetic exchange and the "scattering" effects of random anisotropy. Using renormalization-group techniques Aharony (1975) predicts that there is no ferromagnetism for dimensions $d \leq 4$. The result is in agreement with domain-wall arguments (Jayaprakash and Kirkpatrick, 1980). It has been suggested by several authors (Chen and Lubensky, 1977; Pelcovits et al., 1978; Bray and Moore, 1985b) that a speromagnet (= spin-glass-like phase) may occur instead. Aharony and Pytte (1980), however, have found a novel "infinite-susceptibility phase" in which the magnetization vanishes (calculated to lowest order in D). This unusual property is obtained by an expansion in terms of M/H which becomes singular for $H \to 0$ and might be incorrect. A low-temperature scaling theory by the same authors (Aharony and Pytte, 1983) indicates for the case of small D/J_0 that χ should become very large but not diverge. They suggest for T and $H \to 0$ that the maximum value of χ is given in d = 3 by

$$\chi_0 \propto (J_0/D)^4 \qquad \text{for } T \lesssim T_c \ . \qquad (103)$$

Chudnovsky and Serota (1983) recently have given a phenomenological theory for the RAM problem introducing into the model the length scale R_c of the spatial correlation of the easy axes. Then, the magnetic structure of amorphous magnets is shown to be strongly dependent on the parameter $\Lambda_r = \lambda_r (R_c/a)^2$, where $\lambda_r = D/J_0$ and a is the atomic spacing. For weak random anisotropy ($\Lambda_r < 1$) a new magnetic state is predicted: the "correlated speromagnet" (CSM). This state is characterized by a smooth rotation of the magnetization M over a ferromagnetic correlation length $R_D \gg R_c$, even though the net magnetization is zero. There are no domains separated from each other by thin domain walls, as it is in a crystalline ferromagnet. In the CSM, M is reversible and the zero-field susceptibility becomes very large but remains finite

$$\chi_0 = \frac{1}{8}\,(\Lambda_r/4)^{-4} \propto (J_0/D)^4 \qquad (104)$$

in agreement with eq. 103. In contrast to the CSM, for large random anisotropy ($\Lambda_r \gg 1$) the magnetization is irreversible as discussed by Callen et al. (1977).

9.2 Properties in comparison to spin glasses :

Amorphous binary rare-earth alloys a-$R_x X_{1-x}$ with non-magnetic X atoms are expected to show most clearly the influence of random anisotropy on magnetic properties. Hence, we mainly discuss here results from such materials with X = Cu, Ag, Au, or Al, which have been prepared in the amorphous state over a wide range of concentration by sputtering or evaporation.

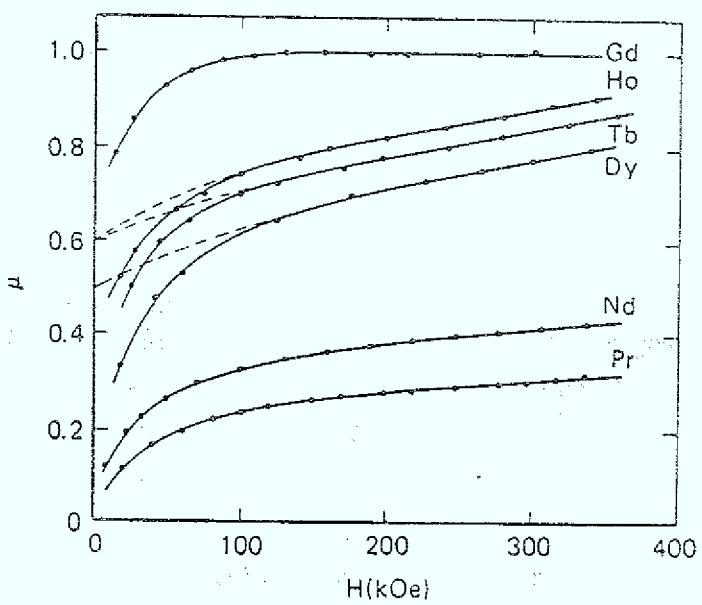

Fig. 103: High-field magnetization, $\mu = M/M_{sat}$, of amorphous RAg alloys at 4.2 K (R = rare earths as indicated). Dashed lines are fits based on the RAM-model in mean-field approximation, eq. 102 (From Boucher, 1977; Moorjani and Coey, 1984).

It is always difficult to obtain saturation of the magnetization in these alloys even in the case of Gd, as demonstrated by pulsed-field measurements in Fig. 103 (Boucher, 1977; Moorjani and Coey, 1984). Gd^{3+} ($4f^7$, J = 7/2) is an S-state ion, thus single-ion anisotropy is expected to be negligible or very small (see also Nigh et al., 1963). The behavior in Fig. 103 indicates the presence of antiferromagnetic interactions which prevent a complete parallel alignment of the moments favored by the generally stronger ferromagnetic interactions in these amorphous a-RX alloys. The corresponding crystalline RX alloys of CsCl-type structure are antiferromagnetic, which corroborates the statement. In the crystallized structure only the second nearest neighbors of a rare-earth ion are rare earths again, while in the amorphous state they are randomly distributed with a finite probability of rare-earth ions to become first as well as second nearest neighbor. Thus, both ferro- and antiferromagnetic interactions are present in amorphous RX alloys with noble metals. In $a\text{-}Gd_xX_{1-x}$ the competing exchange interactions lead to spin-glass behavior for sufficiently low Gd concentration x. Examples are $a\text{-}Gd_xAl_{1-x}$ (Fig. 13), $a\text{-}Gd_xCu_{1-x}$ (McGuire et al., 1978), $a\text{-}Gd_xAg_{1-x}$ (Boucher, 1976) and $a\text{-}Gd_xLa_{0.80-x}Au_{0.20}$ (Poon and Durand, 1978). For high Gd concentrations they become ferromagnets.

Table 4:

Random-anisotropy parameter D and exchange coupling constant J_o obtained from high-field magnetization data (using the model in eq. 102) of three amorphous RAg alloys (From Ferrer et al., 1978).

$a\text{-}Tb_{0.52}Ag_{0.48}$:	D = 4.0 K	D/J_o = 7.6
$a\text{-}Dy_{0.50}Ag_{0.50}$:	D = 3.0 K	D/J_o = 22.0
$a\text{-}Ho_{0.50}Ag_{0.50}$:	D = 1.5 K	D/J_o = 10.0

The approach to saturation in a-RX alloys when R ≠ Gd (Fig. 103) is mainly governed by single-ion anisotropy. The dashed lines in Fig. 103 are fits based on eq. 102 in the molecular-field approximation (Ferrer et al. 1978). The analysis allows one to estimate the values for the random-anisotropy constant D and for the exchange interaction J_0, as summarized in table 4. For the light rare earths (Pr, Nd: Fig. 103) this simple model is inappliable, influences of fourth- and sixth-order electrostatic fields obviously have to be invoked.

While there is good agreement between the RAM model description and the magnetization obtained at high fields, serious deviations are found (Fig. 103) in the low-field region ($H \lesssim 100$ kOe). The deviations originate from the presence of sizable hysteresis loops and magnetic aftereffects. Most detailed informations are available for a-TbAg (Boucher and Barbara, 1979) and a-DyCu (Coey et al., 1981). Fig. 104 displays hysteresis loops measured in a-$Dy_{0.41}Cu_{0.59}$ (anisotropy parameter D = 3 K) at two temperatures. Time-dependent effects are found in the dashed parts of the loop at 4.2 K. The measured value of the coercive field H_c is dependent on temperature and measurement time. H_c will be smaller the longer the time at which it is measured after the application of the field. The intrinsic coercivity (H_c extrapolated to zero temperature) is rather large: 8 kOe for a-DyCu and 23 kOe for a-TbAg. A quite remarkable feature appears in the very-low-T loop at 0.1 K (Fig. 104). Instead of a smooth field dependence in the irreversible part of the loop (as measured at 4.2 K), the magnetization changes in a series of large discrete jumps, reminiscent of the Barkhausen effect in a sample containing about half a dozen domains. Each would have volume 10^{-2} mm^3 and contain some 2×10^{18} Dy ions.

The remanent magnetization in low fields invariably depends on the manner in which it is acquired. This is illustrated for a-DyCu in Fig. 105, where the field dependences of the IRM and TRM are shown, being very similar to the properties of spin glasses.

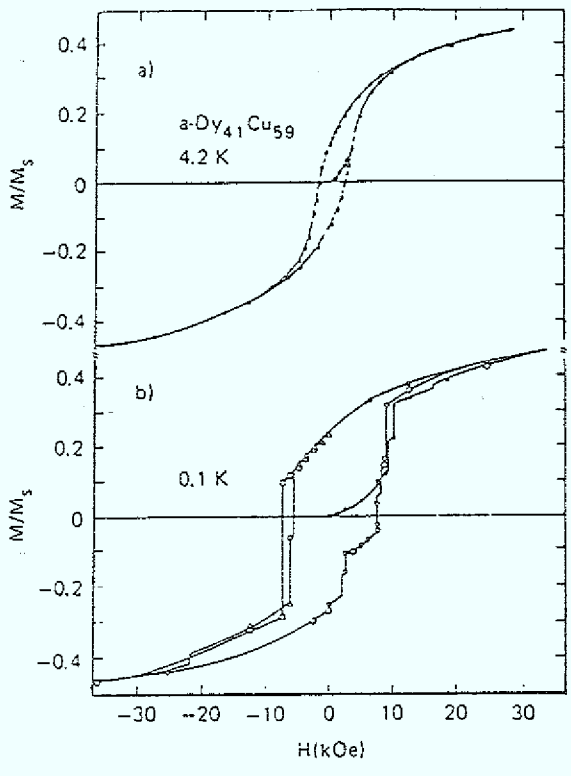

Fig. 104: Initial magnetization curves and hysteresis loops for a-$Dy_{0.41}Cu_{0.59}$ at two temperatures, 4.2 K and 0.1 K. The dashed parts of the loops at 4.2 K indicate the presence of time effects. Triangles, circles, and crosses denote different cycles at 0.1 K (From Coey at al., 1981).

For the time dependence (magnetic aftereffect) a slow lnt-decay is measured, indicating a wide distribution of relaxation times or energy barriers. Very-low-field measurements of the magnetization reveal different behavior after ZFC or FC (Fig. 106). Below a welldefined temperature one can define reversible and irreversible susceptibilities. Thus, the speromagnet a-DyCu, where random anisotropy dominates exchange, exhibits many properties which also characterize spin glasses, i.e. isotropic spin systems where competing exchange interactions are essential.

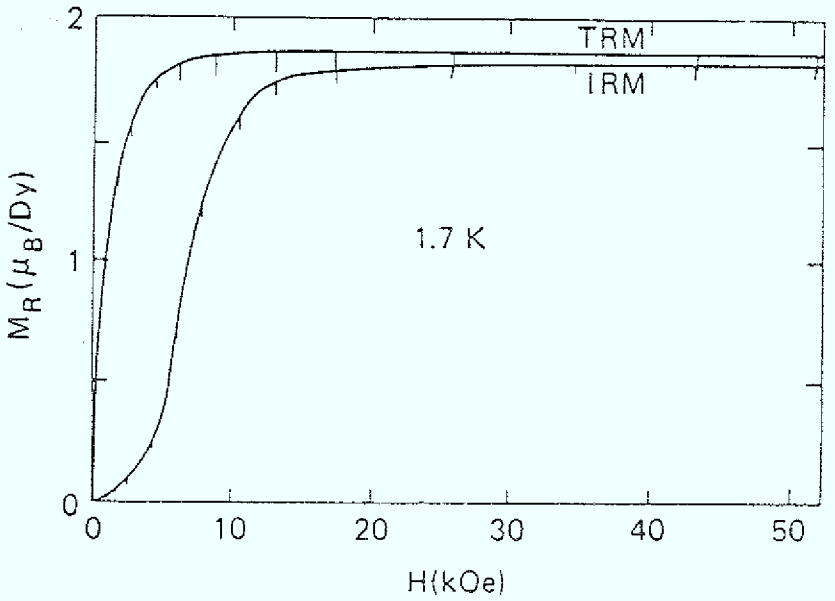

Fig. 105: Isothermal remanence and thermoremanence of a-DyCu at 1.7 K. Vertical lines indicate the time variation in one minute (From Coey et al., 1981).

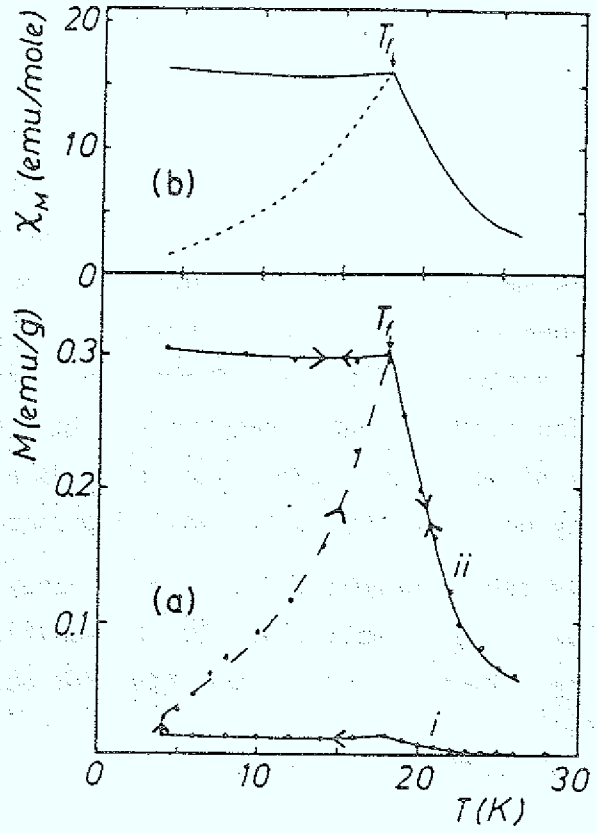

Fig. 106: (a) Magnetization of a-DyCu measured (i) in the earth's field and (ii) in 4.94 Oe applied at 4.2 K. The arrows indicate the sequence of measurements. (b) Reversible (solid lines) and irreversible (dashed line) susceptibilities, derived from these data (From Coey et al., 1981).

In a recent study von Molnar et al. (1982) present a comparison of random-anisotropy and spin-glass properties in the amorphous rare-earth alloys a-$Dy_{0.52}Cu_{0.48}$ (D/J_o large), a-$Gd_{0.52}Ag_{0.48}$ (D/J_o small), and a-$Gd_{0.37}Al_{0.63}$ (a wellknown spin glass). This work has also been stimulated by the theoretical prediction of Aharony and Pytte (1980) of an "infinite-susceptibility phase". Detailed measurements of the magnetization as a function of temperature and applied magnetic field are analyzed in the form of Arrott plots, i.e. M^2 vs. H/M, as shown in Fig. 107. The general features of the Arrott plot for a-DyCu (Fig. 107a) are quite different from those of a-GdAg (Fig. 107b). On the other hand, the behavior in Fig. 107a is similar to the Arrott plot obtained for the spin glass a-GdAl (Fig. 107c). As in spin glasses and contrarily to the low-anisotropy case (Fig. 107b), it is difficult to see on the plot in Fig. 107a at which temperature the transition occurs. Low-field susceptibility measurements (similar to Fig. 106), however, clearly indicate the transition at 23 K. Below T_c = 23 K the susceptibility remains large but finite (χ_o^{-1} = 0.69) (intercept along the abscissa), and there is no spontaneous magnetization at any temperature (no intercept along the positive ordinate).

The disagreement with the theory of Aharony and Pytte (1980) can be ascribed to the fact that the prediction of the "infinite-susceptibility phase" is developed for $D/J_o < 1$. Consequently, a-GdAg is also studied where the anisotropy is small. The data in Fig. 107b show that the susceptibility approaches the demagnetizing limit, i.e. $\chi_o^{-1} \rightarrow 0$. In addition, a careful analysis of the low-field data indicates that the material may develop a small moment despite the apparent vertical drop in M^2 as $H/M \rightarrow 0$; although this conclusion depends critically on the magnitude of any possible extremely small demagnetizing field.

Finally, the spin-glass sample a-GdAl (Fig. 107c) clearly exhibits no spontaneous magnetization, a small value for the initial susceptibility (χ_o^{-1} = 13.7), and the curvature remains positive for all measured temperatures in the Arrott plot. Thus, the spin glass a-GdAl shows many similarities to the speromagnet a-DyCu.

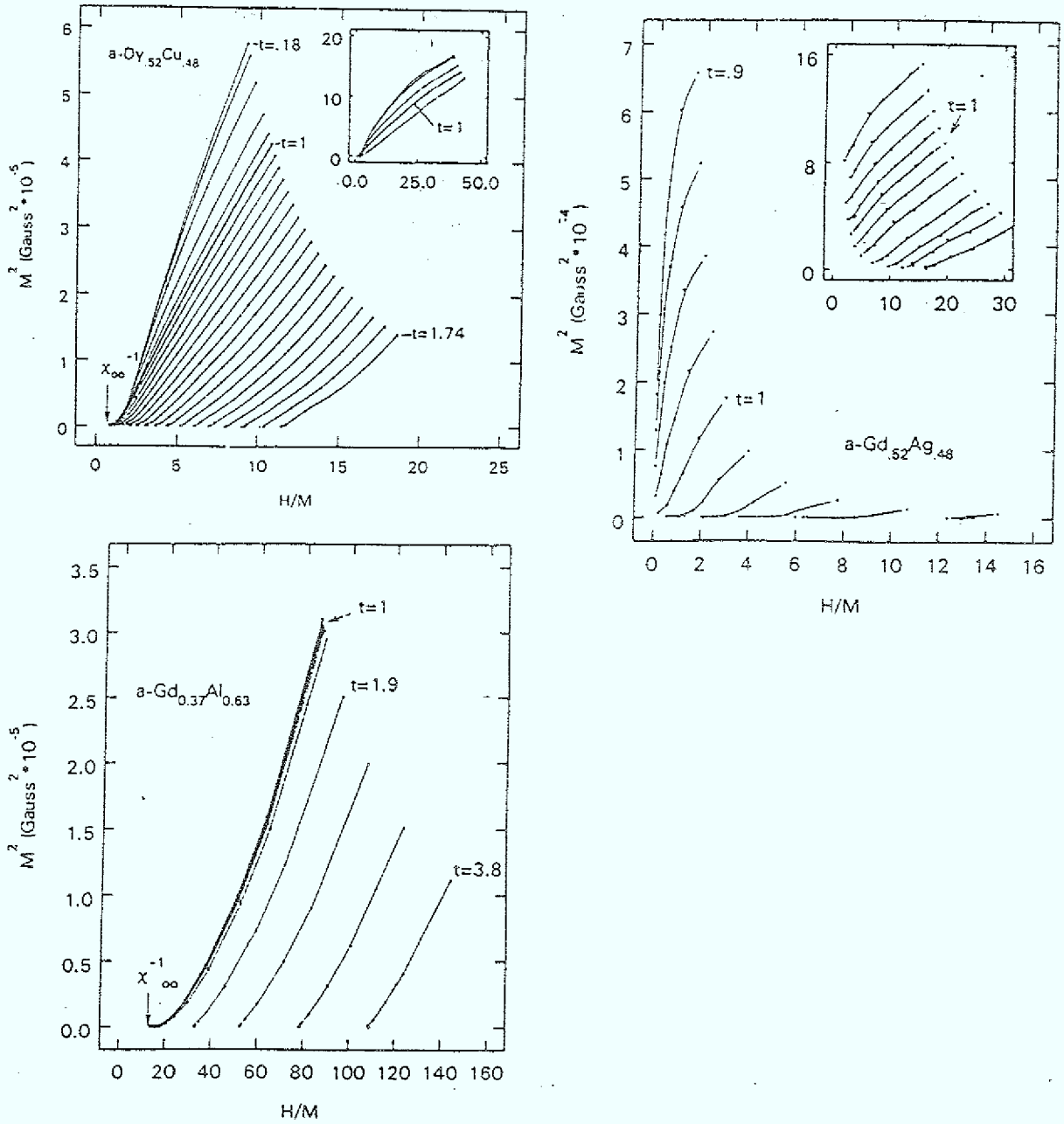

Fig. 107: (a) Arrott plot of a-$Dy_{0.52}Cu_{0.48}$ for applied fields up to 7 kOe. The insert is the same plot extended to 50 kOe. $t = T/T_c$, where T_c = 23 K.
(b) Arrott plot of a-$Gd_{0.52}Ag_{0.48}$ for applied fields up to 400 Oe. The insert is the same plot for intermediate fields 500 Oe $\lesssim H \lesssim$ 6 kOe. $t = T/T_c$, where T_c = 83 K.
(c) Arrott plot of a-$GdAl_2$ for applied fields up to 48 kOe. $t = T/T_c$, where T_c = 15.75 K.
(From v. Molnar et al., 1982).

It would be particularly interesting to know the magnetic behavior in systems with small anisotropy D/J_0. The random anisotropy should destroy ferromagnetic order, but a large or even diverging susceptibility is predicted (Aharony and Pytte, 1980 and 1983; Chudnovsky and Serota, 1983). Barbara and Dieny (1985) have recently studied the properties of a-$Dy_xGd_{1-x}Ni$ (where Ni is nonmagnetic) for various concentrations x. Estimating D and J_0 for different x from high-field magnetization measurements, they find a dependence of χ_0 on the ratio D/J_0 (Fig. 108) which can be represented by the power law of eq. 103 with the exponent 3.8 ± 0.2, in excellent agreement with the result (exponent 4) of non-mean-field theories (Aharony and Pytte, 1983; Chudnovsky and Serota, 1983). The problem of low-anisotropy systems, however, is still open. In particular, it is not known for the present, whether the transition to the infinite-susceptibility phase occurs at $D = 0$ as is theoretically predicted (Aharony and Pytte, 1983) or at $D > 0$.

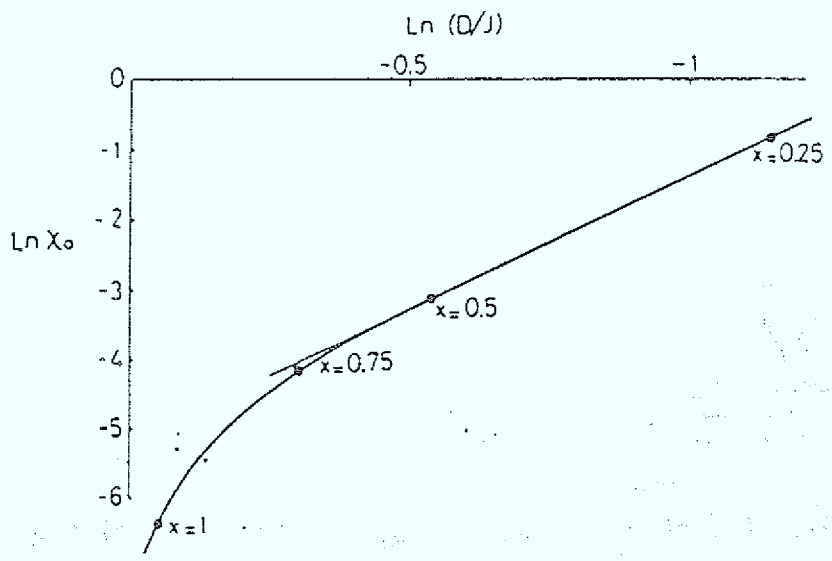

Fig. 108: Susceptibility χ_0 vs. the ratio D/J_0 for a-$Dy_xGd_{1-x}Ni$ alloys. The straight line in the ln-ln plot for $D/J_0 < 0.7$ corresponds to eq. 103 with an exponent 3.8 ± 0.2 (From Barbara and Dieny, 1985).

Sellmyer and Nafis (1985) have also studied this problem. In a-$Gd_{0.72}Fe_{0.10}Ga_{0.18}$ they find no spontaneous magnetization and a completely reversible magnetization below T_c. They suggest that their data may be taken as evidence for the new CSM-state (Fig. 109) predicted by Chudnovsky and Serota (1983). The same authors (1986) also analyze ac-χ data near T_c for a-$Dy_{0.60}Fe_{0.30}B_{0.10}$, taken in various applied fields, in terms of an Ising-type spin-glass transition, i.e. they deduce critical exponents γ and δ from the behavior of the nonlinear susceptibility ($\gamma = 2.4$; $\delta = 2.3$).

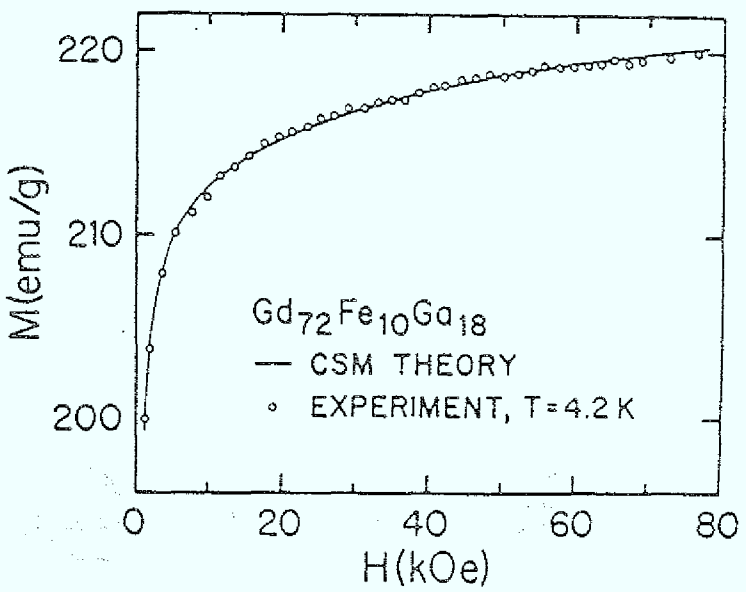

Fig. 109: Magnetization M(H) of a-$Gd_{0.72}Fe_{0.10}Ga_{0.18}$ at 4.2 K and comparison (solid line) to CSM prediction (From Sellmyer and Nafis, 1985).

10. Conclusions

Spin-glass behavior is an intrinsic effect of disorder and competition of the magnetic interactions (sec. 2). In such materials, several unusual properties are observed below the temperature T_f, and the transition at T_f appears as a complicated freezing process. Attempts to interpret this novel phenomenon of magnetic ordering have proved difficult, but in recent years substantial progress has occurred in our understanding of spin glasses.

Up to now no realistic model of a spin glass has been solved analytically. The simple model proposed by Edwards and Anderson (1975) (sec. 4.1), however, is shown by Monte Carlo simulations to reproduce many experimental findings on spin glasses remarkably well (sec. 4.2). Its mean-field theory, as realized in the Sherrington-Kirkpatrick (SK) model (1975) (sec. 4.3), is now fairly well understood (which has taken about eight years). The solution proposed by Parisi (1980) yields a rich structure in the ordered phase, described by an infinite number of pure states related by an ultrametric topology. The onset of irreversibility at T_f is associated with a phase transition which also holds in an applied field. The critical H-T line is different for Ising (AT-line: eq. 15) or Heisenberg spins (GT-line: eq. 27).

A large amount of experimental data shows the intrinsic feature of irreversibilities of spin glasses at temperatures below T_f (sec. 5.1). The picture of the "many-valley structure" in phase space (Fig. 15) is useful to explain the effects phenomenologically, independent of whether at T_f an equilibrium transition occurs. It would be desirable, however, to have more detailed theoretical work for instance on slowly relaxing metastable states. The concept of "isotropic anisotropy" (sec. 5.2), characterized by an anisotropy triad (Saslow, 1982) and anisotropic interactions of the Dzyaloshinskii-Moriya-type, can explain successfully several distinct properties of metallic spin glasses well below T_f. The nature of low-energy excitations in spin glasses is far from being understood (sec. 5.3). In spite of similar observing a linear specific heat in glasses as well as in spin glasses, they are of different origin: The linear specific heat in spin glasses is accounted for by linear (oscillatory) spin excitations, while it is due to two-level tunneling systems in ordinary glasses. In

addition, recent specific heat measurements (Martin, 1985) on the spin glass CuMn 0.88 at% show no time effects, in contrast to the behavior in ordinary glasses. Thus, there are not much analogies between spin glasses and ordinary glasses, except the existence of slowly relaxing metastable states.

Most of recent experimental studies on spin glasses are concerned with the nature of the spin-glass transition at T_f (sec. 6 and 7). The appearance of very long relaxation phenomena and the lack of corresponding reliable analytic theories hamper the interpretation of these experiments. Indeed, until recently no consensus existed as to whether spin glasses exhibit a phase transition at all. A number of experiments on various spin glasses, however, provides now fairly convincing evidence for a phase transition at a nonzero T_f (sec. 7.3). An understanding of the complicated spin dynamics near T_f, however, which includes macroscopic times, would be desirable. For the critical exponents, even numbers close to the Ising values determined from numerical studies are quoted.

Numerical studies of Ising spin glasses in three dimensions corroborate the experimental evidence that a phase transition takes place (sec. 4.4). However, very similar studies of Heisenberg spin glasses indicate that there is no transition in short-range vector-spin systems in three dimensions. In a very recent paper, Bray, Moore and Young (1986) demonstrate that vector-spin glasses with short-range couplings or RKKY couplings are in a different universality class, the lower critical dimension d_l is $d_l > 3$ or $d_l = 3$, respectively. In contrast, Ising spin-glasses have the same critical behavior for both types of couplings ($2 < d_l < 3$). The authors also show that the critical exponents associated with the Ising-type transition in anisotropic vector-spin glasses are always those of the short-range Ising spin-glass. The dependence of T_f on the anisotropy D in d=3-Heisenberg spin glasses is such that as $D \to 0$, $T_f \to 0$, but so slowly that for realistic values of D/J ($\approx 10^{-2}$), the transition temperature is still $T_f \approx J$ (see also: Morris et al., 1986). Thus, one can reconcile the numerical results with the experimental work, where most of the best-studied spin glasses are Heisenberg-type systems, by taking into account a very small anisotropy.

Much confusion, however, exists about the interpretation of spin-glass transitions in an applied magnetic field. As reported in sec. 7.2, there have been extensive efforts in the comparing of experimental results with mean-field theory of spin glasses (AT- and GT-lines).

Such a comparison has to be done with great coutiousness (see sec. 7.2) as pointed out by Fisher and Sompolinsky (1985). In this context it is quite interesting that several authors (McMillan, 1984b; Moore and Bray, 1985; Bray and Moore, 1986; Fisher and Huse, 1986) have proposed a new picture of the Ising-spin-glass phase in short-range systems. In striking contrast to the results of the mean-field model (SK), they conclude that there is only one phase in three dimensions:

Bray and Moore (1986) present a theory, based on a "one-parameter-scaling" picture, the central concept being that of a scale-dependent coupling J(L). The equilibrium properties in the ordered phase are determined from an exponent y which describes the scale dependence of J(L) at zero temperature

$$J(L) \sim JL^{y} \quad . \qquad (105)$$

The sign of y determines whether the system scales to weak or strong coupling for $L \to \infty$, i.e. whether $d > d_1$ $(y > 0)$ or $d < d_1 (y < 0)$. They obtain $y = +0.19 \pm 0.01$ for $d = 3$, which again implies a phase transition at a nonzero temperature. Then, the exponent y determines the decay of correlations in the ordered state which is algebraic $(\sim r^{-y})$ for all $T < T_f$. This result was first suggested by Fisher and Huse (1986) on the basis of a droplet model. It implies that the ordered phase is described by a single pure state, and the short-range model does not exhibit "replica symmetry breaking", in contrast to the mean-field model. The exponent y also governs the response to a weak magnetic field. If the ordered phase is replica symmetric for short-range models, it follows that there can be no AT line; i.e. a magnetic field destroys the spin-glass transition. This would imply that experiments only observe "dynamic AT-lines", at which relaxation times become comparable with experimental observation times.

Summarizing, this new concept would mean that the ordered state of real spin glasses is simpler than the complicated structure obtained from the SK-mean-field theory. Future work will certainly be directed toward further studies on this central issue of the nature of the spin-glass phase.

Finally, systems where long-range periodic (FM, AFM) and spin-glass orderings compete exhibit magnetic properties which obviously are not in accordance with present theories (Fig. 18 and 20). In sec. 8 we made a first attempt to classify the large amount of experimental data on this subject which now needs confirmation by theoretical work beyond the SK-mean-field theory.

References

Aeppli, G., S.M. Shapiro, H. Maletta, R.J. Birgeneau and H.S. Chen, 1984, J. App. Phys. 55, 1628.

Aeppli, G., H. Maletta, S.M. Shapiro, and D. Abernathy, 1986, submitted for publication.

Aharony, A., 1975, Phys. Rev. B12, 1038.

Aharony, A., and E. Pytte, 1980, Phys. Rev. Letters 45, 1583.

Aharony, A., and E. Pytte, 1983, Phys. Rev. B27, 5872.

Alexander, S., C. Laermans, R. Orbach and H.M. Rosenberg, 1983, Phys. Rev. B28, 4615.

Alloul, H., 1979a, Phys. Rev. Letters 42, 603.

Alloul, H., 1979b, J. Appl. Phys. 50, 7330.

Alloul, H., 1983, in: "Heidelberg Colloquium on Spin Glasses", ed. by J.L. van Hemmen and I. Morgenstern (Springer Verlag, Berlin), p. 18.

Alloul, H., and F. Hippert, 1983, J. Magn. and Magn. Mater. 31-34, 1321.

Alloul, H., and P. Mendels, 1985, Phys. Rev. Letters 54, 1313.

Alloul, H., P. Mendels, P. Beauvillain and C. Chappert, 1986, J. Magn. and Magn. Mater. 54-57, 105.

Anderson, P.W., B.I. Halperin, and C.M. Varma, 1972, Phil. Mag. 25, 1.

Anderson, P.W., and C.W. Pond, 1978, Phys. Rev. Letters 40, 903.

Anderson, P.W., 1983, Proc. Natl. Acad. Science USA 80, 3386.

Baberschke, K., P. Pureur, A. Fert, R. Wendler, and S. Senoussi, 1984, Phys. Rev. B29, 4999.

Baberschke, K., C. Pappa, H. Mahdjour and R. Wendler, 1986, J. Magn. and Magn. Mater. 54-57, 179.

Barbara, B., and A.P. Malozemoff, 1983, J. Less-Common Metals 94, 45.

Barbara, B., A.P. Malozemoff and Y. Imry, 1981, Phys. Rev. Letters 47, 1852.

Barbara, B., and B. Dieny, 1985, Physica 130B, 245.

Bauhofer, W., M. Wittmann and H.G. v. Schnering, 1981, J. Phys. Chem. Solids, 42, 687.

Bauhofer, W., E. Gmelin, M. Möllendorf, R. Nesper and H.G. v. Schnering, 1985, J. Phys. C18, 3017.

Bauhofer, W., T. Chattopadhyay, M. Möllendorf, E. Gmelin, and H.G. v. Schnering, 1986, J. Magn. and Magn. Mater. 54-57, 1359.

Baumann, U., D. Schubert, A. Schwotzer, and G. Weber, 1984, J. Magn. and Magn. Mater. 45, 179.

Beauvillain, P., C. Dupas, J.P. Renard and P. Veillet, 1984a, Phys. Rev. B29, 4086.

Beauvillain, P., C. Chappert and J.P. Renard, 1984b, J. Physique Lettres 45, 665.

Beauvillain, P., C. Chappert, J.P. Renard and J. Seiden, 1986, J. Magn. and Magn. Mater. 54-57, 127.

Berton, A., J. Chaussy, J. Odin, R. Rammal, and R. Tournier, 1982, J. Physique Lettres 43, 153.

Bertrand, D., A.R. Fert, M.C. Schmidt, F. Bensamka and S. Legrand, 1982, J. Phys. C15, L883.

Bertrand, D., F. Bensamka, A.R. Fert, J. Gelard, J.P. Redoulès and S. Legrand, 1984, J. Phys. C17, 1725.

Besnus, M.J., and J.P. Kappler, 1980, J. Magn. and Magn. Mater. 15-18, 1237.

Bhatt, R.N., and A.P. Young, 1985, Phys. Rev. Letters 54, 924.

Binder, K., 1977, Z. Physik B26, 339.

Binder, K., 1982, Solid State Comm. 42, 377.

Binder, K., W. Kinzel, and D. Stauffer, 1979, Z. Physik B36, 161.

Binder, K., W. Kinzel, H. Maletta, and D. Stauffer, 1980, J. Magn. and Magn. Mater. 15-18, 189.

Binder, K., and W. Kinzel, 1983, J. Phys. Soc. Japan 52, S-209.

Binder, K., and K. Schröder, 1976, Phys. Rev. B14, 2142.

Binder, K., and A.P. Young, 1984, Phys. Rev. B29, 2864.

Binder, K., and A.P. Young, 1986, Rev. Mod. Phys. (in press).

Birgeneau, R.J., Y. Shapira, G. Shirane, R.A. Cowley and H. Yoshizawa, 1986, Physica 137B, 83.

Bohn, H.G., W. Zinn, B. Dorner, and A. Kollmar, 1980, Phys. Rev. B22, 5447.

Bonjour, E., R. Calemczuk, R. Caudon, H. Safa, P. Gandit, and P. Monod, 1984, Proc. of LT17, (Karlsruhe, North Holland).

Bouchiat, H., 1986, J. Physique 47, 71.

Bouchiat, H., and D. Mailly, 1985, J. Appl. Phys. 57, 3453.

Bouchiat, H., and P. Monod, 1982, J. Magn. and Magn. Mater. 30,175.

Bontemps, N., J. Rajchenbach, and R. Orbach, 1983, J. Physique Lettres 44, 47.

Bontemps, N., J. Rajchenbach, R.V. Chamberlin and R. Orbach, 1984, Phys. Rev. B30, 6514.

Bontemps, N., J. Rajchenbach, R.V. Chamberlin and R. Orbach, 1986, J. Magn. and Magn. Mater. 54-57, 1.

Böni, P., S.M. Shapiro and K. Motoya, 1986, submitted for publication.

Börgermann, F.-J., H. Maletta, and W. Zinn, 1986a, J. Magn. and Magn. Mater. 54-57, 71.

Börgermann, F.-J., H. Maletta, and W. Zinn, 1986b, Phys. Rev. B (submitted for publication).

Brand, R.A., V. Manns and W. Keune, 1983, in: "Heidelberg Colloquium on Spin Glasses", ed. by J.L. van Hemmen and I. Morgenstern (Springer Verlag, Berlin), p. 79.

Brand, R.A., and W. Keune, 1984, Phys. Rev. Letters 52, 2097.

Brand, R.A., J. Lauer and W. Keune, 1985, Phys. Rev. B31, 1630.

Bray, A.J., and M.A. Moore, 1979, J. Phys. C12, 1441.

Bray, A.J., and M.A. Moore, 1980, J. Phys. C13, L469.

Bray, A.J. and M.A. Moore, 1984, J. Phys. C17, L463.

Bray, A.J. and M.A. Moore, 1985a, Phys. Rev. B31, 631.

Bray, A.J., and M.A. Moore, 1985b, J. Phys. C18, L139.

Bray, A.J., M.A. Moore and A.P. Young, 1986, Phys. Rev. Letters 56, 2641.

Bray, A.J., and M.A. Moore, 1986, in: "Heidelberg Colloquium on Glassy Dynamics and Optimization", ed. by J.L. van Hemmen and I. Morgenstern (Springer Verlag, Berlin), preprint.

Brown, P.J., R. Caudron, A. Fert, D. Givord and P. Pureur, 1985, J. Physique Lett. 46, L-1139.

Brown, J.A., R.H. Heffner, T.A. Kitchens, M. Leon, C.E. Olsen, M.E. Schillaci, S.A. Doods, and D.E. Mac Laughlin, 1981, J. Appl. Phys. 52, 1766.

Bruss, F., K. Baberschke, M. Loewenhaupt and H. Scheuer, 1979, Solid State Comm. 32, 135.

Cable, J.W., S.A. Werner, G.P. Felcher and N. Wakabayashi, 1984, Phys. Rev., B29, 1268.

Callen, E., Y.J. Liu, and J.R. Cullen, 1977, Phys. Rev. B16, 263.

Campbell, I.A., D. Arvanitis, and A. Fert, 1983, Phys. Rev. Letters 51, 57.

Campbell, I.A., N. de Courtenay, and A. Fert, 1984, J. Physique Lettres 45, 565.

Cannella, V., and J.A. Mydosh, 1972, Phys. Rev. B6, 4220.

Carlson, N.W., S. Geschwind, G.E. Devlin, B. Batlogg, J.F. Dillon, Jr., L.W. Rupp, Jr., and H. Maletta, 1984, J. Appl. Phys. 55, 1679.

Carnegie, D.W., Jr., and H. Claus, 1979, Phys. Rev. B20, 1280.

Casimir, H.B.G., and F.K. du Pré, 1938, Physica 5, 507.

Caudron, R., P. Costa, J.C. Lasjaunias and B. Levesque, 1981, J. Phys. F11, 451.

Chalupa, J., 1977, Solid State Comm. 24, 429.

Chamberlin, R.V., 1984, Phys. Rev. B30, 5393.

Chamberlin, R.V., 1985, J. Appl. Phys. 57, 3377.

Chamberlin, R.V., M. Hardiman, L.A. Turkevich, and R. Orbach, 1982, Phys. Rev. B25, 6720.

Chen, J.H., and T.C. Lubensky, 1977, Phys. Rev. B16, 2106.

Chattopadhyay, T., P.J. Brown, P. Thalmeier and H.G. v. Schnering, 1986 (in press).

Chikazawa, S., S.Taniguchi, H. Matsuyama and Y. Miyako, 1983, J. Mag. and Magn. Mater. 31-34, 1355.

Child, H.R., and J.W. Cable, 1969, J. Appl. Phys. 40, 1003.

Ching, W.Y., D.L. Huber, and K.M. Leung, 1980, Phys. Rev. B21, 3708.

Chudnovsky, E.M., and R.A. Serota, 1983, J. Phys. C16, 4181.

Coey, J.M.D., T.R. McGuire and B. Tissier, 1981, Phys. Rev. B24, 1261.

Coles, B.R., B.V.B. Sarkissian and R.H. Taylor, 1978, Phil. Mag. B37, 489.

Coles, B.R., 1984, Phil. Mag. B49, L21.

de Courtenay, N., A. Fert, and I.A. Campbell, 1984, Phys. Rev. B30, 6791.

Continentino, M.A., and A.P. Malozemoff, 1986, Phys. Rev. B33, 3591.

Cragg, D.M., D. Sherrington, and M. Gabay, 1982a, Phys. Rev. Letters 49, 158.

Cragg, D.M., and D. Sherrington, 1982b, Phys. Rev. Letters 49, 1190.

Crane, S., and H. Claus, 1981, Phys. Rev. Letters 46, 1693.

Dahlberg, E.D., M. Hardiman, R. Orbach, and J. Souletie, 1979, Phys. Rev. Letters 42, 401.

Dartyge, E., H. Bouchiat and P. Monod, 1982, Phys. Rev. B25, 6995.

De Almeida, J.R.L., and D.J. Thouless, 1978, J. Phys. A11, 983.

De Chatel, P.F., 1981, J. Magn. and Magn. Mater. 23, 28.

De Dominicis, C., 1978, Phys. Rev. B18, 4913.

De Dominicis, C., 1983, in: "Heidelberg Colloquium on Spin Glasses", ed. by J.L. van Hemmen and I. Morgenstern (Springer Verlag, Berlin), p.103.

De Dominicis, C., M. Gabay, T. Garel, and H. Orland, 1980, J. Physique 41, 923.

De Dominicis, C., H. Orland, and F. Lainée, 1985, J. Physique Lettres, 46, 463.

De Dominicis, C., and A.P. Young, 1983a, J. Phys. C16, L641.

De Dominicis, C., and A.P. Young, 1983b, J. Phys. A16, 2063.

De Gennes, P.G., 1962, J. Phys. Radium 23, 630.

Derrida, B., and J. Vannimenus, 1980, J. Phys. C13, 3261.

Deville, A., C. Arzoumanian, B. Gaillard, C. Blanchard, J.P. Jamet, and H. Maletta, 1981a, Physica 107a, 641.

Deville, A., C. Arzoumanian, B. Gaillard, C. Blanchard, J.P. Jamet, and H. Maletta, 1981b, J. Physique 42, 1641.

Duffield, T,, and C.N. Guy, 1985, J. Phys. F15, L17.

Dunlop, M.W., and D. Sherrington, 1985, J. Phys. C18, 1465.

Durand, J., and S.J. Poon, 1979, J. Physique 40, C5-231.

van Duyneveldt, A.J., and C.A.M. Mulder, 1982, Physica 114B, 82.

Dzyaloshinskii, I.E., 1958, J. Phys. Chem. Solids 4, 241.

Dzyaloshinskii, I.E., and G.E. Volovik, 1978, J. Physique 39, 693.

Edwards, S.F., and P.W. Anderson, 1975, J. Phys. F5 965.

Eiselt, G., J. Kötzler, H. Maletta, D. Stauffer, and K. Binder, 1979a, Phys. Rev. B19, 2664.

Eiselt, G., J. Kötzler, H. Maletta, K. Binder, and D. Stauffer, 1979b, J. Magn. and Magn. Mater. 13, 146.

Elliott, R.J., 1961, Phys. Rev. 124, 346.

Emmerich, K., and Ch. Schwink, 1981, Hyperfine Interact. 8, 767.

Emmerich, K., E. Lippelt, R. Neuhaus, H. Pinkvos, Ch. Schwink, F.N. Gygax, A. Hintermann, A. Schenck, W. Studer, and A.J. van der Wal, 1985, Phys. Rev. B31, 7226.

Felsch, W., 1978, Z. Physik B29, 203.

Ferré, J., M. Ayadi, R.V. Chamberlin, R. Orbach and N. Bontemps, 1986, J. Magn. and Magn. Mater. 54-57,211.

Ferré, J., J. Rajchenbach, and H. Maletta, 1981, J. Appl. Phys. 52, 1697.

Ferrer, R., R. Harris, D. Zobin, and M.J. Zuckermann, 1978, Solid State Comm. 26, 451.

Fert, A., and F. Hippert, 1982, Phys. Rev. Letters 49, 1508.

Fert, A., and P.M. Levy, 1980, Phys. Rev. Letters 44, 1538.

Fert, A., and P.M. Levy, 1981, J. Appl. Phys. 52, 1718.

Fert, A., P. Pureur, F. Hippert, K. Baberschke and F. Bruss, 1982, Phys. Rev. B26, 5300.

Fincher, C.R., S.M. Shapiro, A.H. Palumbo and R.D. Parks, 1980, Phys. Rev. Letters 45, 474.

Finnemore, D.K., L.J. Williams, F.H. Spedding, and D.C. Hopkins, 1968, Phys. Rev. 176, 712.

Fisch, R., and A.B. Harris, 1977, Phys. Rev. Letters 38, 785.

Fischer, K.H., 1980, Z. Physik, B39, 37.

Fischer, K.H., 1983a, phys. stat. sol. 116, 357.

Fischer, K.H., 1983b, Z. Physik 53, 215.

Fischer, K.H., 1985, phys. stat. sol. 130, 13.

Fischer, K.H., and W. Kinzel, 1984, J. Phys. C17, 4479.

Fisher, D.S., and H. Sompolinsky, 1985, Phys. Rev. Letters 54, 1063.

Fisher, D.S., and D.A. Huse, 1986, Phys. Rev. Letters 56, 1601.

Fishmann, S., and A. Aharony, 1980, Phys. Rev., B21, 280.

Fogle, W.E., J.B. Boyer, R.A. Fisher, and N.E. Phillips, 1983, Phys. Rev. Letters 50, 1815.

Freeman, A.J., 1972, in: Magnetic Properties of Rare Earth Metals, ed. by R.J. Elliott (Plenums, New York), p. 245.

Gabay, M., and G. Toulouse, 1981, Phys. Rev. Letters 47, 201.

Geohegan, J.A., and S.M. Bhagat, 1981, J. Magn. and Magn. Mater. 25, 17.

Gotaas, J.A., J.J. Rhyne and S.A. Werner, 1985, J. Appl. Phys. 57, 3404.

Gray, E.M., 1979, J. Phys. F9, L167.

Guy, C.N., 1975, J. Phys. F5, L242.

Guy, C.N., 1977, J. Phys. F7, 1505.

Guy, C.N., 1978, J. Phys. F8, 1309.

Guy, C.N., and J.G. Park, 1983, J. Phys. F13, 1955.

Halperin, B.I., and W.M. Saslow, 1977, Phys. Rev. B16, 2154.

Harris, R., M. Plischke and M.J. Zuckermann, 1973, Phys. Rev. Letters 31, 160.

Heffner, R.H., and D.E. MacLaughlin, 1984, Phys. Rev. B29, 6048.

Hein, R.A., R.L. Falge, Jr., B.T. Matthias, and C. Corenzwit, 1959, Phys. Rev. Letters 2, 500.

Hennion, B., M. Hennion, F. Hippert and A.P. Murani, 1983, Phys. Rev. B28, 5365.

Hennion, B., M. Hennion, F. Hippert and A.P. Murani, 1984, J. Phys. F14, 489.

Hippert, F., and H. Alloul, 1982, J. Physique 43, 691.

Hippert, F., H. Alloul, and A. Fert, 1982, J. Appl. Phys. 53, 7702.

Hiraoka, K., T. Hihara, K. Kojima and T. Kino, 1986, J. Magn. and Magn. Mater. 54-57, 1295.

Hoekstra, F.R., G.J. Nieuwenhuys, K. Baberschke, and S.E. Barnes, 1984, Phys. Rev. B29, 1292.

Hohenberg, P.C., and B.I. Halperin, 1977, Rev. Mod. Phys. 49, 435.

Hopfield, J.J., 1982, Proc. Natl. Acad. Science USA, 79, 2554.

Hoogerbeets, R., W.-L. Luo. R. Orbach, and D. Fiorani, 1986, Phys. Rev. B33, 6531.

Houghton, A., S. Jain, and A.P. Young, 1983, J. Phys. C16, L375.

Huang, C.Y., 1985, J. Magn. and Magn. Mater. 51, 1.

Hüser, D., M.J.F.M. Rewiersma, J.A. Mydosh, and G.J. Nieuwenhuys, 1983a, Phys. Rev. Letters 51, 1290.

Hüser, D., L.E. Wenger, A.J. van Duyneveldt and J.A. Mydosh, 1983b, Phys. Rev. B27, 3100.

Krey, U., 1980, Z. Physik B38, 243.

Krey, U., 1981, Z. Physik B42, 231.

Krey, U., 1982, J. Magn. and Magn. Mater. 28, 231.

Krey, U., 1985, J. Physique Lett. 46, 845.

Kubo, R., 1966, Rep. Prog. Phys. 29, 255.

Lauer, J., and W. Keune, 1982, Phys. Rev. Letters 48, 1850.

Lecomte, G.V., H. v. Löhneysen, W. Bauhofer, and G. Güntherodt, 1984, Solid State Comm. 52, 535.

Lecomte, G.V., H. v. Löhneysen, A. Schröder, W. Bauhofer, and G. Güntherodt, 1986a, J. Magn. and Magn. Mater. 54-57, 69.

Lecomte, G.V., N. Schubert, J.A. Heller and E.F. Wassermann, 1986b, J. Magn. and Magn. Mater. (in press).

Levitt, D.A., and R.E. Walstedt, 1977, Phys. Rev. Letters 38, 178.

Levy, P.M., and R. Raghavan, 1986, J. Magn. and Magn. Mater. 54-57, 181.

Levy, P.M., and Q. Zhang, 1986, J. Magn. and Magn. Mater. 54-57, 133.

v. Löhneysen, H., J.L. Tholence, and R. Tournier, 1978a, J. Physique C6, 922.

v. Löhneysen, H., J.L. Tholence, and F. Steglich, 1978b, Z. Physik B29, 319.

v. Löhneysen, H., and J.L. Tholence, 1979, Phys. Rev. B19, 5858.

v. Löhneysen, H., R. van den Berg, G.V. Lecomte, and W. Zinn, 1985, Phys. Rev. B31, 2920.

Lundgren, L., Svedlindh and O. Beckman, 1981, J. Magn. and Magn. Mater. 25, 33.

Lundgren, L., P. Svedlindh, and O. Beckman, 1982, Phys. Rev. B26, 3990.

Lundgren, L., P. Svedlindh, P. Nordblad, and O. Beckman, 1983, Phys. Rev. Letters 51, 911.

Lundgren, L., P. Nordblad, P. Svedlindh, and O. Beckman, 1985, J. Appl. Phys. 57, 3371.

MacLaughlin, D.E., and H. Alloul, 1976, Phys. Rev. Letters 36, 1158.

MacLaughlin, D.E., L.C. Gupta, D.W. Cooke, R.H. Heffner, M. Leon, and M.E. Schillaci, 1983, Phys. Rev. Letters 51, 927.

Maletta, H., and G. Crecelius, 1976, J. Physique 37, C6-645.

Maletta, H., W. Felsch, and J.L. Tholence, 1978a, J. Magn. and Magn. Mater. 9, 41.

Maletta, H., and W. Felsch, 1978b, J. Physique 39, C6-931.

Maletta, H., and P. Convert, 1979a, Phys. Rev. Letters 42, 108.

Maletta, H., and W. Felsch, 1979b, Phys. Rev. B20, 1245.

Maletta, H., 1979c, J. Appl. Phys. 50, 7312.

Maletta, H., 1980a, J. Magn. and Magn. Mater. 15-18, 100.

Maletta, H., W. Felsch, H. Scheuer, and H. Pink, 1980b, J. Magn. and Magn. Mater. 15-18, 167.

Maletta, H., 1980c, J. Physique 41, C5-115.

Maletta, H., and W. Felsch, 1980d, Z. Physik B37, 55.

Maletta, H., W. Zinn, H. Scheuer, and S.M. Shapiro, 1981a, J. Appl. Phys. 52, 1735.

Maletta, H., 1981b, J. Magn. and Magn. Mater. 24, 179.

Maletta, H., 1982a, J. Appl. Phys. 53, 2185.

Maletta, H., G. Aeppli, and S.M. Shapiro, 1982b, Phys. Rev. Letters 21, 1490.

Maletta, H., 1982c, in: "Excitations in Disordered Systems", NATO Advanced Study Institutes, Series B, Vol. 78, p. 431 (Plenums Press).

Maletta, H., G. Aeppli, and S.M. Shapiro, 1983a, J. Magn. and Magn. Mater. 31-34, 1367.

Maletta, H., 1983b, in: "Heidelberg Colloquium on Spin Glasses", Lecture Notes in Physics Vol. 192, p. 90 (Springer Verlag).

Malozemoff, A.P., and I. Imry, 1981b, Phys. Rev. B24, 489.

Malozemoff, A.P., Y. Imry, and B. Barbara, 1982, J. Appl. Phys. 53, 7672.

Malozemoff, A.P., S.E. Barnes, and B. Barbara, 1983, Phys. Rev. Letters 51, 1704.

Malozemoff, A.P., and B. Barbara, 1985, J. Appl. Phys. 57, 3410.

Manheimer, M.A., S.M. Bhagat and H.S. Chen, 1983, J. Magn. and Magn. Mater. 38, 147.

Maple, M.B., 1976, Appl. Phys. 9, 179.

Marshall, W., and S.W. Lovesey, 1971, Theory of Thermal Neutron Scattering, Oxford University Press, Oxford.

Martin, D.L., 1979, Phys. Rev. B20, 368.

Martin, D.L., 1985, Phys. Rev. B31, 4708.

Matsui, M., A.P. Malozemoff, R.J. Gambino, and L. Krusin-Elbaum, 1985, J. Appl. Phys. 57, 3389.

Mattis, D.C., 1976, Phys. Lett. 56A, 421.

McGuire, T.R., T. Mizoguchi, R.J. Gambino and S. Kirkpatrick, 1978, J. Appl. Phys. 49, 1689.

McMillan, W.L., 1983, Phys. Rev. B28, 5216.

McMillan, W.L., 1984a, Phys. Rev. B30, 476.

McMillan, W.L., 1984b, J. Phys. C17, 3179.

Mehran, F., K.W.H. Stevens, F. Holtzberg, R.L. Melcher, W.J. Fitzpatrick, and T.R. McGuire, 1984, Solid State Comm.52, 107.

Mezei, F., 1972, Z. Physik 255, 146.

Mezei, F., and A.P. Murani, 1979, J. Magn. and Magn. Mater. 14, 211.

Mezei, F., 1981, in: "Recent Developments in Condensed Matter Physics, Vol. 1, p. 679, ed. J.T. Devreese (Plenum, New York).

Mezei, F., 1982, J. Appl. Phys. 53, 7654.

Mezei, F., A.P. Murani, and J.L. Tholence, 1983, Solid State Comm. 45, 411.

Mezei, F., 1983, J. Magn. and Magn. Mater. 31-34, 1327.

Meschede, D., F. Steglich, W. Felsch, H. Maletta, and W. Zinn, 1980, Phys. Rev. Letters 44, 102.

Meyer, C., F. Hartmann-Boutron, Y. Gros and I.A. Campbell, 1985, J. Magn. and Magn. Mater. 46, 254.

Mézard, M., G. Parisi, N. Sourlas, G. Toulouse, and M. Virasoro, 1984, Phys. Rev. Letters 52, 1186.

Mizoguchi, T., T.R. McGuire, S. Kirkpatrick, R.J. Gambino, 1977, Phys. Rev. Letters 38, 89.

v. Molnar, S., B. Barbara, T.R. McGuire and R. Gambino, 1982, J. Appl. Phys. 53, 2350.

Monod, P., J.J. Préjean, and B. Tissier, 1979, J. Appl. Phys. 50, 7324.

Monod, P., and Y. Berthier, 1980, J. Magn. and Magn. Mater. 15-18, 149.

Monod, P., and H. Bouchiat, 1982, J. Physique Lettres 43, 46.

Monod, P., and I.A. Campbell, 1984, Phys. Rev. Letters 52, 2096.

Monod, P., A. Landi, C. Blanchard, A. Deville and H. Hurdequint, 1986, J. Magn. and Magn. Mater. 59, 132.

Moore, M.A., and A.J. Bray, 1985, J. Phys. C18, L699.

Moorjani, K., and J.M.D. Coey,: "Magnetic Glasses", Elsevier, 1984.

Morgenstern, I., and K. Binder, 1979, Phys. Rev. Letters 43, 1615.

Morgownik, A.F.J., and J.A. Mydosh, 1983, Solid State Comm. 47, 321 and 325.

Moriya, T., 1960, Phys. Rev. Letters 4, 5.

Morris, B.W., S.G. Colborne, M.A. Moore, A.J. Bray and J. Canisius, 1986, J. Phys. C19, 1157.

Mulder, C.A.M., A.J. van Duyneveldt, and J.A. Mydosh, 1981, Phys. Rev. B23, 1384.

Murani, A.P., and J.L. Tholence, 1977, Solid State Comm. 22, 25.

Murani, A.P., 1978a, Phys. Rev. Letters 41, 1406.

Murani, A.P., 1978b, J. Physique 39, C6-1517.

Murani, A.P., and A. Heidemann, 1978c, Phys. Rev. Letters 41, 1402.

Murani, A.P., 1981, J. Magn. and Magn. Mater. 22, 271.

Murani, A.P., 1983, Phys. Rev. B28, 432.

Murani, A.P., 1985, J. Phys. F15, 417.

Murnick, D.E., A.T. Fiory, and W.J. Kossler, 1976, Phys. Rev. Letters 36, 100.

Nagata, S., P.H. Keesom, and H.R. Harrison, 1979, Phys. Rev. B19, 1633

Néel, L., 1949, Ann. Geophys. 5, 99.

Ngai, K.L., A.K. Rajagopal and C.Y. Huang, 1984, J.Appl. Phys. 55, 1714.

Nigh, H.E., S. Legvold and F.H. Spedding, 1963, Phys. Rev. 132, 1092.

Nordblad, P., L. Lundgren, and L. Sandlund, 1986a, J. Magn. and Magn. Mater. 54-57, 185.

Nordblad, P., P. Svedlindh, L. Lundgren, and L.Sandlund, 1986b, Phys. Rev. B33, 645.

Novak, M.A., O.G. Symko and D.J. Zheng, 1986, J. Magn. and Magn. Mater. 54-57, 129.

Ocio, M., H. Bouchiat, and P. Monod, 1985, J. Physique Lettres 46, 647.

Ocio, M., H. Bouchiat and P. Monod, 1986, J. Magn. and Magn. Mater. 54-57, 11.

Ogielski, A.T., 1985, Phys. Rev. B32, 7384.

Ogielski, A.T., and I. Morgenstern, 1985, Phys. Rev. Letters 54, 928.

Omari, R., J.J. Préjean and J. Souletie, 1983, J. Physique 44, 1069.

Overhauser, A.W., 1959, Phys. Rev. Letters 3, 414.

Overhauser, A.W., 1960, J. Phys. Chem. Solids 13, 71.

Owen, J., M.E. Browne, V. Arp and A.F. Kip, 1957, J. Phys. Chem. Solids 2, 85.

Palmer, R.G., 1982, Adv. Phys. 31, 669.

Palmer, R.G., D.L. Stein, E. Abrahams, and P.W. Anderson, 1984, Phys. Rev. Letters 53, 958.

Parisi, G., 1979, Phys. Rev. Letters 43, 1754.

Parisi, G., and G. Toulouse, 1980, J. Physique Lettres 41, 361.

Parisi, G., 1983, Phys. Rev. Letters 50, 1946.

Paulsen, C.C., J.A. Hamida, S.J. Williamson, and H. Maletta, 1984, J. Appl. Phys. 55, 1652.

Paulsen, C.C., S.J. Williamson, and H. Maletta, 1986a, J. Magn. and Magn. Mater. 54-57, 209.

Paulsen, C.C., S.J. Williamson, and H. Maletta, 1986b, submitted for publication.

Pelcovits, R.A., E. Pytte and J. Rudnick, 1978, Phys. Rev. Letters 40, 476.

Phillips, W.A., 1972, J. Low Temp. Phys. 7, 351.

Poon, S.J., and J. Durant, 1978, Phys. Rev. B18, 6253.

Préjean, J.J., 1978, J. Physique 39, C6-907.

Préjean, J.J., M.J. Joliclerc and P. Monod, 1980, J. Physique 41, 427.

Rainford, B.D., H.B. Stanley and B.V.B. Sarkissian, 1985, Physica 130B, 388.

Rajchenbach, J., J. Ferre, and H. Maletta, 1981, in: "Recent Developments in Condensed Matter Physics", Vol. 2, p. 253 (ed. J.T. DeVresse, L.F. Lemmens, V.E. Van Doren, and J. van Royen), Plenum Publ. Coorp.

Rajchenbach, J., and N. Bontemps, 1983, J. Physique Lettres 44, 799.

Rajchenbach, J., and N. Bontemps, 1984, J. Appl. Phys. 55, 1649.

Rakoto, H., J.C. Ousset, S. Senoussi and I.A. Campbell, 1984, J. Magn. and Magn. Mater. 46, 212.

Rathmann, O., and P. Touborg, 1977, Phys. Rev. B16, 1212.

Reim, W., R.H. Koch, A.P. Malozemoff, M.B. Ketchen and H. Maletta, 1986, Phys. Rev. Letters 57, 905.

Roberts, S.A., and A.J. Bray, 1982, J. Phys. C15, L527.

Rosenbaum, T.F., L.W. Rupp, G.A. Thomas, W.M. Walsh, H.S. Chen, J.R. Banavar and P.B. Littlewood, 1982, Solid State Comm. 42, 725.

Roth, S., 1978, Appl. Phys. 15, 1.

Ruderman, M.A., and C. Kittel, 1954, Phys. Rev. 96, 99.

Salamon, M.B., 1979, Solid State Comm. 31, 781.

Salamon, M.B., K.V. Rao and Y. Yeshurun, 1981, J. Appl. Phys. 52, 1687.

Salamon, B.M., and J.L. Tholence, 1982, J. Appl. Phys. 53, 7684.

Salamon, M.B., and J.L. Tholence, 1983, J.Magn. and Magn. Mater. 31-34, 1375.

Sarkissian, B.V.B., and B.R. Coles, 1976, Comm. on Phys. 1, 17.

Sarkissian, B.V.B., 1977, J. Phys. F7, L139.

Saslow, W.M., 1982, Phys. Rev. Letters 48, 505.

Sato, T., and Y. Miyaka, 1982, J. Phys. Soc. Japan 51, 2153.

Scherzberg, A., H. Maletta, and W. Zinn, 1981, J. Magn. and Magn. Mater. 24, 186.

Schröder, A., H. v. Löhneysen and W. Bauhofer, 1986, submitted for publication.

Schmitt; R.W., and I.S. Jacobs, 1957, J. Phys. Chem. Solids, 3/4, 324.

Schultz, S., F.M. Gullikson, D.R. Fradkin and M. Tovar, 1980, Phys. Rev. Letters 45, 1508.

Sellmyer, D.J., and S. Nafis, 1985, J. Appl. Phys. 57, 3584.

Sellmyer, D.J., and S. Nafis, 1986, J.Magn. and Magn. Mater. 54-57, 113.

Senoussi, S., 1984, J. Physique 45, 315.

Shapiro, S.M., H. Maletta and F. Mezei, 1985, J. Appl. Phys. 57, 3485.

Shapiro, S.M. G. Aeppli, H. Maletta, and K. Motoya, 1986, in: "Frontiers of Neutron Scattering", Physica 137B, 96.

Sherrington, D., and S. Kirkpatrick, 1975, Phys. Rev. Letters 35, 1792.

Sherrington, D., 1983, in: "Heidelberg Colloquium on Spin Glasses", ed. by J.L. van Hemmen and I. Morgenstern (Springer Verlag, Berlin), p. 125.

Shull, R.D., H. Okamoto and P.A. Beck, 1976, Solid State Comm. 20, 863.

Smit, J.J., G.J. Nieuwenhuys, and L.J. de Jongh, 1979a, Solid State Comm. 31, 265.

Smit, J.J. G.J. Nieuwenhuys, and J.L. de Jongh, 1979b, Solid State Comm. 32, 233.

Sompolinsky, H., and A. Zippelius, 1981, Phys. Rev. Letters 47, 359.

Sompolinsky, H., 1981, Phys. Rev. Letters 47, 935.

Sompolinsky, H., and A. Zippelius, 1982, Phys. Rev. B25, 6860.

Sompolinsky, H., and A. Zippelius, 1983, Phys. Rev. Letters 50, 1297.

Southern, B.W., and A.P. Young, 1977, J. Phys. C10, 2179.

Stauffer, D., and K. Binder, 1978, Z. Physik B30, 313.

Suzuki, M., 1977, Prog. Theor. Phys. 58, 1151.

Taniguchi, T., H. Matsuyama, S. Chikazawa, and Y. Miyako, 1983, J. Phys. Soc. Japan 52, 4323.

Taniguchi, T., Y. Miyako and J.L. Tholence, 1985, J. Phys. Soc. Japan, 54, 220.

Tatsumi, T., 1978,Progr. Theor. Phys. 59, 405.

Thalmeier, P., 1986, J. Magn. and Magn. Mater. 54-57, 509.

Thouless, D.J., P.W. Anderson, and R.G. Palmer, 1977, Phil. Mag. 35, 593.

Tholence, J.L., and R. Tournier, 1974, J. Physique 35, C4-229.

Tholence, J.L., 1980, Solid State Comm. 35, 113.

Thomson, J.O., and J.R. Thompson, 1981, J. Phys. F11, 247.

Touborg, P., 1977, Phys. Rev. B16, 1201.

Toulouse, G., 1977, Comm. Phys. 2, 115.

Toulouse, G., 1980, J. Physique Lettres 41, 447.

Tournier, R., and Y. Ishikawa, 1964, Phys. Lett. 11, 280.

Uemura, Y.J., T. Yamazaki, R.S. Hayano, R. Nakai, and C.Y. Huang, 1980, Phys. Rev. Letters 45, 583.

Uemura, Y.J., 1981, Hyperfine Interact. 8, 739.

Uemura, Y.J., and T. Yamazaki, 1982, Physica 109-110B,1915.

Uemura, Y.J., and D.R. Harshman, M. Senba, E.J. Ansaldo and A.P. Murani, 1984, Phys. Rev. B30, 1606.

Uemura, Y.J., T. Yamazaki, D.R. Harshman, M. Senba, and E.J. Ansaldo, 1985, Phys. Rev. B31, 546(1985).

Vannimenus, J., G. Toulouse, and G. Parisi, 1981, J. Physique 42, 565.

Varret, F., A. Hamzić, and I.A. Campbell, 1982, Phys. Rev. B26, 5285.

Velu, E., J.P. Renard and J.P. Miranday, 1981, J. Physique Lett. 42, 237.

Verbeek, B.H., G.J. Nieuwenhuys, H. Stocker and J.A. Mydosh, 1978, Phys. Rev. Letters 40, 586.

Verbeek, B.H., and J.A. Mydosh, 1978, J. Phys. F8, L109.

Viana, L., and A.J. Bray, 1985, J. Phys. C18, 3037.

Violet, C.E., and R.J. Borg, 1983, Phys. Rev. Letters 51, 1073.

Violet, C.E., and R.J. Borg, 1984, Phys. Rev. Letters 52, 2098.

Wachter, P., 1979, in: Handbook on the Physics and Chemistry of Rare Earths, ed. K.A. Gschneidner, Jr. and L. Eyring, North-Holland Publ. Comp., Vol. 2, p. 507.

Walker, L.R., and R.E. Walstedt, 1977, Phys. Rev. Letters 38, 514.

Walker, L.R., and R.E. Walstedt, 1980, Phys. Rev. B22, 3816.

Walstedt, R.E., and L.R. Walker, 1981, Phys. Rev. Letters 47, 1624.

Walstedt, R.E., 1981, Phys. Rev. B24, 1524.

Wendler, R., and K. Baberschke, 1983, Solid State Comm. 48, 91.

Wendler, R., P. Pureur, A. Fert and K. Baberschke, 1984, J. Magn. and Magn. Mater. 45, 185.

Wenger, L.E., and P.H. Keesom, 1975, Phys. Rev. B11, 3497.

Wenger, L.E., and P.H. Keesom, 1976, Phys. Rev. B13, 4053.

Wenger, L.E., 1978, J. Appl. Phys. 49, 1630.

Wenger, L.E., 1983, in: "Heidelberg Colloquium on Spin Glasses", ed. by J.L. van Hemmen and I. Morgenstern (Springer Verlag, Berlin), p.60.

Wenger, L.E., and J.A. Mydosh, 1984a, J. Appl. Phys. 55, 1717.

Wenger, L.E., and J.A. Mydosh, 1984b, J. Appl. Phys. 55, 1850.

Wenger, L.E., G.W. Hunter, J.A. Mydosh, J.A. Gotaas, and J.J. Rhyne, 1986, Phys. Rev. Letters 56, 1090.

Westerholt, K., B. Gosh,K. Siratori, S. Methfessel and T. Petzel, 1977, Physica 86-88B, 740.

Westerholt, K. and H. Bach, 1981a, J. Magn. and Magn. Mater. 24, 191.

Westerholt, K., and H. Bach, 1981b, Phys. Rev. Letters 47, 1925.

Westerholt, K. and H. Bach, 1985, Phys. Rev. B31, 7151.

Wohlfarth, E.P., 1977, Physica 86-88B, 852.

Wolff, W.F., and J. Zittartz, 1985, Z. Physik B60, 185.

Wong, P.-Z., H. Yoshizawa and S.M. Shapiro, 1985a, J. Appl. Phys. 57, 3462.

Wong, P.-z., S. v. Molnar, T.T.M. Palstra, J.A. Mydosh, H. Yoshizawa, S.M. Shapiro and A. Ito, 1985b, Phys. Rev. Letters 55, 2043.

Wosnitza, J., H. v. Löhneysen, W. Zinn, and U. Krey, 1986, Phys. Rev. B33, 3436.

Wu, W.-y., G. Mozurkewich and R. Orbach, 1985, Phys. Rev. B31, 4557.

Yeshurun, Y., M.B. Salamon, K.V. Rao and H.S. Chen, 1980, Phys. Rev. Letters 45, 1366.

Yeshurun, Y., and M.B. Salamon, 1981, J. Phys. C14, L575.

Yeshurun, Y., and H. Sompolinsky, 1982, Phys. Rev. B26, 1487.

Yosida, K., 1957, Phys. Rev. 106, 893.

Young, A.P., 1983a, Phys. Rev. Letters 50, 917.

Young, A.P., 1983b, Phys. Rev. Letters 51, 1206.

Zinn, W., 1976, J. Magn. and Magn. Mater. 3, 23.